Uniwersytet Mikołaja Kopernika w Toruniu
Wydział Nauk Biologicznych i Weterynaryjnych

UNIWERSYTET
MIKOŁAJA KOPERNIKA
W TORUNIU
Wydział Nauk Biologicznych
i Weterynaryjnych

Kinga Walczak

Rozprawa doktorska

Relacje filogenetyczne w obrębie rodziny Muscidae (Diptera): perspektywa oparta na danych filogenomicznych oraz morfologii stadiów preimaginalnych

Promotor: prof. dr hab. Krzysztof Szpila
Promotor zagraniczny: prof. Thomas Pape

Katedra Ekologii i Biogeografii

Toruń, 2025

Nicolaus Copernicus University in Toruń
Faculty of Biological and Veterinary Sciences

Kinga Walczak

PhD thesis

The phylogenetic relationships within Muscidae (Diptera): a perspective illuminated by phylogenomic and immature stages morphology data

Supervisor: prof. dr hab. Krzysztof Szpila
Foreign supervisor: prof. Thomas Pape

Department of Ecology and Biogeography

Toruń, 2025

Acknowledgements

I would like to express my sincere gratitude to ***Dr. Andrzej Grzywacz****, without whose support it would probably not have been possible for me to be where I am today. I am deeply thankful for his academic, methodological and practical guidance, for his time, patience, invaluable support, and for the many insightful comments provided at every stage of this doctoral research, as well as during other scientific projects.*

I would also like to extend my appreciation to ***Prof. Krzysztof Szpila*** *for sharing his extensive professional knowledge, for his thoughtful remarks and constructive criticism, which have greatly contributed to the improvement of the quality of my work.*

My sincere thanks go to ***Prof. Thomas Pape*** *for his remarkable attention to detail, as well as for his always precise and insightful comments and suggestions, which not only enhanced the scientific value of this dissertation but also taught me the importance of accuracy and precision in every aspect of research.*

Finally, I wish to express my heartfelt gratitude to ***My Husband*** *for his unwavering support, understanding, and motivation, both in everyday life and throughout the completion of this dissertation. Thank you for your patience, sense of humour and unshakable faith in me, which helped me maintain balance and calm even in the most challenging moments.*

Funding

- The research constituting part of the doctoral dissertation was financed as part of the OPUS 17 project from the funds of the National Science Centre.
  Project title: A large-scale phylogeny and evolution of immature stages in megadiverse family Muscidae (Diptera)
  Project number: 2019/33/B/NZ8/02316
  Principal Investigator: dr Andrzej Grzywacz

- Part of the research work was carried out during international research internships at the following institutions:
  a) Departmento de Ciencias Ambientales y Recursos Naturales, University of Alicante, Alicante, Spain;
  b) Natural History Museum of Denmark, University of Copenhagen, Copenhagen, Denmark.
  The internships were financed from the "Excellence Initiative – Research University" program.

NARODOWE CENTRUM NAUKI

List of publications included in the doctoral dissertation

No.	Full references	Ref. code (used in text)	IF indicator / MNiSW points
1.	**Walczak, K.**, Pape, T., Ekanem, M., Szpila, K., & Grzywacz, A. (2023). Insights into the systematics of *Alluaudinella* and allied *Aethiopomyia* and *Ochromusca* (Muscidae, Diptera). Zoologica Scripta, 52(3): 279–297. https://doi.org/10.1111/zsc.12584	Article 1	IF (2023) – 2.3 MNiSW – 100 pts
2.	**Walczak, K.**, Pape, T., Wallman, J. F., Szpila, K., & Grzywacz, A. (2024). To see the unseen: notes on the larval morphology and systematic position of *Achanthiptera* Rondani (Diptera: Muscidae). Arthropod Systematics and Phylogeny, 82: 305–322. https://doi.org/10.3897/ASP.82.E116703	Article 2	IF (2024) – 1.8 MNiSW – 100 pts
3.	**Walczak, K.**, & Grzywacz, A. (2024). An illustrated identification key to early instar larvae of forensically important Muscidae (Diptera) of the western Palaearctic region. Forensic Science International, 360:112028. https://doi.org/10.1016/j.forsciint.2024.112028	Article 3	IF (2024) – 2.5 MNiSW – 100 pts
4.	**Walczak, K.**, Piwczyński, M., Pape, T., Johnston, N. P., Wallman, J. F., Szpila, K., & Grzywacz, A. (2025). Unravelling phylogenetic relationships within the genus *Lispe* (Diptera: Muscidae) through genome-assisted and *de novo* analyses of RAD-seq data. Molecular Phylogenetics and Evolution, 204: 108291. https://doi.org/10.1016/j.ympev.2025.108291	Article 4	IF (2025) – 3.6 MNiSW – 140 pts
		Sum	IF – 9.1 MNiSW pts – 440

Other publications published during doctoral studies

No.	Full references	IF indicator / MNiSW points
1.	**Walczak, K.**, Szpila, K., Nelson, L., Pape, T., Hall, M. J. R., Alves, F., & Grzywacz A. (2022). Larval morphology of the avian parasitic genus *Passeromyia*: playing hide and seek with a parastomal bar. Medical and Veterinary Entomology, 37(1): 14–26. https://doi.org/10.1111/mve.12603	IF (2022) – 1.9 MNiSW – 140 pts
2.	Johnston N.P., Piwczyński M., Trzeciak P., **Walczak K.**, & Szpila K. (2023). Integration of mitogenomic and morphological data disentangles the systematics of *Pollenia* and establishes a revised phylogenetic hypothesis for the Polleniidae. Systematic Entomology, 48(2), 296–315. https://doi.org/10.1111/syen.12576	IF (2023) – 4.7 MNiSW – 140 pts
3.	Szpila K., **Walczak K.**, Grzywacz A., Soszyńska A., Akbarzadeh K., Bystrowski C., & Pape T. (2023). Underexplored diversity in Palaearctic *Miltogramma* Meigen, 1803 (Diptera: Sarcophagidae). Zoological Journal of the Linnean Society, zlad141. https://doi.org/10.1093/zoolinnean/zlad141	IF (2023) – 3.0 MNiSW – 140 pts
4.	Szpila K., **Walczak K.**, Soszyńska A., & Pape T. (2024). First data on early instar Afrotropical Miltogramminae (Diptera: Sarcophagidae) reveal unexpected morphological diversity. Zoological Journal of the Linnean Society, zlae030. https://doi.org/10.1093/zoolinnean/zlae030	IF (2024) – 2.8 MNiSW – 140 pts
5.	Tomsia M., Grzywacz A., Szpila K., **Walczak K.**, Mahlerová K., Vanek D., & Matuszewski S. (2025). Human costal cartilage, tooth cavities, and femur nutrient canals – new niches for insects used in forensic entomology. Forensic Sciences Research, 10(2): owae028. https://doi.org/10.1093/fsr/owae028	IF (2025) – 1.8 MNiSW – 20 pts

6.	Piwczyński M., Dinka M.D., Trzeciak P., **Walczak K.**, Puchałka R., Soghigian J., & Spalik K. (2025). Conflicting phylogenetic signals obscure the taxonomic position of *Ferula heuffelii* (Apiaceae), a rare Southeast European endemic. Botanical Journal of the Linnean Society, boaf050. https://doi.org/10.1093/botlinnean/boaf050	IF (2025) – 2.2 MNiSW – 100 pts

Table of contents

List of abbreviations

AHE – Anchored Hybrid Enrichment,

BI – Bayesian analysis,

BIC – Bayesian information criterion,

BS – bootstrap,

CAD – carbamoyl-phosphate synthetase 2,

CLSM – confocal laser scanning microscopy,

COI – cytochrome c oxidase subunit I,

cytB – cytochrome b,

Ef-1α – elongation factor 1-alpha,

EtOH – ethyl alcohol,

gDNA – genomic deoxyribonucleic acid,

KOH – potassium hydroxide,

LM – light microscopy,

MIP – maximum intensity projections,

ML – maximum likelihood,

mS-seq – multilocus Sanger sequencing,

N.A. – numerical aperture,

ONT – Oxford Nanopore Technologies,

PP – posterior probability,

RAD-seq – restriction site-associated DNA sequencing,

SEM – scanning electron microscopy,

SNP – single-nucleotide polymorphism,

Q – Phred quality score,

QV – assembly quality.

Streszczenie

Muchówki (Diptera), jeden z najbogatszych w gatunki rzędów owadów, osiągnęły nadzwyczajny sukces ewolucyjny oraz wykształciły niespotykaną różnorodność strategii życiowych. Jednakże relacje pokrewieństwa i historia ewolucyjna muchówek wciąż pozostają w dużej mierze nierozwiązane, a wyniki analiz morfologicznych postaci dorosłych i danych molekularnych często prowadzą do sprzecznych hipotez filogenetycznych lub słabo wspieranych statystycznie relacji. W niniejszej pracy, oprócz analiz filogenetycznych, szczególny nacisk położono na wykorzystanie morfologii stadiów larwalnych jako źródła danych użytecznych w badaniach taksonomicznych i systematycznych owadów. Badania przeprowadzono na przedstawicielach rodziny Muscidae, jednej z najbogatszych gatunkowo rodzin muchówek, charakteryzującej się wyjątkową różnorodnością morfologiczną i biologiczną zarówno postaci dorosłych, jak i stadiów preimaginalnych. Chociaż obecna koncepcja rodziny Muscidae jest stosunkowo dobrze ugruntowana dzięki jednoznacznym i zgodnym wynikom zarówno analiz morfologicznych, jak i molekularnych, wiele powiązań filogenetycznych w jej obrębie, zwłaszcza dotyczących relacji między gatunkami czy pozycji poszczególnych taksonów w obrębie podrodzin, często wykazuje zmienność w zależności od wykorzystanego źródła danych lub przyjętej metody analizy.

Celem niniejszej pracy było pogłębienie wiedzy o relacjach filogenetycznych wybranych przedstawicieli Muscidae oraz szczegółowe udokumentowanie morfologii wczesnych stadiów larwalnych. W analizach wykorzystano zarówno dane molekularne, stosując metody sekwencjonowania nowej generacji, jak i podejście morfologiczne oparte na nowoczesnych technikach mikroskopowych. Zastosowanie skanującej laserowej mikroskopii konfokalnej umożliwiło szczegółową wizualizację dotąd nieopisanych i niedokumentowanych struktur szkieletu głowowo-gardzielowego larw, dostarczając nowych cech istotnych dla rekonstrukcji filogenezy oraz rewizji systematyki wybranych taksonów.

Szczególną uwagę poświęcono trzem problematycznym taksonom: rodzajowi *Alluaudinella* Giglio-Tos i taksonom siostrzanym *Aethiopomyia* Malloch i *Ochromusca* Malloch, rodzajowi *Achanthiptera* Rondani oraz rodzajowi *Lispe* Latreille. W przypadku *Alluaudinella* i taksonów siostrzanych zastosowano zarówno analizę morfologiczną larw, jak i dane molekularne, co pozwoliło zweryfikować ich dotychczas niejednoznaczną pozycję systematyczną. Dla rodzaju *Achanthiptera* opracowano szczegółową dokumentację larw z wykorzystaniem skaningowej laserowej mikroskopii konfokalnej i

skaningowej mikroskopii elektronowej, umożliwiając ponowną ocenę jego relacji filogenetycznych w obrębie podrodziny Azeliinae. Z kolei w przypadku rodzaju *Lispe* zastosowano sekwencjonowanie fragmentów DNA powiązanych z miejscami restrykcyjnymi (RAD-seq) oraz sekwencjonowanie nanoporowe, uzyskując nowe dane o relacjach wewnątrzrodzajowych i wskazując na potrzebę rewizji niektórych grup gatunkowych. Istotnym elementem pracy było także opracowanie i udokumentowanie morfologii wczesnych stadiów larwalnych (pierwsze i drugie stadium larwalne) gatunków Muscidae o znaczeniu medyczno-sądowym. Uzyskane wyniki pozwoliły na opracowanie pierwszego kompleksowego klucza identyfikacyjnego dla gatunków występujących w zachodniej Palearktyce, wypełniając istotną lukę w wiedzy i stanowiąc cenne narzędzie m.in. dla entomologii sądowej oraz przyszłych badań nad różnorodnością i ewolucją Muscidae.

Słowa kluczowe: *Achanthiptera*, *Alluaudinella*, szkielet głowowo-gardzielowy, mikroskopia konfokalna, mikroskopia świetlna, *Lispe*, filogeneza molekularna, pręcik parastomalny, analiza filogenetyczna

Abstract

Flies (Diptera), one of the most species-rich insect orders, have achieved extraordinary evolutionary success and evolved an unprecedented diversity of life strategies. However, phylogenetic relationships and evolutionary history of Diptera remain largely unresolved, and the results of analyses of morphological and molecular data often lead to conflicting phylogenetic hypotheses or statistically weakly supported relationships. In this study, in addition to phylogenetic analyses, particular emphasis was placed on utilising the morphology of the larval stage as a source of data useful in taxonomic and systematic studies of insects. The study was conducted on representatives of the Muscidae family, one of the most species-rich families of flies, characterised by extraordinary morphological and biological diversity of both adults and preimaginal stages. Although the current concept of the Muscidae as a family is relatively well-established, many phylogenetic relationships within it, particularly those concerning species relationships and the position of individual taxa within subfamilies, often exhibit variation depending on the data source used or the analytical method adopted.

The aim of this study was to better understand the phylogenetic relationships of selected representatives of the Muscidae and to document in detail the morphology of early larval instars. The analyses utilised both molecular data, using next-generation sequencing methods, and a morphological approach based on modern microscopic techniques. Particularly, confocal laser scanning microscopy (CLSM) enabled detailed visualisation of previously undescribed and undocumented structures of the cephaloskeleton of larvae, providing new characters crucial for phylogenetic reconstruction and systematic revision of selected taxa.

Particular attention was paid to three problematic taxa: the clade consisting of the genus *Alluaudinella* Giglio-Tos and its sister taxa *Aethiopomyia* Malloch and *Ochromusca* Malloch, the genus *Achanthiptera* Rondani and the genus *Lispe* Latreille. In the case of *Alluaudinella* and its sister taxa, analyses were carried out on morphological data from the larvae as well as on molecular data, allowing for the clarification of their previously ambiguous systematic position. For the genus *Achanthiptera*, detailed larval documentation was produced using CLSM and scanning electron microscopy (SEM), enabling a reassessment of its phylogenetic relationships within the Azeliinae. For the genus *Lispe*, restriction site-associated DNA sequencing (RAD-seq) combined with nanopore sequencing was used, yielding new data on intrageneric relationships and suggesting the need for revision of some species groups. A significant part of the work

also involved documenting and interpreting the morphology of early immature stages (first and second instar larvae) of necrophagous muscid species. The data obtained allowed for the development of the first comprehensive identification key for species occurring in the western Palearctic region, filling a significant knowledge gap and providing a valuable tool for forensic entomology and future research on the diversity and evolution of Muscidae.

Keywords: *Achanthiptera*, *Alluaudinella*, cephaloskeleton, confocal laser scanning microscopy, light microscopy, *Lispe*, molecular phylogeny, parastomal bar, phylogenetic analysis

1. Introduction

Flies (Diptera) represent one of the most diverse and ecologically significant groups of insects, and their evolutionary relationships have become the subject of extensive molecular and morphological studies. The phylogeny of flies has traditionally been reconstructed based on morphological characters of adults (Meier & Lim, 2009), less frequently on larval morphology, however, recent advances in phylogenomics have significantly improved the resolution of the dipteran Tree of Life, clarifying relationships at deep, intermediate and shallow taxonomic levels. In many cases higher-level taxa, that is families, subfamilies and tribes, are now well defined (Buenaventura et al., 2021; Cohen et al., 2021; Stireman et al., 2019; Winkler et al., 2022; Young et al., 2016). The use of modern molecular tools has, for example, led to a revision of the taxonomic status of blowflies (Diptera: Calliphoridae), in which, despite decades of research, phylogenetic relationships remained controversial (Kutty et al., 2019). Discussions regarding monophyly and the classification or status of some subfamilies remain contentious, although the results of recent analyses have led, among others, to the resurrection of the former subfamilies Polleniinae and Mesembrinellinae to the level of families (Polleniidae and Mesembrinellidae, respectively) (Cerretti et al., 2019; Marinho et al., 2017; Yan et al., 2021) and to the reassessment of the status of Rhiniinae, which was resurrected to family level (Kutty et al., 2010) and is now treated again as a subfamily (Kutty et al., 2019; Yan et al., 2021). Nevertheless, even in the era of phylogenomics, morphological data remain a valuable source of information on phylogenetic relationships, for example, by providing clues to support the interpretation of molecular analyses. Although both morphological and molecular approaches are largely congruent in terms of many key relationships within Diptera, they often lead to divergent conclusions regarding the relationships between main evolutionary lineages, and some nodes of the phylogenetic tree remain poorly supported statistically (Grzywacz et al., 2021; Haseyama et al., 2015). Consequently, the reconstruction of the phylogeny of Diptera still faces significant difficulties, as reflected in conflicting hypotheses derived from different data sources (San Jose et al., 2018).

In cases of conflict, integrating multiple types of data, from morphological and ecological traits to molecular sequences, becomes crucial. A particularly valuable but still underestimated source of information is the morphology of larval instars, the individual

features of which may reflect both deep phylogenetic relationships and adaptations to specific feeding strategies (Meier & Lim, 2009).

House flies (Muscidae), with approximately 6 000 species, are one of the most species-rich dipteran families, found in all biogeographic regions. Several muscid species are well known for their economic, medical or veterinary importance, as they can act as mechanical vectors for pathogens, posing a threat to public health and animal breeding. Nevertheless, these are characteristics of a few notorious species, such as the house fly (*Musca domestica* Linnaeus), the stable fly (*Stomoxys calcitrans* (Linnaeus)), and the cattle fly (*Haematobia irritans* (Linnaeus)), and the great majority of members of this family are harmless. Some of them, however, play a significant ecological role, for example as pollinators or potential biological pest control agents (some species of Azeliinae and Coenosiinae) (Couri & de Carvalho, 2013; Couri & Salas, 2010; Tiusanen et al., 2016). In turn, immature stages exhibit remarkably diverse feeding strategies, as they can parasitise bird nestlings (larvae of *Passeromyia* Rodhain & Villeneuve and *Philornis* Meinert), feed on grasses (*Atherigona* Rondani), feed on dead snails (*Alluaudinella* Giglio-Tos, *Aethiopomyia* Malloch and *Ochromusca* Malloch), live in aquatic habitats (Coenosiinae), decompose organic matter and cause myiasis in humans and animals (*Muscina* Robineau-Desvoidy, *Hydrotaea* Robineau-Desvoidy). The extraordinary diversity of morphology, life histories, behaviour, feeding strategies, and ecological adaptations, both in the immature and adult stages, makes the Muscidae an excellent model for studying the evolution of morphology and behaviour in a phylogenetic context, and for the application of these data sources to verify hypotheses on higher-level relationships.

The modern classification of the family Muscidae (Michelsen, 1991; Roback, 1951) differs significantly from earlier concepts. Previously, this family included taxa currently classified in the families Fanniidae, Anthomyiidae and Scathophagidae (Karl, 1928; van Emden, 1951), as well as in the superfamilies Hippoboscoidea and Oestroidea (Séguy, 1937), resulting in a wide variability in the proposed number of subfamilies, which ranged from four (Hennig, 1955) to fifteen (Séguy, 1937). The classification of Muscidae gained greater clarity in the second half of the 20th century. In particular, studies on female oviscapt have clearly distinguished muscid species from the representatives of modern Anthomyiidae, Fanniidae and Scathophagidae, based on the loss of two postabdominal spiracles in the female abdomen (Herting, 1957). Significant progress in higher-level classification was achieved through the use of morphological

data in realms of phylogenetic concepts (Couri & Pont, 2000; Hennig, 1965; Moura et al., 1998; Nihei & De Carvalho, 2007; Savage & Wheeler, 2004). Nevertheless, most studies were still based solely on adult morphology. The only data on preimaginal stages were included in the work of Skidmore (1985), who, however, did not perform a formal phylogenetic analysis and avoided reclassification when the morphological data of immature stages and adults were at odds. The modern concept of Muscidae and the understanding of relationships within the family were later refined by molecular analyses (mS-seq, AHE, RAD-seq, transcriptomic data (Grzywacz et al., 2017, 2021; Haseyama et al., 2015; Kutty et al., 2008, 2014, 2019)). Despite these advances, numerous relationships, especially at the intermediate and deep taxonomic levels, are still poorly understood and classifications based on adult morphology often do not matc–h with the results of molecular studies. Currently, Muscidae is divided into eight subfamilies: Atherigoninae, Azeliinae, Coenosiinae, Cyrtoneurininae, Muscinae, Mydaeinae, Phaoniinae and Reinwardtiinae. However, most subfamilies and tribes, that have traditionally been recognised based on adult morphology, appear to be either not monophyletic or the various data sources suggest alternative phylogenetic hypotheses, indicating the need to develop a new, robust classification system for Muscidae (Grzywacz et al., 2021; Haseyama et al., 2015; Kutty et al., 2008, 2014).

The morphology of the immature stages is still a rarely implemented source of taxonomic data. One of the key activities in this approach is the analysis of the morphology of the cephaloskeleton, which is located inside the anterior part of the larval body and is responsible for feeding in cyclorrhaphan Diptera (Ferrar, 1979). The analysis of its structure (e.g., the presence/absence of individual elements of the cephaloskeleton, i.e., sclerites, their position, connections, shape, modifications) and functional diversity, which usually correlates with the mode of food acquisition, constitutes the basis for reconstructing higher-level relationships between taxa (Ferrar, 1979; Skidmore, 1985). In practise, traditional light microscopy, routinely used in the study of dipteran larvae, allows only the observation of a limited range of features due to the cephaloskeleton being a small structure, sclerotized to varying degrees and partially hidden by soft tissue. A breakthrough in the study of these minor structures is confocal laser scanning microscopy, which allows for the acquisition of high-resolution three-dimensional images using chitin's autofluorescence properties (Brooker et al., 2012; Grzywacz, Góral, et al., 2014; Lee et al., 2009). In this work, the application of CLSM to the systematics of muscids

opens new possibilities for the interpretation of morphological data of immature stages in the context of phylogenetic inference.

In this doctoral thesis, representative taxa from the family Muscidae that are characterised by ambiguous phylogenetic relationships or problematic taxonomic positions were selected. Each of the Articles 1–4 covers different taxa and employs different analytical approaches: Article 1 combines detailed larval morphology with molecular analyses, Articles 2 and 3 focus solely on morphological data of larvae and Article 4 uses only molecular data to analyse intrageneric relationships. This methodological diversity, and above all, the inclusion of larval morphology, enabled the testing of existing phylogenetic hypotheses, the provision of new and revised morphological descriptions of larval instars and contributed to resolving some questionable nodes within the family Muscidae. Although particular emphasis was placed on integrating larval morphology into phylogenetic inference in this dissertation, this was not feasible for the genus *Lispe* (Article 4). The primary reason was the lack of complete and comprehensive literature data and larval material for a broad set of species, representing major evolutionary lineages in this genus. Where those were present, available morphological descriptions and line drawings did not provide sufficient information to allow for phylogenetic inference (Skidmore, 1985).

1.1 The systematic position of *Alluaudinella* (Article 1)

The phylogenetic position of the genus *Alluaudinella*, along with its relatives *Aethiopomyia* and *Ochromusca*, has remained unclear for decades, and their classification has undergone numerous changes. Previous authors based their hypotheses on adult morphological characters, and only in a few cases took into account the morphology of larvae, placing these taxa in different subfamilies of Muscidae (Dichaetomyiinae, Dichaetomyiini of Phaoniinae, Muscinae, Reinwardtiinae). The only consistent and unambiguous conclusion among authors was the close relationship between *Alluaudinella*, *Aethiopomyia*, and *Ochromusca*, which together form a monophyletic group supported by both immature and adult morphology, as well as by a highly specialised snail-feeding strategy of larval stages. The unclear systematic position of the entire *Alluaudinella-Aethiopomyia-Ochromusca* clade within other muscid species resulted from several reasons: (i) overreliance on single features of adult morphology (e.g., the shape of the lower calypter (Malloch, 1925; van Emden, 1939) or male terminalia (Paterson, 1959) or yellow body colouration and/or setose anepimeron

(Hennig, 1965)), (ii) the use of heterogeneous and often contradictory classification criteria by subsequent authors (mostly the morphology of adult flies with single examples of including larval biology and morphology), (iii) erroneous interpretations of the biology of larvae, initially considered carnivorous (Paterson, 1959), while in fact they are trimorphic saprophagous (Skidmore, 1985), (iv) reliance on homoplastic characters devoid of phylogenetic value (Couri & Carvalho, 2003) and (v) scarcity of data on early instar larvae. The up-to-date concept is that *Alluaudinella* is placed in the subfamily Phaoniinae and is closely related to *Dichaetomyia* Malloch (Pont, 1980). Due to the inconsistency and unclear subfamily position of the clade *Alluaudinella-Aethiopomyia-Ochromusca* the aim of this study was to investigate its position within Muscidae using larval morphology and, for the first time, molecular data. This approach allowed us to test existing concepts and assess the congruence of morphological and molecular data in the context of the systematic position of the *Alluaudinella-Aethiopomyia-Ochromusca* group within the family Muscidae.

1.2 The systematic position of *Achanthiptera* (Article 2)

For many decades, the genus *Achanthiptera* remained one of the most challenging taxa in muscid systematics. The genus has been placed in various tribes and subfamilies (d'Assis Fonseca, 1968; Hennig, 1955, 1965), and even in its own subfamily, Achanthipterinae (Hennig, 1965). This classification was based on a single observation by Hennig (1965) that one postabdominal spiracle is retained in segment 6 of the female abdomen, while all other members of the Muscidae lack postabdominal spiracles. However, as later morphological reanalyses of adult flies showed (Kutty et al., 2014), this peculiar feature was a misinterpretation. The phylogenetic analysis based on molecular data with the addition of revisions of adult morphology (Kutty et al., 2014) demonstrated that *Achanthiptera* did not occupy a unique position within Muscidae, but was closely related to *Potamia* Robineau-Desvoidy and *Australophyra* Malloch, justifying its placement in the subfamily Azeliinae. Nevertheless, detailed morphological documentation of *Achanthiptera* larvae, which could have provided additional systematic evidence, was still lacking. In Article 2, this gap was filled by examining the second and third larval instars of *Achanthiptera* and *Potamia*, and the third larval instar of *Australophyra*, using CLSM and SEM. The use of CLSM in this study proved invaluable due to the poor condition of the 100-year-old museum *Achanthiptera* larvae, which prevented sufficient analysis using LM. The obtained microscopic documentation

allowed for a reanalysis of the systematic position of these taxa and provided new evidence for the position of *Achanthiptera* within the subfamily Azeliinae. Furthermore, CLSM observations revealed peculiar, previously undocumented modifications of the cephaloskeleton, including distinct anterior rod shapes in the second and third instars of *Ac. rohrelliformis* (Robineau-Desvoidy) and *P. littoralis* Robineau-Desvoidy. The analysis also provided evidence for unique similarities between *Achanthiptera*, *Potamia* and *Australophyra*, supporting their close relationship.

1.3 The morphology of early instar muscid larvae (Article 3)

Although the family Muscidae has for decades been the subject of considerable interest among many authors, resulting in substantial descriptions of larval morphology, these efforts have focused predominantly on late (third) instar larvae. Consequently, the morphology of early (i.e., first and second) instars remains poorly understood or even entirely unknown. Knowledge of larval morphology may prove useful, for example, in the context of forensic entomology, where accurate species identification is of paramount importance. This problem is particularly acute for the early larval instars of muscid larvae, a family encompassing several species of medico-legal importance. A common opinion was that first and second instar larvae are difficult to distinguish due to their small size and significant morphological similarity. Current methods, which involve rearing larvae to adults and then identifying them or molecular identification of larvae, are often limited by difficulties in obtaining and properly storing material, as well as potential DNA degradation (Byrd & Castner, 2010; Hajibabaei et al., 2005; Yeo et al., 2020). At the same time, the development of modern microscopic techniques, i.e., CLSM, has opened up new perspectives in the imaging and analysis of such small material, enabling much more detailed morphological studies of early larval instars. In Article 3, a detailed analysis of the morphology of first and second instar larvae of necrophagous muscid species was conducted using LM and CLSM, and for two species, also SEM. Based on the obtained data, the first comprehensive identification key for the first and second instars of muscid larvae from the western Palearctic region was developed, filling a significant gap in morphological knowledge and increasing the precision of early instar identification.

1.4 The phylogenetic relationships within the genus *Lispe* (Article 4)

Lispe Latreille is a monophyletic genus of flies (Diptera: Muscidae) widely distributed worldwide, except for New Zealand. Its monophyly is supported by autapomorphies described by Hennig (1960, 1965) and recent molecular analyses (Gao et al., 2022). *Lispe* is currently classified in the subfamily Coenosiinae and is closely related to the genus *Limnophora* Robineau-Desvoidy (Hennig, 1960), which has been confirmed by molecular studies (Gao et al., 2022; Ge et al., 2016; Grzywacz et al., 2021; Kutty et al., 2014). So far, numerous attempts have been made to systematise species within *Lispe* and classify them within smaller units, i.e., species groups. Initial divisions into species groups were proposed in the mid-20th century (including the *tentaculata*, *uliginosa*, *palposa*, *scalaris*, *caesia* and *longicollis* species groups), and in recent years, Vikhrev has significantly expanded on them, introducing subsequent species groups. Some groups, such as *nivalis*-group and *palposa*-group, are well-defined, while others, such as *caesia*-group, remain unclear. Currently, fourteen species groups are recognised based on morphological data and ecological preferences, however, some of them have an unclear status, as do the relationships between them, and some species still remain unassigned, which requires further study. To better understand species relationships within *Lispe*, RAD-seq was applied in Article 4 using two approaches: *de novo* assembly and reads mapping to a reference genome. For this purpose, the *Lispe tentaculata* (De Geer) reference genome was obtained using long-read nanopore sequencing (Oxford Nanopore Technologies). To obtain the highest possible genome quality, we tested different ONT read assemblers to evaluate their performance in terms of completeness and quality of the obtained genome sequence. Additionally, we compared different RAD-seq analysis schemes, as the choice of analysis parameters is crucial and can significantly impact the final results (Grzywacz et al., 2021). Our findings largely confirm the previous division into species groups that were proposed based on traditional morphology, but at the same time reveal new relationships between them and indicate the need for a thorough revision of the phylogeny of the genus *Lispe*.

2. Aims and objectives

The primary aim of this study was to clarify the phylogenetic relationships between some taxa within the family Muscidae and to describe for the first time and/or revise the morphology of selected immature stages of muscid species. The interpretation of Muscidae as a distinct family (Michelsen, 1991) and the establishment of phylogenetic relationships between taxa within it have been a subject of debate for many years. Despite some progress in the classification of muscids achieved by incorporating molecular data (Grzywacz et al., 2017, 2021; Haseyama et al., 2015; Kutty et al., 2014; Schuehli et al., 2007), many relationships still remain unresolved, mainly due to divergent results (e.g., adult morphology versus molecular analyses) and poor statistical support for the proposed phylogenetic hypotheses. Given the growing importance and abundant evidence (Meier & Lim, 2009) that the morphology of immature stages of insects is a valuable source of phylogenetic information, this work extensively uses morphological data of preimaginal stages for phylogenetic inference. This dissertation utilised both molecular and morphological analyses, with the choice of methods largely dependent on the availability of larval material and research question. In Articles 1–3, morphological analyses were performed (in Article 1, supplemented by molecular analysis using mS-seq), while in Article 4, due to the lack of comprehensive data on immature stages for a broad set of species, only a phylogenomic approach was used.

The specific objectives of the present work were as follows:

Article 1:

- to study and document the morphology of the egg, first, second and third instar of *Alluaudinella flavicornis* (Macquart);
- to provide the first molecular phylogenetic analysis including *Alluaudinella* spp.;
- to incorporate larval morphology into the evaluation of certain nodes on the phylogenetic tree that are consistent or inconsistent with traditional concepts.

Article 2:

- to evaluate the effectiveness of CLSM in visualising over 100-year-old museum larval material exposed to excessive UV radiation;
- to examine and document in detail the morphology of second and third instar larvae of *Achanthiptera rohrelliformis* (Robineau-Desvoidy) and *Potamia*

littoralis Robineau-Desvoidy, and third instar larvae of *Australophyra rostrata* Robineau-Desvoidy, using LM, SEM and CLSM,

- to reexamine the systematic relationships of *Ac*. *rohrelliformis* within the family Muscidae.

Article 3:

- to conduct a detailed morphological analysis of the first and second instar larvae of medico-legal muscid species using LM and CLSM;
- to develop the first illustrated identification key enabling species identification of early instar of forensically significant muscids larvae from the western Palearctic region.

Article 4:

- to obtain the *L*. *tentaculata* genome sequence using nanopore sequencing;
- to examine the phylogenetic relationships within the genus *Lispe* using RAD-seq method.

3. Materials and methods

Each of the four articles constituting this doctoral dissertation addressed different taxa within the family Muscidae. The selection of taxa resulted from the need to fill gaps in knowledge about their systematic position and the morphology of preimaginal stages. Particular attention was paid to species whose early instar larvae were poorly known and insufficiently documented, with the literature often providing only limited descriptions that concerns only diagnostic features of mature larvae. An additional benchmark for selecting taxa was their unresolved systematic position, resulting from the lack of solid molecular or morphological evidence supporting the previously proposed phylogenetic hypotheses.

Table 1. Summary of the taxa studied and methods used in each of the four studies.

Article	**Taxon/taxa under study**	**Morphological analysis methods**	**Molecular analysis methods**
Article 1	*Alluaudinella flavicornis*	LM, CLSM, SEM	mS-seq
Article 2	*Achanthiptera rohrelliformis, Potamia littoralis, Australophyra rostrata*	CLSM, SEM	-
Article 3	*Atherigona orientalis, Hydrotaea aenescens, Hydrotaea armipes, Hydrotaea capensis, Hydrotaea dentipes, Hydrotaea ignava, Hydrotaea pilipes, Hydrotaea similis, Musca domestica, Muscina levida, Muscina prolapsa, Muscina stabulans, Stomoxys calcitrans, Synthesiomyia nudiseta*	LM, CLSM, SEM	-
Article 4	genus *Lispe*	-	RAD-seq, nanopore sequencing

3.1 Materials

Article 1

In Article 1, the main subject of the study was the species *Alluaudinella flavicornis*. The morphological analysis covered the full range of its preimaginal stages, from eggs to third instar larvae. The material was collected in 2018 in Uyo (Nigeria) by Dr. Mfon Ekanem. Briefly, females of *A. flavicornis* were attracted to *Achatina* Lamarck snails as bait and collected using an entomological net. The obtained females were then brought to the laboratory to obtain larval material. After oviposition, some eggs were transferred directly to 70% ethanol, and subsequently larvae of adequate age were killed by immersion in boiling water and preserved in 70% ethanol (Adams & Hall, 2003). Phylogenetic analyses based on molecular data were performed using a total of 55 species representing all recently defined subfamilies of Muscidae (Grzywacz et al., 2021), including five species from the family Anthomyiidae as an outgroup. The material for molecular analysis was obtained from the collections of the Department of Ecology and Biogeography, NCU, Toruń, Poland. A complete list of all species used in the molecular analyses is available in Supplementary Material: Table S1, Article 1.

Article 2

In Article 2, the phylogenetic position of *Achanthiptera rohrelliformis*, *Potamia littoralis* and *Australophyra rostrata* was investigated based on larval morphology. To achieve this, a detailed morphological analysis of the larvae was provided, including the second and third instar larvae of *Ac. rohrelliformis*, the second and third instar larvae of *P. littoralis* and the third instar larvae of *Au. rostrata*. Larvae of *Ac*. *rohrelliformis* were obtained from the Natural History Museum (BMNH) in London (UK), the Natural History Museum of Denmark (NHMD), University of Copenhagen (Denmark) and the Museum für Naturkunde (ZMB), Leibniz Institute for Evolution and Biodiversity Science, Berlin (Germany). Some of the larvae posed a challenge, since they were over 100 years old and faded from overexposure to UV light. Larvae of *P. littoralis* were obtained by capturing adult female flies in Pławin (Poland) in 2013 by Dr. Andrzej Grzywacz and allowing them to oviposit in the laboratory. Larvae of *Au. rostrata* were collected during a police investigation from human cadaver in the Kuitpo Forest (South Australia) by Prof. James F. Wallman.

Article 3

Article 3 focused on muscid species for which early larval morphology was unknown or poorly described or insufficiently documented in the literature. The study also included species that had already been relatively well studied by LM and SEM

methods (i.e., *Atherigona orientalis* Schiner (Grzywacz & Pape, 2014) and *Synthesiomyia nudiseta* (Wulp) (Velásquez et al., 2013)), but the use of CLSM in this study provided new morphological data and more detailed microscopic documentation of the cephaloskeleton. The following species were included in the analyses: *A. orientalis*, *Hydrotaea aenescens* (Wiedemann), *Hydrotaea armipes* (Fallén), *Hydrotaea capensis* (Wiedemann), *Hydrotaea dentipes* (Fabricius), *Hydrotaea ignava* (Harris), *Hydrotaea pilipes* Stein, *Hydrotaea similis* Meade, *Musca domestica*, *Muscina levida* (Harris), *Muscina prolapsa* (Harris), *Muscina stabulans* Fallén, *St. calcitrans* and *Sy. nudiseta*. The larval material was obtained from the collections of the Department of Ecology and Biogeography, NCU, Toruń, Poland. Detailed protocols for material collection and laboratory rearing have been described in previous works (Grzywacz, 2013; Grzywacz et al., 2015; Grzywacz, Lindström, et al., 2014; Grzywacz & Pape, 2014; Velásquez et al., 2013), with the exception of *St. calcitrans*. Larvae of *St. calcitrans* were collected in Pławin (Poland) in 2010 by Dr. Andrzej Grzywacz and preserved in 70% ethanol.

Article 4

Article 4 focuses on the phylogenetic analysis of the genus *Lispe*. Molecular analyses were performed on 49 species representing all currently recognised and/or revised species groups (Gao et al., 2022; Hennig, 1960; Snyder, 1954; N. Vikhrev, 2011; N. E. Vikhrev, 2021; N. E. Vikhrev et al., 2016; N. E. Vikhrev, 2011, 2012c, 2012b, 2012a, 2014, 2015, 2016, 2020). The material included taxa from Afrotropical, Australasian, Nearctic and Palaearctic regions. All species were collected successively since 2008 and pinned or preserved in ethanol. Additionally, four species of the genus *Limnophora* were included in the analysis as an outgroup. The full list of species and metadata with information on collection location and source can be found in Supplementary Material: Table S2, Article 4. Due to the need to obtain DNA with the least degree of degradation, samples intended for genome sequencing were collected just before the initiation of molecular studies. Thus, specimens of *Lispe tentaculata* were collected in Toruń (Poland) (53º00′14.4″N; 18º36′19.2″E) in June 2021 by Dr. Andrzej Grzywacz. Adults were placed in a freezer for a few minutes for immobilisation and subject to further steps.

3.2 Methods

3.2.1 Morphological analyses

The larvae intended for morphological studies were examined using a combination of different types of microscopy: LM, CLSM, SEM (Article 1, Article 3) and CLSM, SEM (Article 2). The application of this approach allows to obtain comprehensive and detailed documentation including all relevant morphological structures. In the present study, CLSM was widely used to visualise muscid larvae because light microscopy turned out to be insufficient for cephaloskeleton analysis. Optical limitations of LM such as problems of resolution, illumination and depth of field, prevented precise visualisation of the edges of small sclerites and their interactions (Grzywacz et al., 2014). The use of innovative microscopy techniques, that is CLSM, effectively overcomes these limitations. Confocal microscopy is particularly desirable for visualising fine, complex, autofluorescent structures of larvae (Grzywacz et al., 2014). Its use guarantees high resolution as well as high-fidelity imaging and 3D reconstruction providing detailed information on examined structures (Szpila et al., 2021).

Due to the reproducibility of the microscopy methods used (LM, CLSM, SEM), the description of the procedures in the following subsections is presented in a general manner. Detailed parameters of the morphological analysis, such as maceration time in 10% KOH or the excitation wavelength used in CLSM, are presented in Articles 1–3.

3.2.1.1 Light microscopy

For light microscopy examination, the whole larvae were mounted in Hoyer's medium (chloral hydrate ($Cl_3CCH(OH)_2$) : gum arabic : glycerol : distilled water = 20 : 3 : 2 : 5) prepared according to Cielecka et al. (2009). The prepared microscope slides were examined and photographed using a M205C Leica Stereomicroscope (Leica Microsystems, Wetzlar, Germany) equipped with an integrated high-resolution Leica DFC495 digital camera or a Nikon Eclipse E200 microscope with a Nikon 8400 digital camera (Nikon Corp., Tokyo, Japan).

3.2.1.2 Confocal laser scanning microscopy

The preparation and acquisition steps for CLSM examination were conducted in accordance with the protocol provided by Walczak et al. (2022). Firstly, effective visualisation of the cephaloskeleton requires maceration of the soft tissues. To achieve

this, whole specimens of first-instar larvae were used, while in the case of second- and third-instar larvae, the anterior part of the body was cut off and then transferred to a 10% KOH solution. Maceration time was controlled by regularly assessing the degree of tissue maceration. It varied depending on the developmental stage and larval size, with durations of 20–24 hours for first-instar larvae, 24–36 hours for second-instar larvae and 24–72 hours for third-instar larvae. After this step, the larvae were transferred to freshly prepared 80% EtOH for 15 minutes to dehydrate and rinse away any residual KOH. Each specimen was then placed in a drop of glycerine or Euparal on a microscopic slide and covered with a coverslip. Since acquisition times varied from 1 to 4 hours, this led to excessive heating of the glycerine and its hydration, resulting in coverslip displacement and loss of image quality. To prevent this, the edges of the coverslip were secured with quick-drying glue.

Prepared slides were scanned using a Leica TCS SP8 Confocal Laser Scanning Microscope (Leica Microsystems, Wetzlar, Germany), using various combinations of excitation wavelengths (488 nm, 561 nm, 633 nm) in sequential scanning mode. The specimens were examined under a 40× or 63× oil immersion objective with a N.A. of 1.3 or 1.4, respectively. Effective 3D visualisation requires collecting more data than necessary to obtain acceptable 2D images, and differences in larval thickness necessitated optimisation of the number of frames collected for each sample (Grzywacz et al., 2014). The Z-axis step size was defined individually and manually for each specimen. After acquisition, all individual images were assembled to generate MIP using *LAS AF* V3.3 software and 3D visualisations were created using *LAS X 3D Viewer*.

3.2.1.3 Scanning electron microscopy

Preparation for SEM analyses included dehydration of specimens at 80.0%, 90.0% and 99.5% EtOH, followed by critical point drying in carbon dioxide (CO_2) with an Autosamdri®-815, Series A critical point dryer (Tousimis Research Corp., Rockville, MD, U.S.A.). Afterwards larvae were mounted on aluminium stubs using double-sided adhesive tape and sputter coated with gold for 210 s or platinum for 140 s (30 nm or 20 nm of coating, respectively) using a JEOL JFC 2300HR high-resolution fine coater (JEOL Ltd, Tokyo, Japan). SEM images were taken with a JEOL scanning microscope (JSM-6335F; JEOL Ltd., Tokyo, Japan).

3.2.2 Molecular analyses

3.2.2.1 Multilocus Sanger sequencing

For molecular analysis using an mS-seq approach (Article 1), *de novo* obtained gene sequences as well as additional sequences retrieved from GenBank were used. The newly obtained sequences were generated by gDNA extraction, gene amplification, purification, Sanger sequencing, capillary electrophoresis and final assembly using *SeqMan II* v.4.0 (DNASTAR, Lasergene, Madison, WI, USA). The mS-seq alignment, including two mitochondrial protein-coding genes (*COI*, *cytB*) and two nuclear genes (*Ef-1α*, *CAD*), was analysed with ML using *RAxML* 8.2.6 (with the GTR + G + I model) and *GARLI* v.2.01 (using the best-fitting model of nucleotide substitution), and by BI using *MrBayes* v.3.2.6. *PartitionFinder* v.1.1.1 was used to select the best partitioning scheme according to the BIC. Branch support was assessed using 1000 nonparametric bootstrap replicates for ML and posterior probabilities for BI, and the convergence of the Bayesian analyses was verified in *TRACER* v.1.7. The phylogenetic tree was rooted using Anthomyiidae species.

3.2.2.2 Genome sequencing (ONT) and data processing

DNA was isolated from freshly collected *L. tentaculata* specimens, and the two extracts with the highest concentration and longest fragments (Qubit 3.0 evaluation and gel electrophoresis) were selected. The selected samples were purified using AMPure XP beads to remove short fragments and prepared for further steps. Due to the relatively low gDNA concentration, two libraries were prepared, one for each *L. tentaculata* individual, using the SQK-LSK110 kit (ONT) according to the manufacturer's protocol with some modifications (extended incubation times). The libraries were sequenced in four runs on two flow cells (SpotON Flow Cell Rev D (R.9.4.1; FLO-MIN106D)) using a MinION Mk1C device. ONT reads were basecalled in super-accuracy mode (*Guppy* v.5.0.7), adapter-cleaned (*PoreChop* v.0.2.4), filtered for length (>500 nucleotides) and quality (Q>10) (*NanoFilt*), and their quality was assessed using *NanoPack*. For genome assembly, five long-read assemblers were compared: *Raven*, *SMARTdenovo*, *wtdbg2*, *Canu* and *Flye*, using default parameters and adjusted to the genome size (~700 Mb). The quality and completeness of the assemblies were assessed using *BUSCO* v.5.2.1 and *Inspector* (number of contigs, total length, the longest contig, N50, QV). The most complete assembly with the highest QV was selected for further analysis.

3.2.2.3 RAD-seq

For each species, individually barcoded RAD-seq libraries were prepared with modifications including double DNA digestion with SbfI-HF restriction enzyme and selection of 300–500 bp fragments (Pippin Prep). The final library was sequenced on an Illumina HiSeq 2500 system (paired-end). Raw reads were quality controlled (*FastQC* v.0.11.9), cleaned from adapters and low-quality sequences (*Trimmomatic* v.0.36) and then analysed in *ipyrad* v.0.9.81. Two approaches of assembly were performed: (i) a *de novo* approach, with a wide range of clustering threshold values (CT 0.70–0.90, incremented by 0.01), and (ii) a reference-based approach, using the *L. tentaculata* genome obtained in this study. For each dataset, phylogenetic trees were constructed using the ML approach in *RAxML* v.8.2.12 with 100 bootstrap repetitions, selecting the optimal CT based on the highest average bootstrap support and the highest number of SNPs. For phylogenetic analysis, the maximum likelihood (*RAxML* v.8.2.6) was applied on four datasets: three *de novo* alignments and one reference-based alignment, using the GTR+G model. For RAD-seq data with CT = 0.74, the multispecies coalescent model in *BPP* v.4.0 was applied, analysing two sets of loci (11 693 retrieved from reference-based assembly and 9 540 retrieved from assembly under 0.74 CT) in four independent MCMC runs. The species tree topology from *RAxML* was used as a starting point, assuming priors for population size and the divergence time of the root between *Lispe* and *Limnophora* based on literature data (Haseyama et al., 2015).

4. Results and discussion

Article 1

The results of all analyses carried out in Article 1 provided full and detailed morphological descriptions of the egg and all three larval instars of *A. flavicornis*. New descriptions prepared on the basis of documentation obtained, covered both the cephaloskeleton and the external morphology of the larvae. Using microscopic images, detailed line drawings for each larval instar were created. Extensive morphological documentation with the use of LM, CLSM and SEM was also provided. The results were compared with published data of *Alluaudinella* and their relatives (*Aethiopomyia* and *Ochromusca*) (Ekanem, 2008; Paterson, 1959; Skidmore, 1985) and any differences were highlighted. The most important differences identified concern the accuracy and completeness of the documentation. This study visualised and described a larger number of sclerites than previously observed by means of light microscopy only, and also captured their structural details. For the eggs, differences in the shape and arrangement of surface structures that have not been adequately explained in the literature were described. Furthermore, more precise information regarding the details of the cephaloskeleton was presented, including, in particular, visualisation of the accessory stomatal sclerites, labial sclerites, the epistomal sclerite, parastomal bars and rami, as well as the spinulation pattern. As a result, a coherent and more complete understanding of the morphology of *A. flavicornis* eggs and larvae has been obtained, which significantly expands current knowledge and corrects previous fragmentary or erroneous interpretations (including misidentification of larval instars (Ekanem, 2008)).

Considering the current systematics of *Alluaudinella* and the state of its close relationship to *Dichaetomyia*, a comparative analysis of the larval morphology of these taxa was conducted, taking into account both the obtained results and published literature data on the biology and morphology of *Dichaetomyia*. Significant differences between these taxa were demonstrated, particularly in the cephaloskeleton, which is crucial for taxonomic diagnosis, as well as in the structure of the posterior spiracles and details of the spinulation pattern. In turn, the larval morphology of representatives of the Reinwardtiinae (i.e., *Muscina* Robineau-Desvoidy, *Passeromyia*, *Philornis*, *Synthesiomyia* Brauer & von Bergenstamm) shows significant similarity to the third larval instar of *Alluaudinella*. A summary of selected larval characters is presented in Table 2.

Table 2. Summary of certain larval characters of *Alluaudinella*, *Ochromusca* and *Aethiopomyia* compared to *Dichaetomyia* as a selected representative of Phaoniinae, and Reinwardtiinae. The data included in the table are based on this study and the available literature data (Paterson, 1959; Pont & Dear, 1976; Skidmore, 1985).

Larval characters	*Alluaudinella*, *Ochromusca, Aethiopomyia*	*Dichaetomyia*	Reinwardtiinae
larval biology	trimorphic saprophages	monomorphic obligatory carnivores	trimorphic saprophages, trimorphic facultative carnivores
mouthhooks	massive	slender	massive
dental sclerites fused with mouthhook	yes	yes	yes
posterior ribbon	absent	present	absent
basal sclerite	robust	elongated	robust
posterior spiracles	massive	small	massive
position of spiracular scar	median	median	median to dorsal
shape of respiratory slits	sinuate to curved	straight	curved to tortuous
arrangement of respiratory slits	radiate	subparallel to convergent	radiate
spinulation	strong	poor	strong to moderate
papillae on anal division	distinct	indistinguishable	distinct
sclerotization of hypopharynx	indistinct	distinct	indistinct
longitudinal ridges in hypopharynx	present	hardly visible to absent	present

Although analysis based on selected molecular markers obtained relatively low support, *Alluaudinella* was not found to be the sister taxon of either *Dichaetomyia* or other Phaoniinae, as would be expected from traditional classification. The systematic position of *Alluaudinella* was not unequivocally confirmed, however, phylogenetic analyses indicate that this genus may be a sister taxon to Reinwardtiinae + *Neomuscina* (BS_{GARLI} = 20%, $PP_{MrBayes}$ = 0.82) or is part of a clade *Alluaudinella-Cyrtoneuropsis-Atherigona* with a sister group relationship to Reinwardtiinae + *Neomuscina* (BS_{RAxML} = 27%).

The phylogenetic tree obtained in this study, based on molecular data, as well as details regarding the morphology of preimaginal stages, are inconsistent with the hypothesis that the genus *Alluaudinella* is a sister taxon to *Dichaetomyia* or even closely related to other members of the subfamily Phaoniinae. Considering the significant larval discrepancies between *Alluaudinella* and Phaoniinae and the strong resemblance of *Alluaudinella* larvae to Reinwardtiinae larvae (Table 2), the transfer of the clade *Alluaudinella–Aethiopomyia–Ochromusca* to the subfamily Reinwardtiinae is proposed.

Article 2

In Article 2 complete and detailed morphological descriptions of the second and third larval instars of *Ac. rohrelliformis* and *P. littoralis*, and the third larval instar of *Au. rostrata* were provided. The second instars of *Ac. rohrelliformis* and *P. littoralis* were visualised and described for the first time. The morphological descriptions presented in this work included both the cephaloskeleton and the external morphology of the larvae. Using microscopic images, detailed line drawings for larvae under study and morphological documentation using CLSM and SEM were provided. A thorough comparative analysis of the morphology of the analysed larvae and existing literature data confirmed the affiliation of the studied species to the subfamily Azeliinae, with particular similarity of the cephaloskeleton and anal division.

Even more importantly, this study revealed morphological details previously unnoticed and undescribed in Muscidae. The most distinctive feature is the presence in the second and third larval instars of *Ac. rohrelliformis* and *P. littoralis* of a dome-shaped anterior rod that closely attached to each mouthhook, enveloping their tips and constituting a kind of extension of them. This type of modification of the cephaloskeleton has not been documented so far, at least within the family Muscidae, and its function remains unclear. Another previously unreported morphological feature is the asymmetry of accessory oral sclerites, i.e., oral bars and anterior rods, particularly pronounced in *Ac. rohrelliformis*. Although asymmetry of the mouthhooks is known in Azeliinae (Grzywacz et al., 2021), such a strong and unambiguous asymmetry of the accessory oral sclerites has not been described before. In *P. littoralis*, the asymmetry is less pronounced, but this species possesses well-developed accessory sclerites, which distinguishes it from most muscids and indicates that previous interpretations, such as that of Skidmore (1985), who described the anterior rods and oral bars as “very slender, short, and weak”, did not reflect the true complexity of these structures, nor did discrepancies in the descriptions of related

species such as *Potamia scabra* (Giglio-Tos) (Calhoun et al., 1956). The study corrects these inconsistencies and shows that both the peculiar shape of anterior rods and the presence and degree of asymmetry of the accessory oral sclerites distinguish these species within the Muscidae.

Detailed morphological analysis and the visualisation of peculiar modifications of the cephaloskeleton allowed conclusions to be drawn regarding the feeding strategy of the studied species. Larvae of *Au. rostrata* remain classified as facultative predators. In contrast, in *Ac. rohrelliformis*, the pronounced asymmetry of the mouthhooks and the modified accessory oral sclerites indicate a saprophagous lifestyle, contradicting Skidmore's (1985) conclusion that *Achanthiptera* larvae are trimorphic facultative carnivores. Similarly, *P. littoralis* larvae, whose larval morphology is similar to that of *Ac. rohrelliformis*, indicate that they are saprophages, although this requires further verification from rearing experiments. It is worth noting that the feeding strategy of *Potamia* larvae has been previously debated. Skidmore (1985) considered them trimorphic facultative carnivores, while Séguy (1923) and Iwasa et al. (1995) suggested a saprophagous or coprophagous lifestyle, pointing out that larvae were found primarily in faecal matter and in nesting materials, rather than feeding on nestlings or their carrion.

Article 3

In Article 3, the early larval instars of 14 muscid species of documented and/or potential forensic importance (first and second instars of *A. orientalis*, *H. aenescens*, *H. capensis*, *H. dentipes*, *H. ignava*, *H. pilipes*, *H. similis*, *Mc. domestica*, *Mu. levida*, *Mu. prolapsa*, *Mu. stabulans*, *St. calcitrans* and *Sy. nudiseta*, and the second instar of *H. armipes*) were analysed. Detailed microscopic documentation (LM, CLSM and SEM) was provided and the first identification key enabling the identification of larvae of these species was developed. The study showed that precise identification of larvae is possible down to at least the genus level, and in many cases to the species level. The morphological features of the cephaloskeleton (i.e., its overall shape, size, sclerite position) were crucial, while external features can only serve a supporting role. In some cases (e.g., *St. calcitrans* or *A. orientalis*), relatively distinctive features allowed for easy identification, while in others, detailed evaluation of multiple morphological features was necessary. Morphological characters of early larval instars, particularly details of the cephaloskeleton, used for species discrimination purposes, did not allowed to draw conclusive statements on higher-level relationships. For example, various degrees of

mouthhooks reduction have been observed in second instars of *Hy. capensis*, *Mu. domestica* and *St. calcitrans*. On the other hand, remaining *Hydrotaea* and other Azeliinae (Walczak et al. 2024) representatives did not reveal such mouthhooks reduction, suggesting possible convergence. The use of first and second instar characters in Muscidae systematics is currently limited due to the lack of free-living larvae of these instars for many species, as Muscidae are characterised by a peculiar feature of a variable number of free-living larval instars (trimorphic, dimorphic and monomorphic larvae) (Skidmore, 1985). While the morphological features of early larval instars indicated in Article 3 are useful for distinguishing some species, their use in inferring higher-level relationships is currently limited. For example, incomplete mouthhooks have been found to have evolved independently in *Musca* Linnaeus, *Stomoxys* Linnaeus and some *Hydrotaea* and they are not informative in a phylogenetic context.

Nevertheless, the use of CLSM allowed for precise visualisation of sclerite connections and shapes, which were difficult or impossible to assess using classical light microscopy. However, the developed identification key can also be used using LM alone, and in doubtful cases, molecular methods are recommended. This study represents the first attempt to develop a tool for identifying early larval instars of Muscidae species of forensic importance. The results demonstrate the potential of combining LM and CLSM in the study of fly larval morphology and emphasise the need for further, in-depth analyses of early larval instars in other insect groups.

Article 4

In Article 4, the previously proposed division of the genus *Lispe* into species groups and the relationships between them and between species within these groups were examined. To do this, second-generation sequencing (RAD-seq) and third-generation sequencing (nanopore sequencing) were employed. The use of nanopore sequencing allowed the generation of long reads, which were later used for the assembly of the *L. tentaculata* genome using five assemblers. Of these, *Flye* appeared to be the most effective, with the highest completeness and quality, and the resulting genome sequence was selected for further analysis. Regarding the results of RAD-seq analysis, different clustering thresholds affected the alignment length, number of recovered loci, percentage of missing data, number of variable sites, percentage of parsimony-informative sites (PIS) and mean bootstrap for nodes. For subsequent phylogenetic analyses, alignments under 0.74, 0.75, and 0.85 CT were used, with 0.74 chosen as the superior due to the highest

number of SNPs and the strength of the phylogenetic signal. Analyses based on the multispecies coalescence model (BPP) yielded topologies largely consistent with ML trees, confirming the monophyly of most groups and highlighting the need for further investigation of problematic taxa and intergroup relationships.

Phylogenetic analyses, both *de novo* and reference-based with the newly obtained *L. tentaculata* genome confirmed the monophyly of the genus *Lispe* and revealed three major, well-supported (BS ≥ 90%) clades. In most species groups, the interrelationships were clearly defined, although for the *palposa*, *caesia* and *kowarzii* groups, they remained ambiguous. Results of this study are partially consistent with the earlier hypotheses of Gao et al. (2022), the only and first study to date using molecular data, but the relationships between species groups remain uncertain and require further investigation. In Article 4, 'Clade A' comprises the *palposa*-group, the *rigida*-group and the *caesia*-group; 'Clade B' consists of *L. albimaculata* Stein, the *nicobarensis*-group, the *nivalis*-group, the *scalaris*-group and the *tentaculata*-group; 'Clade C' is composed of the *longicollis*-group, the *desjardinsii*-group, the *uliginosa*-group and the *kowarzi*-group. Within Clade A, the close relationship of the *palposa* and *rigida* groups was confirmed (Vikhrev, 2015), and an expansion of the *caesia*-group to include *L. polonaise* Vikhrev, as well as *L. cana* (Walker) and its relatives was proposed. In Clade B, results of this study support Gao et al. (2022) proposal to expand the *tentaculata*-group to include the *nana*-group and *L. mirabilis* Stein, and suggest the need to include *L. capensis* Zielke. Furthermore, the previous conclusion that the *tentaculata* supergroup includes species from the *nivalis*-, *scalaris*- and extended *tentaculata*-groups was supported, while also proposing the inclusion of the *nicobarensis*-group. In Clade C, the valid *desjardinsii*-group was maintained, contrary to the proposal to include it in the *longicollis*-group, and the expansion of the *kowarzi*-group to include the *dichaeta* and *geniseta* complexes was confirmed. The position of *L. pumila* Wiedemann, *L. pygmaea* (Fallén) and the *leucospila*-group remains uncertain and varies depending on the analysis method used, indicating the need for further analysis and greater sampling. As explained, larvae were not used in this study due to the lack of complete literature data and the unavailability of larval material for analysis.

In summary, results of this dissertation (Articles 1–3) clearly demonstrate the value of modern microscopic techniques in the morphological analysis of flies, enabling the identification of larval structures previously difficult to capture using classical light

microscopy. For the genus *Lispe*, for which larval morphology was not considered, although RAD-seq analysis ultimately yielded incomplete and unambiguous results (Article 4), it was feasible to deepen our understanding of the relationships between species groups. By applying various approaches to phylogenetic inference, including analyses of larval morphology and molecular data, a more complete and in-depth understanding of the phylogenetic relationships within the family Muscidae was achieved. Particularly, the use of CLSM enabled detailed examination of sclerites, including accessory sclerites, epistomal sclerites, labial sclerites and rami, which were often omitted or misinterpreted in previous descriptions due to the resolution limitations of light microscopy. What is also of key importance, in the third larval instars of *A. flavicornis*, *Ac. rohrelliformis*, *P. littoralis*, and *Au. rostrata*, we were able to visualise a pair of parastomal bars, similar to those previously observed in *Passeromyia* (Walczak et al., 2022). The parastomal bars in some muscid species are clearly visible on the dorsal edge of the intermediate sclerite, as confirmed by the frame-by-frame analysis of CLSM stack images. This finding is highly important because the absence of parastomal bars was previously considered the single larval synapomorphy for Muscidae (Ferrar, 1979; Roback, 1951; Skidmore, 1985). The visualisation of the presence of both parastomal bars and rami in muscid species, for the first time, significantly expands our knowledge of the morphology of the larvae of this family, revealing features that require verification in the light of previous descriptions. The results presented in this paper highlight the importance of integrating diverse approaches, both morphological and molecular, in a comprehensive study of dipteran systematics and evolution. This work, in particular, demonstrates that modern microscopic techniques not only allow for the verification of previous observations but also open up new perspectives in morphological analysis, revealing previously overlooked features that may have significant phylogenetic and taxonomic significance.

5. References

Adams, Z. J. O., & Hall, M. J. R. (2003). Methods used for the killing and preservation of blowfly larvae, and their effect on post-mortem larval length. *Forensic Science International*, *138*(1–3), 50–61. https://doi.org/10.1016/j.forsciint.2003.08.010

Brooker, A. J., Shinn, A. P., & Bron, J. E. (2012). Use of laser scanning confocal microscopy for morphological taxonomy and the potential for digital type specimens (e-types). *Aquatic Biology*, *14*(2), 165–173. https://doi.org/10.3354/ab00389

Buenaventura, E., Lloyd, M. W., Perilla López, J. M., González, V. L., Thomas-Cabianca, A., & Dikow, T. (2021). Protein-encoding ultraconserved elements provide a new phylogenomic perspective of Oestroidea flies (Diptera: Calyptratae). *Systematic Entomology*, *46*(1), 5–27. https://doi.org/10.1111/syen.12443

Byrd, J. H., & Castner, J. L. (2010). Insects of forensic importance. In J. H. Byrd & J. L. Castner (Eds.), *Forensic entomology: the utility of arthropods in legal investigations* (pp. 39–126). CRC Press, Boca Raton.

Calhoun, E. L., Dodge, H. R., & Fay, R. W. (1956). Description and rearing of various stages of *Dendrophaonia scabra* (Giglio-Tos) (Diptera, Muscidae). *Annals of the Entomological Society of America*, *49*(1), 49–54. https://doi.org/10.1093/aesa/49.1.49

Cerretti, P., Stireman, J. O., Badano, D., Gisondi, S., Rognes, K., Giudice, G. Lo, & Pape, T. (2019). Reclustering the cluster flies (Diptera: Oestroidea, Polleniidae). *Systematic Entomology*, *44*(4), 957–972. https://doi.org/10.1111/syen.12369

Cielecka, D., Salamatin, R., & Garbacewicz, A. (2009). Usage of Hoyer's medium for diagnostic and morphological studies of some parasites. [in Polish with English abstract]. *Wiadomości Parazytologiczne*, *55*, 265–270.

Cohen, C. M., Noble, K., Jeffrey Cole, T., & Brewer, M. S. (2021). The phylogeny of robber flies (Asilidae) inferred from ultraconserved elements. *Systematic Entomology*, *46*(4), 812–826. https://doi.org/10.1111/syen.12490

Couri, M. S., & Carvalho, C. J. B. de. (2003). Systematic relations among *Philornis* Meinert, *Passeromyia* Rodhain & Villeneuve and allied genera (Diptera, Muscidae). *Brazilian Journal of Biology*, *63*(2), 223–232. https://doi.org/10.1590/S1519-69842003000200007

Couri, M. S., & de Carvalho, C. J. B. (2013). A new genus and species of Coenosiini from Costa Rica (Diptera, Muscidae, Coenosiinae). *ZooKeys*, *321*, 25–33. https://doi.org/10.3897/zookeys.321.5443

Couri, M. S., & Pont, A. C. (2000). Cladistic analysis of Coenosiini (Diptera: Muscidae: Coenosiinae). *Systematic Entomology*, *25*(3), 373–392. https://doi.org/10.1046/j.1365-3113.2000.00125.x

Couri, M. S., & Salas, C. (2010). First record of *Coenosia attenuata* Stein (Diptera, Muscidae) from Chile, with biological notes. *Revista Brasileira de Entomologia*, *54*(1), 144–145. https://doi.org/10.1590/s0085-56262010000100020

d'Assis Fonseca, E. C. M. (1968). Diptera Cyclorrhapha Calyptrata Section (b) Muscidae. *Handbooks for the Identification of British Insects.*, *10*, 1–118.

Ekanem, M. S. (2008). Immature stages and developmental biology of two muscid flies (Cyclorrhapha: Diptera) which breed in carrion in Southern Nigeria. *Zoologist (The)*, *6*(1), 1–6.

Ferrar, P. (1979). The immature stages of dung-breeding muscoid flies in Australia, with notes on the species, and keys to larvae and puparia. *Australian Journal of Zoology, Supplementary Series*, *73*, 1–106.

Gao, Y., Ge, Y., Yan, L., Vikhrev, N. E., Wang, Q., Butterworth, N. J., & Zhang, D. (2022). Phylogenetic Analyses Support the Monophyly of the Genus *Lispe* Latreille (Diptera: Muscidae) with Insights into Intrageneric Relationships. *Insects*, *13*(11), 1015. https://doi.org/10.3390/insects13111015

Ge, Y., Gao, Y., Yan, L., Liu, X., & Zhang, D. (2016). Review of the *Lispe tentaculata*-group (Diptera: Muscidae) in China, with one new synonym. *Zoosystema*, *38*(3), 339–352. https://doi.org/10.5252/z2016n3a4

Grzywacz, A. (2013). Review and comparative analysis of the morphology of third instar larvae of European and Mediterranean Muscidae (Diptera) of forensic importance. *Nicolaus Copernicus University*, 1–157.

Grzywacz, A., Góral, T., Szpila, K., & Hall, M. J. R. (2014). Confocal laser scanning microscopy as a valuable tool in Diptera larval morphology studies. *Parasitology Research*, *113*(11), 4297–4302. https://doi.org/10.1007/s00436-014-4125-0

Grzywacz, A., Hall, M. J. R., & Pape, T. (2015). Morphology successfully separates third instar larvae of *Muscina*. *Medical and Veterinary Entomology*, *29*(3), 314–329. https://doi.org/10.1111/mve.12117

Grzywacz, A., Lindström, A., & Hall, M. J. R. (2014). *Hydrotaea similis* Meade (Diptera: Muscidae) newly reported from a human cadaver: A case report and larval morphology. *Forensic Science International*, *242*, e34–e43. https://doi.org/10.1016/j.forsciint.2014.07.014

Grzywacz, A., & Pape, T. (2014). Larval morphology of *Atherigona orientalis* (Schiner) (Diptera: Muscidae) - A species of sanitary and forensic importance. *Acta Tropica*, *137*, 174–184. https://doi.org/10.1016/j.actatropica.2014.05.018

Grzywacz, A., Trzeciak, P., Wiegmann, B. M., Cassel, B. K., Pape, T., Walczak, K., Bystrowski, C., Nelson, L., & Piwczyński, M. (2021). Towards a new classification of Muscidae (Diptera): a comparison of hypotheses based on multiple molecular phylogenetic approaches. *Systematic Entomology*, *46*(3), 508–525. https://doi.org/10.1111/syen.12473

Grzywacz, A., Wallman, J. F., & Piwczyński, M. (2017). To be or not to be a valid genus: the systematic position of *Ophyra* R.-D. revised (Diptera: Muscidae). *Systematic Entomology*, *42*(4), 714–723. https://doi.org/10.1111/syen.12240

Hajibabaei, M., DeWaard, J. R., Ivanova, N. V., Ratnasingham, S., Dooh, R. T., Kirk, S. L., Mackie, P. M., & Hebert, P. D. N. (2005). Critical factors for assembling a high volume of DNA barcodes. *Philosophical Transactions of the Royal Society B: Biological Sciences*, *360*(1462), 1959–1967. https://doi.org/10.1098/rstb.2005.1727

Haseyama, K. L. F., Wiegmann, B. M., Almeida, E. A. B., & de Carvalho, C. J. B.

(2015). Say goodbye to tribes in the new house fly classification: A new molecular phylogenetic analysis and an updated biogeographical narrative for the Muscidae (Diptera). *Molecular Phylogenetics and Evolution*, *89*, 1–12. https://doi.org/10.1016/j.ympev.2015.04.006

Hennig, W. (1955). Family Muscidae. In: E. Lindner (Ed.), *Die Fliegen der Paläarktischen Region*, 63b. Schweizerbart'sche Verlagsbuchhandlung, Stuttgart, pp. 625–672.

Hennig, W. (1960). Muscidae (Lieferung 209). In: E. Lindner (Ed.), *Die Fliegen der Palaearktischen Region*. Schweizerbart'sche Verlagsbuchhandlung, Stuttgart, pp. 399–432.

Hennig, W. (1965). Vorarbeiten zu einem phylogenetischen System der Muscidae (Diptera: Cyclorrhapha). *Stuttgarter Beiträge Zur Naturkunde*, *141*, 1–100.

Herting, B. (1957). Das weibliche Postabdomen der calyptraten Fliegen (Diptera) und sein Merkmalswert für die Systematik der Gruppe. *Zeitschrift Für Morphologie Und Ökologie Der Tiere*, *45*(5), 429–461.

Iwasa, M., Hori, K., & Aoki, N. (1995). Fly fauna of bird nests in Hokkaido, Japan (Diptera). *The Canadian Entomologist*, *127*(5), 613–621.

Karl, O. (1928). Zweiflügler oder Diptera. II: Muscidae. In *Die Tierwelt Deutschlands und der angrenzenden Meeresteile nach ihren Merkmalen und nach ihrer Lebensweise* (pp. 1–232).

Kutty, S. N., Pape, T., Pont, A. C., Wiegmann, B. M., & Meier, R. (2008). The Muscoidea (Diptera: Calyptratae) are paraphyletic: Evidence from four mitochondrial and four nuclear genes. *Molecular Phylogenetics and Evolution*, *49*(2), 639–652. https://doi.org/10.1016/j.ympev.2008.08.012

Kutty, S. N., Pape, T., Wiegmann, B. M., & Meier, R. (2010). Molecular phylogeny of the Calyptratae (Diptera: Cyclorrhapha) with an emphasis on the superfamily Oestroidea and the position of Mystacinobiidae and McAlpine's fly. *Systematic Entomology*, *35*(4), 614–635. https://doi.org/10.1111/j.1365-3113.2010.00536.x

Kutty, S. N., Pont, A. C., Meier, R., & Pape, T. (2014). Complete tribal sampling reveals basal split in Muscidae (Diptera), confirms saprophagy as ancestral feeding mode, and reveals an evolutionary correlation between instar numbers and carnivory. *Molecular Phylogenetics and Evolution*, *78*(1), 349–364. https://doi.org/10.1016/j.ympev.2014.05.027

Lee, S., Brown, R. L., & Monroe, W. (2009). Use of confocal laser scanning microscopy in systematics of insects with a comparison of fluorescence from different stains. *Systematic Entomology*, *34*(1), 10–14. https://doi.org/10.1111/j.1365-3113.2008.00451.x

Malloch, J. R. (1925). XLVII. - Exotic Muscaridæ (Diptera).—XVII. *Annals and Magazine of Natural History*, *16*(94), 361–377. https://doi.org/10.1080/00222932508633323

Marinho, M. A. T., Wolff, M., Ramos-Pastrana, Y., de Azeredo-Espin, A. M. L., & Amorim, D. de S. (2017). The first phylogenetic study of Mesembrinellidae (Diptera: Oestroidea) based on molecular data: clades and congruence with

morphological characters. *Cladistics*, *33*(2), 134–152. https://doi.org/10.1111/cla.12157

Meier, R., & Lim, G. S. (2009). Conflict, convergent evolution, and the relative importance of immature and adult characters in Endopterygote phylogenetics. *Annual Review of Entomology*, *54*, 85–104. https://doi.org/10.1146/annurev.ento.54.110807.090459

Michelsen, V. (1991). Revision of the aberrant New World genus *Coenosopsia* with a discussion of anthomyiid relationships. *Systematic Entomology*, *16*, 85–104.

Moura, M. O., de Carvalho, C. J. B., & Monteiro-Filho, E. L. (1998). Carrion attendant arthropods in southern Brazil. *Ciência e Cultura*, *50*, 377–381.

Narayanan Kutty, S., Meusemann, K., Bayless, K. M., Marinho, M. A. T., Pont, A. C., Zhou, X., Misof, B., Wiegmann, B. M., Yeates, D., Cerretti, P., Meier, R., & Pape, T. (2019). Phylogenomic analysis of Calyptratae: resolving the phylogenetic relationships within a major radiation of Diptera. *Cladistics*, *35*(6), 605–622. https://doi.org/10.1111/cla.12375

Nihei, S. S., & De Carvalho, C. J. B. (2007). Phylogeny and classification of Muscini (Diptera, Muscidae). *Zoological Journal of the Linnean Society*, *149*(4), 493–532. https://doi.org/10.1111/j.1096-3642.2007.00252.x

Paterson, H. E. (1959). Notes on the genus *Alluaudinella* G.-T. with the description of a new species and a key to the known species of the genus (Diptera: Muscidae). *Memoires de l'Institut Scientifique de Madagascar*, *11*, 355–367.

Pont, A. C. (1980). Family Muscidae. In R. W. Crosskey (Ed.), *Catalogue of the Diptera of the Afrotropical region* (pp. 719–761). British Museum (Natural History), London.

Pont, A. C., & Dear, J. P. (1976). A synopsis of the genus *Ochromusca* Malloch, 1927 (Diptera: Muscidae). *Annals of the Natal Museum*, *22*(3), 747–753.

Roback, S. S. (1951). A classification of the muscoid Calyptrate, Diptera. *Annals of the Entomological Society of America*, *44*, 327–361.

San Jose, M., Doorenweerd, C., Leblanc, L., Barr, N., Geib, S., & Rubinoff, D. (2018). Incongruence between molecules and morphology: A seven-gene phylogeny of Dacini fruit flies paves the way for reclassification (Diptera: Tephritidae). *Molecular Phylogenetics and Evolution*, *121*(October 2017), 139–149. https://doi.org/10.1016/j.ympev.2017.12.001

Savage, J., & Wheeler, T. A. (2004). Phylogeny of the Azeliini (Diptera: Muscidae). *Studia Dipterologica*, *11*(1), 259–300.

Schuehli, G. S. E., de Carvalho, C. J. B., & Wiegmann, B. M. (2007). Molecular phylogenetics of the Muscidae (Diptera : Calyptratae): new ideas in a congruence context. *Invertebrate Systematics*, *21*(3), 263–278. https://doi.org/10.1071/is06026

Séguy, E. (1923). Dipteres Anthomyides. *Faune de France*, *3*, 306–307.

Séguy, E. (1937). Diptera, family Muscidae. In: P. Wytsmann (ed.). In *Genera Insectorum* (Vol. 205, pp. 1-604 Bruxelles, Desmet-Verteneuil).

Skidmore, P. (1985). The biology of the Muscidae of the World. *Series Entomologica*,

29, 1–550.

Snyder, F. M. (1954). A review of Nearctic *Lispe* Latreille (Diptera, Muscidae). *The American Museum of Natural History*, *1675*, 1–40.

Stireman, J. O., Cerretti, P., O'Hara, J. E., Blaschke, J. D., & Moulton, J. K. (2019). Molecular phylogeny and evolution of world Tachinidae (Diptera). *Molecular Phylogenetics and Evolution*, *139*(September 2018), 106358. https://doi.org/10.1016/j.ympev.2018.12.002

Szpila, K., Walczak, K., Johnston, N. P., Pape, T., & Wallman, J. F. (2021). First instar larvae of endemic Australian Miltogramminae (Diptera: Sarcophagidae). *Scientific Reports*, *11*(1), 1–12. https://doi.org/10.1038/s41598-020-80139-x

Tiusanen, M., Hebert, P. D. N., Schmidt, N. M., & Roslin, T. (2016). One fly to rule them all – Muscid flies are the key pollinators in the arctic. *Proceedings of the Royal Society B: Biological Sciences*, *283*(1839). https://doi.org/10.1098/rspb.2016.1271

van Emden, F. I. (1939). Muscidae: Muscinae and Stomoxydinae. *Ruwenzori Expedition 1934-5*, *II*(3), 49–89.

van Emden, F. I. (1951). Muscidae: C – Scatophaginae, Anthomyiinae, Lispinae, Fanniinae and Phaoninae. *Ruwenzori Expedition 1934–5*, *2*, 325–710.

Velásquez, Y., Ivorra, T., Grzywacz, A., Martínez-Sánchez, A., Magaña, C., García-Rojo, A., & Rojo, S. (2013). Larval morphology, development and forensic importance of *Synthesiomyia nudiseta* (Diptera: Muscidae) in Europe: a rare species or just overlooked? *Bulletin of Entomological Research*, *103*(1), 98–110. https://doi.org/10.1017/S0007485312000491

Vikhrev, N. (2011). Review of the Palaearctic members of the *Lispe tentaculata* species-group (Diptera, Muscidae): Revised key, synonymy and notes on ecology. *ZooKeys*, *84*, 59–70. https://doi.org/10.3897/zookeys.84.819

Vikhrev, N. E. (2011). Taxonomic notes on the *Lispe leucospila* species-group (Diptera: Muscidae). *Russian Entomological Journal*, *20*(1), 215–218. https://doi.org/10.15298/rusentj.20.2.14

Vikhrev, N. E. (2012a). Four new species of *Lispe* Latreille, 1796 (Diptera: Muscidae) with taxonomic notes on related species. *Russian Entomological Journal*, *21*(4), 423–433. https://doi.org/10.15298/rusentj.21.4.08

Vikhrev, N. E. (2012b). Notes on taxonomy of *Lispe* Latreille (Diptera: Muscidae). *Russian Entomological Journal*, *21*(1), 107–112. https://doi.org/10.15298/rusentj.21.1.14

Vikhrev, N. E. (2012c). Revision of the *Lispe longicollis*-group (Diptera, Muscidae). *ZooKeys*, *235*, 23–39. https://doi.org/10.3897/zookeys.235.3306

Vikhrev, N. E. (2014). Taxonomic notes on *Lispe* (Diptera, Muscidae), Parts 1-9. *Amurian Zoological Journal*, *VI*(2), 147–170.

Vikhrev, N. E. (2015). Taxonomic notes on *Lispe* (Diptera, Muscidae), Parts 10-12. *Amurian Zoological Journal*, *7*, 228–247.

Vikhrev, N. E. (2016). Taxonomic notes on *Lispe* (Diptera, Muscidae), Part 13.

Amurian Zoological Journal, *VIII*(3), 171–185.

Vikhrev, N. E. (2020). *Lispe* (Diptera, Muscidae) of the Palaearctic region. In *Amurian Zoological Journal* (Vol. 12, Issue 2). https://doi.org/10.33910/2686-9519-2020-12-2-158-188

Vikhrev, N. E. (2021). *Lispe* (Diptera, Muscidae) of Africa. In *Amurian Zoological Journal* (Vol. 13, Issue 3). https://doi.org/10.33910/2686-9519-2021-13-3-369-400

Vikhrev, N. E., Ge, Y. Q., & Zhang, D. (2016). On taxonomy of the *Lispe caesia*-group (Diptera: Muscidae). *Russian Entomological Journal*, *25*(4), 407–410. https://doi.org/10.15298/rusentj.25.4.10

Walczak, K., Szpila, K., Nelson, L., Pape, T., Hall, M. J. R., Alves, F., & Grzywacz, A. (2022). Larval morphology of the avian parasitic genus *Passeromyia*: playing hide and seek with a parastomal bar. *Medical and Veterinary Entomology*, *March*, 1–13. https://doi.org/10.1111/mve.12603

Winkler, I. S., Kirk-Spriggs, A. H., Bayless, K. M., Soghigian, J., Meier, R., Pape, T., Yeates, D. K., Carvalho, A. B., Copeland, R. S., & Wiegmann, B. M. (2022). Phylogenetic resolution of the fly superfamily Ephydroidea–Molecular systematics of the enigmatic and diverse relatives of Drosophilidae. *PLoS ONE*, *17*(10 October), 1–20. https://doi.org/10.1371/journal.pone.0274292

Yan, L., Pape, T., Meusemann, K., Kutty, S. N., Meier, R., Bayless, K. M., & Zhang, D. (2021). Monophyletic blowflies revealed by phylogenomics. *BMC Biology*, *19*(1), 1–14. https://doi.org/10.1186/s12915-021-01156-4

Yeo, D., Srivathsan, A., & Meier, R. (2020). Longer is not always better: Optimizing barcode length for large-scale species discovery and identification. *Systematic Biology*, *69*(5), 999–1015. https://doi.org/10.1093/sysbio/syaa014

Young, A. D., Lemmon, A. R., Skevington, J. H., Mengual, X., Ståhls, G., Reemer, M., Jordaens, K., Kelso, S., Lemmon, E. M., Hauser, M., De Meyer, M., Misof, B., & Wiegmann, B. M. (2016). Anchored enrichment dataset for true flies (order Diptera) reveals insights into the phylogeny of flower flies (family Syrphidae). *BMC Evolutionary Biology*, *16*(1), 1–13. https://doi.org/10.1186/s12862-016-0714-0

6. Attachments

Article 1

Walczak, K., Pape, T., Ekanem, M., Szpila, K., & Grzywacz, A. (2023). Insights into the systematics of *Alluaudinella* and allied *Aethiopomyia* and *Ochromusca* (Muscidae, Diptera). Zoologica Scripta, 52(3), 279–297.

https://doi.org/10.1111/zsc.12584

Received: 7 December 2022 | Revised: 25 January 2023 | Accepted: 30 January 2023

DOI: 10.1111/zsc.12584

Zoologica Scripta | WILEY

ORIGINAL ARTICLE

Insights into the systematics of *Alluaudinella* and allied *Aethiopomyia* and *Ochromusca* (Muscidae, Diptera)

Kinga Walczak[1,2] | **Thomas Pape**[3] | **Mfon Ekanem**[4] | **Krzysztof Szpila**[1] | **Andrzej Grzywacz**[1,2]

[1]Department of Ecology and Biogeography, Nicolaus Copernicus University in Toruń, Toruń, Poland

[2]Centre for Modern Interdisciplinary Technologies, Nicolaus Copernicus University in Toruń, Toruń, Poland

[3]Natural History Museum of Denmark, University of Copenhagen, Copenhagen, Denmark

[4]Department of Zoology, University of Uyo, Uyo, Nigeria

Correspondence
Kinga Walczak and Andrzej Grzywacz, Department of Ecology and Biogeography, Nicolaus Copernicus University in Toruń, Lwowska 1, Toruń 87-100, Poland.
Email: walczak.kinga00@gmail.com and hydrotaea@gmail.com

Funding information
National Science Centre of Poland, Grant/Award Number: 2019/33/B/NZ8/02316

Abstract

The muscid genera *Alluaudinella* Giglio-Tos, 1895, *Aethiopomyia* Malloch, 1921 and *Ochromusca* Malloch, 1927 form a monophyletic group supported by immature and adult morphology and a highly specialised snail-feeding strategy of immature stages. In contrast to the undoubted monophyly of the *Alluaudinella-Aethiopomyia-Ochromusca* clade, previous studies have provided contradictory hypotheses of the subfamiliar position within the Muscidae, and these three genera have been placed in the subfamily Muscinae, Dichaetomyiinae, Phaoniinae and Reinwardtiinae. The systematic position of *Alluaudinella*, as a representative of *Alluaudinella*, *Aethiopomyia* and *Ochromusca* group, is revised by means of larval morphology, biology and molecular data. Light microscopy (LM), confocal laser scanning microscopy (CLSM) and scanning electron microscopy (SEM) are used to study the egg and all larval instars of *Alluaudinella flavicornis* (Macquart, 1855) and a multilocus Sanger sequencing (mS-seq) approach to examine position within Muscidae. Results are inconsistent with the traditional, morphology-based concept of the *Alluaudinella-Aethiopomyia-Ochromusca* clade as closely related to *Dichaetomyia* Malloch, 1921, and the phylogenetic analysis revealed no support for inclusion within subfamily Phaoniinae. Larval morphology in *Alluaudinella* differs significantly from that of *Dichaetomyia* (and other Phaoniinae), but resembles that of genera nested in Reinwardtiinae. Based on molecular data and larval morphology a transfer of *Alluaudinella*, *Aethiopomyia* and *Ochromusca* to the subfamily Reinwardtiinae is proposed.

KEYWORDS

confocal laser scanning microscopy, light microscopy, molecular phylogeny, scanning electron microscopy

1 | INTRODUCTION

Alluaudinella Giglio-Tos, 1895 is a small muscid genus, including seven species widespread in the continental part of the Afrotropical region (Paterson, 1959; Pont, 1980). *Alluaudinella bivittata* Macquart, 1843 has also been reported from Mauritius, Madagascar, Réunion and Seychelles, whereas *A. stuckenbergi* Paterson, 1960 is endemic to Madagascar (Couri & de Sousa, 2020). Species of *Alluaudinella* are moderate to large, yellow or yellowish-brown flies (Paterson, 1959). Adults of *A. bivittata* have been reported on human faeces in scrubland or forests (Couri et al., 2006), but knowledge of adult life history is otherwise scarce. Larvae of *Alluaudinella* are

trimorphic saprophages and are known to feed on dying or dead snails, mostly of the genus *Achatina* Lamarck, 1799 (Paterson, 1959; Skidmore, 1985). Any attempts to induce females of *A. bivittata* to oviposit on living snails were unsuccessful (Paterson, 1959). *Alluaudinella flavicornis* (Macquart, 1855) has been considered as a species of forensic importance due to its breeding in animal carrion, and successful larval development has been obtained on decaying beef meat (Ekanem, 2008). Based on their shared, highly specialised larval life history related to feeding on snails, Paterson (1959) and Hennig (1965) suggested that *Alluaudinella*, *Aethiopomyia* Malloch, 1921 and *Ochromusca* Malloch, 1927 form a monophyletic group. *Aethiopomyia* is represented by five species (de Sousa et al., 2020), *Ochromusca* by two species (Pont & Dear, 1976), and both genera are also confined to the Afrotropical region. This concept was supported by Couri and de Carvalho (2003), who documented that adults of *Alluaudinella*, *Aethiopomyia* and *Ochromusca* share 'remarkably short stubby spines on the upper side of the palpi'. In contrast to their undoubted close relationship, the systematic position of these three genera within the family Muscidae has seen several changes over the years and is still unclear. The classifications proposed so far have been based mainly on the morphology of adult flies (Hennig, 1965; Paterson, 1959; Pont & Dear, 1976; van Emden, 1939), occasionally including features of the larval biology (Hennig, 1965; Skidmore, 1985). Nonetheless, the results are inconsistent and *Alluaudinella*, *Aethiopomyia* and *Ochromusca* have been classified either in the subfamily Muscinae, Dichaetomyiinae, Dichaetomyiini of Phaoniinae or Reinwardtiinae. Malloch (1921) initially included *Alluaudinella* and *Aethiopomyia* in the subfamily Phaoniinae, yet 4 years later he moved them to the subfamily Muscinae, based on the shape of the lower calypter (Malloch, 1925). van Emden (1939) accepted a position of *Alluaudinella* and *Aethiopomyia* within the Muscinae as defined by Malloch (1925) solely on the basis of the details of the lower calypter, and he also considered *Ochromusca* in Muscinae. Paterson (1959) considered these three genera in Phaoniinae and supported his hypothesis by similarities in the morphology of the male terminalia, but also included features of the egg and larval instars. Paterson (1959) erroneously regarded the larvae to be carnivorous, which he considered would additionally confirm their relationship with other Phaoniinae, known for obligate carnivory. Hennig (1965), following Paterson (1959), and further based on a setose anepimeron as well as yellow body colouration, placed *Alluaudinella*, *Aethiopomyia* and *Ochromusca* within the *Dichaetomyia*-group of Phaoniinae. This concept was adopted by Pont (1980), who classified *Alluaudinella*, *Aethiopomyia*, *Ochromusca* and *Dichaetomyia* Malloch, 1921 within the tribe Dichaetomyiini of Phaoniinae. The latest phylogenetic analysis, carried out by Couri and de Carvalho (2003), placed *Alluaudinella*, *Aethiopomyia* and *Ochromusca* in the subfamily Dichaetomyiinae together with *Dichaetomyia*, *Cyrtoneurina* Giglio-Tos, 1893, *Cyrtoneuropsis* Malloch, 1925 and *Charadrella* Wulp, 1896, albeit this subfamily was supported by homoplastic character states, that is setose anepimeron and prosternum.

The morphology of dipteran immature stages is an invaluable source of data in taxonomic and phylogenetic analyses (Grzywacz et al., 2014; Skidmore, 1985). Despite the increasing number of papers documenting the importance of the morphology of immature stages (Grzywacz et al., 2021; Piwczyński et al., 2017; Skidmore, 1985; Szpila, 2010; Szpila & Pape, 2007), this approach is used less frequently than adult characters (Meier & Lim, 2009). In the case of *Alluaudinella*, *Aethiopomyia* and *Ochromusca*, however, Skidmore (1985) proposed an alternative classification that was in contradiction with previous concepts based on adult morphology. Taking into account the biology and morphology of the immature stages, he placed *Alluaudinella*, *Aethiopomyia* and *Ochromusca* in the subfamily Reinwardtiinae stating a close relationship with *Muscina* Robineau-Desvoidy, 1830 and *Synthesiomyia* Brauer & Bergenstamm, 1893. Furthermore, Skidmore (1985) noted that he did not find any specific similarities in the larval morphology between Reinwardtiinae and Phaoniinae. Moreover, in contradiction to Paterson (1959), who considered larvae of *Alluaudinella* to be carnivorous, Skidmore (1985) found no evidence of larval carnivory, and based on the dark gut contents, he concluded that the larvae of *Alluaudinella* are saprophagous, which has later been confirmed by Ekanem (2008). Larvae of Phaoniinae are monomorphic to dimorphic obligate carnivores, whereas *Alluaudinella*, *Aethiopomyia* and *Ochromusca* are trimorphic saprophages (Skidmore, 1985).

Current knowledge of the morphology of the preimaginal stages of *Alluaudinella*, *Aethiopomyia* and *Ochromusca* is non-exhaustive and limited mainly to third instar larvae and puparia. The morphology of the immature stages of *Aethiopomyia* and *Ochromusca* has been presented only by Skidmore (1985) and de Sousa et al. (2020), but only the former included a short description in addition to the line drawings. More information can be found in the literature on *Alluaudinella* larvae. The third instar larva of *A. bivittata* was described by Paterson (1959) and Skidmore (1985), whereas Ekanem (2008) presented all the larval instars of *A. flavicornis*. Nevertheless, these results are limited to line drawings and short descriptions of the morphology. On the other hand, the morphology of the eggs of *Alluaudinella* has been provided by several authors (Paterson, 1959; Skidmore, 1985; Ekanem, 2008;

Couri & de Sousa, 2020), and Pont & Dear (1976), who stated that *Ochromusca* eggs are similar to those of *Alluaudinella*.

Due to the inconsistency and unclear subfamily position of *Alluaudinella*, *Aethiopomyia* and *Ochromusca* the aim of the study is to investigate the position of this group within Muscidae with application of immature morphology and molecular data. To achieve this goal, *Alluaudinella* was chosen as a representative of the entire *Alluaudinella-Aethiopomyia-Ochromusca* group. In particular, the objectives are to: (i) study and document the morphology of the egg, first, second and third instar of *A. flavicornis*; (ii) provide the first molecular phylogenetic analysis including *Alluaudinella* spp.; and (iii) incorporate larval morphology to evaluate certain nodes on the phylogenetic tree that are either in agreement or conflict with traditional concepts.

2 | MATERIALS AND METHODS

2.1 | Sampling

In total, 55 species, representing all recently defined muscid subfamilies (Grzywacz et al., 2021), were included in the analysis (see Table S1). The outgroup included 5 representatives of the family Anthomyiidae. All adult specimens were identified by AG using keys provided by Pont (1974), de Carvalho (2002), Gregor et al. (2002) and Shinonaga (2003). Our sampling focused particularly on species in the subfamily Reinwardtiinae and Phaoniinae. We obtained sequences of *COI* (cytochrome c oxidase subunit), *cytB* (cytochrome b) and *Ef-1α* (elongation factor 1-alpha) genes for 18 species, while the *CAD* (carbamoylphosphate synthetase 2) gene sequences, where possible, were acquired from GenBank. To extend species and gene sequence sampling, we also included gene sequences of 45 other species retrieved from GenBank as provided by previous authors (Grzywacz et al., 2021; Haseyama et al., 2015; Kutty et al., 2014).

2.2 | DNA isolation, amplification and sequencing

Flies stored in ethanol were soaked three times for 30 min in distilled water or rehydration buffer (STE) at room temperature (Kim et al., 2021). After drying on a thermoblock at 40°C, total genomic DNA was isolated from entire specimens, detached legs or thoracic muscles using a DNeasy Blood & Tissue Kit (Qiagen) following the manufacturer's instructions. The extracted DNA was quantified with a Qubit 3.0 fluorometer using a dsDNA High Sensitivity Assay Kit (Life Technologies, Inc.) following manufacturer's protocol. Mitochondrial *COI* barcode region was obtained with COI-Fex-MP/COI-Rex-MP (Grzywacz et al., 2017) or TY-J-1460/C1-N-2191 (Bernasconi et al., 2000), mitochondrial *cytB* with cytB-F-MP /cytB-R-MP (Grzywacz et al., 2017) or cytB-J-10933/TSI-N-11683 (Simon et al., 1994) and in case of *Ef-1α* we used Ef1α-F-MP/Ef1α-R-MP or Ef1α-F-MPa/Ef1α-R-MPa (Grzywacz et al., 2017). For all three genes, the first given pair of primers was used, which resulted in a longer sequence. If no PCR product was obtained, a second pair of primers was used, resulting in a shorter gene sequence. A standard 25-μL PCR was performed using 1× PCR buffer, 0.2 mM dNTPs, 0.2 μM of each primer, 2 mM $MgCl_2$, 1.25 U of DreamTaq Green DNA Polymerase (Thermo Fisher) and 1.0 μL of the DNA template. The PCR products were checked by electrophoresis on a 1% agarose gel, and samples with a poorly visible band were re-amplified. The PCR cycles consisted of an initial denaturation at 94°C for 2 min, followed by 30 cycles (or 35 in case of *Ef-1α*) comprising 94°C for 30 s, annealing at temperatures ranging from 45–54°C for 30 s, extension at 70°C for 60–90 s and a final extension at 70°C for 10 min. The PCR products were purified with AMPure XP (Beckman Coulter) at a ratio of 1:1 and then re-suspended in TE buffer. The purified products were quantified with a Qubit 3.0 fluorometer using the dsDNA High Sensitivity Assay Kit following manufacturer's protocol. Cycle sequencing reactions were performed using the PCR product and a BrilliantDye Terminator v.3.1 Cycle Sequencing Kit (Nimagen B.V.). The final sequencing products were resolved with an automated DNA sequencer at the Laboratory of Molecular Biology Techniques, UAM (Poznań, Poland). The obtained sequences were assembled and edited using *SeqMan II* ver. 4.0 (DNASTAR). All newly obtained sequences were deposited in GenBank.

2.3 | Phylogenetic analysis

The sequence alignment was analysed using a maximum likelihood (ML) approach in RAxML v.8.2.6 (Stamatakis, 2014) and GARLI v.2.01 (Zwickl, 2006), as well as with a Bayesian (BI) approach using MrBayes v.3.2.6 (Ronquist et al., 2012). PartitionFinder v.1.1.1 (Lanfear et al., 2012), with the option: branchlengths = linked, was used to identify best-partitioning scheme from models available in each software (by gene and codon position) and nucleotide substitution models based on the Bayesian information criterion (BIC; Table 1). Due to software constraints, for RAxML we searched for the best-partitioning scheme using the GTR + G + I model; for GARLI and MrBayes we searched for the best model of nucleotide substitution according to partitioning scheme. The ML analysis in GARLI included

TABLE 1 Partitioning scheme for different data analysis approaches

Partitioning scheme		Model
GARLI		
1	*cytB* _codon2, *COI*_codon1	GTR + I + G
2	*cytB* _codon3, *COI*_codon2	K81UF + I + G
3	*cytB* _codon1, *COI*_codon3	HKY + I + G
4	*Ef-1a* _codon1	GTR + I + G
5	*Ef-1a* _codon2, *Ef-1a*_codon3	K81 + I + G
6	*CAD* _codon1	GTR + G
7	*CAD* _codon2	F81 + I + G
8	*CAD* _codon3	SYM + I + G
RAxML		
1	*COI* _codon1, *cytB*_codon2	GTR + I + G
2	*COI* _codon2, *cytB*_codon3	GTR + I + G
3	*COI* _codon3	GTR + I + G
4	*cytB* _codon1	GTR + I + G
5	*Ef-1a* _codon1	GTR + I + G
6	*Ef-1a* _codon2, *CAD*_codon1	GTR + I + G
7	*CAD* _codon2, *Ef-1a*_codon3	GTR + I + G
8	*CAD* _codon3	GTR + I + G
MrBayes		
1	*COI* _codon1, *cytB*_codon2	GTR + I + G
2	*COI* _codon2, *cytB*_codon3	HKY + I + G
3	*COI* _codon3	HKY + I + G
4	*cytB* _codon1	HKY + G
5	*Ef-1a* _codon1	GTR + I + G
6	*Ef-1a* _codon2, *Ef-1a*_codon3	K80 + I + G
7	*CAD* _codon1	GTR + G
8	*CAD* _codon2	F81 + I + G
9	*CAD* _codon3	SYM + I + G

Note: Maximum likelihood was performed in GARLI v.2.01 and RAxML v.8.2.6., and Bayesian inference in MrBayes v.3.2.6.

50 independent search replicates (searchreps = 50) for 20,000 generations (genthreshfortopoterm = 20,000), all other settings were left as default values. Branch support was evaluated with 1000 nonparametric bootstrap replicates (bootstrapreps = 1000) and summarised on the best tree with SumTrees in DendroPy v.4.5.2 (Sukumaran & Holder, 2010). In RAxML, we summarised (−f b -t bestTree -z bootstrap -m GTRGAMMA) 1,000 nonparametric bootstrap replicates (−m GTRGAMMA -p 12345 -b 29,812 -N 1000 –asc-corr lewis -q partition) on the best-scoring maximum likelihood tree (−m GTRGAMMA -p 12345 -N 500 -q partition –asc-corr lewis). Two BI runs were carried out in MrBayes, each using a random starting tree, one cold and three heated chains (temperature at default = 0.1), for 40 million generations sampled every 2000 generations. All priors for estimated parameters were left as defaults. The initial 25% of saved trees were discarded as burn-in, then the 50% majority-rule consensus tree and posterior probabilities (PPs) of each clade were calculated based on the remaining trees from both runs. We visually assessed runs for convergence in TRACER v.1.7 (Rambaut et al., 2018) by checking for effective sample sizes that were >200 for all model parameters.

2.4 | Morphological analysis

Material for the morphological part of the present study was collected in 2018 in Uyo, Nigeria. Females were collected from the field with the use of *Achatina* sp. snails as bait, and larvae were obtained by keeping these flies in the laboratory until oviposition. Specimens were reared in the laboratory, eggs were transferred directly to 70% ethanol, while larvae of appropriate age were killed by soaking in boiling water and preserved in 70% ethanol. The larvae intended for morphological studies were examined using a combination of three types of microscopy: light microscopy (LM), confocal laser scanning microscopy (CLSM) and scanning electron microscopy (SEM). The application of this approach allows to obtain comprehensive and detailed documentation including all relevant morphological structures. CLSM observations were performed with a Leica TCS SP8 Confocal Laser Scanning Microscope (Leica Microsystems). The preparation and acquisition steps were conducted in accordance with the protocol provided by Walczak et al. (2022). The maceration time in 10% potassium hydroxide (KOH) ranged from 20 h for the first instar, 24–30 h for the second instar and 36 h for the third instar larvae. All larvae were mounted on cavity slides using glycerine as medium. The autofluorescence signal of the cephaloskeleton was collected with two excitation wavelengths: 561 and 633 nm. A weak signal was also observed with 405 and 488 nm lasers, but they were abandoned as neither of these lasers provided additional information to the final images. The microscopic slides were scanned with a 40× oil lens with a numerical aperture of 1.3 (N.A. = 1.3). Following acquisition of sequential images, maximum intensity projections (MIP) and 3D visualisation were built using LAS AF V3.3 and LAS X 3D Viewer (Leica Microsystems), respectively.

SEM observations were performed with a JEOL scanning microscope (JSM-6335F; JEOL Ltd.). The preparation of the samples for SEM included cleaning with a fine brush, dehydration at 80.0%, 90.0% and 99.5% ethanol (EtOH) and critical point drying in carbon dioxide (CO_2) with an Autosamdri®-815, Series A critical point dryer (Tousimis Research Corp.). The larvae were then mounted on aluminium stubs with double-sided adhesive tape and

coated with platinum for 140 s (20 nm of coating) using a JEOL JFC 2300HR high-resolution fine coater (JEOL Ltd.).

The larvae for LM examination were prepared by immersion in Hoyer's medium on a cavity slide. The light microscopy observations were conducted with a Nikon Eclipse E200 microscope (Nikon Corp.) with an integrated Nikon 8400 digital camera. Specimens were stored in Hoyer's medium after study and deposited in the collection of the Department of Ecology and Biogeography, Nicolaus Copernicus University, Toruń, Poland. Egg terminology follows Hinton (1981) with some clarification described by Grzywacz et al. (2012). Larval terminology follows Courtney et al. (2000) with a few modifications proposed by Szpila and Pape (2005). Family-specific structures follow the terminology of Skidmore (1985) with modifications proposed by Grzywacz (2013) and Walczak et al. (2022).

3 | RESULTS

3.1 | Morphology

3.1.1 | Egg

Egg is creamy white in the centre to translucent white on the sides, elongated and oval in lateral view (Figure 1a). The dorsal surface is distinctly convex and the ventral surface is flat to slightly convex (Figure 1f). The anterior pole carries a bulge-like fold bearing the micropyle (*mcp*), the posterior pole is wavy (Figure 1d,e). The micropyle is in the form of a funnel-shaped area with distinctly raised walls (Figure 1e). Eggs are laterally broadly foliaceous through the entire length into folds resembling hatching pleats (*hp*). The hatching line (*hl*) runs along the lateral edge of the egg (Figure 1a,f) divides the median area (*ma*) and the remaining chorion (*c*). The shape of the *ma* and the *c* is defined by the whole dorsal and ventral surface of the egg, respectively (Figure 1b,d). The *ma*, which bears a plastron function, consists of two different configurations simultaneously (Figure 1d). The ovoid central area of the *ma* is covered with an island pattern (Figure 1c), whereas the remaining surface, up to the *hl*, is covered with a hexagonal pattern (Figure 1d). The island pattern consists of two different in size and shape islands, forming long undulating groups of adjacent islands or clearly separated islands (Figure 1c). The first are fine, mesh-like sparsely islands, the second are slightly bigger neighbouring islands, tightly adjacent (Figure 1c). A shallow depression parallel to the *hl* is present on the *c* (Figure 1b). The chorion along the depression is covered with an angular and longitudinal pattern. The anterior and posterior poles of the *c* are covered with a poorly defined hexagonal pattern, whereas the hexagonal pattern with elevated boundaries reaches the *mp*. The remaining chorion is almost smooth (Figure 1e).

3.1.2 | Larva

3.1.2.1 | *Cephaloskeleton*

In the first instar the cephaloskeleton consists of suprabuccal teeth (*sub*), paired mouthhooks (*mh*), an unpaired labrum (*lb*), an unpaired intermediate sclerite (*is*), paired parastomal bars (*pb*) and a basal sclerite (*bs*) (Figures 2a,b, 3a,b and 4a). The anteriormost sclerites are the *sub*, composed of several small closely adjacent teeth directed ventrally (Figures 2a,b and 4a). The *sub* varies in size and show an overall decrease in the ventral direction (Figure 4a). The blunt-ended apical part of each *mh* adjoins anteroventrally to the first of the *sub* (Figures 2a and 4a). The *mh* is a slightly arched rod with the basal part curved upwards and equipped with a lateral arm (*la*) directed medially (Figure 4a). Mouthhooks are symmetrical and well-separated, except for the converging apical part (Figure 3b). The suprabuccal teeth, the *mh*, in particular the *la*, are the least sclerotized parts of the cephaloskeleton (Figure 3a). The labrum (*lb*), located above the basal part of the *mh*, is robust and apically pointed. The basal part of the *lb* is fused with an anterior part of the *pb* and *is* (Figure 4a). In dorsal view, the area just behind the posterior edge of the *lb* and between the anterior part of paired *pb* is strongly sclerotized up to the posterior margin of the epistomal sclerite (*es*) (Figures 3b and 4a). The anterior part of the *pb* and the anterior part of the intermediate sclerite (*is*) are strongly elongated (Figure 2a,b). The *es* is fused with the *pb* and easily visible in lateral view. Anteriorly to the *es* are two symmetrical tear-shaped appendages pointed upwardly (Figure 3b). In ventral view, the *is* has two strong transverse sclerotizations, the first in the elongated part of the *is*, located just below the fusion with the *lb* and the *pb* and the second corresponding to the crossbeam. A strongly sclerotized basal sclerite (*bs*) consists of paired vertical plates (*vp*) with dorsal (*dc*) and ventral cornua (*vc*) connected anterodorsally by sclerotized dorsal bridge (*db*) (Figure 3a). The *dc* is shorter than the *vc*. The posterior part of the *vc* is poorly sclerotized and carries ventrally a sensory organ X (*x*) equipped with paired sensilla (Figure 2a). The hypopharynx bears longitudinal ridges.

The *mh* of the second instar are symmetrical and tightly appressed (Figure 3d). The anterior part of *mh* adjoins laterally to the *sub* (Figures 2c,d and 4b). The ventral part of *mh* is fused with the dental sclerite (*ds*) (Figure 4b). Paired roundish accessory stomal sclerites

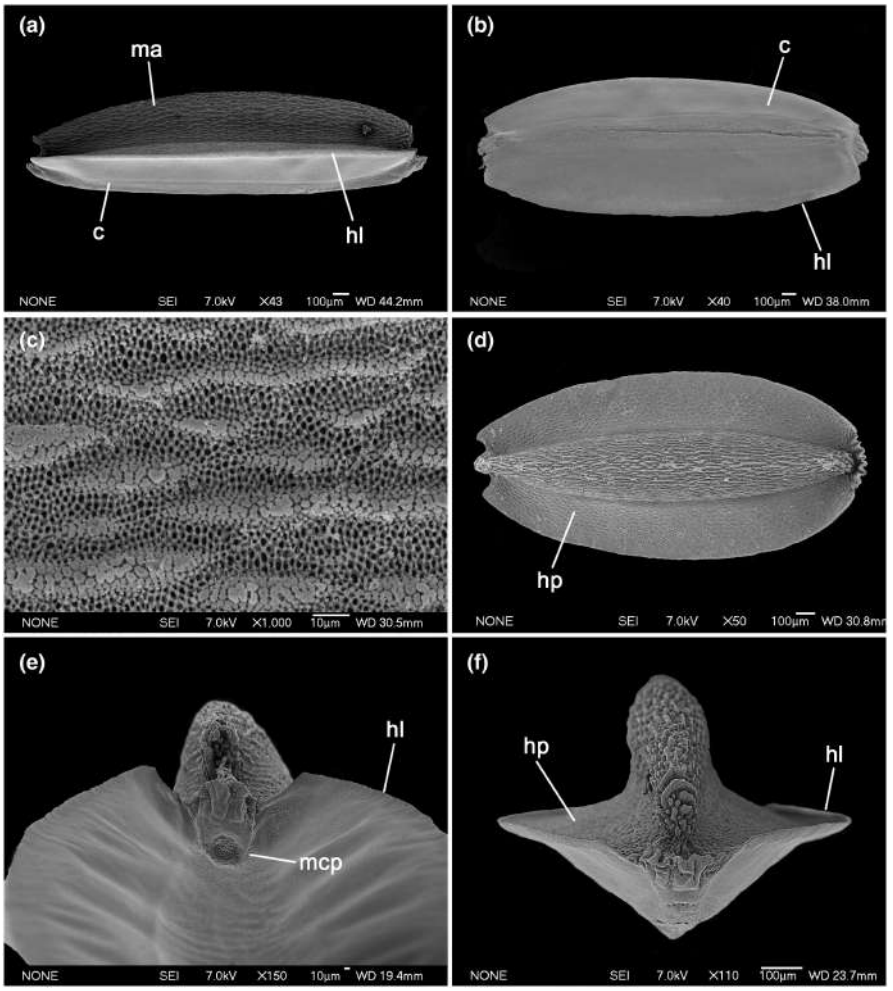

FIGURE 1 *Alluaudinella flavicornis*, details of egg [SEM]. (a) habitus, lateral view; (b) habitus, ventral view; (c) central part of median area covered with an island pattern; (d) habitus, dorsal view; (e) anterior part with micropyle, anteroventral view; (f) habitus, posterior view. Abbreviations: c, chorion; hl, hatching line; hp, hatching pleat; ma, median area; mcp, micropyle.

(*acc*) are present ventrally to the area where the *mh* join with the *ds* (Figures 2d and 3d). The *is* elongated and H-shaped. The *es* is hemispherical and situated anterodorsally to the *is*, well visible in the lateral view, while anteroventrally is a pair of labial sclerites (*lb*) (Figures 2d and 3d). A pair of rod-like rami (*r*) is present between the lateral arms of the *is* (Figure 4d). The rami varies intraspecifically being rod-shaped and strongly sclerotized in some individuals, in others is cracked and indistinct. The *bs* is connected anterodorsally with tightly appressed dorsal bridge (*db*) and anteroventrally fused with the ventral bridge (*vb*) (Figures 2c,d, 3d and 4c). The *db* is well-perforated (Figure 3c). The *vb* is equipped with the expansion directed posteriorly (Figure 2c). The length of the *dc* and the *vc* is similar, both are further elongated with poorly sclerotized lobe-like extensions. The hypopharynx bears longitudinal ridges.

The cephaloskeleton of the third instar consists of paired *mh* with additional sclerites, an unpaired *is* and a *bs* (Figures 2e and 3e). Third instar *mh* are symmetrical and well-separated throughout their entire length. The basal part of the *mh* is robust, whereas the apical part is slender and curved downwards (Figures 2e, 3e and 4e). Parallel to and below the *mh* is a pair of irregular anterior rods (*aro*) and a pair of oral bars (*ob*) with serrated tips (Figures 2e and 4e). The accessory rectangular process (*rp*) is indistinct. The *ob* is posteriorly adjacent to the basal part of the *mh* (Figure 4e). The *sub* lies freely ventrally to the apical part of *ob* (Figures 3e and 4e). Paired accessory stomal sclerites (*acc*) and triangular *ds* are placed ventrally to the *mh*. The *ds* and the *mh* are connected by a narrow sclerotized hinge (Figure 4e). The *es* and the pair of *ls* lie between the posterior part of the *mh* and the anterior part of the *is*. The *es* bears four, slightly elongated appendages (Figure 4f). The *ls* are fused together. The *is* is robust and H-shaped with a broad crossbeam (*crs*) in ventral view. The *is* is closely appressed anteriorly to the *mh* and posteriorly to the *bs* (Figure 4g). The lateral arms of the *is* are irregularly formed with a distinct protuberance anteriorly (Figure 4g). Each of the parastomal bars (*pb*) is in the form of an anterodorsal extension of *is*. Paired rami (*r*), located ventrally to the *is*, are bar-like, slender and well sclerotized (Figure 4f). The massive basal sclerite consists of paired broad *vp* each with an arched dorsal (*dc*) and ventral cornua (*vc*) connected anterodorsally by a perforated dorsal bridge (*db*) and anteroventrally by a

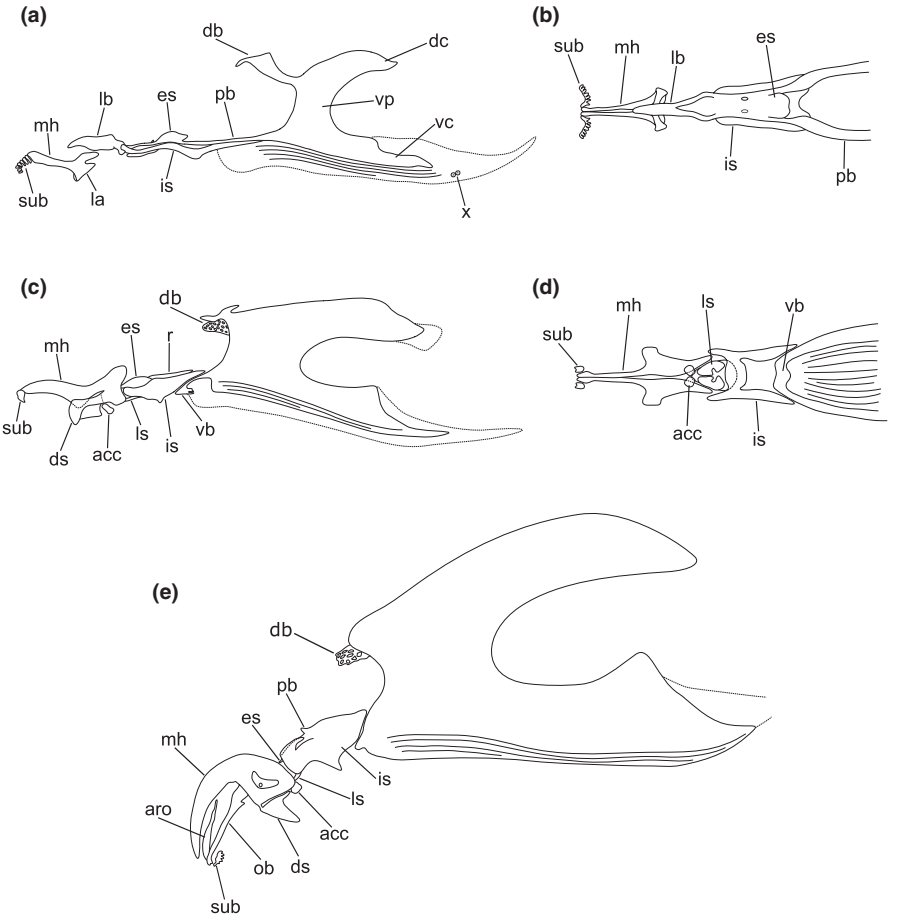

FIGURE 2 *Alluaudinella flavicornis*, details of larva I–III. (a) cephaloskeleton of the first instar larva, lateral view; (b) cephaloskeleton of the first instar larva, dorsal view; (c) cephaloskeleton of the second instar larva, lateral view; (d) cephaloskeleton of the second instar larva, ventral view; (e) cephaloskeleton of the third instar larva, lateral view. Abbreviations: acc, accessory stomal sclerite; aro, anterior rod; db, dorsal bridge; dc, dorsal cornu; ds, dental sclerite; es, epistomal sclerite; is, intermediate sclerite; la, lateral arm; lb, labrum; ls, labial sclerite; mh, mouthhook; ob, oral bar; pb, parastomal bar; r, rami; sub, suprabuccal teeth; vb, ventral bridge; vc, ventral cornu; vp, vertical plate; x, sensory organ X.

ventral bridge (*vb*) (Figures 2e and 3e). The *dc* and *vc* are of similar length. The dorsal extension (*de*) of the *vc* is well marked (Figure 3e). The hypopharynx bears longitudinal ridges.

3.1.2.2 | *Pseudocephalon*

Each lobe of the bilobate pseudocephalon of all instars carries an antennal complex (*an*), maxillary palpus (*mp*), ventral organ (*vo*) and oral ridges (*or*) as well as labial lobe (*ll*) (Figures 5b, 7b and 8a,b). The antennal complex consists of an antennal dome (*and*) situated on an antennal basal ring (*abr*) (Figure 5c). The oblong antennal dome is slightly longer than the height of the basal ring. The *abr* carries dorsally a lateral pore equipped with a sensillum (Figure 5c). The *mp* in the first and second instar is surrounded by irregular folds (Figures 5d and 7c), while in the third instar folds are circular and form five distinguishable rings (Figure 8c). The *mp* in all instars consists of three sensilla coelonica (*sc*), three sensilla basiconica (*sb*), several additional sensilla placed between the *sc* and the *sb* and two sensilla coeloconica of non-maxillary origin (*ns*) located laterodorsally (Figures 5d, 7c and 8c). The facial mask in the first instar is composed of oral ridges (*or*), cirri and suprabuccal teeth (*sub*) (Figure 5b). The cirri are arranged in one short row and are pointed apically. The oral ridges in the subsequent instars are more numerous and cover most of the latero-ventral surface of pseudocephalon (Figures 7a,b and 8a,b). In the second and third instar the *vo* is located anteriorly to the margin of the oral ridges and is bulge-shaped (Figures 7b and 8b). The *vo* is equipped with three sensilla ampullacea and one sensillum resembling a sensillum placodeum.

3.1.2.3 | *Thorax*

The first thoracic segment carries an anterior band of sclerotized spines (Figure 3a,c,e). The band is broad and complete, forming a strong wreath, followed by a transverse cleft approximately reaching the middle of the segment. The width of the band is not constant and is twice as wide ventrally as dorsally. The spines of the anterior spinose band are massive, tapered, pointed and posteriorly directed (Figures 5a,b, 7b and 8a). Spines in the first instar are arranged separately, in the second instar are fused into short rows of one to three spines, while in the third instar the spines are arranged in the transverse and adjacent rows fused at the base (Figures 5b, 7b and 8a). In the third instar spinose band is broadened ventrally by an additional patch of spines, present beyond the main broad band and the cleft (Figure 8a). The degree of sclerotization of spines increases from the first to the third instar

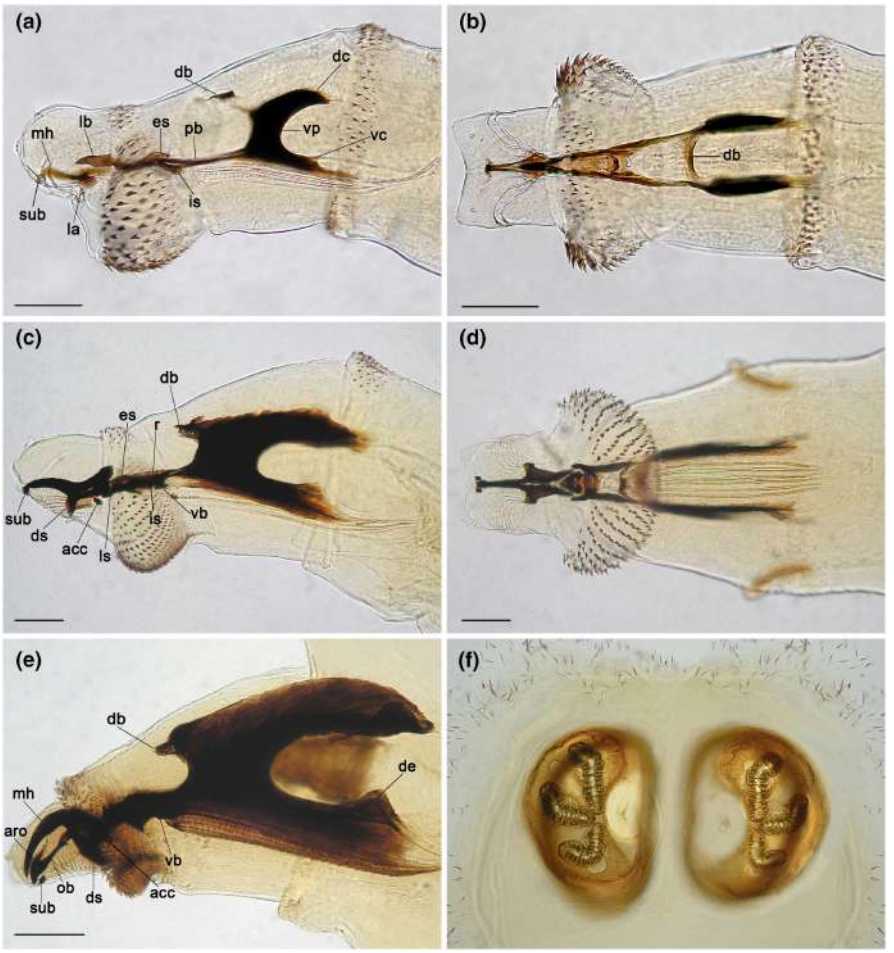

FIGURE 3 *Alluaudinella flavicornis*, details of larva I–III [LM]. (a) cephaloskeleton of the first instar larva, lateral view; (b) cephaloskeleton of the first instar larva, dorsal view; (c) cephaloskeleton of the second instar larva, lateral view; (d) cephaloskeleton of the second instar larva, ventral view; (e) cephaloskeleton of the third instar larva, lateral view; (f) posterior spiracles of the third instar larva. Abbreviations: acc, accessory stomal sclerite; aro, anterior rod; db, dorsal bridge; dc, dorsal cornu; de, dorsal extension; ds, dental sclerite; es, epistomal sclerite; is, intermediate sclerite; la, lateral arm; lb, labrum; ls, labial sclerite; mh, mouthhook; ob, oral bar; pb, parastomal bar; r, rami; sub, suprabuccal teeth; vb, ventral bridge; vc, ventral cornu; vp, vertical plate. Scale bars: 0.05 mm.

(Figure 3a,c,e). Anterior spinose bands on the second and third thoracic segments are complete and of a constant width, but less frequently arranged than on the first thoracic segment (Figures 5a, 7a and 8a). The shape and arrangement of spines in all instars correspond to those of the first thoracic segment. In the first instar are arranged individually, in the second instar are single-, double- or three-pointed, while in the third instar are arranged in short rows (Figures 6a, 7a and 8a). The thoracic segments are ventrally equipped with paired Keilin's organs (*ko*) with trichoid sensilla (Figures 6a, 7b and 8a). The first instar anterior spiracles (*as*) are in the form of a simple opening (Figure 5a), while in the second and third instar, each anterior spiracle consists of 11 lobes tightly arranged (Figures 7a and 8a).

3.1.2.4 | *Abdomen*

Only in the second instar the first abdominal segment has colourless, fine and singly scattered spines placed anterodorsally (Figure 7d). The remaining abdominal segments in the second instar, as well as all abdominal segments in the first and third instar are devoid of spines placed anterodorsally. Abdominal segments I–VII in the third instar carry ventrally a transverse crevice (*cr*) (Figure 8d). In all instars strongly pronounced lateral creeping welts (*lcw*) are placed posteriorly and run parallel to the edge of each abdominal segment (Figures 7d and 8d). Abdominal segments carry anteriorly ventral creeping welts (*vcw*) with the welt on the anal division termed the pre-anal welt (*pre*) (Figures 6a,b, 7d,e and 8d). The *vcw* bears rows of spines, which on successive abdominal segments are similar in size and shape. In the first instar, the *vcw* carries a row of oblong, tapered spines pointing backwards (Figure 6a). The regular row of spines is followed by three rows of shorter spines perpendicular to the surface of abdominal segments (Figure 6b). Spines of the *vcw* are separated in half by a narrow split. In the second instar, the *vcw* carries two rows of massive spines (Figure 7e). The spines arranged in a row on a delicate bulge are cylindrical and blunt, while behind them are conical and irregularly arranged. In the third instar the *vcw* is equipped with a row of tightly contiguous spines with a broad base and blunt ends (Figure 8d). The row of spines is followed by irregularly arranged conical and massive spines, which are followed by short rows of tiny, pointed spines. In all instars, above the pre-anal welt, additional spines are present on the aVII, creating an almost complete posterior spinose band (Figures 6e, 7f,g

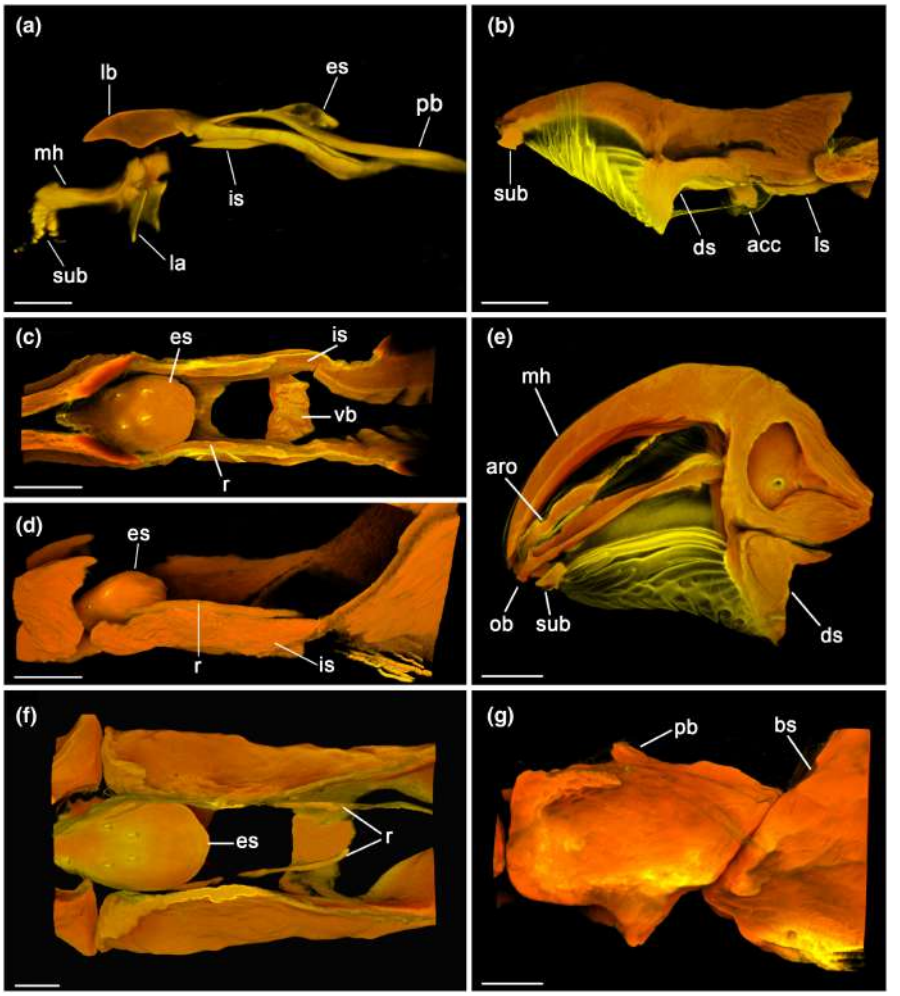

FIGURE 4 *Alluaudinella flavicornis*, cephaloskeleton of larva I–III [CLSM]. (a) cephaloskeleton of the first instar larva, lateral view; (b) mouthhooks of the second instar larva, lateral view; (c) intermediate sclerite of the second instar larva, dorsal view; (d) intermediate sclerite of the second instar larva, dorso-lateral view; (e) mouthhooks of the third instar larva, lateral view; (f) intermediate sclerite of the third instar larva, dorsal view; (g) intermediate sclerite of the third instar larva, lateral view. Abbreviations: acc, accessory stomal sclerite; aro, anterior rod; bs, basal sclerite; ds, dental sclerite; es, epistomal sclerite; is, intermediate sclerite; la, lateral arm; lb, labrum; ls, labial sclerite; mh, mouthhook; ob, oral bar; pb, parastomal bar; r, rami; sub, suprabuccal teeth; vb, ventral bridge. Scale bars: 0.05 mm.

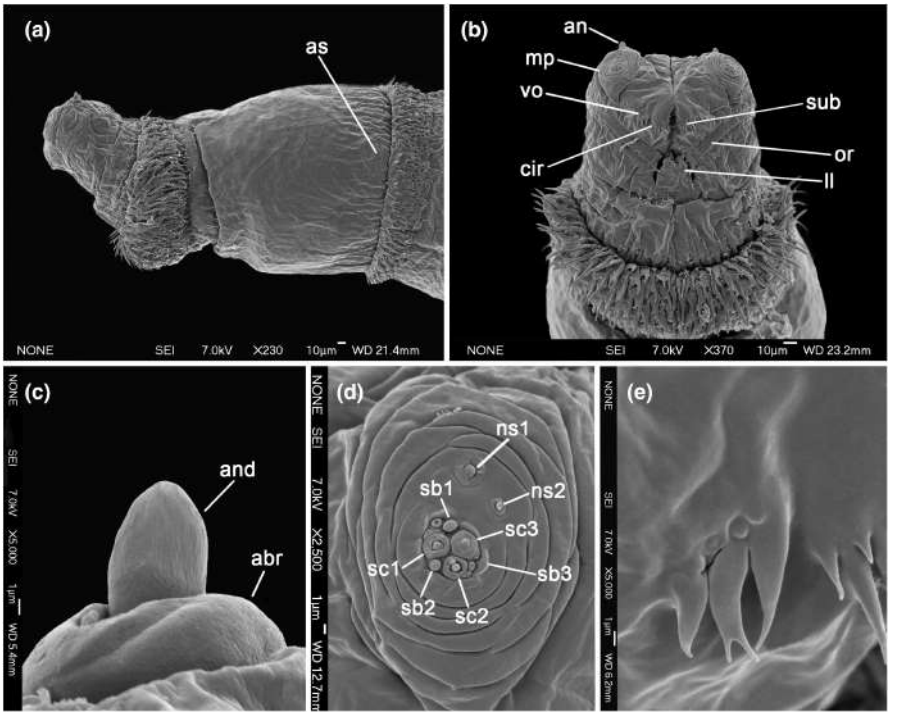

FIGURE 5 *Alluaudinella flavicornis*, pseudocephalon of the first instar larva [SEM]. (a) anterior end of body, lateral view; (b) anterior end of body, ventral view; (c) antennal complex; (d) maxillary palpus; (e) ventral organ. Abbreviations: abr, antennal basal ring; an, antennal complex; and, antennal dome; as, anterior spiracle; cir, cirri; ll, labial lobe; mp, maxillary palpus; ns1–2, first and second additional sensillum coeloconicum; or, oral ridges; sb1–3, sensillum basiconicum 1–3; sc1–3, sensillum coeloconicum 1–3; sub, suprabuccal teeth; vo, ventral organ.

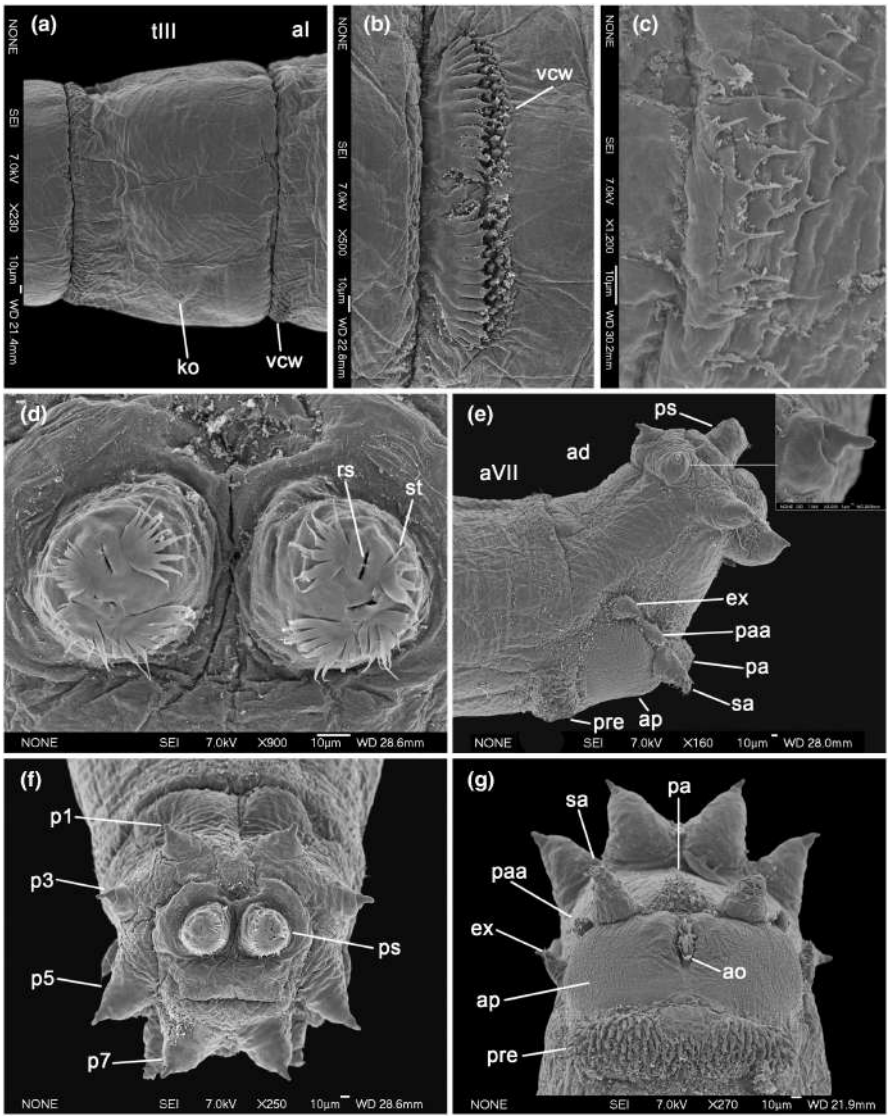

FIGURE 6 *Alluaudinella flavicornis*, thorax and abdomen of the first instar larva [SEM]. (a) thoracic and abdominal segments, lateral view; (b) ventral creeping welt, ventral view; (c) spines on the seventh abdominal segment, lateral view; (d) posterior spiracles; (e) posterior end of body, lateral view; (f) anal division, posterior view; (g) posterior end of body, ventral view. Abbreviations: aI, aVII, abdominal segments 1 and 7; tIII, thoracic segment 3; ad, anal division; ao, anal opening; ap, anal plate; ex, extra-anal papilla; ko, Keilin's organ; p1–p7, papillae 1–7 surrounding spiracular field; pa, post-anal papilla; paa, para-anal papilla; pre, pre-anal welt; ps, posterior spiracle; rs, respiratory slit; sa, sub-anal papilla; st, spiracular tuft; vcw, ventral creeping welt.

and 8e). On the dorsal and lateral surface of aVII spines are less numerous, and the shape and distribution at the subsequent instars correspond to those of the anterior spinose bands. The spines on the anterior spinose band are directed posteriorly, while the pre-anal welt spines point forward (Figures 5a, 6e, 7a,h and 8d,e). The anal division carries an anal plate (*ap*) with a ventrally located anal opening (*ao*) and anal papillae (Figures 6f,g, 7f,g and 8e,h). The *ap* is porous, broadened laterally and well visible in lateral view (Figures 6e,g, 7g and 8h). The *ap* is limited anteriorly by the *pre*, posteriorly by the anal papillae and laterally by a slight prominence of the integument. Directly behind the *ao* lies an unpaired, slightly flattened post-anal papilla (*pa*), and laterally to the *pa* lie pairs of sub-anal (*sa*), para-anal (*paa*) and extra-anal (*ex*) papillae (Figures 6g, 7g and 8h). All papillae are conical in shape and covered with pointed spines (Figures 6g, 7g and 8h). In the first and second instar the *sa* are twice as high as the other papillae (Figures 6g and 7f), while in the third instar, all papillae are of equal size (Figure 8h). Each *sa* is equipped with a sensillum basiconicum and two sensilla resembling sensilla ampullacea. The spiracular field carries posterior spiracles and seven pairs of papillae (*p1–p7*; Figures 6e,f, 7f and 8e). Posterior spiracles are clearly raised on the stem. Each of the posterior spiracle carries four branched spiracular tufts (*st*) and two respiratory slits (*rs*) in the first and second instar, and three *rs* in the third instar. In the second and third instar spiracular scar (*ss*) is located medially (Figures 3f, 6d, 7f and 8f,g). The *rs* in the first and second instar are straight and unevenly distributed, while in the third instar the *rs* are crescent-shaped and arranged in a radiating configuration. The *ss* is placed on the inner margin of each posterior spiracle (Figures 7f and 8f,g). Papillae *p1*, *p3*, *p5* and *p7* are arranged in the margins of the spiracular field, forming a strong stellar wreath, while papillae *p2*, *p4* and *p6* are shifted forward (Figures 6f, 7f and 8e). The former are conical and equipped with a sensillum

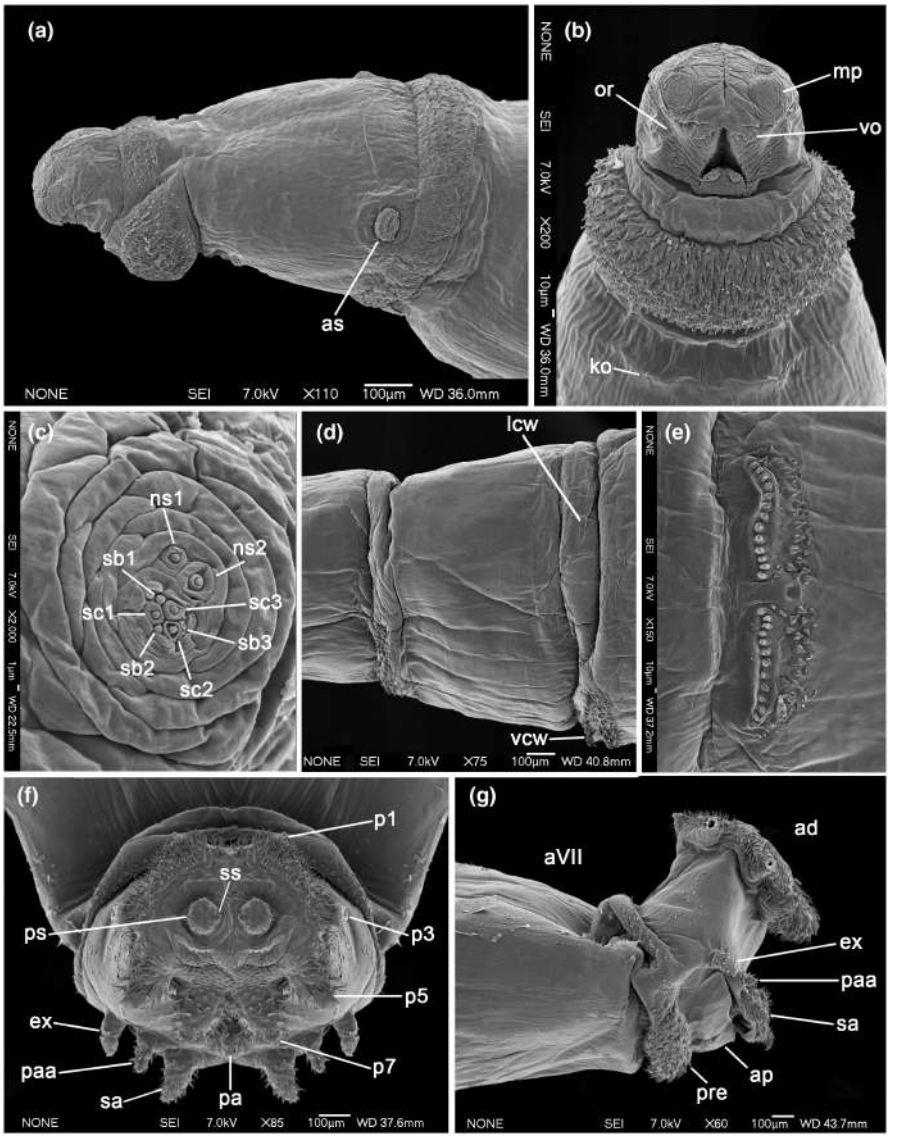

FIGURE 7 *Alluaudinella flavicornis*, pseudocephalon, thorax and abdomen of the second instar larva [SEM]. (a) anterior end of body, lateral view; (b) anterior end of body, ventral view; (c) maxillary palpus; (d) first abdominal segment, lateral view; (e) ventral creeping welt, ventral view; (f) anal division, posterior view; (g) posterior end of body, lateral view. Abbreviations: aVII, abdominal segment 7; ad, anal division; ap, anal plate; as, anterior spiracle; ex, extra-anal papilla; ko, Keilin's organ; lcw, lateral creeping welt; mp, maxillary palpus; ns1–2, first and second additional sensillum coeloconicum; or, oral ridges; p1–p7, papillae 1–7 surrounding spiracular field; pa, post-anal papilla; paa, para-anal papilla; pre, pre-anal welt; ps, posterior spiracle; sa, sub-anal papilla; sb1–3, sensillum basiconicum 1–3; sc1–3, sensillum coeloconicum 1–3; ss, spiracular scar; vo, ventral organ; vcw, ventral creeping welt.

resembling a sensillum basiconicum. Papillae *p1*, *p3*, *p5* and *p7* in the second and third instar are covered with long, narrow spines (Figures 7f and 8e). Papillae *p2*, *p4* and *p6* are indistinct and each equipped with a sensillum resembling a sensillum ampullaceum. The surface of the spiracular field above papillae *p7* in the second and third instar is covered with fine protuberances that resemble small grains (Figures 7f and 8e). The posterior spiracles in young third instar larvae are convex and closely appressed to one another, while in mature larvae are raised and distinctly spaced apart (Figure 8f,g).

3.2 | Phylogenetic inference

A highly supported dichotomy splits Muscidae into one clade composed of Azeliinae + Muscinae and a second clade containing the remaining Muscidae ($BS_{GARLI} = 100\%$, $BS_{RAxML} = 100\%$ and $PP_{MrBayes} = 1.0$; Figure 9). In the second clade, a moderately supported dichotomy ($BS_{GARLI} = 73\%$, $BS_{RAxML} = 66\%$ and $PP_{MrBayes} = 1.0$) splits the clade into (Phaoniinae + (Mydaeinae + (Coenosiinae + Phaoniinae))) and (Phaoniinae + ((Atherigoniinae + Cyrtoneurininae) + (*Alluaudinella* + (Reinwardtiinae + Cyrtoneurininae)))). Phaoniinae are found to be polyphyletic. *Phaonia* Robineau-Desvoidy, 1830 spp. are placed in all analyses as sister taxon to (Mydaeinae + (Coenosiinae + Phaoniinae)) with high branch support ($BS_{GARLI} = 96\%$, $BS_{RAxML} = 98\%$ and $PP_{MrBayes} = 1.0$), while *Prohardyia* Pont, 1969, *Metopomyia* Malloch, 1922 and *Lophosceles* Ringdahl, 1922 as sister group to Cyrtoneurininae, Atherigoniinae, Reinwardtiinae and *Alluaudinella* ($BS_{GARLI} = 34\%$, $BS_{RAxML} = 22\%$ and $PP_{MrBayes} = 1.0$). Cyrtoneurininae are recovered as non-monophyletic, with *Cyrtoneuropsis* Malloch, 1925 as the sister taxon of Atherigoninae, and *Neomuscina* as the sister taxon of *Synthesiomyia nudiseta* van der Wulp, 1883 and nested within Reinwardtiinae. *Xenotachina* Malloch, 1921 sp.

and *Eginia ocypterata* (Meigen, 1826) are placed within Reinwardtiinae, as the sister group of *Calliphoroides antennatis* Hutton, 1881 + *Passeromyia* Rodhain and Villeneuve, 1915 (BS_{GARLI} = 42%, BS_{RAxML} = 44% and $PP_{MrBayes}$ = 1.0). *Alluaudinella* emerges as the sister taxon of Reinwardtiinae + *Neomuscina* spp., yet with poor support (BS_{GARLI} = 20%, $PP_{MrBayes}$ = 0.82). In RAxML *Alluaudinella* emerges as the sister taxon of *Cyrtoneuropsis* (BS_{RAxML} = 23%), and both, in turn, as the sister taxa of *Atherigona* Rondani, 1856 (BS_{RAxML} = 9%). In RAxML (Atherigoniinae + (*Alluaudinella* + *Cyrtoneuropsis*)) emerges as the sister group of (Reinwardtiinae + Cyrtoneurininae) (BS_{RAxML} = 27%). No sister group relationship is observed between *Alluaudinella* spp. and *Dichaetomyia* spp. or any other representative of Phaoniinae.

4 | DISCUSSION

4.1 | Systematic position of *Alluaudinella*

All previous studies have treated *Alluaudinella*, *Aethiopomyia* and *Ochromusca* as undoubtedly forming a natural grouping (Couri et al., 2006; Couri & de Carvalho, 2003; Couri & de Sousa, 2020; Hennig, 1965; Paterson, 1959; Pont & Dear, 1976; Séguy, 1937; Skidmore, 1985; van Emden, 1939); therefore, in this study, *Alluaudinella* is considered as a representative for this group. Since immature stages have been recognised as a valuable source of phylogenetic information (Meier & Lim, 2009), larval morphology and life history were applied to assess the traditional concept of *Alluaudinella* closely related to *Dichaetomyia* (Table 2). *Alluaudinella*,

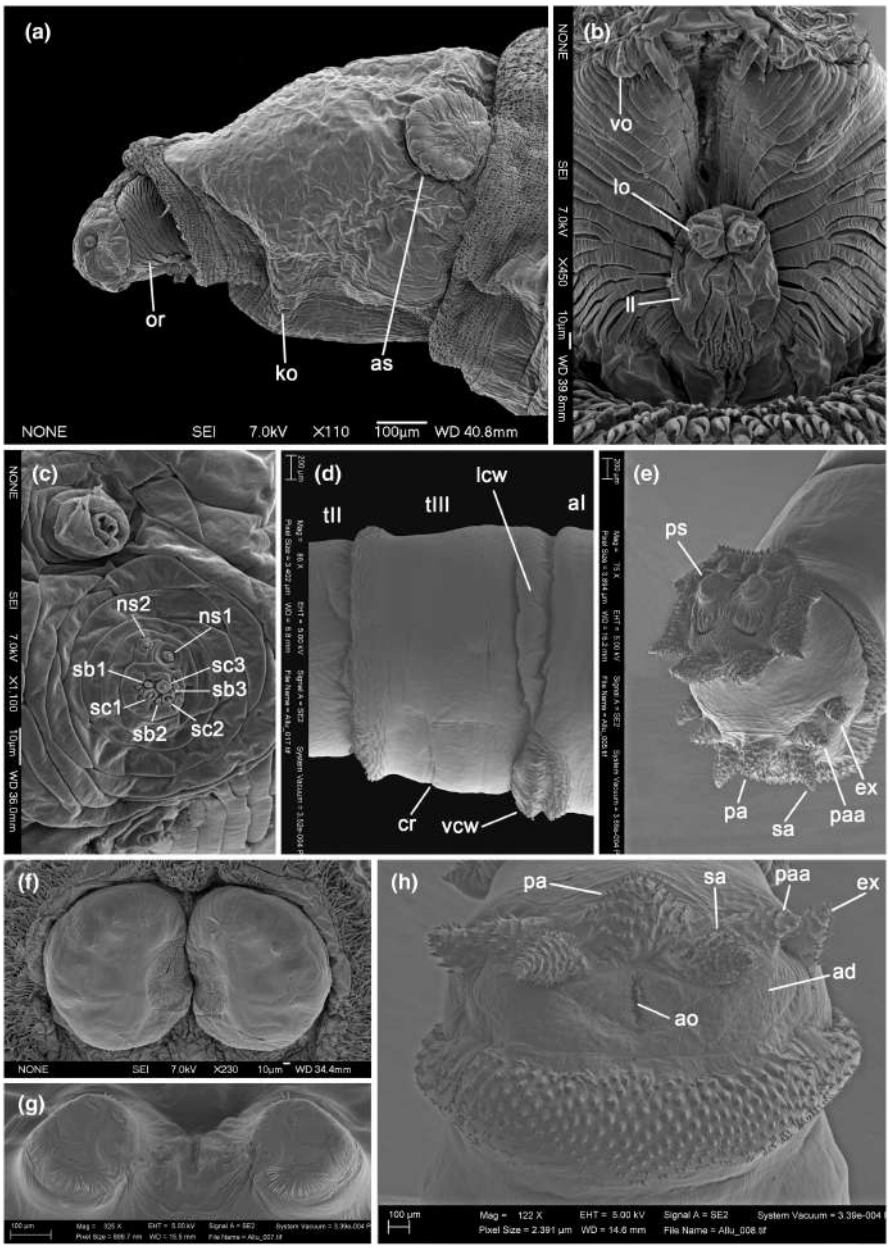

FIGURE 8 *Alluaudinella flavicornis*, pseudocephalon, thorax and abdomen of the third instar larva [SEM]. (a) anterior end of body, lateral view; (b) facial mask, ventral view; (c) maxillary palpus; (d) thoracic and abdominal segments, lateral view; (e) posterior end of body, posterior-lateral view; (f) posterior spiracles in young larvae, posterior view; (g) posterior spiracles in mature larvae, posterior view; (h) posterior end of body, ventral view. Abbreviations: aI, abdominal segment 1; tII, tIII, thoracic segments 2 and 3; ad, anal division; ao, anal opening; as, anterior spiracle; cr, transverse crevice; ex, extra-anal papilla; ko, Keilin's organ; lcw, lateral creeping welt; ll, labial lobe; lo, labial organ; ns1–2, first and second additional sensillum coeloconicum; or, oral ridges; pa, post-anal papilla; paa, para-anal papilla; ps, posterior spiracles; sa, sub-anal papilla; sb1–3, sensillum basiconicum 1–3; sc1–3, sensillum coeloconicum 1–3; vcw, ventral creeping welt; vo, ventral organ.

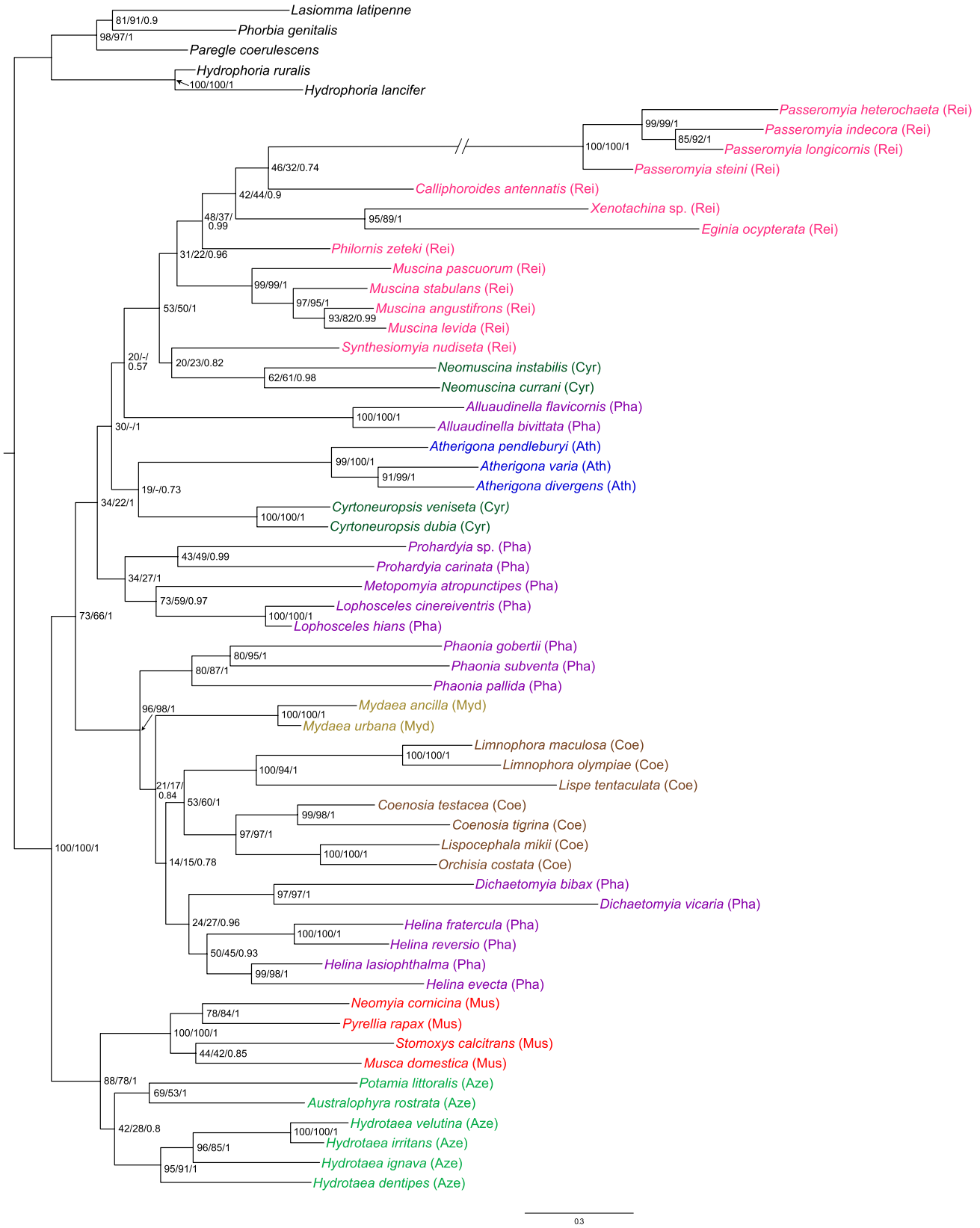

FIGURE 9 The best maximum likelihood tree inferred from the analysis of mitochondrial and nuclear sequences data for 55 representatives of Muscidae in GARLI. Node support values are shown for maximum likelihood (bootstrap) using GARLI and RAxML as well as Bayesian inference (posterior probability) analyses using MrBayes. Nodes that were not recovered in RAxML are marked with hyphen (−). Branch lengths were estimated using the GTR + G substitution model (see scale bar). Outgroups marked with black colour. Representatives of Muscidae subfamily marked with other colours. Ath, Atherigoninae; Aze, Azeliinae; Coe, Coenosiinae; Cyr, Cyrtoneurininae; Mus, Muscinae; Myd, Mydaeinae; Pha, Phaoniinae; Rei, Reinwardtiinae.

Aethiopomyia and *Ochromusca* include species with trimorphic larvae (i.e. three free-living larval instars), while Phaoniinae, including *Dichaetomyia*, have mono- or dimorphic larvae (i.e. one or two free-living larval instars, respectively; Table 2). The cephaloskeleton, which is of primary importance for taxonomic purposes, as well as posterior spiracles and spinulation details differ significantly between these two groups. In *Alluaudinella*, the entire cephaloskeleton is well sclerotized, with massive mouthhooks and a robust basal sclerite, while in *Dichaetomyia* the cephaloskeleton is slender, and the basal sclerite is elongated. Third instar larvae of Coenosiinae, Mydaeinae and Phaoniinae, including *Dichaetomyia*, are equipped with a posterior ribbon in the cephaloskeleton, while this structure is absent in *Alluaudinella*. Another distinguishing feature between *Alluaudinella* and *Dichaetomyia* larvae is the hypopharynx. In *Alluaudinella*, the indistinctly sclerotized hypopharynx bears visible longitudinal ridges, while in *Dichaetomyia* the hypopharynx is distinctly sclerotized with hardly visible or absent longitudinal ridges. With a few exceptions (Ferrar, 1979), the presence or absence of longitudinal ridges is assumed to indicate a larval feeding strategy (Courtney et al., 2000; Keilin & Tate, 1930; Roberts, 1970; Skidmore, 1985). Saprophagous larvae have been reported to show a hypopharynx with well-developed longitudinal ridges, used for filtering food particles (Courtney et al., 2000), while longitudinal ridges are poorly developed or not distinguishable in carnivorous species (Keilin & Tate, 1930). The third instar of *Alluaudinella* is characterised by massive posterior spiracles with curved respiratory slits arranged in a radiating configuration. Larvae of *Dichaetomyia* have small posterior spiracles with straight, subparallel to convergent respiratory slits. Another distinguishing feature is the presence of strong anal papilla and all of *p1*, *p3*, *p5*, *p7* in *Alluaudinella*. Larval morphology of Reinwardtiinae (i.e. *Muscina*, *Passeromyia*, *Philornis*, *Synthesiomyia*) is similar to that of third instar *Alluaudinella* (Table 2), that is extensive spinulation, massive and heavily sclerotized cephaloskeleton (also in the earlier instars), well-separated and symmetrical mouthhooks as well as broad intermediate sclerite with a distinct protuberance and/or anterodorsal extension and rod-like paired rami. The distribution and the size of accessory oral sclerites below the apical region of curved mouthhooks, the shape of the dental sclerite and its fusion with the basal part of the mouthhooks through sclerotized junction are other distinctive larval features of Reinwardtiinae, which comply with *Alluaudinella* larvae.

Although phylogenetic analyses do not provide unambiguous results regarding the position of *Alluaudinella*, certain tree topologies that conflict with traditional classification of *Alluaudinella* within Phaoniinae (Figure 9) are repeatedly observed. Similar to the recently proposed changes (Grzywacz et al., 2021), these results support both the resurrection of subfamily Reinwardtiinae as well as the transfer of *Eginia ocypterata* + *Xenotachina* sp. into this subfamily.

TABLE 2 Summary of certain larval characters of *Alluaudinella*, *Aethiopomyia* and *Ochromusca* compared to *Dichaetomyia* as a selected representative of Phaoniinae.

Larval characters	*Alluaudinella*, *Aethiopomyia*, *Ochromusca*	*Dichaetomyia*	Reinwardtiinae
Larval biology	Trimorphic saprophages	Monomorphic obligatory carnivores	Trimorphic saprophages, trimorphic facultative carnivores
Mouthhooks	Massive	Slender	Massive
Dental sclerites fused with mouthhook	Yes	Yes	Yes
Posterior ribbon	Absent	Present	Absent
Basal sclerite	Robust	Elongated	Robust
Posterior spiracles	Massive	Small	Massive
Position of spiracular scar	Median	Median	Median to dorsal
Shape of respiratory slits	Sinuate to curved	Straight	Curved to tortuous
Arrangement of respiratory slits	Radiate	Subparallel to convergent	Radiate
Spinulation	Strong	Poor	Strong to moderate
Papillae on anal division	Distinct	Indistinguishable	Distinct
Sclerotization of hypopharynx	Indistinct	Distinct	Indistinct
Longitudinal ridges in hypopharynx	Present	Hardly visible to absent	Present

Note: The data included in the table is based on this study and the available literature data (Paterson, 1959; Pont & Dear, 1976; Skidmore, 1985).

Alluaudinella, included for the first time in a molecular phylogenetic analysis, clusters in all trees within a clade composed of Atherigoninae, Cyrtoneurininae, Phaoniinae and Reinwardtiinae. The systematic position of *Alluaudinella* is the only difference that is observed between analyses. While the GARLI and MrBayes trees are congruent and *Alluaudinella* emerges as the sister taxon of Reinwardtiinae + *Neomuscina*, in the RAxML tree *Alluaudinella* forms a clade with *Cyrtoneuropsis* and Atherigoninae as a sister group of Reinwardtiinae + *Neomuscina*. Nevertheless, *Alluaudinella* is not found to be the sister taxon of neither *Dichaetomyia* nor other Phaoniinae as would be expected from traditional classification (Couri & de Carvalho, 2003; Paterson, 1959; Pont & Dear, 1976). Previous studies relied solely on adult morphology, and little data on immature stages were included in the analysis. Phylogenetic tree obtained in this study from molecular data and the details of the morphology and natural history of the immature stages are inconsistent with the position of *Alluaudinella* as the sister taxon of *Dichaetomyia* and even in close relationships with other representatives of Phaoniinae.

4.2 | Immature stages morphology

A literature search revealed that the larval morphology of *Alluaudinella* provided so far is unsatisfactorily documented and at some points inconsistent with the present study. Most of the discrepancies relate to the recognition of sclerites of the cephaloskeleton and details of the spinulation pattern. The misidentification or overlooking of some sclerites is a common issue due to the resolution limitations of light microscopes, which do not allow for obtaining details of minute morphological structures (Grzywacz et al., 2014). It is noteworthy that none of the previous morphology descriptions identified all the sclerites documented in this study.

The egg morphology of *A. flavicornis* provided here closely resembles those of *A. bivittata* (Paterson, 1959) and *A. flavicornis* (Ekanem, 2008). Nevertheless, none of the previous authors has provided a description of the egg, and illustrations are limited to the outline of the shape only. On the other hand, an illustration of *A. jennyae* egg, provided by de Sousa et al. (2020) does not allow to discern whether the dorsal or the ventral surface was presented. SEM images presented in this study and line drawings or statements of previous authors clearly show that eggs of *Alluaudinella* (Ekanem, 2008; Paterson, 1959; Skidmore, 1985) and *Ochromusca* (Pont & Dear, 1976) have a peculiar shape, referred to by other authors as 'flanged' (Paterson, 1959) and classified as *Phaonia*-type sensu Thomson (1937). The junction between the median area and the remaining chorion forms longitudinal folds named 'hatching pleats', and these can be only slightly raised in *Musca*-type eggs or broadly foliaceous in *Phaonia*- and *Mydaea*-type (Grzywacz, Szpila, & Pape, 2012; Skidmore, 1985). Eggs of *Alluaudinella* are distinctly expanded, which may be regarded as folds of hatching pleats. However, contrary to other Muscidae where hatching pleats are clearly marked on the dorsal surface of the egg, in *Alluaudinella* the expansion is moved towards the latero-ventral surface and there is no distinct transition between the median area and expansions. Furthermore, in *Alluaudinella*, the dorsal surface is convex and the ventral surface is flat or slightly convex, while the opposite is present in other muscid eggs. Nevertheless, the egg cell and subsequently developing embryo, are located in the ventral part of the egg, not in the convex dorsal part. The description of the egg provided in this study differs from the types of muscid eggs listed and described so far (Ferrar, 1979; Grzywacz & Pape, 2010; Skidmore, 1985; Thomson, 1937). *Phaonia*-type egg and its modification, *Mydaea*-type, are common within Muscidae and have so far been reported in Atherigoninae, Coenosiinae, Mydaeinae, Phaoniinae and Reinwardtiinae (Ferrar, 1979; Skidmore, 1985; van Emden, 1965). Taking into consideration the current knowledge of the muscid eggs, as well as the peculiar morphology of *Alluaudinella* eggs, it seems reasonable not to conclude on the classification of *Alluaudinella* based on eggs morphology.

Ekanem (2008) provided drawings of the egg, larval body, the cephaloskeleton for all instars as well as the anal division and both anterior and posterior spiracles for the third instar. Cephaloskeleton considered as the first instar larva is in fact a second instar larva (Figure 2b in Ekanem, 2008). Additionally, this study confirms the presence of anterior spiracles in the first instar larva (Figure 5a). So far it has been proven that the first instar anterior spiracles are widespread in Cyclorrhapha and appear as a simple aperture almost invisible under the light microscope (Grzywacz, Pape, & Szpila, 2012; Kitching, 1976). Furthermore, the dorsal bridge is clearly smooth in the first instar, and porosity is only present in the remaining instars. As for the second instar, Ekanem (2008) presented the mouthhooks with suprabuccal teeth, the intermediate sclerite and the basal sclerite. In this study non-hooked mouthhooks, dental sclerites, accessory stomal sclerites, the epistomal sclerite, labial sclerites, rami and the ventral bridge are discerned. Moreover, we do not recognise a rupture of the posterior part of the basal sclerite, and instead, the whole cephaloskeleton is well sclerotized. In the third instar Ekanem (2008) presented mouthhooks, the intermediate sclerite and the basal sclerite. In this study suprabuccal teeth, anterior rods, oral bars, dental sclerites, accessory stomal sclerites, as well as paired rami and the ventral bridge are also revealed. As in the second instar, the basal

sclerite does not have a posterior rupture. What is more, single-, double- and triple-pointed spines on the spiracular field are revealed (Figure 8e), instead of the previous recognition of single-pointed spines only.

Following Skidmore (1985), the cephaloskeleton of the third instar larva of *Alluaudinella* is very similar to *Ochromusca*. Skidmore's (1985) examination of third instar larva of *O. trifaria* (Bigot, 1878) from puparium is incomplete due to the lack of recognition of accessory stomal sclerites, the epistomal sclerite, labial sclerites and rami. Nevertheless, a strong and massive cephaloskeleton, with properly recognised oral bars and anterior rods in the area below the apical part of the mouthhooks, as well as suprabuccal teeth are consistent with this study. Moreover, Skidmore (1985) stated that 'larval mouthparts, anal spiracles, and anal plate' of *A. bivittata* were presented by Paterson (1959), but only an outline of the shape of an egg and a puparium with schematically drawn posterior spiracles can be found in Paterson (1959).

4.3 | Identification of *Alluaudinella* larvae

This study provides descriptions that allow the determination of *Alluaudinella* specimens to subsequent larval stages and also to distinguish them from other Muscidae species. All larval stages of *Alluaudinella* are characterised by strong spinulation. This is particularly visible in the first thoracic segment, where sclerotized and prominent spines form a continued wreath. For each instar, the strongly developed post-anal papillae, sub-anal papillae, para-anal papillae and extra-anal papillae as well as four pairs of conical papillae (*p1*, *p3*, *p5*, *p7*) surrounding the spiracular field are other unique character states within Muscidae (Ferrar, 1979; Keilin & Tate, 1930; Schumann, 1954; Skidmore, 1985). The arrangement and size of the latter papillae resemble a distinct eight-pointed star. The first instar of *Alluaudinella* is characterised by the simple cephaloskeleton construction, typical of Cyclorrhapha (Ferrar, 1979; Schumann, 1954; Skidmore, 1985). Nevertheless, certain features allow them to be easily identified among other muscid species. The epistomal sclerite was overlooked by many previous authors or treated as an integral part of the labrum (Arnaldos et al., 2014; Skidmore, 1985; Szpila & Pape, 2005; Velásquez et al., 2013). In the first instar, the epistomal sclerite is placed between the anterior arms of parastomal bars (Grzywacz & Pape, 2014), however, this study reveals that the epistomal sclerite in *Alluaudinella* is neither fused nor even closely adjacent to the labrum, and the space between these two is filled with elongated parastomal bars. In the second instar, it would seem unique for *Alluaudinella* that the dental sclerite is fused with the base of mouthhooks. However, CLSM analysis of selected muscid species showed that it is not exclusive within Muscidae and the fusion of the dental sclerite with the mouthhook also occurs in *S. nudiseta* and species of the genera *Atherigona* and *Muscina*, what was not recognised by previous authors (Grzywacz & Pape, 2014; Velásquez et al., 2013). In the third instar, in turn, CLSM analysis revealed a prominent connection of the dental sclerite with the base of mouthhooks through the sclerotized junction. Previous studies on muscid morphology treated the dental sclerite as a separate sclerite (Grzywacz et al., 2015; Skidmore, 1985; Velásquez et al., 2013), however, this feature is not uncommon among the Muscidae and additional CLSM observations confirm that the dental sclerite is clearly fused with the base of mouthhooks in third instar larvae of *Coenosia* Meigen, 1826, *Lispe* Latreille, 1796, *Muscina*, *Phaonia* and *Synthesiomyia* (KW & AG; data unpublished).

According to Grzywacz et al. (2015), spiracular distance factor (SDF) defined by van Emden (1965) is not a constant ratio in a particular species and is useless for taxonomic purposes; therefore, it should not be considered as a diagnostic feature in the identification keys. This study confirms that the distance between posterior spiracles increases with the maturation of larva (Figure 8g,h).

Walczak et al. (2022) stated that muscid larvae possess parastomal bars in a modified form of rod-like anterodorsal extension of intermediate sclerite, and with or without posterior connection with the basal sclerite. In this study, the third instar of *Alluaudinella* is also reported to possess parastomal bars, easily discerned on the dorsal edge of the intermediate sclerite (Figure 4g), further confirmed by the frame-by-frame analysis of CLSM stack images.

5 | CONCLUSIONS

This study provides the first DNA-based phylogenetic analysis including newly obtained gene sequences of *Alluaudinella* spp. Although the systematic position of *Alluaudinella* has not been unambiguously confirmed, the phylogenetic analyses show that *Alluaudinella* either emerged as the sister taxon of Reinwardtiinae + *Neomuscina* or is the part of a clade *Alluaudinella-Cyrtoneuropsis-Atherigona* with a sister group relationship to Reinwardtiinae+*Neomuscina*. Results provided in this study are incongruent with the traditional concept of *Alluaudinella*, *Aethiopomyia* and *Ochromusca* as closely related to Dichaetomyia. Neither the results of molecular analysis nor the features of the larval morphology

support the placement of *Alluaudinella* in the subfamily Phaoniinae. Taking into consideration significant larval discrepancies between *Alluaudinella* and Phaoniinae, and simultaneously the strong resemblance of *Alluaudinella* with Reinwardtiinae larvae (Table 2), a transfer of *Alluaudinella*, *Aethiopomyia* and *Ochromusca* into the subfamily Reinwardtiinae is proposed.

ACKNOWLEDGEMENTS

We would like to express our appreciation to Mr. Nikita Vikhrev (Zoological Museum of Moscow University, Moscow, Russia), Drs. Alessandra Rung, Martin Hauser and Stephen D. Gaimari (California Department of Food and Agriculture, Sacramento, California, USA), Assoc. Profs. Alexey Solodovnikov and Lars Vilhelmsen (Natural History Museum of Denmark, University of Copenhagen, Copenhagen, Denmark) and Prof. Thai Hong Pham (Vietnam National Museum of Nature, Hanoi, Vietnam) for help in obtaining material. This research was supported by the National Science Centre of Poland (grant no. 2019/33/B/NZ8/02316 to AG).

ORCID

Kinga Walczak https://orcid.org/0000-0002-7413-9828
Thomas Pape https://orcid.org/0000-0001-6609-0609
Krzysztof Szpila https://orcid.org/0000-0002-3039-3146
Andrzej Grzywacz https://orcid.org/0000-0003-3745-5992

REFERENCES

Arnaldos, M. I., Ubero-Pascal, N., García, R., Carles-Tolrá, M., Presa, J. J., & García, M. D. (2014). The first report of *Telomerina flavipes* (Meigen, 1830) (Diptera, Sphaeroceridae) in a forensic case, with redescription of its pupa. *Forensic Science International*, *242*, e22–e30. https://doi.org/10.1016/j.forsciint.2014.07.023

Bernasconi, M. V., Valsangiacomo, C., Piffaretti, J. C., & Ward, P. I. (2000). Phylogenetic relationships among Muscoidea (Diptera: Calyptratae) based on mitochondrial DNA sequences. *Insect Molecular Biology*, *9*, 67–74. https://doi.org/10.1046/j.1365-2583.2000.00158.x

Couri, M. S., & de Carvalho, C. J. B. (2003). Systematic relations among *Philornis* Meinert, *Passeromyia* Rodhain & Villeneuve and allied genera (Diptera, Muscidae). *Brazilian Journal of Biology*, *63*, 223–232. https://doi.org/10.1590/S1519-69842003000200007

Couri, M. S., & de Sousa, V. R. (2020). On *Alluaudinella* Giglio-Tos (Diptera, Muscidae) with the revision of the type specimens deposited in the museum für Naturkunde, Berlin (Berlin, Germany) and the description of a new species. *Studies on Neotropical Fauna and Environment*, *56*, 1–6. https://doi.org/10.1080/01650521.2020.1783483

Couri, M. S., Pont, A. C., & Penny, N. D. (2006). Muscidae (Diptera) from Madagascar: Keys to identification, descriptions of new species, and new records. *Proceedings of the California Academy of Sciences*, *57*, 799–923.

Courtney, G. W., Sinclair, B. J., & Meier, R. (2000). Morphology and terminology of Diptera larvae. In L. Papp & B. Darvas (Eds.), *Contributions to a manual of Palaearctic Diptera (with special reference to flies of economic importance)* (pp. 85–161). Science Herald Press.

de Carvalho, C. J. B. (2002). *Muscidae (Diptera) of the neotropical region: Taxonomy* (pp. 1–287). Editora Universidade Federal do Paraná.

de Sousa, V. R., Pereira, A. F. M., & Couri, M. S. (2020). On *Aethiopomyia* Malloch (Diptera, Muscidae) with the revision of the type specimens deposited in the museum für Naturkunde, Berlin (Germany) with a key to species. *ZooKeys*, *926*, 73–80. https://doi.org/10.3897/zookeys.926.49210

Ekanem, M. S. (2008). Immature stages and developmental biology of two muscid flies (Cyclorrhapha: Diptera) which breed in carrion in southern Nigeria. *The Zoologist*, *6*, 1–6. https://doi.org/10.4314/tzool.v6i1.41354

Ferrar, P. (1979). The immature stages of dung-breeding muscoid flies in Australia, with notes on the species, and keys to larvae and puparia. *Australian Journal of Zoology, Supplementary Series*, *73*, 1–106. https://doi.org/10.1071/AJZS073

Gregor, F., Rozkošný, R., Barták, M., & Vaňhara, J. (2002). The Muscidae (Diptera) of Central Europe. Folia Facultatis Scientiarum Naturalium Universitatis Masarykianae Brunensis. *Biologia*, *107*, 1–280.

Grzywacz, A. (2013). Third instar larva morphology of *Hydrotaea cyrtoneurina* (Zetterstedt, 1845) (Diptera: Muscidae) – A species of forensic interest. *Polish Journal of Entomology*, *82*(4), 303–315. https://doi.org/10.2478/v10200-012-0044-5

Grzywacz, A., Góral, T., Szpila, K., & Hall, M. J. R. (2014). Confocal laser scanning microscopy as a valuable tool in Diptera larval morphology studies. *Parasitology Research*, *113*, 4297–4302. https://doi.org/10.1007/s00436-014-4125-0

Grzywacz, A., Hall, M. J. R., & Pape, T. (2015). Morphology successfully separates third instar larvae of *Muscina*. *Medical and Veterinary Entomology*, *29*, 314–329. https://doi.org/10.1111/mve.12117

Grzywacz, A., & Pape, T. (2010). Egg morphology of *Mydaea lateritia* (Rondani, 1866) (Diptera: Muscidae). *Entomologica Fennica*, *21*, 187–192. https://doi.org/10.33338/ef.84530

Grzywacz, A., & Pape, T. (2014). Larval morphology of *Atherigona orientalis* (Schiner) (Diptera: Muscidae) – A species of sanitary and forensic importance. *Acta Tropica*, *137*, 174–184. https://doi.org/10.1016/j.actatropica.2014.05.018

Grzywacz, A., Pape, T., & Szpila, K. (2012). Larval morphology of the lesser housefly, *Fannia canicularis*. *Medical and Veterinary Entomology*, *26*, 70–82. https://doi.org/10.1111/j.1365-2915.2011.00968.x

Grzywacz, A., Szpila, K., & Pape, T. (2012). Egg morphology of nine species of *Pollenia* Robineau-Desvoidy, 1830 (Diptera: Calliphoridae). *Microscopy Research and Technique*, *75*, 955–967. https://doi.org/10.1111/j.1365-2915.2011.00968.x

Grzywacz, A., Trzeciak, P., Wiegmann, B. M., Cassel, B. K., Pape, T., Walczak, K., Bystrowski, C., Nelson, L., & Piwczyński, M. (2021). Towards a new classification of Muscidae (Diptera): A comparison of hypotheses based on multiple molecular

phylogenetic approaches. *Systematic Entomology*, *46*, 508–525. https://doi.org/10.1111/syen.12473

Grzywacz, A., Wallman, J. F., & Piwczyński, M. (2017). To be or not to be a valid genus: The systematic position of *Ophyra* R.-D. revised (Diptera: Muscidae). *Systematic Entomology*, *42*, 714–723. https://doi.org/10.1111/syen.12240

Haseyama, K. L. F., Wiegmann, B. M., Almeida, E. A. B., & de Carvalho, C. J. B. (2015). Say goodbye to tribes in the new house fly classification: A new molecular phylogenetic analysis and an updated biogeographical narrative for the Muscidae (Diptera). *Molecular Phylogenetics and Evolution*, *89*, 1–12. https://doi.org/10.1016/j.ympev.2015.04.006

Hennig, W. (1965). Vorarbeiten zu einem phylogenetischen System der Muscidae (Diptera: Cyclorrhapha). *Stuttgarter Beiträge Zur Naturkunde*, *141*, 1–100.

Hinton, H. E. (1981). *The biology of insect eggs*. Pergamon Press.

Keilin, D., & Tate, P. (1930). On certain semi-carnivorous anthomyid larvae. *Parasitology*, *22*, 168–181.

Kim, B. Y., Wang, J. R., Miller, D. E., Barmina, O., Delaney, E., Thompson, A., Comeault, A. A., Peede, D., ERR, D.'. A., Pelaez, J., Aguilar, J. M., Haji, D., Matsunaga, T., Armstrong, E. E., Zych, M., Ogawa, Y., Stamenković-Radak, M., Jelić, M., Veselinović, M. S., … Petrov, D. A. (2021). Highly contiguous assemblies of 101 drosophilid genomes. *eLife*, *10*, 1–32. https://doi.org/10.7554/eLife.66405

Kitching, R. L. (1976). On the prothoracic spiracles of the first instar larvae of calyptrate Cyclorrhapha (Diptera). *Australian Journal of Entomology*, *15*, 233–235. https://doi.org/10.1111/j.1440-6055.1976.tb01698.x

Kutty, S. N., Pont, A. C., Meier, R., & Pape, T. (2014). Complete tribal sampling reveals basal split in Muscidae (Diptera), confirms saprophagy as ancestral feeding mode, and reveals an evolutionary correlation between instar numbers and carnivory. *Molecular Phylogenetics and Evolution*, *78*, 349–364. https://doi.org/10.1016/j.ympev.2014.05.027

Lanfear, R., Calcott, B., Ho, S. Y. W., & Guindon, S. (2012). PartitionFinder: Combined selection of partitioning schemes and substitution models for phylogenetic analyses. *Molecular Biology and Evolution*, *29*, 1695–1701. https://doi.org/10.1093/molbev/mss020

Malloch, J. R. (1921). Exotic Muscaridae (Diptera).–II. *Annals and magazine of Natural History*, *9*(7), 420–431.

Malloch, J. R. (1925). Exotic Muscaridae (Diptera).–XVII. *Annals and magazine of Natural History*, *9*(16), 361–377.

Meier, R., & Lim, G. S. (2009). Conflict, convergent evolution, and the relative importance of immature and adult characters in Endopterygote phylogenetics. *Annual Review of Entomology*, *54*, 85–104. https://doi.org/10.1146/annurev.ento.54.110807.090459

Paterson, H. E. (1959). Notes on the genus *Alluaudinella* G.-T. with the description of a new species and a key to the known species of the genus (Diptera: Muscidae). *Mémoires de l'Institut Scientifique de Madagascar*, *11*, 355–367.

Piwczyński, M., Pape, T., Deja-Sikora, E., Sikora, M., Akbarzadeh, K., & Szpila, K. (2017). Molecular phylogeny of Miltogramminae (Diptera: Sarcophagidae): Implications for classification, systematics and evolution of larval feeding strategies. *Molecular Phylogenetics and Evolution*, *116*, 49–60. https://doi.org/10.1016/j.ympev.2017.07.001

Pont, A. C. (1974). A revision of the genus *Passeromyia* Rodhain & Villeneuve (Diptera: Muscidae). *Bulletin of the British Museum (Natural History) Entomology*, *30*, 341–372. https://doi.org/10.5962/bhl.part.24943

Pont, A. C. (1980). Family Muscidae. In R. W. Crosskey (Ed.), *Catalogue of the Diptera of the Afrotropical region* (pp. 719–761). British Museum (Natural History).

Pont, A. C., & Dear, J. P. (1976). A synopsis of the genus *Ochromusca* Malloch, 1927 (Diptera: Muscidae). *Annals of the Natal Museum*, *22*, 747–753 https://hdl.handle.net/10520/AJA03040798_598

Rambaut, A., Drummond, A. J., Xie, D., Baele, G., & Suchard, M. A. (2018). Posterior summarization in Bayesian phylogenetics using Tracer 1.7. *Systematic Biology*, *67*, 901–904. https://doi.org/10.1093/sysbio/syy032

Roberts, M. J. (1970). The structure of the mouthparts of syrphid larvae (Diptera) in relation to feeding habits. *Acta Zoologica*, *51*, 43–65.

Ronquist, F., Teslenko, M., van der Mark, P., Ayres, D. L., Darling, A., Höhna, S., Larget, B., Liu, L., Suchard, M. A., & Huelsenbeck, J. P. (2012). MrBayes 3.2: Efficient Bayesian phylogenetic inference and model choice across a large model space. *Systematic Biology*, *61*, 539–542. https://doi.org/10.1093/sysbio/sys029

Schumann, H. (1954). Morphologisch-systematische Studien an Larven von hygienisch wichtigen mitteleuropäischen Dipteren der Familien Calliphoridae-Muscidae. In *Matematisch-naturwissenschaftliche Reihe III (4/5)* (pp. 245–274). Wiss. Z. Univ. Greifswald Jahrgang 1953/54.

Séguy, E. (1937). Diptera, family Muscidae. In P. Wytsmann (Ed.), *Genera Insectorum, 205* (pp. 1–604). Desmet-Verteneuil.

Shinonaga, S. (2003). *A monograph of the Muscidae of Japan* (pp. 1–347). Tokai University Press.

Simon, C., Frati, F., Beckenbach, A., Crespi, B., Liu, H., & Flook, P. (1994). Evolution, weighting, and phylogenetic utility of mitochondrial gene sequences and a compilation of conserved polymerase chain reaction primers. *Annals of the Entomological Society of America*, *87*, 651–701. https://doi.org/10.1093/aesa/87.6.651

Skidmore, P. (1985). The biology of the Muscidae of the world. *Series Entomologica*, *29*, 1–550.

Stamatakis, A. (2014). RAxML version 8: A tool for phylogenetic analysis and post-analysis of large phylogenies. *Bioinformatics*, *30*, 1312–1313. https://doi.org/10.1093/bioinformatics/btu033

Sukumaran, J., & Holder, M. T. (2010). DendroPy: A python library for phylogenetic computing. *Bioinformatics*, *26*, 1569–1571. https://doi.org/10.1093/bioinformatics/btq228

Szpila, K. (2010). *The first instar of European Miltogramminae (Diptera, Sarcophagidae)* (pp. 1–272). Wydawnictwo Naukowe UMK.

Szpila, K., & Pape, T. (2005). The first instar larva of *Apodacra pulchra* (Diptera: Sarcophagidae, Miltogramminae). *Insect Systematics & Evolution*, *36*, 293–300. https://doi.org/10.1163/187631205788838447

Szpila, K., & Pape, T. (2007). Rediscovery, redescription and reclassification of *Beludzhia phylloteliptera* (Diptera: Sarcophagidae: Miltogramminae). *European Journal of Entomology*, *104*, 119–137. https://doi.org/10.14411/eje.2007.018

Thomson, R. C. M. (1937). Observations on the biology and larvae of the Anthomyiidae. *Parasitology*, *29*, 273–358. https://doi.org/10.1017/S0031182000024847

van Emden, F. I. (1939). Muscidae: A.–Muscinae and Stomoxydinae. Ruwenzori Expedition *1934-5*, **II**, 49-89.

van Emden, F. I. (1965). Diptera. Muscidae, part 1. In R. B. S. Sewell & M. L. Roonwal (Eds.), *The fauna of India and the adjacent countries* Vol. 7. pp. xiv + 647, 2 pls. Government of India.

Velásquez, Y., Ivorra, T., Grzywacz, A., Martínez-Sánchez, A., Magaña, C., García-Rojo, A., & Rojo, S. (2013). Larval morphology, development and forensic importance of *Synthesiomyia nudiseta* (Diptera: Muscidae) in Europe: A rare species or just overlooked? *Bulletin of Entomological Research*, *103*, 98–110. https://doi.org/10.1017/S0007485312000491

Walczak, K., Szpila, K., Nelson, L., Pape, T., Hall, M. J. R., Alves, F., & Grzywacz, A. (2023). Larval morphology of the avian parasitic genus *Passeromyia*: playing hide and seek with a parastomal bar. *Medical and Veterinary Entomology*, *37*(1), 14–26. https://doi.org/10.1111/mve.12603

Zwickl, D. J. (2006). Genetic algorithm approaches for the phylogenetic analysis of large biological sequence datasets under the maximum likelihood criterion. Unpublished Ph.D. Thesis, University of Texas, Austin. https://repositories.lib.utexas.edu/handle/2152/2666

SUPPORTING INFORMATION

Additional supporting information can be found online in the Supporting Information section at the end of this article.

How to cite this article: Walczak, K., Pape, T., Ekanem, M., Szpila, K., & Grzywacz, A. (2023). Insights into the systematics of *Alluaudinella* and allied *Aethiopomyia* and *Ochromusca* (Muscidae, Diptera). *Zoologica Scripta*, *00*, 1–19. https://doi.org/10.1111/zsc.12584

Table S1. List of species used in study, including authorship, classification, voucher ID, collecting data and GenBank accession numbers. Voucher ID and collecting data are provided for newly obtained sequences. Accession numbers of newly obtained sequences are bolded.

Species/classification	Voucher ID	Collecting data	COI	cytB	CAD	Ef1α
Atherigoninae						
Atherigona divergens Stein, 1913	KEIB_DIP_02208	Ethiopia	**OP800289**	**OP807859**	-	**OP837972**
Atherigona pendleburyi Malloch, 1935	KEIB_DIP_01861	Malaysia	**OP800290**	**OP807860**	-	**OP837973**
Atherigona varia (Meigen, 1826)	KEIB_DIP_00997 KEIB_DIP_00827	Spain	**OP800291**	**OP807861**	-	MN555710
Azeliinae						
Australophyra rostrata (Robineau-Desvoidy, 1830)	KEIB_DIP_00832	Australia	MN555650	KU932153	-	KU932180
Hydrotaea dentipes (Fabricius, 1805)	KEIB_DIP_00244	Poland	KU932132	KU932161	FJ025579	KU932187
Hydrotaea ignava (Harris, [1780])	KEIB_DIP_00242	Poland	KU932134	KU932164	-	KU932190
Hydrotaea irritans (Fallén, 1823)	KEIB_DIP_01413	Poland	KU932135	FJ025723	FJ025580	FJ025680
Hydrotaea velutina Robineau-Desvoidy, 1830	KEIB_DIP_00243	Poland	KU932141	KU932172	-	KU932197
Potamia littoralis Robineau-Desvoidy, 1830	KEIB_DIP_00241	Poland	KU932145	KU932176	FJ025598	KU932201
Cyrtoneurininae						
Cyrtoneuropsis dubia Snyder, 1954	KEIB_DIP_02318	French Guiana	**OP800292**	**OP807862**	-	**OP837974**
Cyrtoneuropsis veniseta (Stein, 1904)	KEIB_DIP_02311	French Guiana	**OP800293**	**OP807863**	KP161819	**OP837975**
Neomuscina currani Snyder, 1949	-	Brazil	KP161705	-	KP161833	-
Neomuscina instabilis Snyder, 1949	-	-	KJ510634	KJ510567	-	KJ510598
Reinwardtiinae						
Alluaudinella bivittata	KEIB_DIP_01495	Mozambique	**OP800287**	-	-	**OP837970**

(Macquart, 1943)						
Alluaudinella flavicornis Macquart, 1855	KEIB_DIP_01114	Nigeria	**OP800288**	**OP807858**	-	**OP837971**
Calliphoroides antennatis (Hutton, 1881)	KEIB_DIP_02217	New Zealand	-	**OP807872**	-	**OP837983**
Eginia ocypterata (Meigen, 1826)	KEIB_DIP_00834	Poland	MN555654	KJ510551	-	KJ510589
Muscina angustifrons (Loew, 1858)	-	Japan	MF511758	-	KP161831	MK292741
Muscina levida (Harris, 1780)	-	-	FJ025638	FJ025735	-	FJ025688
Muscina pascuorum (Meigen, 1826)	KEIB_DIP_01930	Poland	**OP800296**	**OP807866**	-	**OP837977**
Muscina stabulans (Fallén, 1817)	KEIB_DIP_00238	Poland	MN555671	MN555690	EF531167	MN555706
Passeromyia heterochaeta (Villeneuve, 1915)	KEIB_DIP_02220A	Ethiopia	MN410989	**OP807873**	-	**OP837984**
Passeromyia indecora (Walker, 1858)	KEIB_DIP_01135	Australia	KJ510635	KJ510568	-	KJ510599
Passeromyia longicornis (Macquart, 1851)	KEIB_DIP_00976	Australia	KY937944	**OP807874**	-	**OP837985**
Passeromyia steini Pont, 1970	KEIB_DIP_02066	Australia	**OP800297**	**OP807867**	-	**OP837978**
Philornis zeteki Dodge & Aitken, 1963	-	Brazil	KP161718	-	KP161839	KP161748
Synthesiomyia nudiseta (van der Wulp, 1883)	KEIB_DIP_00825	Spain	MN555677	MN555693	KP161849	MN555709
Xenotachina sp. Malloch, 1921	KEIB_DIP_02225	Vietnam	**OP800301**	**OP807871**	-	**OP837982**
Phaoniinae						
Dichaetomyia bibax (Wiedemann, 1830)	-	-	KJ510615	KJ510549	KP161821	KJ510588
Dichaetomyia vicaria (Walker, 1959)	KEIB_DIP_00833	Australia	MN555652	MN555680	-	MN555694
Helina evecta (Harris, 1780)	-	-	FJ025619	FJ025719	-	FJ025675
Helina fratercula	-	-	KJ510621	KJ510555	-	KJ510592

(Zetterstedt, 1845)						
Helina lasiophthalma (Macquart, 1835)	-	-	FJ025621	FJ025720	KJ510577	-
Helina reversio (Harris, [1780])	KEIB_DIP_00823	Poland	MN555659	MN555685	-	MN555700
Lophosceles hians (Zetterstedt, 1837)	KEIB_DIP_01845	Russia	**OP800295**	**OP807865**	-	-
Lophosceles cinereiventris (Zetterstedt, 1845)	-	-	KJ510629	KJ510562	KJ510579	-
Metopomyia atropunctipes Malloch, 1922	-	-	KJ510630	KJ510563	-	KJ510596
Phaonia gobertii (Mik, 1881)	-	-	KJ510638	KJ510571	-	KJ510602
Phaonia pallida (Fabricius, 1787)	KEIB_DIP_01899	Poland	**OP800298**	**OP807868**	FJ025596	**OP837979**
Phaonia subventa (Harris, 1780)	-	-	FJ025652	FJ025748	-	-
Prohardyia carinata (Stein, 1910)	KEIB_DIP_02068	Australia	**OP800300**	**OP807870**	FJ025596	**OP837981**
Prohardyia sp. Pont, 1969	-	Australia	KP161672	-	KP161840	KP161751
Muscinae						
Musca domestica Linnaeus, 1758	KEIB_DIP_00247	Poland	KU932143	KU932174	FJ025591	KU932199
Neomyia cornicina (Fabricius, 1781)	KEIB_DIP_00248	Poland	KU932144	KU932175	KP161834	KU932200
Pyrellia rapax (Harris, [1780])	KEIB_DIP_00979	Poland	KU932146	KU932177	-	KU932202
Stomoxys calcitrans (Linnaeus, 1758)	KEIB_DIP_00835	Portugal	KU932147	KU932178	EF531173	KU932203
Mydaeinae						
Mydaea ancilla (Meigen, 1826)	-	-	FJ025639	FJ025737	FJ025592	FJ025690
Mydaea urbana (Meigen, 1826)	-	-	FJ025641	FJ025739	FJ025593	FJ025691
Coenosiinae						
Coenosia testacea	-	-	FJ025605	FJ025707	FJ025569	-

(Robineau-Desvoidy, 1830)						
Coenosia tigrina (Fabricius, 1775)	-	-	FJ025606	FJ025708	FJ025570	-
Limnophora maculosa (Meigen, 1826)	-	-	FJ025627	FJ025726	FJ025582	FJ025685
Limnophora olympiae Lyneborg, 1965	-	-	FJ025628	FJ025727	FJ025583	FJ025686
Lispe tentaculata (De Geer, 1776)	KEIB_DIP_01118	Spain	MN555667	MN555687	FJ025585	MN555703
Lispocephala mikii (Strobl, 1893)	-	Japan	KP161692	-	KP161825	KP161739
Orchisia costata (Meigen, 1826)	-	Japan	KP161668	-	KP161836	KP161744
OUTGROUP						
Hydrophoria lancifer (Harris, 1780)	-	-	DQ657043	DQ657058	EF531164	FJ025677
Hydrophoria ruralis (Meigen, 1826)	KEIB_DIP_01049	Poland	**OP800294**	**OP807864**	-	**OP837976**
Lasiomma latipenne (Zetterstedt, 1838)	-	-	DQ657044	DQ657060	-	FJ025683
Paregle coerulescens (Strobl, 1893)	-	-	FJ025645	FJ025741	-	FJ025693
Phorbia genitalis Schnabl, 1911	KEIB_DIP_01047	Poland	**OP800299**	**OP807869**	-	**OP837980**

Article 2

Walczak, K., Pape, T., Wallman, J. F., Szpila, K., & Grzywacz, A. (2024). To see the unseen: notes on the larval morphology and systematic position of *Achanthiptera* Rondani (Diptera: Muscidae). Arthropod Systematics and Phylogeny, 82: 305–322.

https://doi.org/10.3897/ASP.82.E116703

PENSOFT
SENCKENBERG world of biodiversity
Leibniz Association

To see the unseen: notes on the larval morphology and systematic position of *Achanthiptera* Rondani (Diptera: Muscidae)

Kinga Walczak[1,2], Thomas Pape[3], James F. Wallman[4,5], Krzysztof Szpila[1], Andrzej Grzywacz[1,2]

1 *Department of Ecology and Biogeography, Faculty of Biological and Veterinary Sciences, Nicolaus Copernicus University in Toruń, Poland*
2 *Centre for Modern Interdisciplinary Technologies, Nicolaus Copernicus University in Toruń, Poland*
3 *Natural History Museum of Denmark, University of Copenhagen, Copenhagen, Denmark*
4 *Faculty of Science, University of Technology Sydney, Ultimo, NSW, Australia*
5 *School of Earth, Atmospheric and Life Sciences, University of Wollongong, Wollongong, NSW, Australia*

https://zoobank.org/AB3BBC89-3032-4827-B39A-0EB3086E4086

Corresponding authors: Kinga Walczak (walczak.kinga00@gmail.com), Andrzej Grzywacz (hydrotaea@gmail.com)

Received 1 December 2023
Accepted 1 February 2024
Published 25 April 2024

Academic Editors Bradley Sinclair, Klaus-Dieter Klass

Citation: Walczak K, Pape T, Wallman JF, Szpila K, Grzywacz A (2024) To see the unseen: notes on the larval morphology and systematic position of *Achanthiptera* Rondani (Diptera: Muscidae). Arthropod Systematics & Phylogeny 82: 305–322. https://doi.org/10.3897/asp.82.e116703

Abstract

The muscid genus *Achanthiptera* Rondani (Diptera: Muscidae) was classified within its own subfamily Achanthipterinae for decades due to a misinterpretation of adult morphology. Conversely, the larval morphology suggested that *Achanthiptera* should be classified within Azeliinae, yet no formal changes were implemented based on this source of data. Using scanning electron microscopy (SEM) and confocal laser scanning microscopy (CLSM), we examined the larval morphology of *Ac. rohrelliformis* (Robineau-Desvoidy), *Potamia littoralis* Robineau-Desvoidy and *Australophyra rostrata* Robineau-Desvoidy. Despite the challenges posed by the poor condition of hundred-year-old museum specimens of *Ac. rohrelliformis* for light microscopy, CLSM examination yielded satisfactory results. Additionally, CLSM observations revealed peculiar modifications to the cephaloskeleton, including a dome-shaped (second instar) or spade-like (third instar) anterior rod attached to each mouthhook in *Ac. rohrelliformis* and *P. littoralis*. These structural modifications are likely to enhance the efficiency of food collecting by enlarging the surface of the mouthhooks. The results of our morphological analyses lead to the conclusion that larvae of *Au. rostrata* are facultative carnivores, while modified accessory oral sclerites in *Ac. rohrelliformis* and *P. littoralis* suggest a saprophagous feeding strategy. This study contributes new evidence that *Achanthiptera* is the sister taxon to *Potamia* Robineau-Desvoidy, and both are nested within the subfamily Azeliinae.

Key words

Achanthiptera rohrelliformis, anterior rod, confocal laser scanning microscopy, oral bar, saprophagy

1. Introduction

Achanthiptera rohrelliformis (Robineau-Desvoidy) is the sole representative of the muscid genus *Achanthiptera* Rondani. Most records and observations of this species are from the European part of the Palaearctic Region (Zielke 2018), but it has also been recorded from China (Shanxi), Siberia and Tajikistan (Skidmore 1985; Sorokina and Pont 2010). Since *Ac. rohrelliformis* is an uncommon species (Lobanov 1975; Bloxham 1982) with

short-lived adults (Skidmore 1985), information about its biology is scarce and found in only a handful of publications. Until now, adults of *Achanthiptera* have been noticed visiting colonies of aphids (Homoptera: Aphididae) (Cuny 1978), and females have been observed near vespid (Hymenoptera: Vespidae) nests where they lay eggs containing fully formed first-instar larvae, which hatch immediately after oviposition (Séguy 1923) and feed on decaying matter (Skidmore 1985). Larvae have been reported from nests of species of *Vespa* Linnaeus and *Vespula* Thomson (Hennig 1965; Bloxham 1978; Skidmore 1985), yet Lobanov (1975) also found them under moss on a drying swamp and in soil under decaying honey fungi *Armillaria* (Fr.) Staude. The fact that *Achanthiptera* larvae have been found in different substrates was overlooked, leading to a common belief that this genus is associated exclusively with social Hymenoptera (Skidmore 1985). Taking this into consideration, as well as the morphology of the third-instar cephaloskeleton, Skidmore (1985) concluded that larvae of *Achanthiptera* are trimorphic facultative carnivores, signifying the presence of three free-living larval instars.

The systematic position of *Achanthiptera* has long been a matter of great interest. *Achanthiptera* was assigned to the tribe Achanthipterini (Hennig 1955) and later to the tribe Phaoniini (Assis Fonseca 1968), in both cases of the paraphyletic subfamily Phaoniinae. Hennig (1965) concluded that *Achanthiptera* should be classified in its own subfamily based on his earlier observation (Hennig 1955) that a spiracle is retained in the female abdominal segment 6, distinguishing it from all other adult Muscidae, which lack spiracles distal to abdominal segment 5 (except *Cariocamyia* Snyder (Vockeroth 1972)). Later authors have widely accepted and implemented this classification over the years (Lobanov 1975; Michelsen 1977; Cuny 1978; Bloxham 1982; Pont 1986; Rognes 1986; de Carvalho 1989; Couri 2007; Fan 2008; Kutty et al. 2008). Also Skidmore (1985) adopted Hennig's classification, despite recognising the similarity in the biology and morphology of larvae of *Ac. rohrelliformis* with species from the subfamily Azeliinae (Lobanov 1975; Skidmore 1985). Later re-examination of *Ac. rohrelliformis* revealed, however, that Hennig's (1955, 1965) observation was a misinterpretation (Kutty et al. 2014), thereby rejecting the sole morphological support for the monospecific subfamily Achanthipterinae. Based on this observation and results of molecular phylogeny reconstruction in which *Ac. rohrelliformis* formed a sister group with *P. littoralis* Robineau-Desvoidy, the genus *Achanthiptera* was assigned to the subfamily Azeliinae (Kutty et al. 2014, fig. 2). The close relationship between *Achanthiptera* and *Potamia* has been confirmed in subsequent morphological (Jorge 2016) and molecular studies (Haseyama et al. 2015; Grzywacz et al. 2017), and these two genera appear to be closely related to *Australophyra* Malloch (Grzywacz et al. 2017).

Australophyra and *Potamia* are both small muscid genera. *Australophyra* is limited to only one species, *Au. rostrata* Robineau-Desvoidy, restricted to the Australotropical Region (Pont 1973; Savage and Wheeler 2004) and *Potamia* is represented by seven species (Evenhuis and Pape 2023). *Australophyra* has been considered for some time a synonym of *Ophyra* Robineau-Desvoidy (Hardy 1939; Sabrosky 1948; Hennig 1955) or *Hydrotaea* Robineau-Desvoidy (Pont 1989) or regarded as a subgenus of *Ophyra* (Emden 1965). Recently *Australophyra* was resurrected as a valid genus based on adult morphology by Savage and Wheeler (2004), which was later supported by molecular analyses (Grzywacz et al. 2017). *Australophyra rostrata*, the black carrion fly, has been frequently found on human cadavers (Archer et al. 2006; Dawson et al. 2020) and animal carrion (Archer and Elgar 2003a, 2003b; McIntosh et al. 2017), particularly in the advanced stage of decomposition (Fuller 1932; Pont 1973). As a tertiary agent of myiasis, its veterinary importance is negligible as larvae develop in contaminated wool rather than causing fly strike (Zumpt 1965). Fuller (1934) and Skidmore (1985) stated that larvae of *Au. rostrata* are primarily saprophagous, but ultimately, because they have been observed preying on blow fly larvae and conspecific larvae, Skidmore (1985) regarded them as trimorphic facultative carnivores. The genus *Potamia* is widespread in the Holarctic and present in the Neotropical and Oriental regions (Pont 1986; Barták and Roháček 2011). Adults of the most common *Potamia* species, *P. littoralis*, have been frequently collected on tree trunks, honeydew, flowers, and visiting aphid colonies (Cuny 1978; Skidmore 1985), as well as on human cadavers and animal carrion (Grzywacz et al. 2017). In turn, larvae have been found in human faeces, animal dung, rotten wood, fungi, nests of yellow jackets, hornets (Zimin 1948; Skidmore 1985) and various hole-nesting birds (Iwasa and Hori 1993; Iwasa et al. 1995). Skidmore (1985) considered *Potamia* larvae as trimorphic facultative carnivores, however Séguy (1923) and Iwasa et al. (1995) believed the larvae to be saprophages or coprophages since they were found in faecal matter and in nesting materials, rather than feeding on nestlings or their carrion.

Despite numerous changes in the tribal and subfamilial classification of the family Muscidae, *Potamia* (since Hennig (1955, 1965)) and *Australophyra* (since Malloch (1923, 1925)) have consistently been considered as closely related to *Hydrotaea*. Whenever muscid classifications were rearranged, these genera were classified together in a higher-level taxon and assigned to the subfamily Azeliinae (Hennig 1965; Lobanov 1965; Pont 1973), supported by the morphology of both immatures and adults (Hennig 1955, 1965; Skidmore 1985; Pont 1986; de Carvalho 1989; Savage and Wheeler 2004; Couri 2010; Jorge 2016; Michelsen 2022) as well as by molecular analyses (Kutty et al. 2010, 2014; Haseyama et al. 2015; Grzywacz et al. 2017, 2021; Walczak et al. 2023). However, the composition and relationships among the remaining species within Azeliinae have undergone numerous changes over the years. Currently, this subfamily includes 13 genera (Savage and Wheeler 2004; Grzywacz et al. 2021) represented by at least 400 species worldwide (Pont, unpublished). Although species of Azeliinae have been the subject of relatively frequent phylogenetic inferences based primarily

on adult morphology and molecular studies, the systematic position of some azeliines, such as *Azelia* Robineau-Desvoidy, remains questionable (Savage and Wheeler 2004; Kutty et al. 2014; Haseyama et al. 2015; Grzywacz et al. 2017, 2021). Comprehensive analysis of larval morphology has already proven highly informative for inferring phylogenetic relationships (Piwczyński et al. 2017; Grzywacz et al. 2021). Thus, generating detailed morphological documentation of immature stages from taxa of uncertain or questionable taxonomic position is highly desirable. Nevertheless, with the exception of *Hydrotaea*, for which some species have well-described and documented larval stages, immature stage morphology of the remaining Azeliinae is poorly known, e.g., *Drymeia* Meigen and *Thricops* Rondani, or remains unknown. Current knowledge of the morphology of the preimaginal stages of *Ac. rohrelliformis* (Lobanov 1975; Skidmore 1985) and *P. littoralis* (Zimin 1948; Skidmore 1985) is limited to the third larval instar. Due to the attention from forensic studies, more information can be found on the larvae of *Au. rostrata*. O'Flynn and Moorhouse (1980) produced line drawings and short descriptions of the first and second instars of *Au. rostrata*, allowing for their differentiation from other carrion-breeding larvae, whereas Fuller (1932), Skidmore (1985) and Zumpt (1965) documented the morphology of the third instar. Published data are often superficial, encompassing only a few selected features and frequently lacking detailed illustrations. By utilising museum material in morphological studies, researchers can gain a better understanding of the evolutionary history and relationships of different taxa, especially for taxa difficult to obtain (Buenaventura et al. 2021). The morphological examination of museum specimens, however, may face obstacles due to damage caused by the passage of time as well as inappropriate storage conditions, including overexposure to UV light. In this paper, taking advantage of extensive material of immature stages of *Achanthiptera* recently revealed in European museum collections, we evaluate the efficiency of confocal laser scanning microscopy (CLSM) in visualising UV-overexposed and more than 100-year-old museum material. To achieve this, we study and document in detail the second- and third-instar larvae of *Ac. rohrelliformis* and *P. littoralis* as well as the third-instar larva of *Au. rostrata* using light microscopy (LM), scanning electron microscopy (SEM) and CLSM. Based on the results, we reinvestigate the systematic relationships between *Ac. rohrelliformis* and other Muscidae.

2. Materials and methods

Larvae of *Ac. rohrelliformis* were obtained from the Natural History Museum (BMNH), London (UK), the Natural History Museum of Denmark (NHMD), University of Copenhagen, Copenhagen (Denmark) and the Museum für Naturkunde (ZMB), Leibniz Institute for Evolution and Biodiversity Science, Berlin (Germany). The museum material from BMNH and NHMD was preserved in ethanol, while samples from ZMB were dried and collapsed (due to evaporation of ethanol). After this was revealed, the material was re-preserved in ethanol. Procedures for obtaining *P. littoralis* larvae, including collection of gravid females during fieldwork and laboratory rearing and killing of larvae, followed the protocols described by Grzywacz et al. (2014). Briefly, adults of *P. littoralis* were attracted to baits (decomposed chicken liver) in Pławin (Poland) in 2013 and collected using an entomological net. Females were then transported to the laboratory in 2-mL Eppendorf tubes with air exchange provided by incaps punctures. In the laboratory, flies were transferred to plastic containers with a thin layer of wet sand and supplied with water, sugar and a small piece of chicken liver as an oviposition and feeding medium. Larvae of appropriate instars were transferred to a Petri dish and immersed in sub-boiling water (~97°C) for 60 s and then transferred to 70% ethanol. Larvae of *Au. rostrata* were collected from a human cadaver as part of a police investigation (Kuitpo Forest, South Australia). Soft forceps were used to collect the larvae, which were brought to the laboratory and preserved as described for *P. littoralis*. Larvae of *P. littoralis* and *Au. rostrata* are deposited in the Department of Ecology and Biogeography, Nicolaus Copernicus University in Toruń, Toruń, Poland (NCUT).

Third-instar larvae were prepared for SEM examination by cleaning with a fine brush, dehydration in 80.0%, 90.0% and 99.5% ethanol (EtOH) and critical-point-drying in carbon dioxide (CO_2) with an Autosamdri®-815, Series A critical-point-dryer (Tousimis Research Corp., Rockville, MD, U.S.A.). Larvae were then mounted on aluminium stubs with double-sided adhesive tape and coated with platinum for 140 s (20 nm of coating) using a JEOL JFC 2300HR high-resolution fine coater (JEOL Ltd., Tokyo, Japan). Scanning electron microscopy images were obtained with a JEOL scanning microscope (JSM-6335F; JEOL Ltd.).

CLSM observations were performed with a Leica TCS SP8 confocal laser scanning microscope (Leica Microsystems, Wetzlar, Germany). Larvae intended for CLSM analysis were prepared according to the protocol by Szpila et al. (2021). Second-instar larvae of *Ac. rohrelliformis* and *P. littoralis* were macerated by immersion in 10% potassium hydroxide (KOH) for 16 hours at room temperature. Third-instar larvae of *Ac. rohrelliformis* had faded due to exposure from UV light and, to avoid over-macerating, the material was macerated twice, initially for 12 hours and subsequently for an additional 5 hours after an assessment showed that the first maceration was insufficient due to large amounts of remaining soft tissue residues. Third-instar larvae of *P. littoralis* and *Au. rostrata* were macerated for 26 hours. Subsequently, all larvae were washed by placing them in 99.5% EtOH, transferred to a microscope slide with a drop of glycerine and covered with a coverslip. The acquisition steps were conducted in accordance with the protocol provided by Walczak et al. (2022). The autofluorescence signal of the cephaloskeleton was collected with two excitation wavelengths: 561 nm and 633 nm, as well as 488 nm in case of the mouthhooks of *Ac. rohrelliformis*. The microscope

Table 1. Abbreviations of morphological structures.

a1–7	abdominal segments 1–7	*mh*	mouthhook
abr	antennal basal ring	*mp*	maxillary palpus
acc	accessory stomal sclerites	*ns1–2*	additional sensillum coeloconicum 1–2
ad	anal division	*ob*	oral bar
an	antennal complex	*ol*	optic lobe
and	antennal dome	*or*	oral ridges
ao	anal opening	*p1–p7*	papillae 1–7
ap	anal plate	*pa*	post-anal papilla
aro	anterior rod	*paa*	para-anal papilla
as	anterior spiracle	*pb*	parastomal bar
asb	anterior spinose band	*pc*	pseudocephalon
bm	bubble membrane	*pp*	posterior projection
bs	basal sclerite	*pre*	pre-anal welt
cir	cirri	*ps*	posterior spiracle
cl	cleft	*r*	rami
cut	cutaneous teeth	*rp*	rectangular accessory process
db	dorsal bridge	*rs*	respiratory slit
dc	dorsal cornu	*sa*	sub-anal papilla
de	dorsal extension	*sb1–3*	sensillum basiconicum 1–3
ds	dental sclerite	*sc1–3*	sensillum coeloconicum 1–3
es	epistomal sclerite	*ss*	spiracular scar
ex	extra-anal papilla	*st*	spiracular tuft
is	intermediate sclerite	*sub*	suprabuccal teeth
ko	Keilin's organ	*t1–3*	thoracic segments 1–3
lcw	lateral creeping welt	*vb*	ventral bridge
ll	labial lobe	*vc*	ventral cornu
lo	labial organ	*vcw*	ventral creeping welt
lr	longitudinal ridges	*vo*	ventral organ
ls	labial sclerite	*vp*	vertical plate

slides were scanned with a 40x oil lens with a numerical aperture of 1.3 (N.A.=1.3). Following the acquisition of sequential images, maximum intensity projections (MIP) and 3D visualisation were built using LAS AF V3.3 and LAS X 3D Viewers (Leica Microsystems, Wetzlar, Germany), respectively.

Larval terminology follows Courtney et al. (2000) with a few modifications proposed by Szpila and Pape (2005). Family-specific structures follow the terminology of Skidmore (1985) with modifications proposed by Grzywacz (2013a) and Walczak et al. (2022). All abbreviations used in this study are listed in Table 1.

3. Results

3.1. Specimens examined

Achanthiptera rohrelliformis (Robineau-Desvoidy) (Figs 1A, B, 2A–F, 3A–G, 4A–I): 2 third-instar larvae, labelled: "C.27:1"; **BMNH** — 15 third-instar larvae, labelled: "April 1912 / Kryger / W. Lundbeck col."; **NHMD** — 35 second- and 27 third-instar larvae, labelled: "Berlin / Jungfernheide / 1909"; **ZMB** — 8 third-instar larvae, labelled: "Berlin / Wittenau / 1911"; **ZMB**

Potamia littoralis Robineau-Desvoidy (Figs 1C, D, 5A–C, E, G, 6A–I): 5 second- and 8 third-instar larvae, labelled: 21 Jul. 2013, Pławin, Poland, A. Grzywacz leg.; **NCUT**

Australophyra rostrata (Robineau-Desvoidy) (Figs 1E, 5D, F, H, 7A–I): 5 third-instar larvae, labelled: 1 Feb. 1995, Kuitpo Forest, South Australia, Australia, J. F. Wallman leg.; **NCUT**

3.2. General larval morphology

To avoid repetition, general morphology of all species is described jointly, and the species-specific details are highlighted in the following subsections. Due to the poor condition of the second-instar larva of *Ac. rohrelliformis*, it was only feasible to examine its cephaloskeleton using CLSM.

Pseudocephalon. Bilobate and equipped with paired antennal complex (*an*), maxillary palpus (*mp*) and ventral organ (*vo*) (Figs 3B, 6B, 7B). Functional mouth opening surrounded by facial mask consisting of numerous oral ridges (*or*) and a pair of labial lobes (*ll*) equipped apically with sensilla of the labial organ (*lo*) (Figs 3B, E, 6B, 7B). Anterior margin of the facial mask with a row of

cirri (*cir*). Antennal complex with conical antennal dome (*and*) situated on antennal basal ring (*abr*) (Figs 3C, 6B, 7B); the length of *and* half the height of *abr* (Figs 3C, 6B, 7B). The *mp* consists of three sensilla coeloconica (*sc*), three sensilla basiconica (*sb*), several small additional sensilla arranged in a tight cluster and two sensilla coeloconica of non-maxillary origin (*ns*) positioned laterodorsally (Figs 3D, 6C, 7C). The bulge-shaped *vo* equipped with four sensilla (Figs 3B, E, F, 6D, 7D) and placed at the anterior margin of *or* (Figs 3B, E, 6B, 7B).

Cephaloskeleton. Paired mouthhooks (*mh*), unpaired intermediate sclerite (*is*) and basal sclerite (*bs*) (Figs 1A–E).

Second instar with several well-sclerotized, ventrally directed suprabuccal teeth (*sub*) (Figs 2A, 5A) placed anterior to *mh*. The *mh* L-shaped in lateral view (Figs 1A, C, 2A, 5A) with slender base and distal parts symmetrical and closely appressed (Fig. 2B). Apical part of *mh* enveloped in the dome-shaped anterior rod (*aro*) (Figs 1A, C, 2A, B, 5A). Dental sclerite (*ds*) and irregular accessory stomal sclerites (*acc*) located below each *mh* (Figs 2A, 5A). Convex epistomal sclerite (*es*) and a pair of labial sclerites (*ls*) placed anteriorly between anterior arms of *is* (Figs 2A, 5A, B). Paired rod-like rami (*r*) lie freely between lateral arms of *is* (Figs 2B, 5B). Basal sclerite (*bs*) with paired vertical plates (*vp*), with dorsal (*dc*) and ventral cornua (*vc*) connected anteroventrally by strongly sclerotized ventral bridge (*vb*) (Figs 1A, C, 5A, B) and anterodorsally by tightly appressed horseshoe-shaped dorsal bridge (*db*) (Figs 1A, C, 5A). The *vp* broad, *dc* shorter than *vc* (Fig. 1A, C). Posterior parts of *dc* and *vc* poorly sclerotized, the latter with dorsal extension (*de*). Hypopharynx with distinctly developed longitudinal ridges.

Third instar with asymmetric, closely appressed *mh*, the left being shorter (Figs 2C, D, 5C, D). Distal parts curved ventrally (Figs 1B, D, E, 2C, D, 5C, D). Triangular *ds* and *acc* situated ventrally to base of each *mh* (Figs 2C, D, 5C, D). The *ds* connected with base of *mh* by slender, sclerotized hinge along anterodorsal margin (Figs 2C, D, 5C, D). Elongated and convex *es* and paired *ls* lie freely between anterior arms of *is* (Figs 2E, F, 5E, F). The *is* H-shaped in dorsal view (Figs 2F, 5E, F). Parastomal bar (*pb*) fused with dorsal margin of *is*, creating anterodorsal extension (Figs 2E, 5F, G, H). Paired well-sclerotized, rod-like rami (*r*) lie between arms of *is* (Figs 2F, 5E, F). The *bs* consists of paired, broad *vp* each with *dc* and *vc* (Fig. 1B, D, E). The *vp* connected anteroventrally by *vb* and anterodorsally by *db* (Figs 1B, D, E, 2F, 5E, F). Hypopharynx with longitudinal ridges.

Thoracic and abdominal segments. Anterior spinose band (*asb*) on first thoracic segment (*t1*) broad and complete (Figs 3A, B, 6A, B, 7A, B). Spines of *asb* colourless

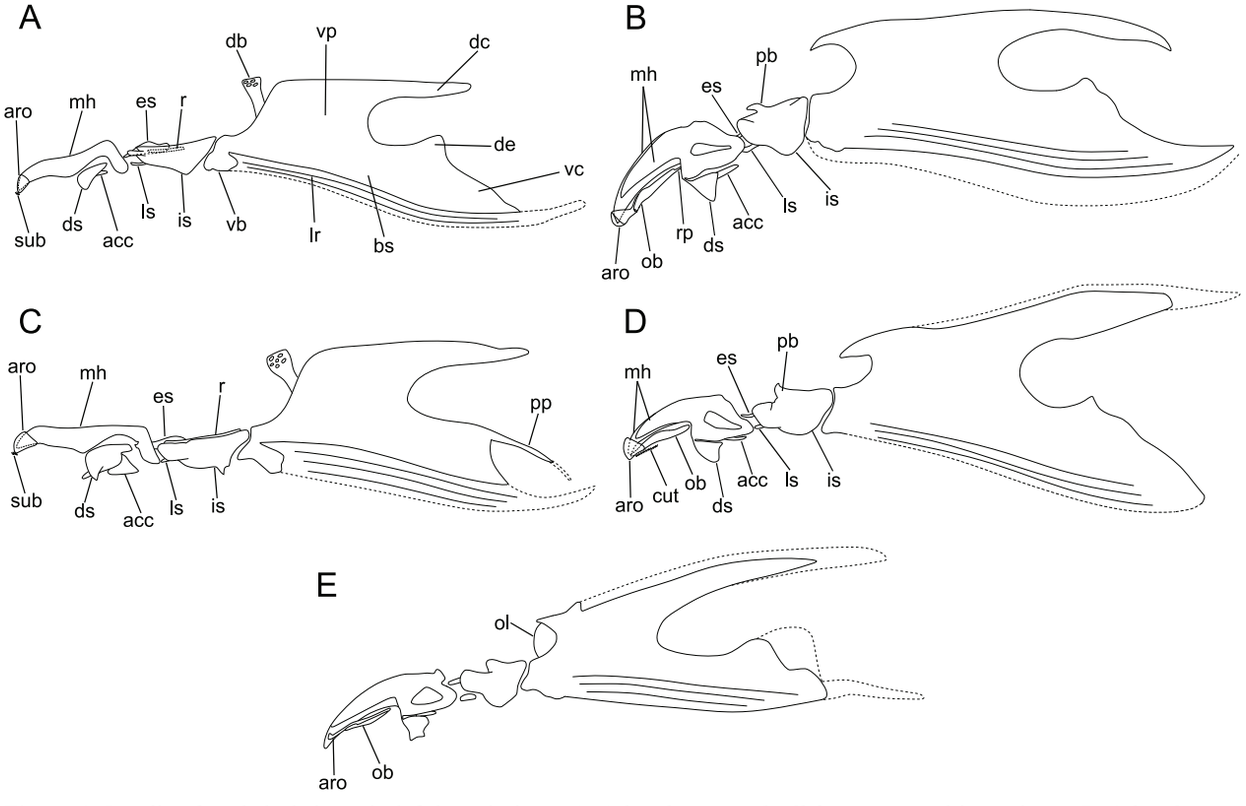

Figure 1. Details of cephaloskeleton in left-lateral views. **A** *Achanthiptera rohrelliformis*, second-instar larva. **B** *Achanthiptera rohrelliformis*, third-instar larva. **C** *Potamia littoralis*, second-instar larva. **D** *Potamia littoralis*, third-instar larva. **E** *Australophyra rostrata*, third-instar larva. — Abbreviations: *acc*, accessory stomal sclerites; *aro*, anterior rod; *bs*, basal sclerite; *cut*, cutaneous teeth; *db*, dorsal bridge; *dc*, dorsal cornu; *de*, dorsal extension; *ds*, dental sclerite; *es*, epistomal sclerite; *is*, intermediate sclerite; *lr*, longitudinal ridges in hypopharynx; *ls*, labial sclerite; *mh*, mouthhook; *ob*, oral bar; *ol*, optic lobe; *pb*, parastomal bar; *pp*, posterior projection; *r*, rami; *rp*, rectangular accessory process; *sub*, suprabuccal teeth; *vb*, ventral bridge; *vc*, ventral cornu; *vp*, ventral cornu.

and arranged densely in long rows, closely adjacent ventrally and slightly separated dorsally (Figs 3A, 6A, 7A). Anterior third of *t1* with transverse cleft (*cl*), followed ventrally by several rows of spines (Figs 3A, 6A, 7A). Each thoracic segment ventrally with a pair of trichoid sensilla of Keilin's organ (*ko*) (Figs 3B, 4B, 7A, E). Second (*t2*) and third (*t3*) thoracic and first abdominal (*a1*) segments in second instar with single short row of fine spines. Third instar with complete anterior spinose bands on *t2* and *t3* arranged in relatively short rows (Figs 3A, 6A, 7A). Abdominal segments (*a2–a7*) anteroventrally with creeping welts (*vcw*) and anal division (*ad*) with pre-anal welt (*pre*) (Figs 4C, I, 6F, I, 7F, I). Elliptical lateral creeping welts (*lcw*) present between abdominal segments, barely visible, never covered by spines (Fig. 7F). The posterolateral margin of *a1* with circular bubble membrane (*bm*) of many globules clustered together and level with the adjacent integument (Figs 4D, 6F, 7F). All spines of *asb* on *t1–t3* and *a1–a3*, as well as of *vcw* on *a2–a7* directed posteriorly (Figs 3A, B, G, 4A, C, 6A, B, F, 7A, B, F), while spines of *pre* point anteriorly (Figs 4I, 6I, 7I). Scars from muscle attachments strongly visible on surface of all thoracic and abdominal segments.

Anal division. Ventrally with anal opening (*ao*), porous anal plate (*ap*) and distinct anal papillae (Figs 4I, 6I, 7I). An unpaired post-anal papilla (*pa*) present directly posterior to *ao*. Paired sub-anal (*sa*), para-anal (*paa*) and extra-anal (*ex*) papillae shifted anteriorly relative to the *pa* (Figs 4I, 6I, 7I). Each *sa* with a sensillum basiconicum and two sensilla resembling sensilla ampullacea. Spiracular field with seven pairs of papillae (*p1–p7*) and a pair of posterior spiracles (*ps*) located centrally (Figs 4G, H, 6H, 7H). Each papilla composed of a sensillum plus the surrounding area. Papillae *p1*, *p3*, *p5* and *p7* with a sensillum basiconicum. Papillae *p2*, *p4* and *p6* indistinct, placed ventral to the spiracular field and equipped with a sensillum ampullaceum.

3.3. Specific morphology

3.3.1. Second instar: *Achanthiptera rohrelliformis*

Cephaloskeleton. Arched *ds*, *acc* and the pair of *r* weakly sclerotized (Fig. 2A, B).

3.3.2. Second instar: *Potamia littoralis*

Pseudocephalon. The *and* encircled with equidistantly spaced pores. The perimeter of the *mp* composed of two nearly circular folds. The *cir* angular and serrated. The *or* digitate along their entire length.

Cephaloskeleton. Base of *mh* with a hooked appendage on the ventral side (indicated by an asterisk in Fig. 5A). The *ds*, *acc* and a pair of *r* robust and strongly sclerotized (Fig. 5A, B). The *de* equipped with a sclerotized posterior projection (*pp*) directed ventrally (Fig. 1C).

Anal division. The *ao* surrounded by convex, W-shaped *ap*, which is anteriorly bounded by the *pre*, posteriorly by a row of conical spines. The *pa*, *sa* and *ex* bulge-like, *paa* flattened. Papillae *p1*, *p3*, *p5* and *p7* positioned level with adjacent integument. The *ps* slightly elevated and each *ps* bears two slightly sinuate and subparallel respiratory slits (*rs*), four branched spiracular tufts (*st*) and a median spiracular scar (*ss*).

3.3.3. Third instar: *Achanthiptera rohrelliformis*

Pseudocephalon. The perimeter of the *mp* composed of two nearly circular folds (Fig. 3B, D). The *or* serrated along entire length (Fig. 3A, B, E).

Cephaloskeleton. Left *mh* considerably shorter than right *mh* (Fig. 2C, D). Distal part of right *mh* massive, left one slender (Fig. 2C, D). Basal part of *mh* on right side joins with *ob* through a small rectangular accessory process (*rp*) (Fig. 2C). The *ob* serrated apically and parallel to the distal part of *mh* through entire length (Fig. 2C). A transformed *aro* embedded anteriorly to *ob* (Fig. 2C). The *aro* narrow at the base and strongly expanded apically. The apical part of *aro* covers the tip of right (and longer) *mh* (Fig. 2C, D). The irregular *ob* and short *aro* tightly appressed to *mh* (Fig. 2D, lateral view from left *mh*). The *dc* slender and slightly shorter than *vc*, which carries *de* (Fig. 1B).

Thoracic and abdominal segments. Spines of *asb* trapezoid with serrated posterior margin (Fig. 3B). The anterior spiracle (*as*) equipped with four or five lobes (Fig. 3A). Spines of anterior spinose bands on *t2* and *t3* of various shape from slightly pointed to blunt-ended (Fig. 3A, G). First three abdominal segments (*a1–a3*) with complete anterior spinose band of colourless, mostly blunt-ended spines that are arranged in short rows (Fig. 4A). In the middle of each *vcw* is a protuberance with at least two rows of conical spines surrounded by several rows of fine, single- and double-pointed spines (Fig. 4C). Anterior part of *pre* with small spines arranged in short rows similar to those of *vcw*, posterior part with irregularly arranged, more or less conical spines that are twice as large (Fig. 4I). Lateral creeping welts (hardly distinguishable) present posterolaterally on each abdominal segment.

Anal division. The *ao* surrounded by W-shaped *ap*, anteriorly limited by *pre* and posteriorly by bulge-shaped *pa* and *sa* (Fig. 4I). The *pa* covered with tiny spines and bigger than *sa*. Beyond each *sa* are paired, relatively flattened *paa* and *ex*, the latter larger than other anal papillae and covered with small spines (Fig. 4I). Anal papillae followed by several rows of tiny spines (Fig. 4I). Each of *p1*, *p3*, *p5* and *p7* in the form of a small integumental protuberance (Fig. 4G, H). The *ps* slightly elevated and relatively small, comparable in size to *p1* (Fig. 4H). Each *ps* with three straight *rs* in convergent arrangement, four branched *st* and *ss* in median position (Fig. 4E).

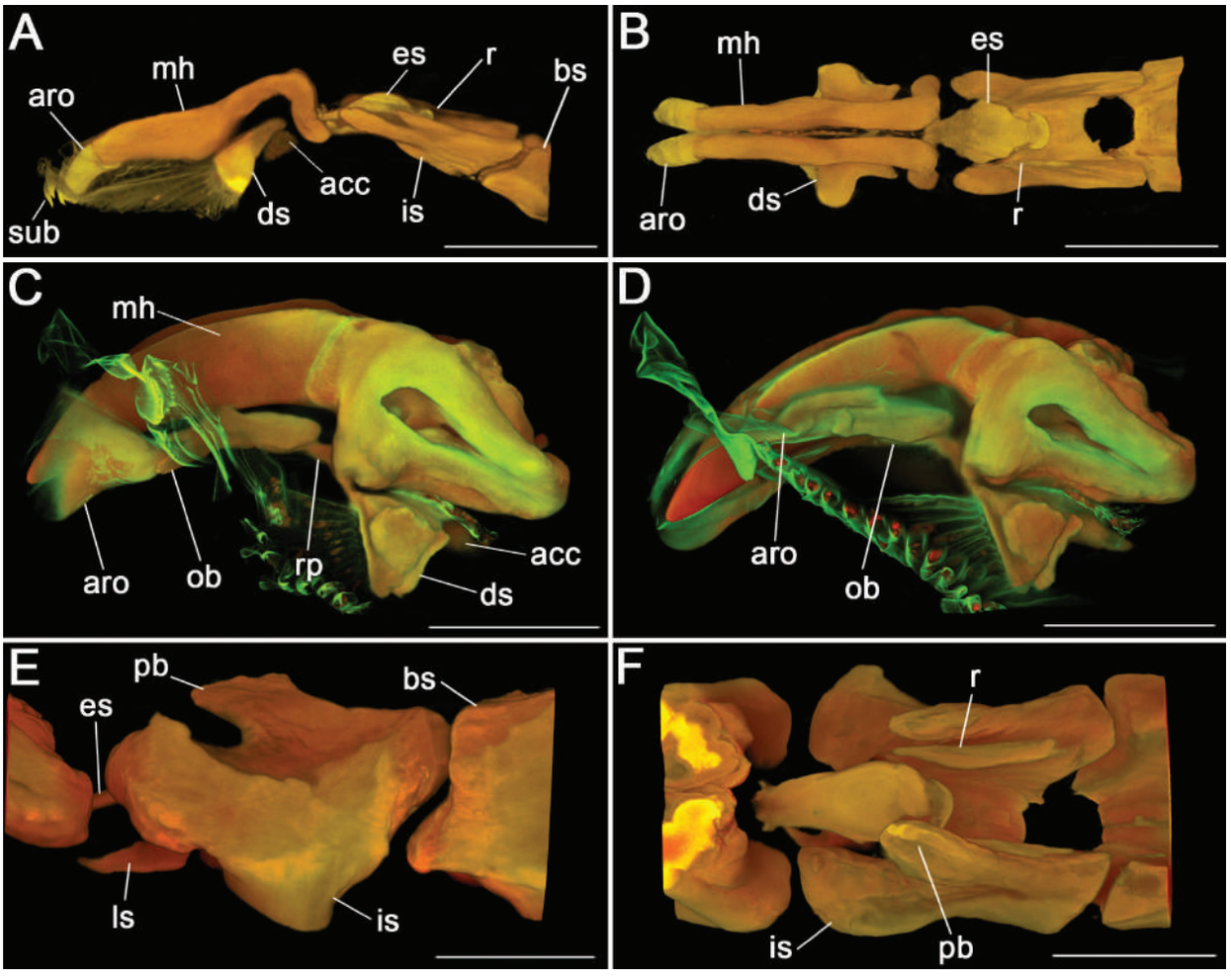

Figure 2. *Achanthiptera rohrelliformis*, cephaloskeleton of larvae II and III [CLSM]. **A** anterior end of cephaloskeleton of second-instar larva, lateral view. **B** mouthhooks and intermediate sclerite of second-instar larva, dorsal view. **C** mouthhooks of third-instar larva, lateral view of right mouthhook. **D** mouthhooks of third-instar larva, lateral view of left mouthhook. **E** intermediate sclerite of third-instar larva, lateral view. **F** intermediate sclerite of third-instar larva, dorsal view. — Abbreviations: *acc*, accessory stomal sclerites; *aro*, anterior rod; *bs*, basal sclerite; *ds*, dental sclerite; *es*, epistomal sclerite; *is*, intermediate sclerite; *ls*, labial sclerite; *mh*, mouthhook; *ob*, oral bar; *pb*, parastomal bar; *r*, rami; *rp*, rectangular accessory process; *sub*, suprabuccal teeth. Scale bars: 0.05 mm.

3.3.4. Third instar: *Potamia littoralis*

Pseudocephalon. The perimeter of the *mp* consists of an inner fold with four crescents and an outer circular fold (Fig. 6B, C). The *or* bluntly serrated along entire length (Fig. 6A, B). The *cir* trapezoid (Fig. 6B).

Cephaloskeleton. The *mh* asymmetrical with tip of *mh* covered by a transformed *aro* in right lateral view (Figs 1D, 5C). Right *aro* with narrow basal part tightly attached to *ob* and strongly expanded apical part in the form of an incomplete dome (Figs 1D, 5C). Two rows of minute cutaneous teeth (*cut*) ventral to the rod-like *ob* (Fig. 5C). The *ds* connected to base of *mh* through narrow, sclerotized hinge [ruptured in the examined specimen] (Fig. 5C). The *es* massive, convex in lateral view, elliptical in dorsal view, with two perforations located on anterolateral margin (Fig. 5E). A pair of rod-like *r* adheres ventrally to each arm of *is* (Fig. 5E). The *dc* slightly shorter and half the height of *vc*, the latter with well-developed *de* posterodorsally. The *vb* well-sclerotized, *db* less sclerotized and finely perforated (Fig. 1D).

Thoracic and abdominal segments. Spines of *asb* trapezoidal, mostly double- or triple-pointed (Fig. 6B, E). The *as* equipped with six lobes (Fig. 6A). Spines of anterior spinose bands on *t2* and *t3* single-pointed (Fig. 6A). Spines on abdominal segments limited to anterior margin only ventrally (Fig. 6F). The *a1* anteroventrally covered by short rows of small, colourless spines. Spines of *vcw* arranged in transverse rows separated in the middle by narrow strip. Spines of two inner rows relatively massive, somewhat hook-shaped, mostly single-pointed, adjacent short rows consist of tiny single- and double-pointed spines (Fig. 6F). The *pre* consists of three irregular rows of robust, conical spines and is preceded with one or two rows of fine spines (Fig. 6I). Lateral creeping welts barely visible but present on posterolateral part of each abdominal segment.

Anal division. The *ao* surrounded by convex, W-shaped *ap* (Fig. 6I). The *ap* anteriorly bound by *pre*, posteriorly

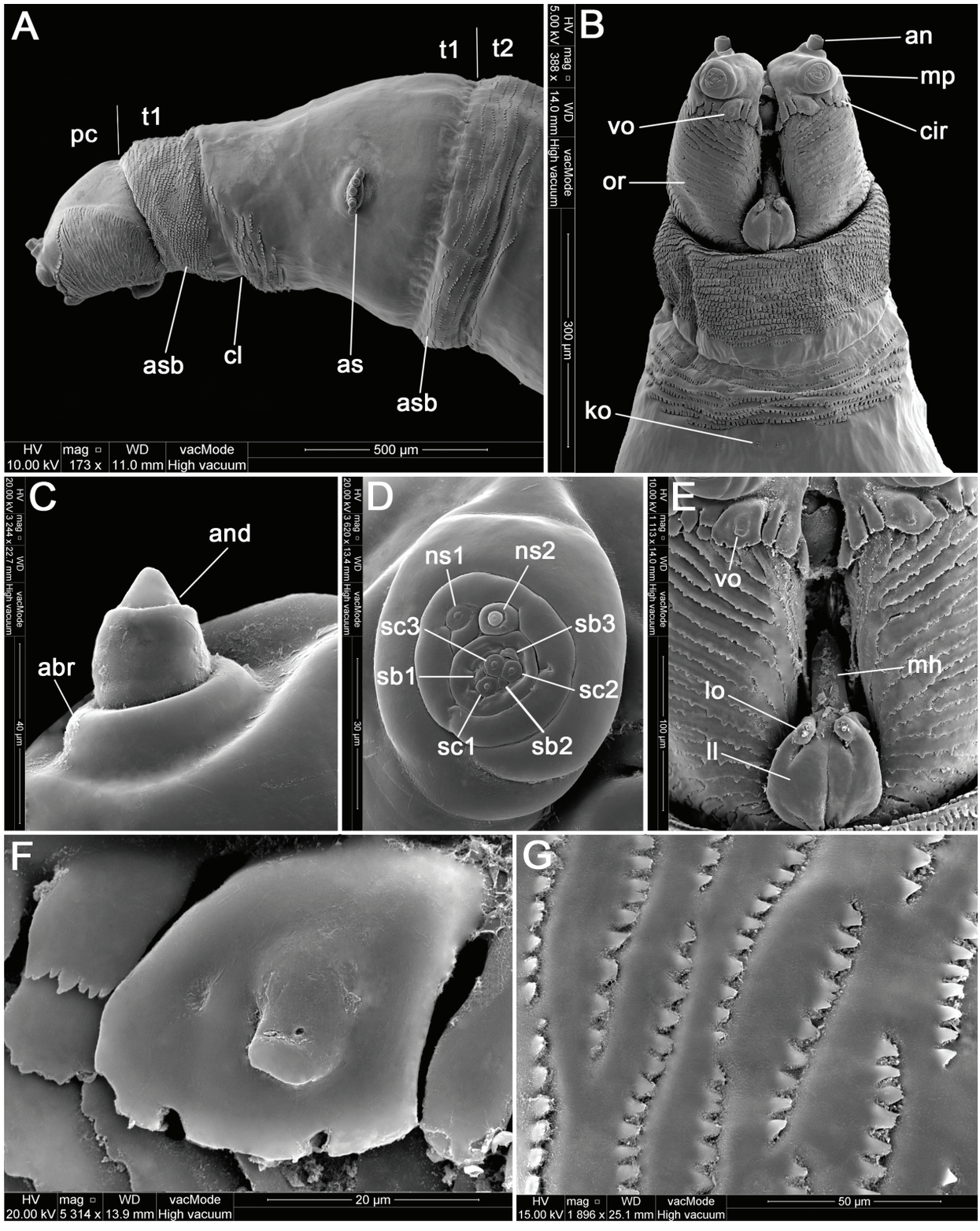

Figure 3. *Achanthiptera rohrelliformis*, pseudocephalon of third-instar larva [SEM]. **A** anterior end of body, lateral view. **B** anterior end of body, ventral view. **C** antennal complex. **D** maxillary palpus. **E** facial mask, ventral view. **F** ventral organ. **G** spines on first thoracic segment. — Abbreviations: *abr*, antennal basal ring; *an*, antennal complex; *and*, antennal dome; *as*, anterior spiracle; *asb*, anterior spinose band; *cir*, cirri; *cl*, cleft; *ko*, Keilin's organ; *ll*, labial lobe; *lo*, labial organ; *mh*, mouthhook; *mp*, maxillary palpus; *ns1–2*, first and second additional sensillum coeloconicum; *pc*, pseudocephalon; *or*, oral ridges; *sb1–3*, sensillum basiconicum 1–3; *sc1–3*, sensillum coeloconicum 1–3; *t1*, thoracic segment 1; *t2*, thoracic segment 2; *vo*, ventral organ.

by a row of spines similar in size and shape to those of the *pre* and further followed by several rows of small, conical spines (Fig. 6I). All anal papillae bulge-like, with *paa* being smallest and *ex* the largest. The *pa* covered with sharply pointed spines. Several irregularly scattered spines between *paa* and *ex*. The *p1*, *p3*, *p5* and *p7* po-

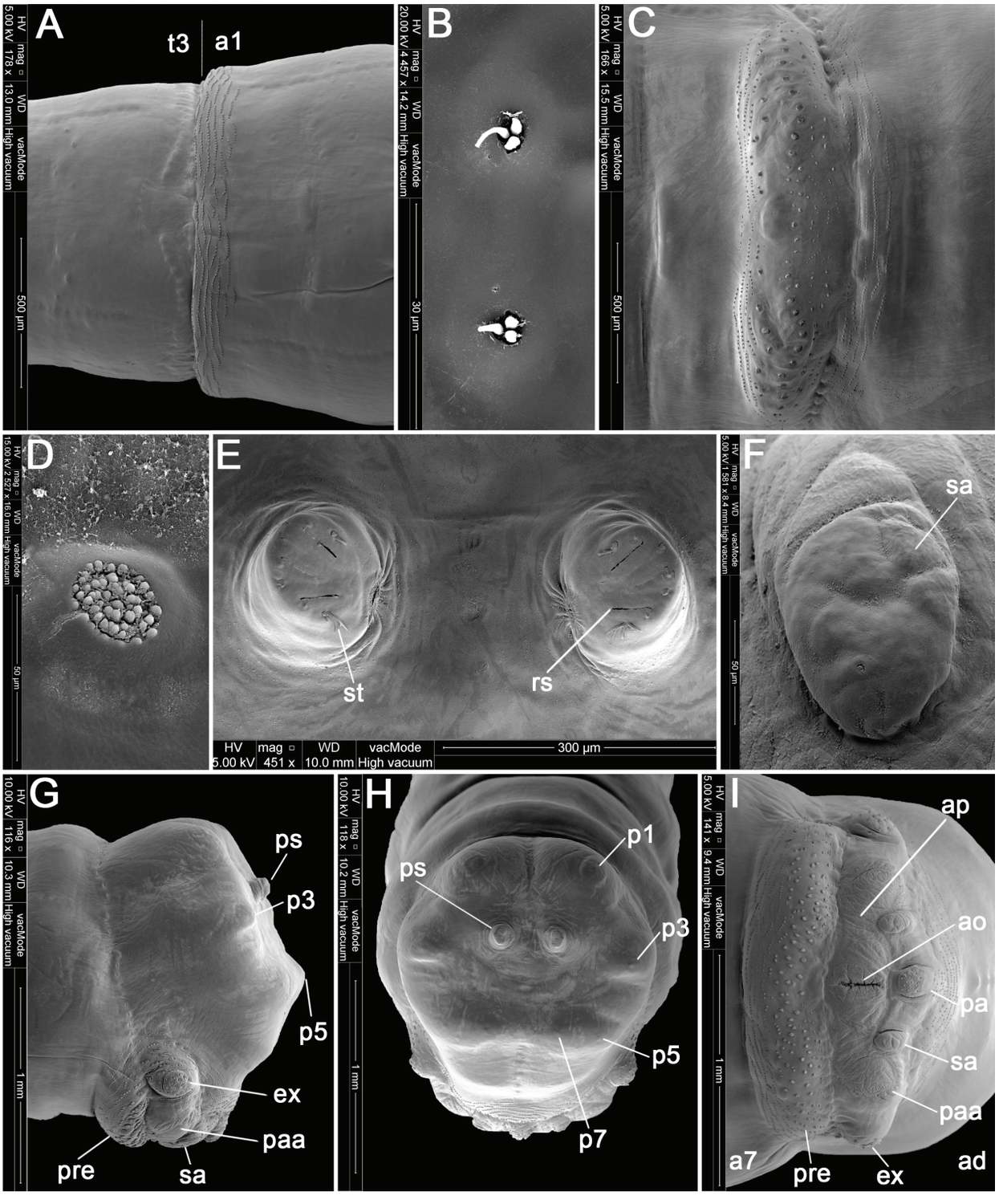

Figure 4. *Achanthiptera rohrelliformis*, thorax and abdomen of third-instar larva [SEM]. **A** third thoracic and first abdominal segments, lateral view, dorsal side up. **B** Keilin's organ on ventral side of third thoracic segment. **C** pre-anal welt on seventh abdominal segment, ventral view. **D** bubble membrane. **E** posterior spiracles. **F** sub-anal papilla. **G** posterior end of body, lateral view. **H** anal division, posterior view. **I** posterior end of body, ventral view. — Abbreviations: *a1*, abdominal segment 1; *a7*, abdominal segment 7; *ad*, anal division; *ao*, anal opening; *ap*, anal plate; *ex*, extra-anal papilla; *p1–p7*, papillae 1–7 surrounding spiracular field; *pa*, post-anal papilla; *paa*, para-anal papilla; *pre*, pre-anal welt; *ps*, posterior spiracle; *rs*, respiratory slit; *sa*, sub-anal papilla; *ss*, spiracular scar; *st*, spiracular tuft; *t3*, thoracic segment 3.

sitioned level with adjacent integument (Fig. 6H). The *ps* slightly elevated, each with three slightly sinuate and subparallel *rs*, four branched *st* and *ss* in median position (Fig. 6G).

3.3.5. Third instar: *Australophyra rostrata*

Pseudocephalon. The perimeter of the *mp* composed of three semi-circular folds (Fig. 7B, C). The *or* gently ser-

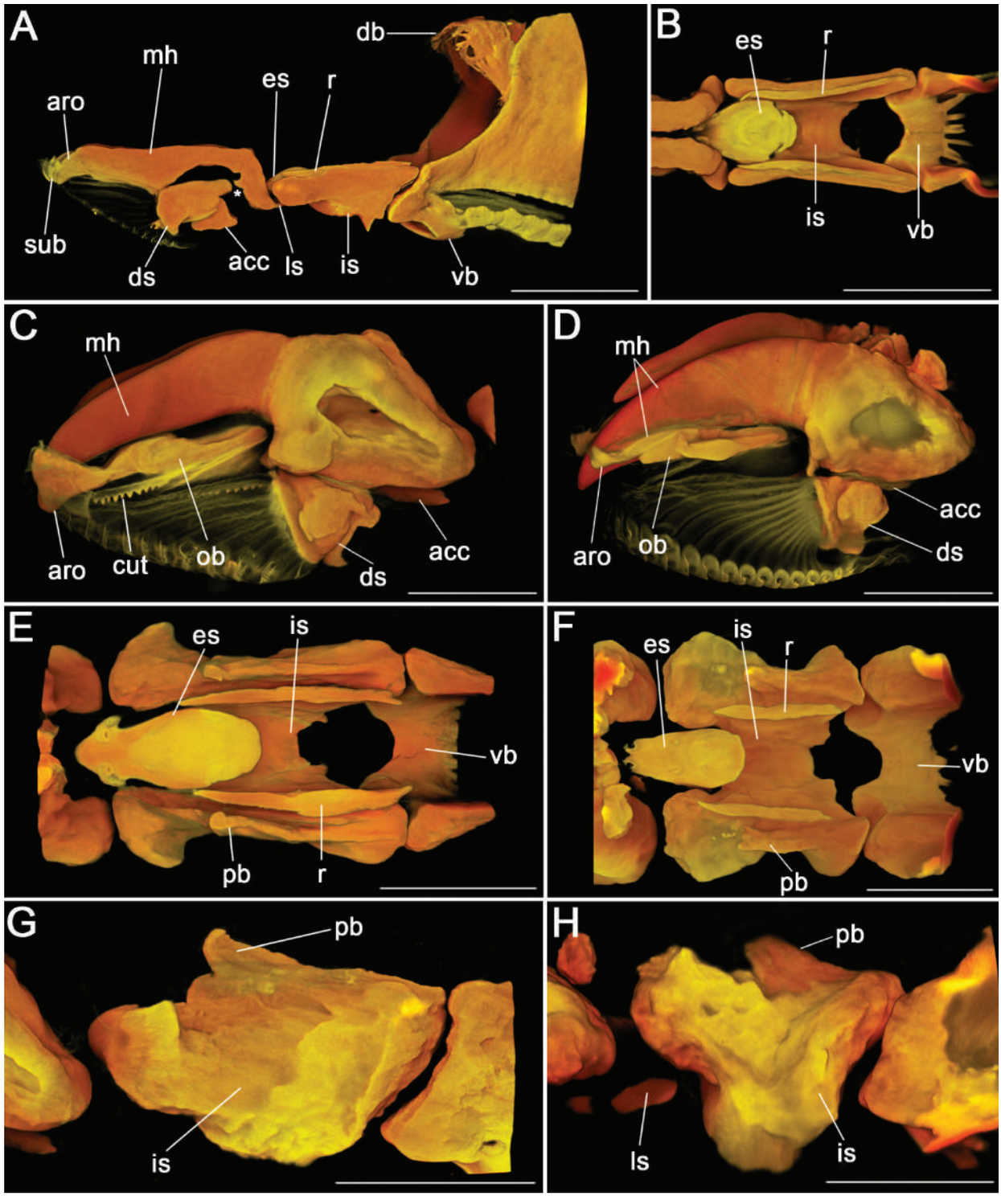

Figure 5. CLSM images of *Potamia littoralis* (A, B, C, E, G) and *Australophyra rostrata* (D, F, H). **A** anterior end of cephaloskeleton of second-instar larva with hooked appendage on ventral side of basal part of mouthhook (indicated by asterisk), left-lateral view. **B** intermediate sclerite and neighbouring elements of second-instar larva; dorsal view. **C** mouthhooks of third-instar larva, right-lateral view. **D** mouthhooks of third-instar larva, right-lateral view. **E** intermediate sclerite of third-instar larva; dorsal view. **F** intermediate sclerite and neighbouring elements of third-instar larva; dorsal view. **G** intermediate sclerite of third-instar larva; lateral view. **H** intermediate sclerite of third-instar larva; lateral view. — Abbreviations: *acc*, accessory stomal sclerite; *aro*, anterior rod; *cut*, cutaneous teeth; *db*, dorsal bridge; *ds*, dental sclerite; *es*, epistomal sclerite; *is*, intermediate sclerite; *ls*, labial sclerite; *mh*, mouthhook; *ob*, oral bar; *pb*, parastomal bar; *r*, rami; *sub*, suprabuccal teeth; *vb*, ventral bridge. Scale bars: 0.05 mm.

rated. The *vo* in the form of an irregularly rounded bulge in the cuticle (Fig. 7B, D). The *cir* only visible in lateral view (Fig. 7A).

Cephaloskeleton. The *ob* rod-like and not connected to base of asymmetrical *mh* (Fig. 5D). The *aro* toothed anteriorly and the elongated basal part tightly appressed to an-

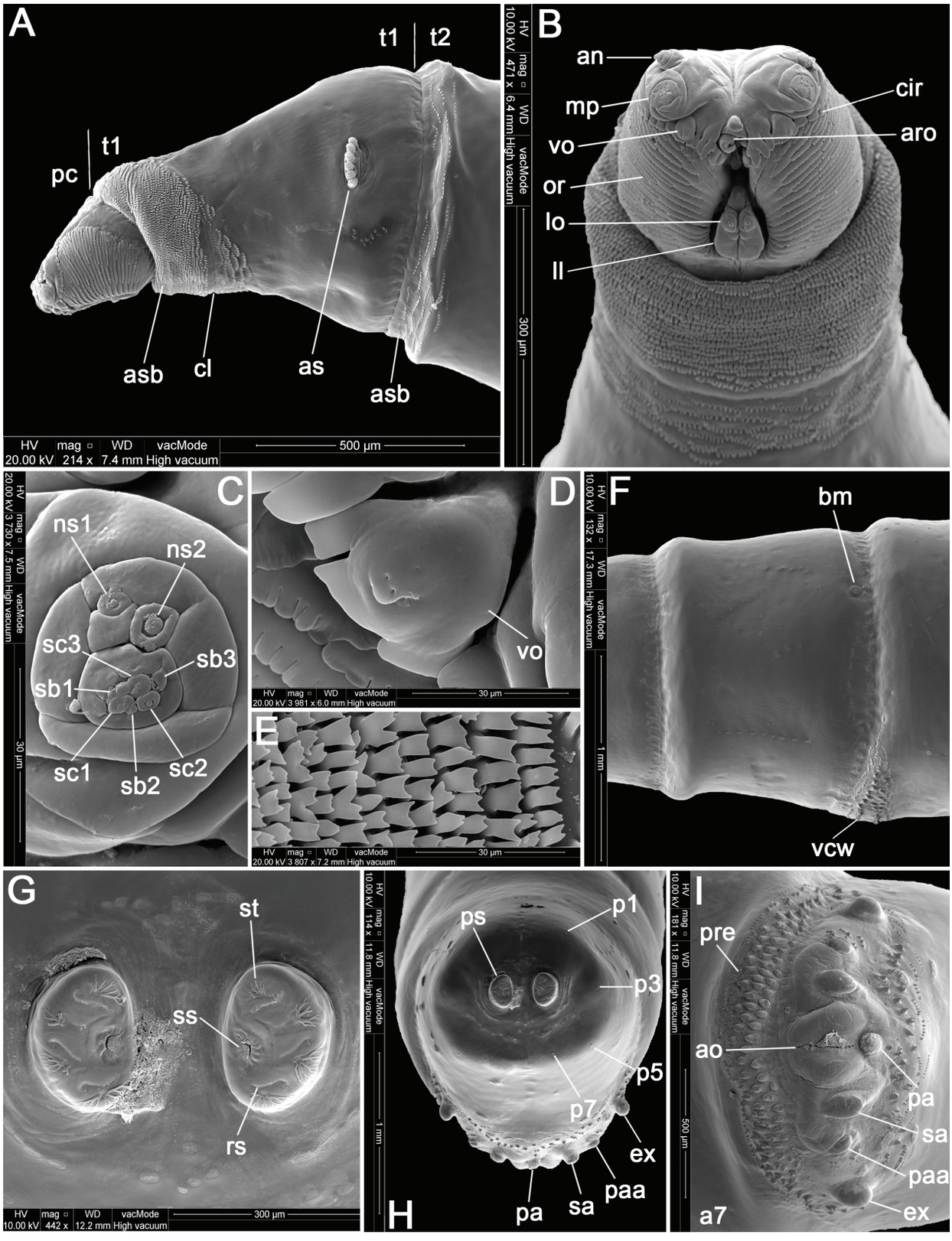

Figure 6. *Potamia littoralis*, pseudocephalon, thorax and abdomen of third-instar larva [SEM]. **A** anterior end of body, lateral view. **B** anterior end of body, ventral view. **C** maxillary palpus. **D** ventral organ. **E** spines on first thoracic segment. **F** first abdominal segment, lateral view, dorsal side up. **G** posterior spiracles. **H** anal division, posterior view. **I** posterior end of body, ventral view. — Abbreviations: *a7*, abdominal segment 7; *an*, antennal complex; *ao*, anal opening; *aro*, anterior rod; *as*, anterior spiracle; *asb*, anterior spinose band; *bm*, bubble membrane; *cir*, cirri; *cl*, cleft; *ex*, extra-anal papilla; *ll*, labial lobe; *lo*, labial organ; *mp*, maxillary palpus; *ns1–2*, first and second additional sensillum coeloconicum; *or*, oral ridges; *p1–p7*, papillae 1–7 surrounding spiracular field; *pa*, post-anal papilla; *paa*, para-anal papilla; *pc*, pseudocephalon; *pre*, pre-anal welt; *ps*, posterior spiracle; *rs*, respiratory slit; *sa*, sub-anal papilla; *sb1–3*, sensillum basiconicum 1–3; *sc1–3*, sensillum coeloconicum 1–3; *ss*, spiracular scar; *st*, spiracular tuft; *t1*, thoracic segment 1; *t2*, thoracic segment 2; *vcw*, ventral creeping welt; *vo*, ventral organ.

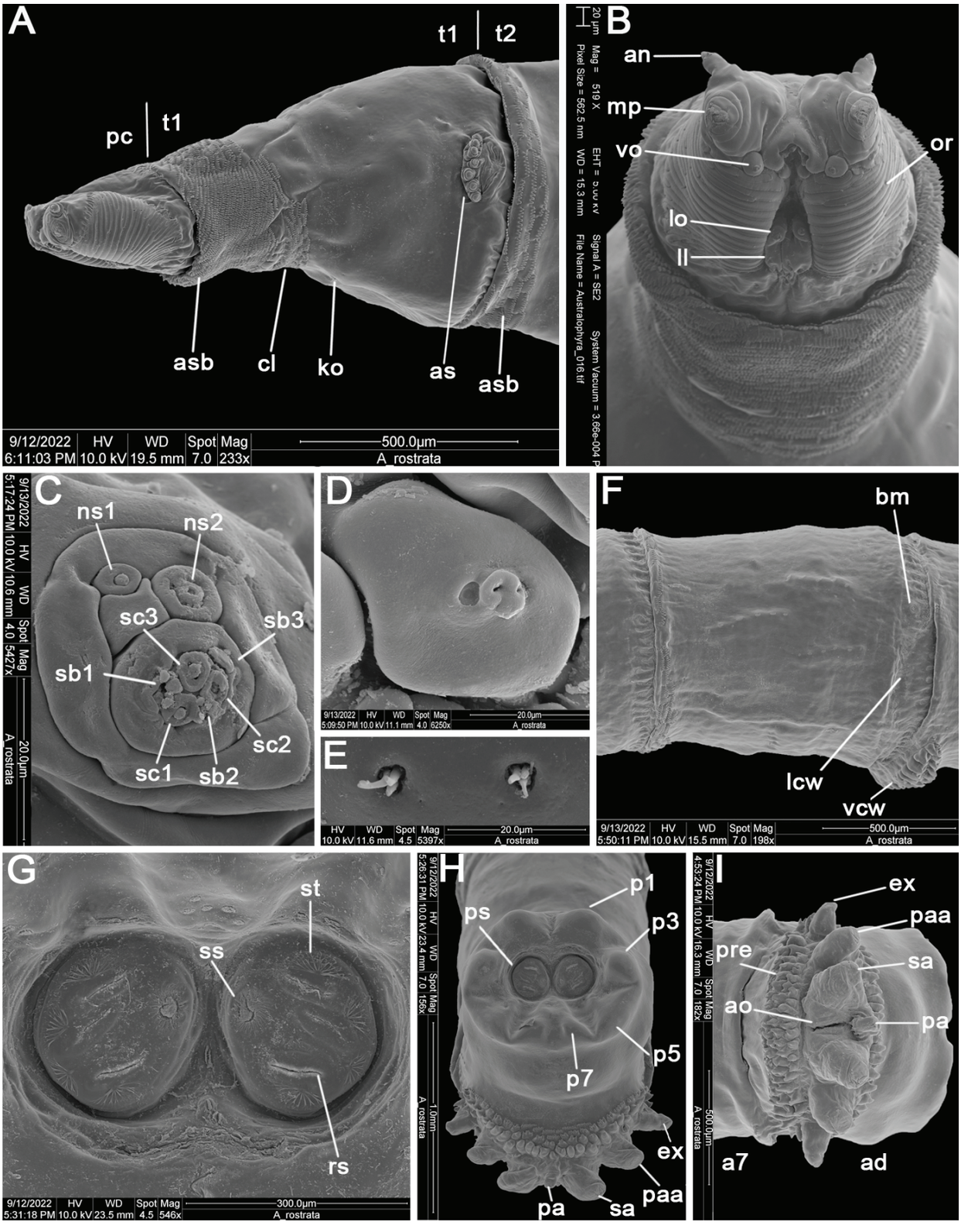

Figure 7. *Australophyra rostrata*, pseudocephalon, thorax and abdomen of third-instar larva [SEM]. **A** anterior end of body, lateral view. **B** anterior end of body, ventral view. **C** maxillary palpus. **D** ventral organ. **E** Keilin's organ on ventral side of third thoracic segment. **F** first abdominal segment, lateral view, dorsal side up. **G** posterior spiracles. **H** anal division, posterior view. **I** posterior end of body, ventral view. — Abbreviations: *a7*, abdominal segment 7; *ad*, anal division; *an*, antennal complex; *ao*, anal opening; *as*, anterior spiracle; *asb*, anterior spinose band; *bm*, bubble membrane; *cir*, cirri; *cl*, cleft; *ex*, extra-anal papilla; *ko*, Keilin's organ; *lcw*, lateral creeping welt; *ll*, labial lobe; *lo*, labial organ; *mp*, maxillary palpus; *ns1–2*, first and second additional sensillum coeloconicum; *or*, oral ridges; *p1–p7*, papillae 1–7 surrounding spiracular field; *pa*, post-anal papilla; paa, para-anal papilla; *pc*, pseudocephalon; pre, pre-anal welt; *ps*, posterior spiracle; *rs*, respiratory slit; *sa*, sub-anal papilla; *sb1–3*, sensillum basiconicum 1–3; *sc1–3*, sensillum coeloconicum 1–3; *ss*, spiracular scar; *st*, spiracular tuft; *t1*, thoracic segment 1; *t2*, thoracic segment 2; *vcw*, ventral creeping welt; *vo*, ventral organ.

terodorsal margin of *ob* (Figs 1E, 5D). Each *aro* slightly curved, forming an incomplete arch in dorsal view. The *is* relatively short (Figs 1E, 5F). Optic lobe (*ol*) present and weakly sclerotized (Fig. 1E). The *bs* is the least sclerotized part of the cephaloskeleton. The *dc* and *vc* of similar length (Fig. 1E). The *dc* slender, and *vc* twice as wide as *dc* and with weakly sclerotized *de* (Fig. 1E).

Thoracic and abdominal segments. Spines of *asb* slender and single-pointed, occasionally double-pointed (Fig. 7B). The *as* with seven to eight lobes (Fig. 7A). Spines of anterior spinose bands on *t2* and *t3* single- or double-pointed (Fig. 7A). The *a1* with *asb* incomplete laterally, ventrally with more rows of spines than dorsally (Fig. 7F). Spines of *asb* colourless and single-pointed, arranged in short rows. Spines of *vcw* relatively robust, conical and blunt-tipped, arranged in two transverse rows separated in middle by narrow strip and followed by row of smaller spines (Fig. 7F). The *pre* consists of three irregular rows of robust and conical spines that are preceded by one row of single-pointed spines (Fig. 7I). A transverse crevice present ventrally in middle part of segments *a1–a7*. A lateral creeping welt is distinctly developed posterolaterally on each abdominal segment.

Anal division. The *ap* almost entirely covered with massive anal papillae (Fig. 7I). Anterior margin of *ap* covered by the *pre*, posterior margin covered by broad strip of spines equal to those of the *pre*. All anal papillae enlarged and conical, together resembling a crown in dorsal and ventral view (Fig. 7H). Paired *sa*, *paa* and *ex* of similar size (Fig. 7I). The *p1*, *p3*, *p5* and *p7* form distinct bulges (Fig. 7H). The *ps* placed slightly below the surface of spiracular field (Fig. 7G, H), with three subparallel and slightly sinuous *rs*, four branched *st* and *ss* placed submedially (Fig. 7G, H).

4. Discussion

4.1. Systematic position of *Ac. rohrelliformis*

Phylogenetic implications based on larval morphology have been discussed for Muscidae by several authors (Roback 1951; Schumann 1954; Ferrar 1979; Skidmore 1985), and, among all larval structures, the cephaloskeleton has been identified as of particular importance. For instance, having observed a striking resemblance of the cephaloskeleton, including the shape and arrangement of sclerites between the larvae of *P. littoralis* and *Hydrotaea dentipes* (Fabricius), Hennig (1965) ultimately concluded that *Potamia* was more closely related to *Hydrotaea* than to *Phaonia* Robineau-Desvoidy. The asymmetry of the mouthhooks in the third-instar larva supports the placement of *Achanthiptera* as well as *Potamia* and *Australophyra* within the Azeliinae + Muscinae clade (Grzywacz et al. 2021). All species examined in this study are nested within the subfamily Azeliinae and have larvae closely resembling those azeliines for which descriptions and drawings are available. Similarities in general morphology and in the details of the cephaloskeleton and anal division with the *dentipes*-group within *Hydrotaea* are particularly compelling (Skidmore 1985; Grzywacz et al. 2014). Shared features are the shape of the anal division: angular outline of the segment in lateral view, spiracular field directed posterodorsally often with dorsal-most part of *ad* distinctly above the level of the dorsal surface of preceding abdominal segments, a W-shaped anal plate with all anal papillae well developed, mostly bulge-like, as well as posterior spiracles with straight to sinuate respiratory slits in a parallel to radiate arrangement (Skidmore 1985; Grzywacz 2013b; Grzywacz et al. 2014). In Muscinae, the spiracular field is directed posteriorly and the dorsal surface of the segment is not above the level of preceding abdominal segments, the anal plate is either small to enlarged, with partially reduced anal papillae, while the slits of the posterior spiracles are serpentine to torturous and arranged in a peripheral to encircling configuration (Skidmore 1985; Grzywacz 2013a). As for the differences in the cephaloskeleton, Azeliinae larvae usually possess well-developed accessory oral sclerites, while in larvae of the Muscinae these are absent or reduced (Skidmore 1985; Grzywacz 2013b; Grzywacz et al. 2014). In addition, the intermediate sclerite of Azeliinae is equipped with a visible anterodorsal extension derived from the reduced parastomal bar, while in Muscinae this sclerite is short and robust, and its dorsal surface is strongly modified (Fig. 8E, F).

4.2. Comparative morphology

Our results provide the first description of the morphology of the second-instar larva of *Ac. rohrelliformis* and *P. littoralis*. The species exhibit numerous similarities in their cephaloskeletons. Notably, the presence of a dome-shaped anterior rod closely attached to each mouthhook differentiates them from other muscid species. CLSM images revealed that each rod envelops the tips of the mouthhooks and further extends forward in relation to them. To the best of our knowledge, this specific shape of the anterior rod has not been documented previously and its function remains uncertain. Although previous studies have provided relatively detailed descriptions of spinulation pattern, arrangement of anal papillae and shape of posterior spiracles in the third-instar larva of *Ac. rohrelliformis*, *P. littoralis* and *Au. rostrata*, details of the cephaloskeleton have either been briefly described or not described at all. Illustrations of the third-instar larval body, the cephaloskeleton and the posterior spiracles were provided by Lobanov (1975) for *Ac. rohrelliformis*, by Zimin (1948) for *P. littoralis*, by Fuller (1932) and Zumpt (1965) for *Au. rostrata* and by Skidmore (1985) for all three species. Examination of these figures reveals that the authors observed all sclerites recognised in this study, except for the epistomal sclerite, parastomal bars, a pair of labial sclerites and a pair of rami in all exam-

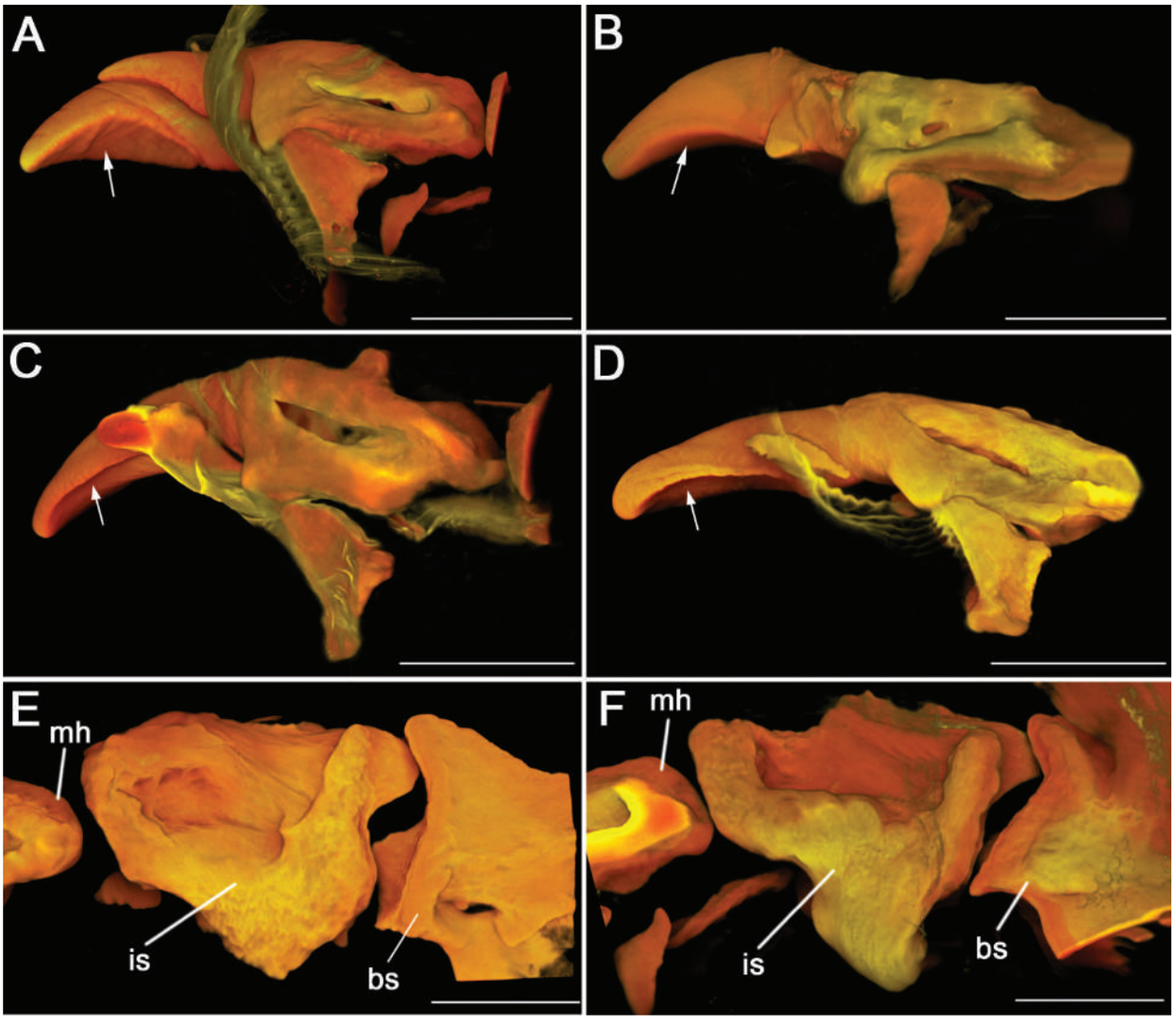

Figure 8. CLSM images of mouthhook of third-instar larvae of some representatives of *Musca*, *Stomoxys* and *Neomyia*. Expanded apical part of mouthhook assists coprophagous and saprophagous species to more efficiently collect food mass (A–D). **A** *Musca conducens* Walker, left-ventrolateral view. **B** *Stomoxys calcitrans* (Linnaeus), left-ventrolateral view. **C** *Neomyia gavisa* (Walker), right-ventrolateral view. **D** *Neomyia lauta* (Wiedemann), right-ventrolateral view. **E** intermediate sclerite of *N. lauta*, lateral view. **F** intermediate sclerite of *M. conducens*, lateral view. — Abbreviations: *bs*, basal sclerite; *is*, intermediate sclerite; *mh*, mouthhook. Scale bars: 0.05 mm.

ined species as well as the rectangular accessory process in *Ac. rohrelliformis*. Additionally, CLSM revealed that the dental sclerite in all examined species is connected to the base of the mouthhook by a narrow, sclerotized hinge. Skidmore (1985) noted that the intermediate sclerite of *Ac. rohrelliformis*, *P. littoralis* and *Au. rostrata* is equipped with a "very strong acute dorsal tooth", which corresponds to the location of the parastomal bar that has fused with the dorsal edge of the intermediate sclerite (Walczak et al. 2022). Despite the long-standing belief that the absence of a parastomal bar was considered a distinctive feature of the family Muscidae (Schumann 1954; Ferrar 1979; Skidmore 1985), recent evidence has demonstrated its presence in reduced form in muscid species (Walczak et al. 2022, 2023). Most importantly, all authors correctly observed the presence of additional sclerites below the apical part of the mouthhooks, however they did not recognise the asymmetry of the oral bars and anterior rods in *Ac. rohrelliformis*, as well as the peculiar shape of anterior rods in both *Ac. rohrelliformis* and *P. littoralis*. The right mouthhook in *Ac. rohrelliformis* is fused basally to a serrated oral bar through a rectangular accessory process, while its apical part is closely attached to a spade-like anterior rod. Below the left mouthhook, these structures are reduced, irregular and unconnected to the base of the mouthhook. Although asymmetry of the mouthhooks is a feature shared by all species in the subfamily Azeliinae (Grzywacz et al. 2021), the pronounced asymmetry of the accessory oral sclerites documented in this study has not been reported previously. While the mouthhooks and accessory oral sclerites do not exhibit such pronounced asymmetry in *P. littoralis*, they do possess comparably well-developed accessory oral sclerites as observed in *Ac. rohrelliformis*. This is in comparison with Skidmore (1985), who misinterpreted the anterior rod and oral bar in *P. littoralis* as

"very slender, short and weak". A similar inconsistency exists in the description of the morphology of *P. scabra* (Giglio-Tos). Skidmore (1985) mentioned the absence of accessory oral sclerites in this species, misinterpreting the line drawings presented by Calhoun et al. (1956), and thus considering *P. scabra* a sole representative of Azelinae devoid of accessory oral sclerites. A re-examination of fig. 3 in Calhoun et al. (1956) revealed that the third instar of *P. scabra* has accessory oral sclerites that are as well-developed or even more strongly developed than in *P. littoralis*. Similarly to *Ac. rohrelliformis*, the oral bar of *P. scabra* closely adjoins the basal part, and the anterior rod adjoins the apical part of the mouthhook. All aforementioned morphological structures, in particular the shape of accessory oral sclerites, and the connection between them, might have been overlooked by previous authors due to the limitations of light microscopy techniques. On the other hand, this might also have resulted from the process of microscopical preparation itself. This study revealed how maceration time in potassium hydroxide may critically impact the visibility of fine sclerites, making them nearly invisible. Individually adjusted maceration time is therefore strongly recommended for each specimen under study. Furthermore, Skidmore's cephaloskeletons of *Ac. rohrelliformis* and *P. littoralis* were dissected from puparia, which could have caused the displacement or rupture of small, weakly sclerotized morphological structures.

4.3. Functional morphology and notes on larval feeding strategy

The function of the modified anterior rods in *Ac. rohrelliformis* and *P. littoralis* remains ambiguous, and further investigation of larval biology would be necessary to unravel its significance. Keilin (1917) demonstrated a close relationship between larval feeding habits and the presence/absence and shape of cephaloskeletal elements, which was later refined by other authors (Keilin and Tate 1930; Thomson 1937; Roberts 1971; Ferrar 1979; Skidmore 1985). Based on the presence of additional oral sclerites and following the conclusions of previous authors, larvae of *Achanthiptera*, *Australophyra* and *Potamia* should be considered facultative carnivores. This larval feeding strategy is particularly indicated by relatively blunt-tipped mouthhooks, well-developed accessory oral sclerites composed of oral bars and anterior rods and well visible longitudinal ventral pharyngeal ridges. Accessory oral sclerites are known to play a vital role in facilitating the movement of mouthhooks when piercing the cuticle of the prey (Roberts 1971). When the mouthhooks are flexed downwards, the oral bars emerge from the functional mouth opening being held in place by the anterior rods to grip the cuticle of potential prey, as shown in fig. 5H in Grzywacz et al. (2014) (Roberts 1971; Skidmore 1973). While accessory oral sclerites in *Au. rostrata* resemble those of the majority of species within the genus *Hydrotaea* (Grzywacz et al. 2014), their modified shape in *Achanthiptera* and *Potamia* seems unlikely to support this function. It is therefore proposed here that the modified anterior rods in the second- and third-instar larvae of both *Achanthiptera* and *Potamia*, in conjunction with the mouthhooks, increase the surface area for collecting food mass. A similar modification for increasing the surface area of the mouthhooks for shovelling liquefied food has already been reported in some saprophagous and coprophagous species within the subfamily Muscinae. For example, species of *Musca* Linnaeus, *Neomyia* Walker and *Stomoxys* Geoffroy are known to have a laterally expanded apical part of the mouthhook (Fig. 8A–D), enabling more efficient collection of food mass (Ferrar 1979; Skidmore 1985). In *Atherigona* Rondani, in turn, a distinct modification of accessory oral sclerites is well known, reflecting the adaptive transition from facultative carnivory (e.g. *At. culicivora* Kovac, Pont and Deeming and *At. orientalis* Schiner) to phytophagy (e.g. *At. reversura* Villeneuve) (Skidmore 1985; Grzywacz and Pape 2013, 2014; Kovac et al. 2023). In the subgenus *Atherigona* s. str., the massively enlarged oral bar and the reduced mouthhook are fused, thereby functioning as a single structure. As a result, lateral movement is inhibited, and the fused sclerites functionally resemble the broadened mouthhooks of phytophagous Anthomyiidae (Roberts 1971; Ferrar 1987).

In summary, based on the current study and literature data, the larval instars of *Au. rostrata* are considered facultative carnivores, while strong asymmetry of mouthhooks and modified accessory oral sclerites in *Ac. rohrelliformis* indicate a saprophagous lifestyle. The larval morphology of the second and third instars of *P. littoralis* closely corresponds to that of *Ac. rohrelliformis*, the only difference being that in *P. littoralis* both oral bars lie freely. Nonetheless, considering similar modifications of accessory oral sclerites, we assume that both *P. littoralis* and *P. scabra* are saprophages, although this requires corroboration, such as through observations from rearing experiments.

5. Declarations

Funding statement. This research was supported by the National Science Centre of Poland (grant no. 2019/33/B/NZ8/02316 to AG) and the SYNTHESYS+ Projects http://www.synthesys.info/, which are financed by the European Community Research Infrastructure Action under the FP7 Integrating Activities Programme (grants nos. DE-TAF-3859, DK-TAF-3856, GB-TAF-3301 and GB-TAF-125 to AG and KW).

CRediT authorship contribution statement. Kinga Walczak: Conceptualization, Methodology, Investigation, Writing – Original draft, Writing – Review and Editing, Visualization. **Thomas Pape:** Resources, Writing – Review and Editing. **James F. Wallman:** Resources, Writing – Review and Editing. **Krzysztof Szpila:** Resources, Writing – Review and Editing. **Andrzej Grzywacz:** Conceptualization, Methodology, Writing – Review and Editing, Visualization, Funding Acquisition.

Declaration of Competing Interests. The authors have declared no competing interests.

6. Acknowledgements

We express our appreciation to Dr Joachim Ziegler (Museum für Naturkunde Leibniz-Institut für Evolutions- und Biodiversitätsforschung, Berlin, Germany), Mr Jaime A. Florez Fernandez (Australian National Insect Collection, CSIRO Ecosystem Sciences, Canberra, Australia) and Dr David K. Yeates (Australian National Insect Collection, CSIRO Ecosystem Sciences, Canberra, Australia) for help in obtaining material.

7. References

Archer MS, Elgar MA (2003a) Effects of decomposition on carcass attendance in a guild of carrion-breeding flies. Medical and Veterinary Entomology 17: 263–271. https://doi.org/10.1046/j.1365-2915.2003.00430.x

Archer MS, Elgar MA (2003b) Yearly activity patterns in southern Victoria (Australia) of seasonally active carrion insects. Forensic Science International 132: 173–176. https://doi.org/10.1016/S0379-0738(03)00034-3

Archer MS, Elgar MA, Briggs CA, Ranson DL (2006) Fly pupae and puparia as potential contaminants of forensic entomology samples from sites of body discovery. International Journal of Legal Medicine 120: 364–368. https://doi.org/10.1007/s00414-005-0046-x

Assis Fonseca ECM d' (1968) Diptera Cyclorrhapha Calyptrata Section (b) Muscidae. Handbooks for the Identification of British Insects 10: 1–118.

Barták M, Roháček J (2011) Records of interesting flies (Diptera) attracted to meat baited pyramidal trap on sapping stump of European walnut (*Juglans regia*) in Central Bohemia (Czech Republic). Časopis Slezského Zemského Muzea 60: 223–233. https://doi.org/10.2478/v10210-011-0026-3

Bloxham MG (1978) Notes on Diptera bred from the remains of a nest of *Vespula vulgaris* (common wasp). Bulletin of the Amateur Entomologists' Society 37: 194–196.

Bloxham MG (1982) The Diptera (Calyptratae) of the Sandwell Valley, West Bromwich. In: Chalmers-Hunt JM (Ed.) The Entomologist's Record and Journal of Variation 94: 28–31.

Buenaventura E, Lloyd MW, Perilla López JM, González VL, Thomas-Cabianca A, Dikow T (2021) Protein-encoding ultraconserved elements provide a new phylogenomic perspective of Oestroidea flies (Diptera: Calyptratae). Systematic Entomology 46: 5–27. https://doi.org/10.1111/syen.12443

Calhoun EL, Dodge HR, Fay RW (1956) Description and rearing of various stages of *Dendrophaonia scabra* (Giglio-Tos) (Diptera, Muscidae). Annals of the Entomological Society of America 49: 49–54. https://doi.org/10.1093/aesa/49.1.49

Carvalho de CJB (1989) Classificação de Muscidae (Diptera): uma proposta através da análise cladística. Revista Brasileira de Zoologia 6(4): 627–648. https://doi.org/10.1590/S0101-81751989000400009

Couri MS (2007) A key to the Afrotropical genera of Muscidae (Diptera). Revista Brasileira de Zoologia 24: 175–184. https://doi.org/10.1590/S0101-81752007000100022

Couri MS (2010) Key to the Australasian and Oceanian genera of Muscidae (Diptera). Revista Brasileira de Entomologia 54: 529–544. https://doi.org/10.1590/S0085-56262010000400002

Courtney GW, Sinclair BJ, Meier R (2000) Morphology and terminology of Diptera larvae. In: Papp L, Darvas B (Eds) Contributions to a Manual of Palaearctic Diptera (with Special Reference to Flies of Economic Importance). Science Herald Press, Budapest, Hungary, 85–161.

Cuny R (1978) Muscidae und Calliphoridae (Insecta: Diptera) der Lägern (Schweiz: Jura). Mitteilungen der Schweizerischen Entomologischen Gesellschaft 51: 377–394. https://doi.org/10.5169/seals-401897

Dawson BM, Barton PS, Wallman JF (2020) Contrasting insect activity and decomposition of pigs and humans in an Australian environment: A preliminary study. Forensic Science International 316: 110515. https://doi.org/10.1016/j.forsciint.2020.110515

Emden FI van (1965) The fauna of India and the adjacent countries. Diptera, Muscidae. Government of India, Delhi, 7: 1–647.

Evenhuis NL, Pape T (2023) Systema Dipterorum. In: Bánki O et al. Catalogue of Life Checklist (4.2.2, May 2023). Natural History Museum of Denmark. https://doi.org/10.15468/k7gwad

Fan Z (2008) Fauna Sinica, Insecta vol. 49. Diptera Muscidae (I). Science Press, Beijing, 1–1180.

Ferrar P (1979) The immature stages of dung-breeding muscoid flies in Australia, with notes on the species, and keys to larvae and puparia. Australian Journal of Zoology, Supplementary Series 73: 1–106. https://doi.org/10.1071/AJZS073

Ferrar P (1987) A guide to the breeding habits and immature stages of Diptera Cyclorrhapha. Entomonograph 8: 1–907.

Fuller ME (1932) The larvae of Australian sheep blowflies. Proceedings of The Linnean Society of New South Wales 57: 77–91.

Fuller ME (1934) The insect inhabitants of carrion: a study in animal ecology. Melbourne: Council for Scientific and Industrial Research; Bulletin no. 82: 1–63.

Grzywacz A (2013a) Review and comparative analysis of the morphology of third instar larvae of European and Mediterranean Muscidae (Diptera) of forensic importance. Nicolaus Copernicus University, 1–157.

Grzywacz A (2013b) Third instar larva morphology of *Hydrotaea cyrtoneurina* (Zetterstedt, 1845) (Diptera: Muscidae) – a species of forensic interest. Polish Journal of Entomology 82: 303–315. https://doi.org/10.2478/v10200-012-0044-5

Grzywacz A, Pape T (2013) Morphology of immature stages of *Atherigona reversura* (Diptera: Muscidae), with notes on the recent invasion of North America. Journal of Natural History 47: 1055–1067. https://doi.org/http:10.1080/00222933.2012.742244

Grzywacz A, Pape T (2014) Larval morphology of *Atherigona orientalis* (Schiner) (Diptera: Muscidae) – a species of sanitary and forensic importance. Acta Tropica 137: 174–184. https://doi.org/10.1016/j.actatropica.2014.05.018

Grzywacz A, Lindström A, Hall MJR (2014) *Hydrotaea similis* Meade (Diptera: Muscidae) newly reported from a human cadaver: A case report and larval morphology. Forensic Science International 242: e34–e43. https://doi.org/10.1016/j.forsciint.2014.07.014

Grzywacz A, Wallman JF, Piwczyński M (2017) To be or not to be a valid genus: the systematic position of *Ophyra* R.-D. revised (Diptera: Muscidae). Systematic Entomology 42: 714–723. https://doi.org/10.1111/syen.12240

Grzywacz A, Trzeciak P, Wiegmann BM, Cassel BK, Pape T, Walczak K, Bystrowski C, Nelson L, Piwczyński M (2021) Towards a new classification of Muscidae (Diptera): a comparison of hypotheses based on multiple molecular phylogenetic approaches. Systematic Entomology 46: 508–525. https://doi.org/10.1111/syen.12473

Hardy GH (1939) Notes on Australian Muscoidea (Calyptrata). Proceedings of the Royal Society of Queensland 45: 30–37. https://doi.org/10.5962/p.272112

Haseyama KLF, Wiegmann BM, Almeida EAB, Carvalho de CJB (2015) Say goodbye to tribes in the new house fly classification: A new molecular phylogenetic analysis and an updated biogeographical narrative for the Muscidae (Diptera). Molecular Phylogenetics and Evolution 89: 1–12. https://doi.org/10.1016/j.ympev.2015.04.006

Hennig W (1955) 63 b. Muscidae. In: Lindner E (Ed.) Die Fliegen der Paläarktischen Region. Schweizerbart'sche Verlagsbuchhandlung, Stuttgart, 625–672.

Hennig W (1965) Vorarbeiten zu einem phylogenetischen System der Muscidae (Diptera: Cyclorrhapha). Stuttgarter Beiträge zur Naturkunde 141: 1–100.

Iwasa M, Hori K (1993) A new record of *Potamia littoralis* Robineau-Desvoidy (Diptera: Muscidae) bred from birds' nests in Japan. Japanese Journal of Sanitary Zoology 44(4): 395–396. https://doi.org/10.7601/mez.44.395

Iwasa M, Hori K, Aoki N (1995) Fly fauna of bird nests in Hokkaido, Japan (Diptera). The Canadian Entomologist 127(5): 613–621. https://doi.org/10.4039/Ent127613-5

Jorge SC (2016) Revisão taxonômica e análise cladística do gênero Neotropical *Micropotamia* Carvalho (Diptera, Muscidae). Universidade Federal do Paraná, 1–62.

Keilin D (1917) Recherches sur les Anthomyiidaes a larves carnivores. Parasitology 9(3): 325–450. https://doi.org/10.1017/S0031182000006132

Keilin D, Tate P (1930) On certain semi-carnivorous anthomyid larvae. Parasitology 22(2): 168–181. https://doi.org/10.1017/S0031182000011045

Kovac D, Pont AC, Deeming JC (2023) *Atherigona culicivora*, new species (Insecta: Diptera: Muscidae), a bamboo shoot-fly feeding on mosquito larvae. The Raffles Bulletin of Zoology 71: 583–595. https://doi.org/10.26107/RBZ-2023-0044

Kutty SN, Pape T, Wiegmann BM, Meier R (2010) Molecular phylogeny of the Calyptratae (Diptera: Cyclorrhapha) with an emphasis on the superfamily Oestroidea and the position of Mystacinobiidae and McAlpine's fly. Systematic Entomology 35: 614–635. https://doi.org/10.1111/j.1365-3113.2010.00536.x

Kutty SN, Pont AC, Meier R, Pape T (2014) Complete tribal sampling reveals basal split in Muscidae (Diptera), confirms saprophagy as ancestral feeding mode, and reveals an evolutionary correlation between instar numbers and carnivory. Molecular Phylogenetics and Evolution 78: 349–364. https://doi.org/10.1016/j.ympev.2014.05.027

Kutty SN, Pape T, Pont AC, Wiegmann BM, Meier R (2008) The Muscoidea (Diptera: Calyptratae) are paraphyletic: Evidence from four mitochondrial and four nuclear genes. Molecular Phylogenetics and Evolution 49: 639–652. https://doi.org/10.1016/j.ympev.2008.08.012

Lobanov AM (1965) The morphology of the third instar larvae of the synanthropic flies of the genus *Hydrotaea* R.-D. (Diptera, Muscidae). Zoologicheskii Zhurnal 47: 85–90.

Lobanov AM (1975) On the morphology of the larva *Achanthiptera rohrelliformis* R.-D. (Diptera, Muscidae). Entomologicheskoe Obozrenie 54: 442–445.

Malloch JR (1923) Notes on Australian Diptera with descriptions. [No. i.]. Proceedings of the Linnean Society of New South Wales 48: 601–622.

Malloch JR (1925) Notes on Australian Diptera. [No. vi.]. Proceedings of the Linnean Society of New South Wales 50: 80–97.

McIntosh CS, Dadour IR, Voss SC (2017) A comparison of carcass decomposition and associated insect succession onto burnt and unburnt pig carcasses. International Journal of Legal Medicine 131: 835–845. https://doi.org/10.1007/s00414-016-1464-7

Michelsen V (1977) Oversigt over Danmarks Muscidae (Diptera). Entomologiske Meddelelser 45: 109–163.

Michelsen V (2022) Costal vein chaetotaxy, a neglected character source in Fanniidae and Muscidae (Diptera: Calyptratae). European Journal of Taxonomy 826: 94–134. https://doi.org/10.5852/ejt.2022.826.1839

O'Flynn MA, Moorhouse DE (1980) Identification of early immature stages of some common Queesland carrion flies. Journal of Australian Entomology Society 19: 53–61. https://doi.org/10.1111/j.1440-6055.1980.tb00961.x

Piwczyński M, Pape T, Deja-Sikora E, Sikora M, Akbarzadeh K, Szpila K (2017) Molecular phylogeny of Miltogramminae (Diptera: Sarcophagidae): Implications for classification, systematics and evolution of larval feeding strategies. Molecular Phylogenetics and Evolution 116: 49–60. https://doi.org/10.1016/j.ympev.2017.07.001

Pont AC (1973) Studies on Australian Muscidae (Diptera). IV. A revision of the subfamilies Muscinae and Stomoxyinae. Australian Journal of Zoology, Supplementary Series 21: 129–296. https://doi.org/10.1071/AJZS021

Pont AC (1986) Family Muscidae. In: Soós A, Papp L (Eds) Catalogue of Palaearctic Diptera. Vol. 11. Scatophagidae – Hypodermatidae. Akadémiai Kiadó, Budapest, 57–215.

Pont AC (1989) Family Muscidae. In: Evenhuis NL (Ed.) Catalog of the Diptera of the Australasian and Oceanian Regions. Special Publications of the Bernice Pauahi Bishop Museum 86, Bishop Museum Press, Honolulu. Brill, Leiden, 675–699.

Roback SS (1951) A classification of the muscoid calyptrate Diptera. Annals of the Entomological Society of America 44(3): 327–361. https://doi.org/10.1093/aesa/44.3.327

Roberts MJ (1971) The structure of the mouthparts of some calypterate dipteran larvae in relation to their feeding habits. Acta Zoologica 52: 171–188. https://doi.org/10.1111/j.1463-6395.1971.tb00556.x

Rognes K (1986) A check-list of Norwegian Muscidae (Diptera). Fauna Norvegica Series B 33: 77–85.

Sabrosky CW (1948) The muscid genus *Ophyra* in the Pacific Region (Diptera). Proceedings of the Hawaiian Entomological Society 13: 423–432.

Savage J, Wheeler TA (2004) Phylogeny of the Azeliini (Diptera: Muscidae). Studia Dipterologica 11: 259–299.

Schumann H (1954) Morphologisch-systematische Studien an Larven von hygienisch wichtigen mitteleuropäischen Dipteren der Familien Calliphoridae-Muscidae. Wissenschaftliche Zeitschrift der Universität Greifswald III 1953–54: 245–274.

Séguy E (1923) Diptéres Anthomyides. Faune de France 6: 1–393.

Skidmore P (1973) Notes on the biology of Palaearctic Muscids. The Entomologist 106: 25–59.

Skidmore P (1985) The biology of the Muscidae of the World. Series Entomologica 29: 1–550.

Sorokina VS, Pont AC (2010) An annotated catalogue of the Muscidae (Diptera) of Siberia. Zootaxa 2597: 1–87. https://doi.org/10.11646/zootaxa.2597.1.1

Szpila K, Pape T (2005) The first instar larva of *Apodacra pulchra* (Diptera: Sarcophagidae, Miltogramminae). Insect Systematics & Evolution 36: 293–300. https://doi.org/10.1163/187631205788838447

Szpila K, Walczak K, Johnston NP, Pape T, Wallman JF (2021) First instar larvae of endemic Australian Miltogramminae (Diptera: Sarcophagidae). Scientific Reports 11: 1–12. https://doi.org/10.1038/s41598-020-80139-x

Thomson BCM (1937) Observations on the biology and larvae of the Anthomyiidae. Parasitology 29(3): 273–358. https://doi.org/10.1017/S0031182000024847

Vockeroth JR (1972) A review of the world genera od Mydaeinae, with a revision of the species of New Guinea and Oceania (Diptera: Muscidae). Pacific Insects Monograph 29: 1–134.

Walczak K, Pape T, Ekanem M, Szpila K, Grzywacz A (2023) Insights into the systematics of *Alluaudinella* and allied *Aethiopomyia* and *Ochromusca* (Muscidae, Diptera). Zoologica Scripta 52: 279–297. https://doi.org/10.1111/zsc.12584

Walczak K, Szpila K, Nelson L, Pape T, Hall MJR, Alves F, Grzywacz A (2022) Larval morphology of the avian parasitic genus *Passeromyia*: playing hide and seek with a parastomal bar. Medical and Veterinary Entomology 37: 14–26. https://doi.org/10.1111/mve.12603

Zielke E (2018) On two remarkable species of Azeliinae (Diptera: Muscidae), previously unknown from the Balkans, but collected from Bulgaria already in the 20th century. Historia Naturalis Bulgarica 30: 1–5. https://doi.org/10.48027/hnb.30.01001

Zimin LS (1948) Opredeliteli lichinok sinantropnykh mukh Tadzhikistana. Opredeliteli po Faune CCCP 28: 1–116.

Zumpt F (1965) Myiasis in Man and Animals in the Old World: A Textbook for Physicians, Veterinarians and Zoologists. London: Butterworths, 1–267.

Article 3

Walczak, K., & Grzywacz, A. (2024). An illustrated identification key to early instar larvae of forensically important Muscidae (Diptera) of the western Palaearctic region. Forensic Science International. 2024 July; 360:112028.

https://doi.org/10.1016/j.forsciint.2024.112028

Forensic Science International 360 (2024) 112028

Contents lists available at ScienceDirect

Forensic Science International

journal homepage: www.elsevier.com/locate/forsciint

An illustrated identification key to early instar larvae of forensically important Muscidae (Diptera) of the western Palaearctic region

Kinga Walczak [a,b,*], Andrzej Grzywacz [a,b,*]

[a] Department of Ecology and Biogeography, Faculty of Biological and Veterinary Sciences, Nicolaus Copernicus University in Toruń, Poland
[b] Centre for Modern Interdisciplinary Technologies, Nicolaus Copernicus University in Toruń, Poland

ARTICLE INFO

Keywords:
Confocal laser scanning microscopy
Forensic entomology
Identification
Immature stages
Muscidae

ABSTRACT

There is a significant gap in the availability of comprehensive identification keys for the early larval stages of forensically important fly species. While well-documented identification keys exist for the third instar larvae, particularly for the Calliphoridae, Muscidae and Sarcophagidae families, there is a notable scarcity of keys for the first, except Calliphoridae, and the second instar larvae, with no such resources available for muscid species. The second instar larvae suffer the most from the lack of morphological descriptions and available identification keys. The Muscidae is one of the most frequently reported dipteran families of forensic importance colonising animal cadavers and human corpses. Nevertheless, descriptions of the morphology of their early instars remain scarce and limited to only a few species, thus their larval identification is challenging or impossible. Considering the numerous challenges associated with studying small-sized entomological material, we tested whether it is feasible to identify muscid flies to the species or at least genus level based predominantly on the details of the cephaloskeleton. To overcome the obstacle of observing details of small sclerites, especially their shapes and interconnections, we effectively employed confocal laser scanning microscopy (CLSM) as a supplementary method for light microscopy (LM). This study provides an identification key for first and second instar larvae of forensically important muscid species from the western Palaearctic (Europe, North Africa, Middle East). The proposed key primarily utilises details of the cephaloskeleton with only addition of external morphology.

1. Introduction

The utilisation of entomological material in forensic investigations most often enables the estimation of the time that has elapsed since death [1,2]. This estimation of minimum post-mortem interval (mPMI) has proven invaluable in cases where traditional methods of determining the time of death might be imprecise or no longer applicable [3]. One method is to determine the age of the oldest immature stages, primarily dipteran flies, as they are usually the first colonisers of human bodies [1]. The first step for the successful application of any entomological method, however, is a thorough and precise identification of the entomological material. Identification of adult stages is more straightforward due to the availability of well-documented identification keys [4,5] or semi-automated identification by means of wing venation patterns [6], whereas identification of larval stages poses a significantly greater challenge. The guidelines developed so far recommend identifying the immature stages using reliable identification keys, followed by rearing eggs or larvae to their adult stage under controlled laboratory conditions [2,7]. Nevertheless, in practice, this process is fraught with many challenges. The morphological diagnosis of immature stages is limited due to their morphological similarities as well as their small size, which hinders accurate examination [8]. Despite the significant increase in morphological descriptions of immature stages of necrophagous species in recent years [9–16], well-documented and user-friendly identification keys are still missing. Consequently, obtaining adult specimens becomes essential either to confirm the initial identification of eggs or larvae, if established, or as the only means of identification. On the other hand, successful rearing requires proper collection and delivery of live immature specimens [17], which is often unfulfilled due to the infrequent involvement of entomologists in the initial phase of forensic investigation. Although molecular methods have been shown to be effective for identifying preimaginal stages, this method depends not solely on the proper preservation of the material, which can significantly affect DNA degradation, but also on the potential challenge of obtaining

* Correspondence to: Department of Ecology and Biogeography, Faculty of Biological and Veterinary Sciences, Nicolaus Copernicus University in Toruń, Lwowska 1, Toruń 87-100, Poland.
E-mail addresses: walczak.kinga00@gmail.com (K. Walczak), hydrotaea@gmail.com (A. Grzywacz).

https://doi.org/10.1016/j.forsciint.2024.112028
Received 26 February 2024; Received in revised form 1 April 2024; Accepted 15 April 2024
Available online 16 April 2024

adequate amount of material in case of small-sized specimens. Combination of inappropriate preservation, small size of examined samples and extended time [18] from material collection to DNA extraction may contribute to potential failure of molecular taxonomy approach. To overcome the issue of degraded DNA, shorter fragments, c. 100–150 bp, can be amplified, but barcodes shorter than 200 bp may perform poorly in species identification [19]. The literature search highlights a scarcity of identification keys for preimaginal stages of forensically important Diptera species [20–23]. Among the dipteran families, well-documented identification keys have been established for all instars of Calliphoridae [10,13,14,24,25], as well as for the third instar larvae of Piophilidae [26], Sarcophagidae [27] and Muscidae [28].

The Muscidae is a large cosmopolitan family, whose potential forensic significance was already recognised by Mégnin [29] in the late 19th century. This family has since become a subject of growing interest in forensic entomology and has frequently been collected in experimental research and forensic investigations. Although Muscidae is represented by *ca*. 6000 species [30], only a few species are considered necrophagous [28]. Nonetheless, muscid specimens have been consistently observed colonising human corpses or animal cadavers under diverse conditions. These range from buried [31,32] and burnt remains [33,34] to those wrapped [35] or submerged in water [36]. They have also been collected during various seasons [37,38], inside building [39,40] and vehicles [41], in urban and rural areas [42–44], in sunny and shaded ones [45,46] and during early and advanced stages of decomposition [47,48]. Despite their widespread occurrence, this family faces a conspicuous absence of identification keys for the first and second instar larvae. The need to provide such a tool is demonstrated by the number of papers in which muscid larvae have been identified only to a family or genus level [36,49–51].

The primary objective of this study is to conduct a detailed morphological analysis of the early instars of necrophagous muscid species using both a light microscope (LM) and a confocal laser scanning microscope (CLSM). For two species, a scanning electron microscope (SEM) was utilised to achieve more precise identification to the species level. Based on the findings from our study, we provide the identification key for the first and second instar muscid larvae, increasing the precision and reliability of distinguishing forensically important Muscidae species from the western Palaearctic (Europe, North Africa, Middle East).

2. Material and methods

The choice of species for examination followed a review of the literature to identify Muscidae species documented in real forensic cases or in forensic entomology experiments. Larvae of selected species were obtained by keeping field-collected females in the laboratory until oviposition. Detailed protocols have been provided in Grzywacz & Pape [12] for *Atherigona orientalis* Schiner, 1868, Grzywacz et al. [52] for *Hydrotaea dentipes* (Fabricius, 1805) and *Hydrotaea similis* Meade, 1887, Grzywacz et al. [53] for *Muscina levida* (Harris, 1780), *Muscina prolapsa* (Harris, 1780) and *Muscina stabulans* Fallén, 1817, Velásquez et al. [11] for *Synthesiomyia nudiseta* Brauer & von Bergenstamm, 1893 as well as Grzywacz [54] for *Hydrotaea aenescens* (Wiedemann, 1830), *Hydrotaea armipes* (Fallén, 1825), *Hydrotaea capensis* (Wiedemann, 1818), *Hydrotaea ignava* (Harris, 1780), *Hydrotaea pilipes* Stein, 1903 and *Musca domestica* Linnaeus, 1758. Larvae of *Stomoxys calcitrans* (Linnaeus, 1758) were collected in Pławin (Poland) in 2010. The material was collected in accordance with the protocol described in Grzywacz et al. [53].

Light microscopy examination was prepared by immersion larvae in Hoyer's medium on cavity microscope slides. The light microscopy observations were conducted with a M205C Leica Stereomicroscope (Leica Microsystems, Wetzlar, Germany) with an integrated high-resolution Leica DFC495 digital camera. All examined specimens are stored in Hoyer's medium and deposited in the collection of the Department of Ecology and Biogeography, Nicolaus Copernicus University in Toruń, Toruń, Poland.

The preparation of the material for the CLSM examination was conducted in accordance with the protocol provided by Walczak et al. [55]. Firstly, the anterior part of each specimen was cut off, taking care not to damage the cephaloskeleton. This step may be omitted if there is no need to preserve the posterior part of the larval body. The subsequent step involves maceration in a 10% potassium hydroxide (KOH) solution, which stands as a pivotal step in the preparation of specimens for CLSM examination. Inadequate maceration time might result in insufficient maceration of soft tissues, consequently obscuring the desired morphological structures. Conversely, excessively prolonged maceration leads to over-maceration of the tissue, causing a significant decrease in image quality and resulting in blurred edges of sclerites. It is therefore preferable to choose a shorter initial maceration and, if necessary, carry out a second maceration. We recommend beginners, if possible, to test this step in advance on less important entomological material. Given that the first and second larval stages are relatively small and maceration makes them almost transparent, this step should be conducted in the smallest container possible. To facilitate later visibility of the macerated material, it may also be helpful to cover the bottom of the container with black tape. In this study, the maceration time in 10% KOH ranged from 8 h to 12 h for the first instar larvae and from 12 h to 20 h for the second instar larvae. Following tissue maceration, specimens were transferred to 80% EtOH for 15 min (or even kept overnight) to wash out KOH. After that, all first instar larvae were mounted on flat microscope slides using glycerine as medium and gently covered with a coverslip. When using flat microscope slides, the coverslip should be gently placed to avoid crushing or displacement of the fine sclerites. It is also possible to place first instars on cavity slides, but due to the limited focal plane of CLSM, the material should be placed on the edge of the cavity. In turn, all second instars were placed on cavity microscope slides in a drop of viscous glycerine. CLSM examination was performed with a Leica TCS SP8 Confocal Laser Scanning Microscope (Leica Microsystems, Wetzlar, Germany). The autofluorescence signal of the cephaloskeleton was collected with two excitation wavelengths: 561 and 633 nm using the sequential scanning option. The microscopic slides were scanned with a 40× oil lens with a numerical aperture of 1.3 (N.A. = 1.3). Following the acquisition of sequential images, maximum intensity projections (MIP) and 3D visualisation were built using a LAS AF V3.3 and a LAS X 3D Viewer (Leica Microsystems, Wetzlar, Germany), respectively.

First and second instar larvae of *H. dentipes* and *H. similis* were additionally prepared for SEM examination by cleaning with a fine brush, dehydration in 80.0%, 90.0% and 99.5% ethanol (EtOH) and critical point drying in carbon dioxide (CO_2) with an Autosamdri®-815, Series A critical point dryer (Tousimis Research Corp., Rockville, MD, U.S.A.). Larvae were then mounted on aluminium stubs with double-sided adhesive tape and coated with platinum for 140 s (20 nm of coating) using a JEOL JFC 2300HR high-resolution fine coater (JEOL Ltd., Tokyo, Japan). Scanning electron microscopy images were obtained with a JEOL scanning microscope (JSM-6335 F; JEOL Ltd.).

Larval terminology follows Courtney et al. [56] with a few modifications proposed by Szpila and Pape [57]. Family-specific structures follow the terminology of Skidmore [58] with modifications proposed by Grzywacz [59] and Walczak et al. [55]. For each species, observations were made on five to ten individuals, except for the first instar of *Hydrotaea pilipes*, which was limited to two individuals due to limited access to the material.

3. Results and discussion

Our literature search showed almost 250 muscid species collected on human corpses or animal cadavers, however, for the vast majority of them there was only one record. Given the frequency of their appearances, we ultimately selected 14 muscid species, occurring in the western Palaearctic, of documented and/or potential forensic

importance. In this study, we analysed the first and second instar of *A. orientalis*, *H. aenescens*, *H. capensis*, *H. dentipes*, *H. ignava*, *H. pilipes*, *H. similis*, *Mc. domestica*, *Mu. levida*, *Mu. prolapsa*, *Mu. stabulans*, *St. calcitrans* and *Sy. nudiseta* and the second instar of *H. armipes*. Larvae of *H. armipes* are dimorphic, which means that the number of free-living instars is reduced, and the second instar hatches directly from the egg.

The morphology of the cephaloskeleton, spinulation pattern and posterior spiracles in the third instar larvae have proven to be crucial for taxonomic purposes [53,58]. However, when it comes to early instars, detailed analysis of these features can be difficult or even impossible due to their small size and mostly colourless spines. Our study has demonstrated that it is feasible to identify first and second instar larvae to the species, or at least genus level, based solely on the details of the cephaloskeleton. To overcome the challenges of observing fine details in small-sized entomological specimens, we effectively applied CLSM. Although for some larvae the results of both LM and CLSM are comparable, the latter allowed precise visualisation of the shapes, positions and interconnections between sclerites. For example, in the first instar of *A. orientalis* CLSM provided information on the shapes of suprabuccal teeth and mouthhooks, as well as the interconnections of the labrum, parastomal bars and intermediate sclerite, which could not be assessed using LM.

Identification key to first and second instar larvae of forensically important Muscidae

1. Cephaloskeleton with labrum (Figs. 1–3); anterior spiracles indistinguishable, present as simple aperture …… first instar larva 2

   Cephaloskeleton without labrum (Figs. 4–6); anterior spiracles with distinct lobes …… second instar larva 14
2. Parastomal bars interrupted. Mouthhooks strongly reduced and labrum long, slender and of equal width. Basal sclerite connected only with intermediate sclerite. Intermediate sclerite in half strongly curved ventrally. Vertical plate very broad and at least 2.5 times as wide as ventral cornu. The posterior part of dorsal cornu pointed and directed posterodorsally (Fig. 3G–H) …… *Stomoxys calcitrans*

   Parastomal bars uninterrupted through its entire length. Mouthhooks curved, well-developed or reduced. Vertical plate relatively narrow and no more than 1.5 times as wide as ventral cornu …… 3
3. Suprabuccal teeth strong, sclerotized and well-visible (Fig. 1A, B; Fig. 2G, H; Fig. 3A–F) …… 4

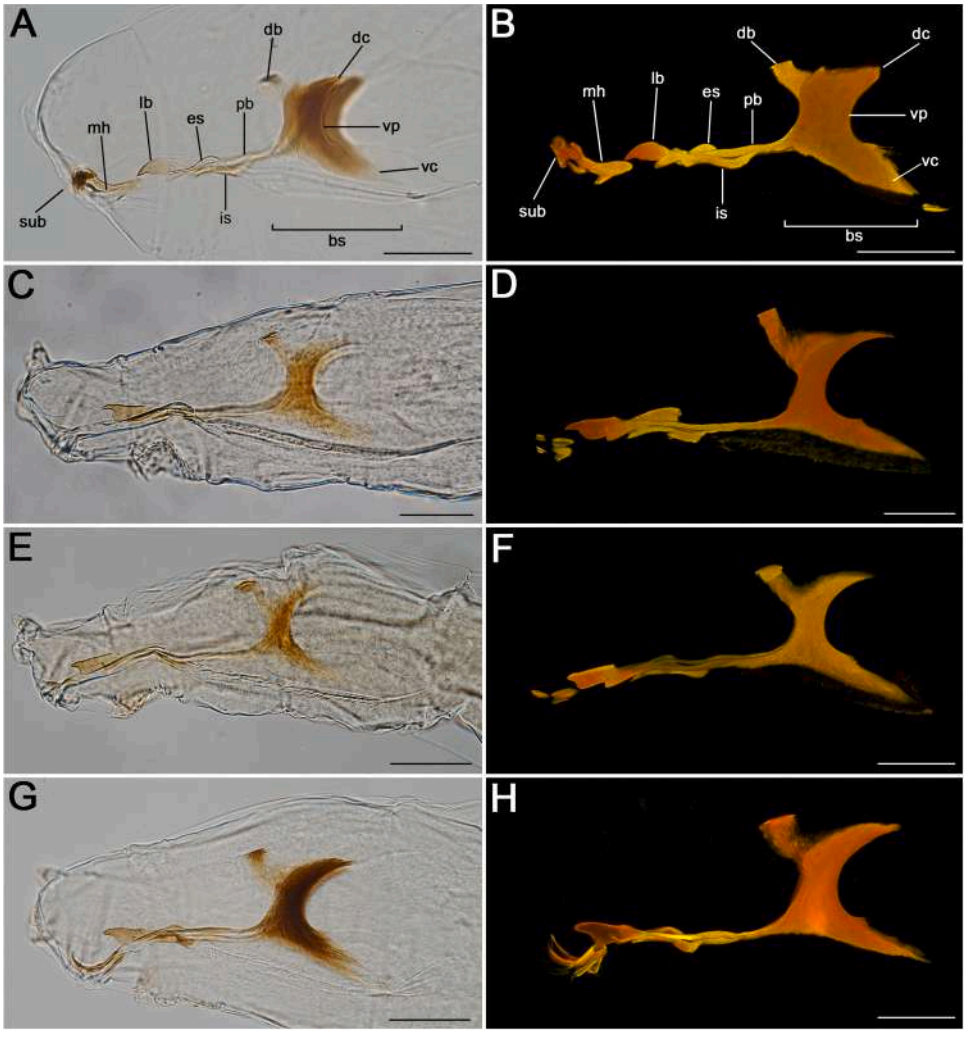

Fig. 1. Cephaloskeletons of first instar larvae using LM (A, C, E, G) and CLSM (B, D, F, H); lateral view. A, B: *Atherigona orientalis*; C, D: *Hydrotaea aenescens*; E, F: *Hydrotaea capensis*; G, H: *Hydrotaea dentipes*. Abbreviations: bs, basal sclerite; db, dorsal bridge; dc, dorsal cornu; es, epistomal sclerite; is, intermediate sclerite; lb, labrum; mh, mouthhook; pb, parastomal bar; sub, suprabuccal teeth; vc, ventral cornu; vp, ventral plate. Scale bars: 0.1 mm.

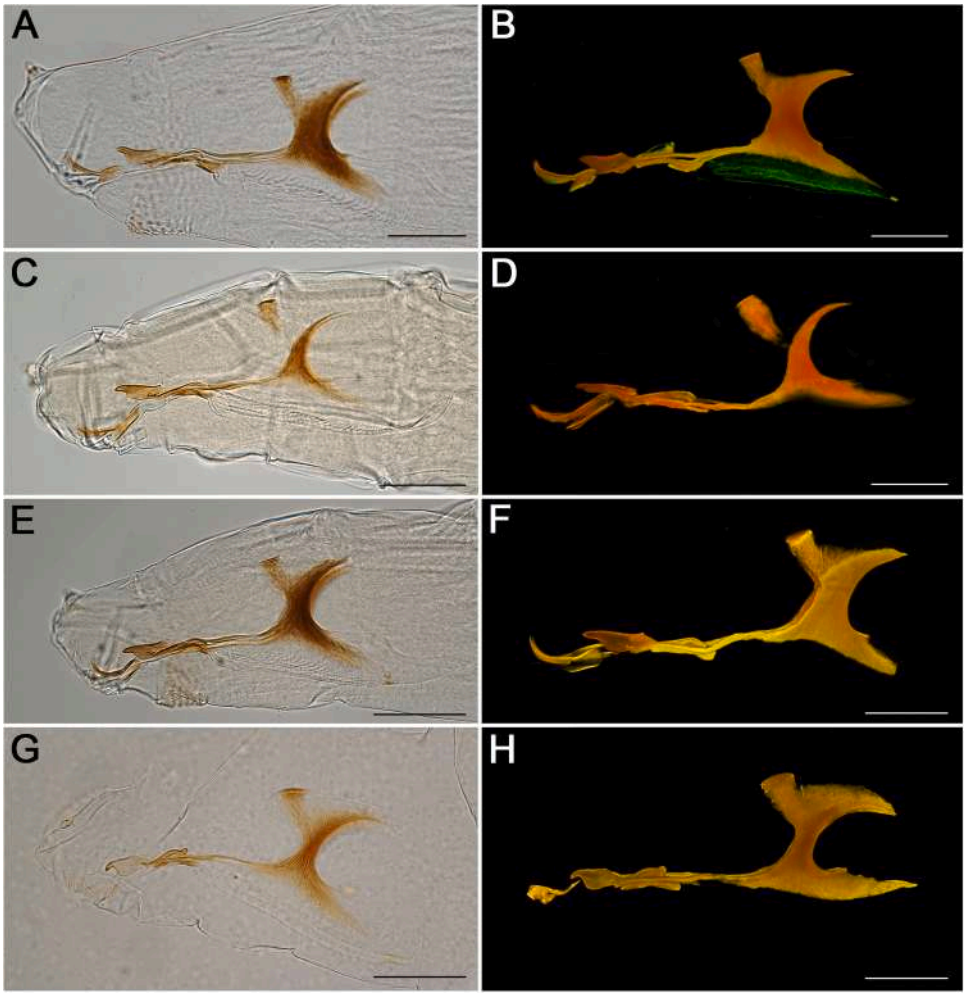

Fig. 2. Cephaloskeletons of first instar larvae using LM (A, C, E, G) and CLSM (B, D, F, H); lateral view. A, B: *Hydrotaea ignava*; C, D: *Hydrotaea pilipes*; E, F: *Hydrotaea similis*; G, H: *Musca domestica*. Scale bars: 0.1 mm.

Suprabuccal teeth reduced or not distinctly sclerotized (Fig. 1C–H; Fig. 2A–F; Fig. 3I, J) …… 8

4. Labrum tear-shaped, with dorsal surface curved. Suprabuccal teeth blunt-ended. The anterior part of intermediate sclerite sinuous. The tips of the anterior arms of parastomal bars placed between epistomal sclerite and intermediate sclerite (Fig. 1A, B) …… *Atherigona orientalis*

   Labrum elongated, with dorsal surface straight. Suprabuccal teeth sharply pointed. Vertical plate narrow, no more than 1.5 times as wide as ventral cornu (Fig. 2G, H; Fig. 3A–F) …… 5

5. The narrow apical part of labrum no more than one-fourth the length of the broad basal part and labrum broadly rounded anteroventrally. Dorsal bridge broadly sclerotized. Dorsal cornu broad and slightly shorter than ventral cornu. Dorsal and ventral cornua 1.5 times as wide as vertical plate (Fig. 2G, H) …… *Musca domestica*

   The narrow apical part of labrum no more than half the length of the basal part and labrum not broadly rounded anteroventrally. Dorsal bridge narrow and/or basally less sclerotized. Ventral cornu twice as long as dorsal cornu (Fig. 3A–F) …… *Muscina* spp. 6

6. Mouthhooks with numerous pointed and strongly sclerotized suprabuccal teeth (more than eight). The basal part of labrum bulged ventrally in lateral view. Intermediate sclerite sinuous in lateral view (Fig. 3A, B) …… *Muscina levida*

   Mouthhooks with 2–4 suprabuccal teeth. The basal part of labrum flat ventrally (Fig. 3C–F) …… 7

7. In lateral view, intermediate sclerite uniformly broad through its entire length. Mouthhooks weakly sclerotized (Fig. 3C, D) …… *Muscina prolapsa*

   In lateral view, intermediate sclerite not uniformly broad through its entire length, with broadened apical and posterior parts. Mouthhooks strongly sclerotized (Fig. 3E, F) …… *Muscina stabulans*

8. Mouthhooks well-developed with the basal part more than 2 times as wide as the apical part. The basal part of each mouthhook with distinct lateral arm. The ventral edge of labrum with protuberance. The tips of the anterior arms of intermediate sclerite bifurcated (Fig. 3I, J) …… *Synthesiomyia nudiseta*

   Mouthhooks with the basal part less than 2 times as wide as the apical part. Sometimes mouthhooks reduced, with apical and basal parts separated. Labrum at most rounded ventrally. Dorsal cornu pointed (Fig. 1C–H; Fig. 2A–F) …… *Hydrotaea* spp. 9

9. Mouthhooks reduced and weakly sclerotized, especially in the apical part. The apical and basal parts of mouthhooks with rupture (Fig. 1C–F) …… 10

   Mouthhooks well-developed and strongly sclerotized. The apical and basal parts of mouthhooks without rupture (Figs. 1G, H, Fig. 2A–F) …… 11

10. The narrow apical part of labrum short, as long as wide. In lateral view, the basal part of labrum angular anteroventrally (Fig. 1E, F)

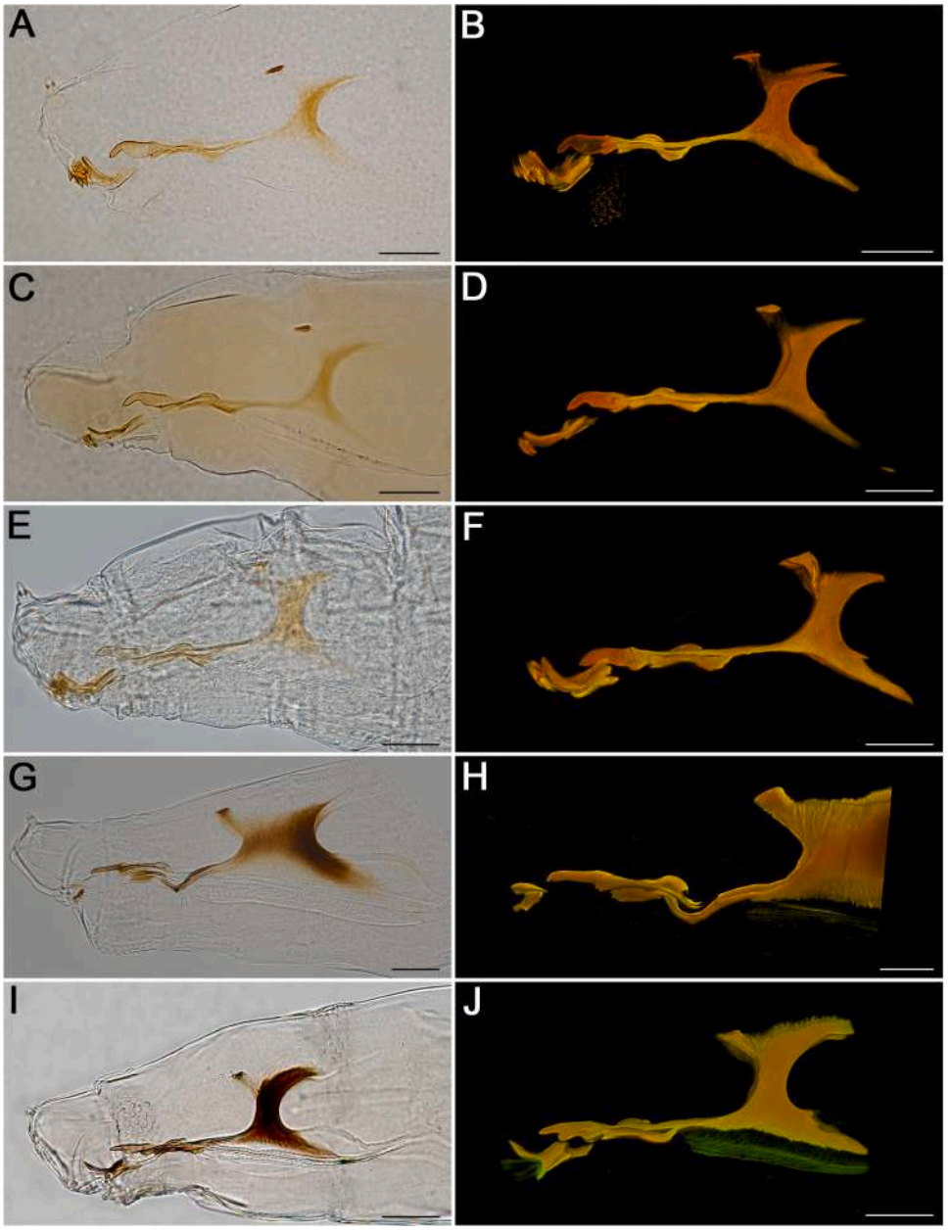

Fig. 3. Cephaloskeletons of first instar larvae using LM (A, C, E, G, I) and CLSM (B, D, F, H, J); lateral view. A, B: *Muscina levida*; C, D: *Muscina prolapsa*; E, F: *Muscina stabulans*; G, H: *Stomoxys calcitrans*; I, J: *Synthesiomyia nudiseta*. Scale bars: 0.1 mm.

…… *Hydrotaea capensis*

The narrow apical part of labrum long and sharply pointed, longer than wide in the widest part. In lateral view, the basal part of labrum rounded anteroventrally (Fig. 1C, D) …… *Hydrotaea aenescens*

11. Labrum elongated and slender, without distant anteroventral expansion of the basal part (Fig. 2C, D) …… *Hydrotaea pilipes*

    Labrum broadened in the basal part, with distinct anteroventral expansion (Fig. 1G, H; Fig. 2A, B, E, F) …… 12

12. The apical part of labrum directed anterodorsally (Fig. 2A, B) …… *Hydrotaea ignava*

    The apical part of labrum directed anteriorly (Fig. 1G, H; Fig. 2E, F) …… 13

13. Cirri long and pointed apically. Anterior spinose band broad ventrally and narrow (almost incomplete) dorsally. Transverse cleft clearly distinguishable on the first thoracic segment (Fig. 7A, B) …… *Hydrotaea dentips*

    Cirri short and trapezoid. Anterior spinose band uniformly broad and complete. Transverse cleft indistinguishable on the first thoracic segment (Fig. 7D, E) …… *Hydrotaea similis*

14. The apical and basal parts of mouthhooks broadly ruptured with the apical part almost entirely reduced. Lateral arms of intermediate sclerite long, slender and directed anterodorsally and posterodorsally (Fig. 6G, H) …… *Stomoxys calcitrans*

    The apical and basal parts of mouthhooks fused, at most narrowly ruptured, yet still with distinct apical part (Fig. 4G, H). Lateral arms of intermediate sclerite not directed upwardly (Fig. 4A–H; Fig. 5A–J; Fig. 6A–F, I, J) …… 15

15. Each mouthhook separated into two pieces, i.e., rod-like apical part and boomerang-like basal part (Fig. 4G, H; Fig. 5 I, J) …… 16

    Each mouthhook in one piece (Fig. 4A–F; Fig. 5A–H; Fig. 6A–F; I, J) …… 17

16. Suprabuccal teeth well-developed. Mouthhooks robust. The basal part of mouthhooks with distinct prominence directed posteriorly

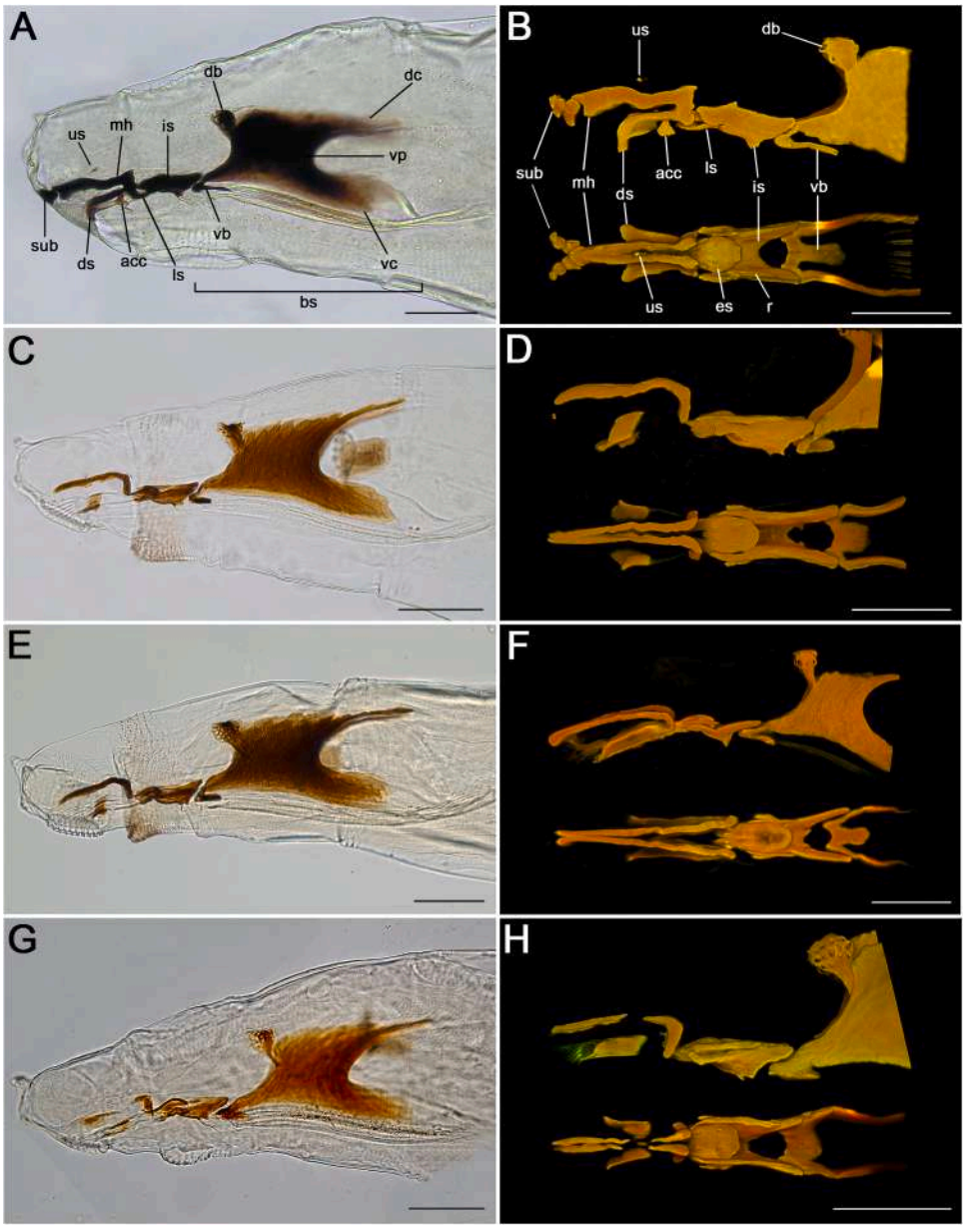

Fig. 4. Cephaloskeletons of second instar larvae using LM (A, C, E, G) and CLSM (B, D, F, H); lateral and dorsal view. A, B: *Atherigona orientalis*; C, D: *Hydrotaea aenescens*; E, F: *Hydrotaea armipes*; G, H: *Hydrotaea capensis*. Abbreviations: acc, accessory stomal sclerite; bs, basal sclerite; db, dorsal bridge; dc, dorsal cornu; es, epistomal sclerite; is, intermediate sclerite; ls, labial sclerite; mh, mouthhook; pb, parastomal bar; r, rami; sub, suprabuccal teeth; us, unpaired sclerite; vb, ventral bridge; vc, ventral cornu; vp, ventral plate. Scale bars: 0.1 mm.

(Fig. 5I, J) …… *Musca domestica*

Suprabuccal teeth absent. Mouthhooks slender. The basal part of mouthhooks without distinct prominence directed posteriorly (Fig. 4G, H) …… *Hydrotaea capensis*

17. Suprabuccal teeth well-developed (Fig. 4A, B; Fig. 6A–F, I, J) …… 18

    Suprabuccal teeth reduced or absent (Fig. 4C–F; Fig. 5A–H) …… *Hydrotaea* spp. 21

18. Mouthhooks F-shaped in lateral view. Dorsal cornu longer than ventral cornu (Fig. 6I, J) …… *Synthesiomyia nudiseta*

    Mouthhooks with irregular L-shape in lateral view. The base of each mouthhook fused with dental sclerite, hence these two sclerites form a U-shaped structure in lateral view (Fig. 4A, B; Fig. 6A–F) …… 19

19. The tip of the apical part of mouthhooks bifurcated. Vertical plate broad, at least 3 times as wide as the width of dorsal cornu. Dorsal cornu somewhat shorter than ventral cornu (Fig. 4A, B) …… *Atherigona orientalis*

    The apical part of mouthhooks blunt-ended. Vertical plate less than 3 times as wide as the width of dorsal cornu. Dorsal and ventral cornua of similar length (Fig. 6A–F) …… *Muscina* spp. 20

20. Suprabuccal teeth numerous, strongly developed in dorsal view and the apical part of mouthhooks distinctly expanded anteriorly in lateral view (Fig. 6A, B) …… *Muscina levida*

    Suprabuccal teeth consist of 3–4 teeth and the apical part of mouthhooks slightly expanded, but not more than half the posterior part. The apical part of dental sclerite directed ventrally (Fig. 6C, D) …… *Muscina prolapsa*

    Suprabuccal teeth consist of 3–4 teeth and the apical part of mouthhooks of uniform width along entire length. The apical part of dental sclerite directed posteroventrally (Fig. 6E, F) …… *Muscina stabulans*

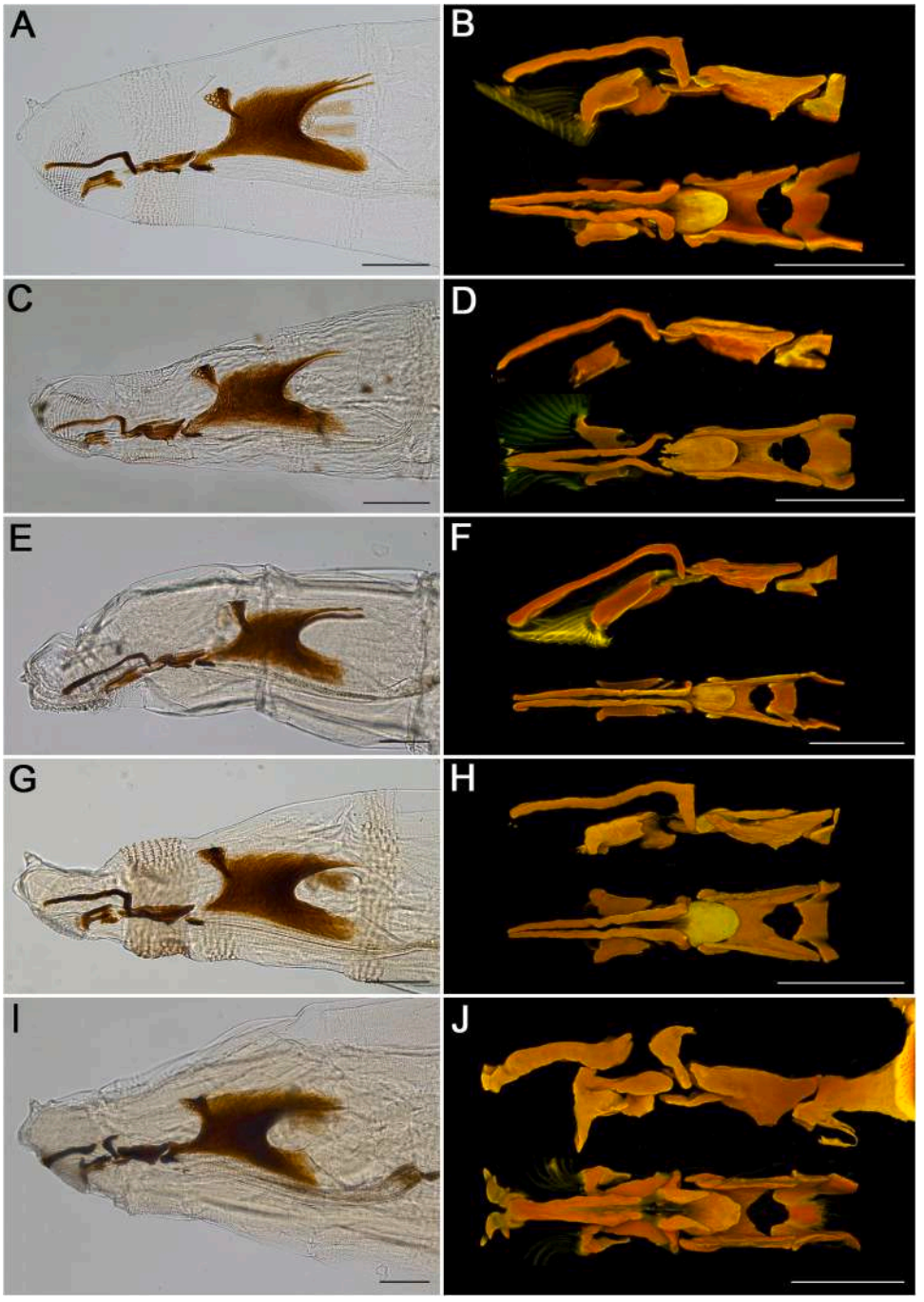

Fig. 5. Cephaloskeletons of second instar larvae using LM (A, C, E, G, I) and CLSM (B, D, F, H, J); lateral and dorsal view. A, B: *Hydrotara dentipes*; C, D: *Hydrotaea ignava*; E, F: *Hydrotaea pilipes*; G, H: *Hydrotaea similis*; I, J: *Musca domestica*. Scale bars: 0.1 mm.

21. Dental sclerite, excluding accessory stomal sclerite, at least half the length of mouthhook or dorsal cornu uniformly narrow through its entire length (Fig. 4E, F; Fig. 5E, F) …… 22

    Dental sclerite, excluding accessory stomal sclerite, less than half the length of mouthhook or dorsal cornu narrowing posteriorly (Fig. 4C, D; Fig. 5A–D, G, H) …… 23
22. Mouthhooks converging in dorsal view. Intermediate sclerite short and pointed ventrally in lateral view (Fig. 4E, F) …… *Hydrotaea armipes*

    Mouthhooks parallel in dorsal view and closely appressed to each other (Fig. 5E, F) …… *Hydrotaea pilipes*
23. Dental sclerite very short, less than one-third of mouthhook length (Fig. 4C, D) …… *Hydrotaea aenescnes*

    Dental sclerite at least one-third as long as mouthhook (Fig. 5A–D, G, H) …… 24
24. Junction between the apical and basal parts of mouthhooks rounded. Accessory stomal sclerite reduced and weakly sclerotized (Fig. 5C, D) …… *Hydrotaea ignava*

    Junction between the apical and basal parts of mouthhooks angular. Accessory stomal sclerite well-developed (Fig. 5A, B, G, H) …… 25
25. Anterior spinose band on the first thoracic segment uniformly broad; spines do not reach transverse cleft (Fig. 7C) …… *Hydrotaea dentipes*

    Anterior spinose band on the first thoracic segment not

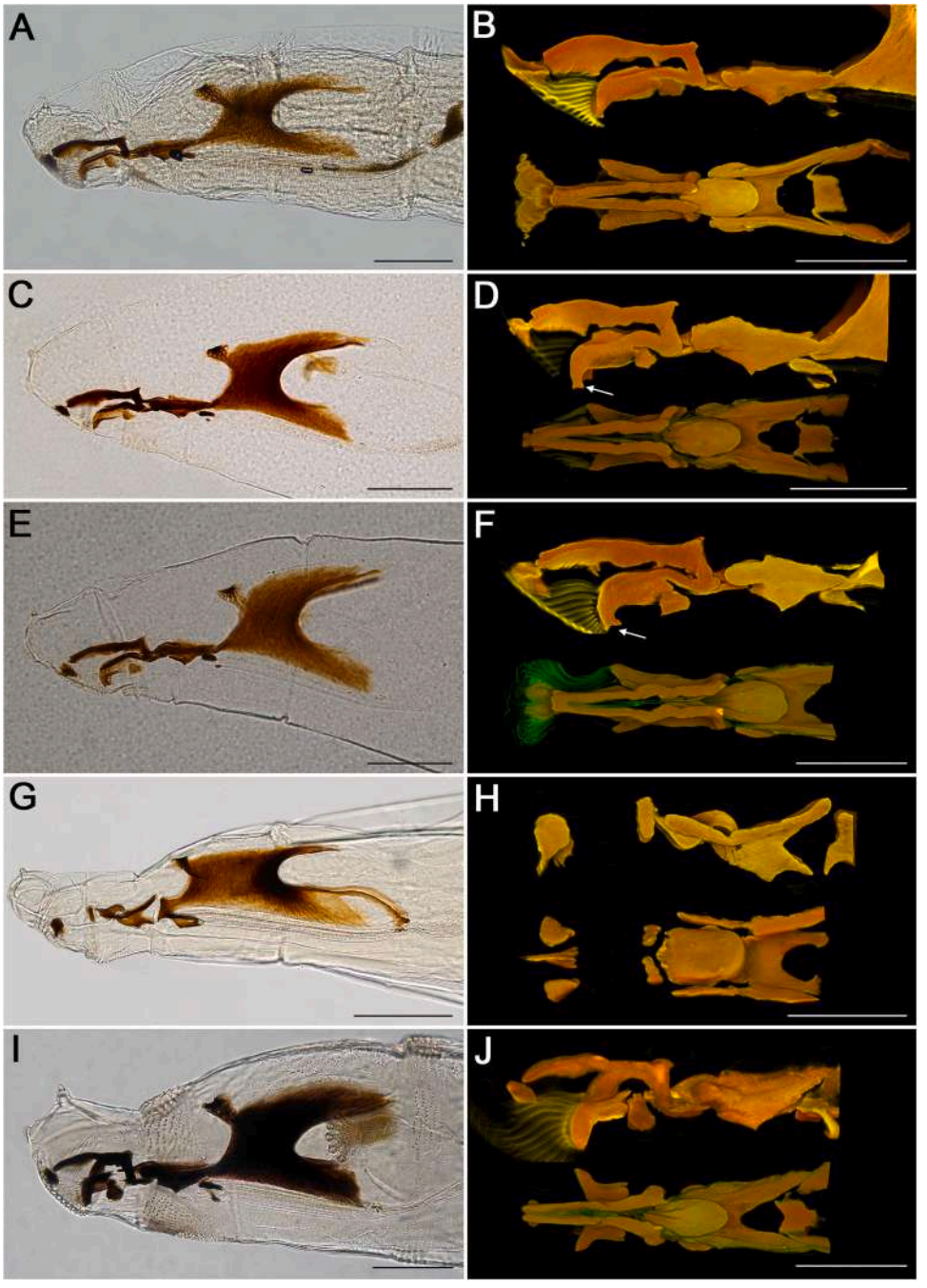

Fig. 6. Cephaloskeletons of second instar larvae using LM (A, C, E, G, I) and CLSM (B, D, F, H, J); lateral and dorsal view. A, B: *Muscina levida*; C, D: *Muscina prolapsa*; E, F: *Muscina stabulans*; G, H: *Stomoxys calcitrans*; I, J: *Synthesiomyia nudiseta*. The arrows indicate the apical part of the dental sclerite directed ventrally (D) or posteroventrally (F). Scale bars: 0.1 mm.

uniformly broad and ventrally with a few additional rows of spines just behind transverse cleft Fig. 7F) …… *Hydrotaea similis*

The identification key provided in this manuscript is considered the first-choice tool that can be used by practitioners to identify first and second instars of muscid larvae in a relatively short time. While CLSM approach has been used in this study to illustrate fine details of the cephaloskeleton of early larval stages, the key itself can be used with only classical light microscopy methods. In case of difficulties in material identification or ambiguous results, users should support themselves with alternative methods of molecular taxonomy. Our examination revealed that precise identification of early instars of muscid larvae is possible by observing the shape, size and position of the cephaloskeleton's sclerites. Examination of details of external morphology in some cases may be used as a supplementary source of information, however, it does not allow for unambiguous discrimination of all species. It is in contrast to third instar muscid larvae, which may be precisely identified by means of external morphology examination [28]. Some of the examined species display peculiar characters that allow relatively easy and straightforward identification, while others require a thorough assessment based on a combination of morphological features. As for the first instar larvae, *St. calcitrans* can be easily identified by its robust basal sclerite with a broad vertical plate and it is the only species examined in which the basal sclerite is fused only with the intermediate sclerite and the connection with the labrum through parastomal bars is interrupted. Previous authors did not report incomplete parastomal bars

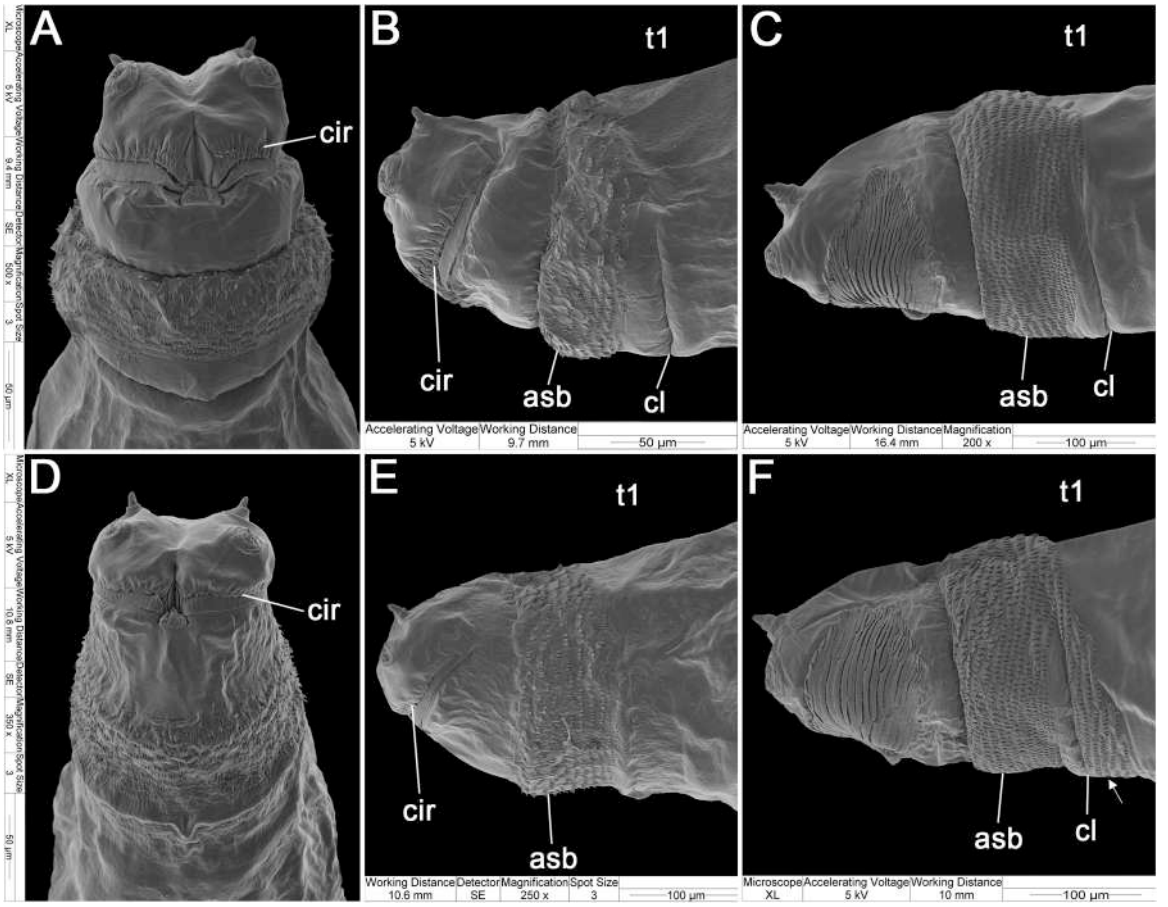

Fig. 7. SEM images of *Hydrotaea dentipes* (A, B, C) and *Hydrotaea similis* (D, E, F). A: first instar larva, anterior end of body, ventral view; B: first instar larva, anterior end of body, lateral view; C: second instar larva, anterior end of body, lateral view; D: first instar larva, anterior end of body, ventral view; E: first instar larva, anterior end of body, lateral view; F: second instar larva, anterior end of body with transverse cleft followed with additional rows of spines (arrow), lateral view. Abbreviations: asb, anterior spinose band; cir, cirri; cl, transverse cleft; t1, first thoracic segment.

in *St. calcitrans* [58,60,61] and in some cases misinterpreted the connection of the basal sclerite with the intermediate sclerite as a parastomal bar [58]. The first instar of *A. orientalis* is another species in which interconnections between sclerites have proven to be useful for taxonomic purposes. In this species, the labrum is fused with the intermediate sclerite, whereas in all other species examined, the labrum is fused to the parastomal bars. Another helpful aspect in the initial identification is the presence/absence of suprabuccal teeth, since species of *Atherigona*, *Musca* and *Muscina* typically exhibit strong and well-sclerotized suprabuccal teeth, while in species of *Hydrotaea* and *Synthesiomyia*, they are either absent or greatly reduced. The ratio of the length of the narrow apical part of the labrum to the height of the labrum can be used to distinguish species of *Musca* and *Muscina*. In *Mc. domestica*, this part is much shorter than half of the height of the labrum, while in *Muscina* the apical part of the labrum is longer than its height. Species of *Muscina* can be distinguished based on the number of suprabuccal teeth (most numerous in *Mu. levida*), the shape of the labrum in lateral view and the degree of sclerotization of the mouthhooks. Species without or with reduced suprabuccal teeth can be distinguished by the shape of the labrum. In *Sy. nudiseta* the ventral edge of the labrum is equipped with a strong protuberance, and additionally, the base of each mouthhook carries a well-sclerotized lateral arm, i.e. a dental sclerite. In turn, the width, length and shape of the labrum are helpful for species-level identification of *Hydrotaea*. However, due to subtle differences between *H. dentipes* and *H. similis* in both the first and second instar larvae, these species could not be identified to the species level based solely on LM and CLSM examination. In this case, the observation and comparison of external morphology proved advantageous (Fig. 7). Given the obscure yet significant differences in cirri and the anterior spinose band on the first thoracic segment morphology between *H. dentipes* and *H. similis*, it becomes possible to reliably distinguish them to the species level.

Second instar larvae can be readily classified to genus level based on the shape of the mouthhooks. Firstly, the second instar larva of *St. calcitrans* has strongly reduced mouthhooks which are placed apart from the rest of the cephaloskeleton's sclerites. On the other hand, the second instar of *Sy. nudiseta* can be easily identified by its F-shaped mouthhooks, *Hydrotaea* species by L-shaped mouthhooks, while *Atherigona* and *Muscina* species by U-shaped sclerite resulting from the fusion of mouthhooks with dental sclerites. Another easily distinguishable feature is that the mouthhooks in *H. capensis* and *Mc. domestica* consist of two parts: the rod-like apical part and the boomerang-like basal part. These species, however, show differences in the orientation of the basal parts of the mouthhooks: in *H. capensis* concave part is directed anteriorly, while in *Mc. domestica* posteriorly. Additionally, in *H. capensis* the anterior part of mouthhooks and dental sclerites are slender, whereas in *Mc. domestica*, are robust. When it comes to distinguishing between *Atherigona* and *Muscina* species, the former is characterised by a small unpaired sclerite just above the mouthhooks and a broad vertical plate. On the other hand, *Muscina* species are recognised by their strongly developed and well-sclerotized dental sclerites. Further identification of *Muscina* to the species level involves assessing the number of suprabuccal teeth (most numerous in *Mu. levida*) and the shape of the dental sclerite. Species identification within *Hydrotaea* can be performed based on the exact shape of the mouthhooks, the length of the dental sclerites and intermediate sclerites and the degree of sclerotization of the

accessory stomal sclerites.

Although some muscid species have received significant attention and comprehensive morphological descriptions are available for them [11,12,58,60,61], previous authors focused mostly on the differentiation of the third instar larvae [53], with the exception of dung-breeding muscid fauna [60]. This work is the first attempt to provide a key allowing for discrimination of the first and second instar larvae of a broad range of muscid species of forensic importance. The present study, although making a significant contribution, fills only a small gap in the analysis of the morphology of necrophagous Diptera larvae. Further in-depth examinations of larval morphology with particular emphasis on early instar larvae are strongly desirable. The use of CLSM in this study proved helpful in obtaining much more detailed insight into the morphology of most of the species studied, confirming its potential in future studies of larval morphology. A combination of LM and CLSM not only enriched our knowledge of the morphology of the specimens, but also facilitated their accurate identification.

Funding statement

This work was supported by the National Science Centre of Poland (grant no. 2019/33/B/NZ8/02316 to AG) and the SYNTHESYS+ Projects http://www.synthesys.info/, which are financed by the European Community Research Infrastructure Action under the FP7 Integrating Activities Programme (grant no. GB-TAF-125 to AG and KW).

CRediT authorship contribution statement

Andrzej Grzywacz: Writing – review & editing, Supervision, Resources, Methodology, Funding acquisition, Conceptualization. **Kinga Walczak:** Writing – original draft, Visualization, Methodology, Funding acquisition, Conceptualization.

Declaration of Competing Interest

The authors declare that they have no known competing financial interests or personal relationships that could have appeared to influence the work reported in this paper.

References

[1] K.G.V. Smith, A Manual of Forensic Entomology. British Museum (Natural History), London, and Cornell University Press, Ithaca, NY, 1986.
[2] J. Amendt, C.P. Campobasso, E. Gaudry, C. Reiter, H.N. LeBlanc, M.J.R. Hall, Best practice in forensic entomology-standards and guidelines, Int. J. Leg. Med. 121 (2007) 90–104, https://doi.org/10.1007/s00414-006-0086-x.
[3] M. Benecke, R. Lessig, Child neglect and forensic entomology, Forensic Sci. Int. 120 (2001) 155–159, https://doi.org/10.1016/S0379-0738(01)00424-8.
[4] L. Lutz, K.A. Williams, M.H. Villet, M. Ekanem, K. Szpila, Species identification of adult African blowflies (Diptera: Calliphoridae) of forensic importance, Int. J. Leg. Med. 132 (2018) 831–842, https://doi.org/10.1007/s00414-017-1654-y.
[5] C.J.B. de Carvalho, C.A. de Mello-Patiu, Key to the adults of the most common forensic species of Diptera in South America, Rev. Bras. Entomol. 52 (2008) 390–406, https://doi.org/10.1590/S0085-56262008000300012.
[6] K. Szpila, N.P. Johnston, K. Akbarzadeh, R. Richet, A. Tofilski, Wing measurements are a possible tool for the identification of European forensically important Sarcophagidae, Forensic Sci. Int. 340 (2022) 111451, https://doi.org/10.1016/j.forsciint.2022.111451.
[7] E.P. Catts, M.L. Goff, Forensic entomology in criminal investigations, Annu. Rev. Entomol. 37 (1992) 253–272, https://doi.org/10.1146/annurev.en.37.010192.001345.
[8] M. GilArriortua, M.I. Salona Bordas, S. Koehnemann, H. Pfeiffer, M.M. de Pancorbo, Molecular differentiation of Central European blowfly species (Diptera, Calliphoridae) using mitochondrial and nuclear genetic markers, Forensic Sci. Int. 242 (2014) 274–282, https://doi.org/10.1016/j.forsciint.2014.07.018.
[9] K. Szpila, T. Pape, A. Rusinek, Morphology of the first instar of *Calliphora vicina*, *Phormia regina* and *Lucilia illustris* (Diptera, Calliphoridae), Med. Vet. Entomol. 22 (2008) 16–25, https://doi.org/10.1111/j.1365-2915.2008.00715.x.
[10] K. Szpila, M.J.R. Hall, K.L. Sukontason, T.I. Tantawi, Morphology and identification of first instars of European and Mediterranean blowflies of forensic importance. Part I: Chrysomyinae, Med. Vet. Entomol. 27 (2013) 181–193, https://doi.org/10.1111/j.1365-2915.2012.01030.x.
[11] Y. Velásquez, T. Ivorra, A. Grzywacz, A. Martínez-Sánchez, C. Magaña, A. García-Rojo, S. Rojo, Larval morphology, development and forensic importance of *Synthesiomyia nudiseta* (Diptera: Muscidae) in Europe: a rare species or just overlooked? Bull. Entomol. Res. 103 (2013) 98–110, https://doi.org/10.1017/S0007485312000491.
[12] A. Grzywacz, T. Pape, Larval morphology of *Atherigona orientalis* (Schiner) (Diptera: Muscidae) - A species of sanitary and forensic importance, Acta Trop. 137 (2014) 174–184, https://doi.org/10.1016/j.actatropica.2014.05.018.
[13] K. Szpila, M.J.R. Hall, T. Pape, A. Grzywacz, Morphology and identification of first instars of the European and Mediterranean blowflies of forensic importance. Part II. Luciliinae, Med. Vet. Entomol. 27 (2013) 349–366, https://doi.org/10.1111/j.1365-2915.2012.01059.x.
[14] K. Szpila, T. Pape, M.J.R. Hall, A. Madra, Morphology and identification of first instars of European and Mediterranean blowflies of forensic importance. Part III: Calliphorinae, Med. Vet. Entomol. 28 (2014) 133–142, https://doi.org/10.1111/mve.12021.
[15] K.P. Vairo, M.M.C. Queiroz, P.M. Mendonça, R.R. Barbosa, C.J.B. de Carvalho, Description of immature stages of the flesh fly *Peckia* (*Sarcodexia*) *lambens* (Wiedemann) (Diptera: Sarcophagidae) provides better resolution for taxonomy and forensics, Trop. Zool. 28 (2015) 114–125, https://doi.org/10.1080/03946975.2015.1057435.
[16] K. Szpila, T. Pape, Rediscovery, redescription and reclassification of *Beludzhia phylloteliptera* (Diptera: Sarcophagidae: Miltogramminae), Eur. J. Entomol. 104 (2007) 119–137, https://doi.org/10.14411/eje.2007.018.
[17] J.H. Byrd, W.D. Lord, J.R. Wallace, J.K. Tomberlin, Collection of Entomological Evidence during Legal Investigations, Forensic Entomol. Util. Arthropods Leg. Investig. (2010) 127–176.
[18] M. Hajibabaei, J.R. DeWaard, N.V. Ivanova, S. Ratnasingham, R.T. Dooh, S.L. Kirk, P.M. Mackie, P.D.N. Hebert, Critical factors for assembling a high volume of DNA barcodes, Philos. Trans. R. Soc. B Biol. Sci. 360 (2005) 1959–1967, https://doi.org/10.1098/rstb.2005.1727.
[19] D. Yeo, A. Srivathsan, R. Meier, Longer is not always better: optimizing barcode length for large-scale species discovery and identification, Syst. Biol. 69 (2020) 999–1015, https://doi.org/10.1093/sysbio/syaa014.
[20] M.A. O'Flynn, D.E. Moorhouse, Identification of early immature stages of some common Queesland carrion flies, J. Aust. Entomol. Soc. 19 (1980) 53–61, https://doi.org/10.1111/j.1440-6055.1980.tb00961.x.
[21] S. Sanit, P. Sribanditmongkol, K.L. Sukontason, K. Moophayak, T. Klong-Klaew, T. Yasanga, K. Sukontason, Morphology and identification of fly eggs: application in forensic entomology, Trop. Biomed. 30 (2013) 325–337.
[22] P.J. Thyssen, Keys for identification of immature insects, in: J. Amendt, M.L. Goff, C. Pietro Campobasso, M. Grassberger (Eds.), Curr. Concepts Forensic Entomol., Springer, Dordrecht, 2010, pp. 25–42, https://doi.org/10.1007/978-1-4020-9684-6_2.
[23] Y. Velásquez, C. Magaña, A. Martínez-Sánchez, S. Rojo, Diptera of forensic importance in the Iberian Peninsula: larval identification key, Med. Vet. Entomol. 24 (2010) 293–308, https://doi.org/10.1111/j.1365-2915.2010.00879.x.
[24] J. Wallman, Third-instar larvae of common carrion-breeding blowflies of the genus *Calliphora* (Diptera: Calliphoridae) in South Australia, Invertebr. Taxon. 15 (2001) 37–51, https://doi.org/10.1071/IT99024.
[25] S. Yusseff-Vanegas, Description of third instars of *Cochliomyia minima* (Diptera: Calliphoridae) from West Indies, and updated identification key, J. Med. Entomol. 51 (2014) 1051–1056, https://doi.org/10.1603/ME13088.
[26] D. Martín-Vega, L.M. Díaz-Aranda, A. Baz, The immature stages of the necrophagous fly *Liopiophila varipes* and considerations on the genus *Liopiophila* (Diptera: Piophilidae), Dtsch. Entomol. Z. 61 (2014) 37–42, https://doi.org/10.3897/dez.61.7534.
[27] K. Szpila, R. Richet, T. Pape, Third instar larvae of flesh flies (Diptera: Sarcophagidae) of forensic importance—critical review of characters and key for European species, Parasitol. Res. 114 (2015) 2279–2289, https://doi.org/10.1007/s00436-015-4421-3.
[28] A. Grzywacz, M.J.R. Hall, T. Pape, K. Szpila, Muscidae (Diptera) of forensic importance – an identification key to third instar larvae of the western Palaearctic region and a catalogue of the muscid carrion community, Int. J. Leg. Med. 131 (2017) 855–866, https://doi.org/10.1007/s00414-016-1495-0.
[29] P. Mégnin, La faune des cadavers: application de l'entomologie a la medecine legale, G. Masson and Gauthier-Villars et Fils, Paris, 1894.
[30] A. Grzywacz, P. Trzeciak, B.M. Wiegmann, B.K. Cassel, T. Pape, K. Walczak, C. Bystrowski, L. Nelson, M. Piwczyński, Towards a new classification of Muscidae (Diptera): a comparison of hypotheses based on multiple molecular phylogenetic approaches, Syst. Entomol. 46 (2021) 508–525, https://doi.org/10.1111/syen.12473.
[31] S.L. Vanlaerhoven, G.S. Anderson, Insect Succession on Buried Carrion in Two Biogeoclimatic Zones of British Columbia, J. Forensic Sci. 44 (1999) 32–43.
[32] E.C. Pastula, R.W. Merritt, Insect arrival pattern and succession on buried carrion in Michigan, J. Med. Entomol. 50 (2013) 432–439, https://doi.org/10.1603/ME12138.
[33] A.M.A. Mashaly, Entomofaunal succession patterns on burnt and unburnt rabbit carrion, J. Med. Entomol. 53 (2016) 296–303, https://doi.org/10.1093/jme/tjv202.
[34] F.W. Avila, M.L. Goff, Arthropod succession patterns onto burnt carrion in two contrasting habitats in the Hawaiian Islands, J. Forensic Sci. 43 (1998) 581–586, https://doi.org/10.1520/JFS16184J.
[35] J.A. Kelly, T.C. van der Linde, G.S. Anderson, The influence of wounds, severe trauma, and clothing, on carcass decomposition and arthropod succession in South

Africa, J. Can. Soc. Forensic Sci. 44 (2011) 144–157, https://doi.org/10.1080/00085030.2011.10768149.
[36] N.R. Hobischak, G.S. Anderson, Freshwater-related death investigations in British Columbia in 1995–1996. A review of coroners cases, J. Can. Soc. Forensic Sci. 32 (1999) 97–106, https://doi.org/10.1080/00085030.1999.10757492.
[37] E.J. Watson, C.E. Carlton, Insect succession and decomposition of wildlife carcasses during fall and winter in Louisiana, J. Med. Entomol. 42 (2005) 193–203, https://doi.org/10.1603/0022-2585(2005)042[0193:ISADOW]2.0.CO;2.
[38] J.A. Payne, A summer carrion study of the baby pig *Sus scrofa* Linnaeus, Ecology 46 (1965) 592–602, https://doi.org/10.2307/1934999.
[39] R.A. Syamsa, B. Omar, R.M. Zuha, M.N. Faridah, M.S. Swarhib, O. Hidayatulfathi, A.W. Shahrom, Forensic entomology of high-rise buildings in Malaysia: three case reports, Trop. Biomed. 32 (2015) 291–299.
[40] T.K. Kumara, R.H.L. Disney, A.A. Hassan, M. Flores, T.S. Hwa, Z. Mohamed, M. R. Chesalmah, S. Bhupinder, Occurrence of oriental flies associated with indoor and outdoor human remains in the tropical climate of north Malaysia, J. Vector Ecol. 37 (2012) 62–68, https://doi.org/10.1111/j.1948-7134.2012.00200.x.
[41] S.C. Voss, S.L. Forbes, I.R. Dadour, Decomposition and insect succession on cadavers inside a vehicle environment, Forensic Sci. Med. Pathol. 4 (2008) 22–32, https://doi.org/10.1007/s12024-007-0028-z.
[42] L.M. Díaz-Aranda, D. Martín-Vega, A. Gómez-Gómez, B. Cifrián, A. Baz, Annual variation in decomposition and insect succession at a periurban area of central Iberian Peninsula, J. Forensic Leg. Med. 56 (2018) 21–31, https://doi.org/10.1016/j.jflm.2018.03.005.
[43] M.L. Cavallari, F.N. Baltazar, S.S. Nihei, D.R. Muñoz, J.E. Tolezano, Dipterofauna associated with *Sus scrofa* Linné, 1758, carcasses in urban and coastal regions of São Paulo State, Brazil, Psyche A J. Entomol. 2015 (2015) 1–12, https://doi.org/10.1155/2015/983980.
[44] L.S. Faria, M.L. Paseto, F.T. Franco, V.C. Perdigão, G. Capel, J. Mendes, Insects breeding in pig carrion in two environments of a rural area of the state of minas gerais, Brazil, Neotrop. Entomol. 42 (2013) 216–222, https://doi.org/10.1007/s13744-012-0099-8.
[45] C.P. e Castro, J.P. Sousa, M.I. Arnaldos, J. Gaspar, M.D. García, Blowflies (Diptera: Calliphoridae) activity in sun exposed and shaded carrion in Portugal, Ann. La Soc. Entomol. Fr. 47 (2011) 128–139, https://doi.org/10.1080/00379271.2011.10697704.
[46] B.J. Sharanowski, E.G. Walker, G.S. Anderson, Insect succession and decomposition patterns on shaded and sunlit carrion in Saskatchewan in three different seasons, Forensic Sci. Int. 179 (2008) 219–240, https://doi.org/10.1016/j.forsciint.2008.05.019.
[47] A. Farinha, C.G. Dourado, N. Centeio, A.R. Oliveira, D. Dias, M.T. Rebelo, Small bait traps as accurate predictors of dipteran early colonizers in forensic studies, J. Insect Sci. 14 (1) (2014) 17, https://doi.org/10.1093/jis/14.1.77.
[48] S. Pittner, V. Bugelli, K. Weitgasser, A. Zissler, S. Sanit, L. Lutz, F. Monticelli, C. P. Campobasso, P. Steinbacher, J. Amendt, A field study to evaluate PMI estimation methods for advanced decomposition stages, Int. J. Leg. Med. (2020), https://doi.org/10.1007/s00414-020-02278-0.
[49] S. Vanin, M. Gherardi, V. Bugelli, M. Di Paolo, Insects found on a human cadaver in central Italy including the blowfly *Calliphora loewi* (Diptera, Calliphoridae), a new species of forensic interest, Forensic Sci. Int. 207 (2011) e30–e33, https://doi.org/10.1016/j.forsciint.2010.12.004.
[50] M.I. Arnaldos, M.D. García, E. Romera, J.J. Presa, A. Luna, Estimation of postmortem interval in real cases based on experimentally obtained entomological evidence, Forensic Sci. Int. 149 (2005) 57–65, https://doi.org/10.1016/j.forsciint.2004.04.087.
[51] F. Lefebvre, E. Gaudry, Forensic entomology: a new hypothesis for the chronological succession pattern of necrophagous insect on human corpses, Ann. La Soci. été Entomol. Fr. 45 (2009) 377–392, https://doi.org/10.1080/00379271.2009.10697622.
[52] A. Grzywacz, A. Lindström, M.J.R. Hall, *Hydrotaea similis* Meade (Diptera: Muscidae) newly reported from a human cadaver: A case report and larval morphology, Forensic Sci. Int. 242 (2014) e34–e43, https://doi.org/10.1016/j.forsciint.2014.07.014.
[53] A. Grzywacz, M.J.R. Hall, T. Pape, Morphology successfully separates third instar larvae of *Muscina*, Med. Vet. Entomol. 29 (2015) 314–329, https://doi.org/10.1111/mve.12117.
[54] A. Grzywacz, Review and comparative analysis of the morphology of third instar larvae of European and Mediterranean Muscidae (Diptera) of forensic importance, Nicolaus Copernic. Univ. (2013) 1–157.
[55] K. Walczak, K. Szpila, L. Nelson, T. Pape, M.J.R. Hall, F. Alves, A. Grzywacz, Larval morphology of the avian parasitic genus *Passeromyia*: playing hide and seek with a parastomal bar, Med. Vet. Entomol. 13 (1) (2022), https://doi.org/10.1111/mve.12603.
[56] G.W. Courtney, B.J. Sinclair, R. Meier, Morphology and terminology of Diptera larvae, in: L. Papp, B. Darvas (Eds.), Contrib. to a Man. Palaearct. Diptera (with Spec. Ref. to Flies Econ. Importance), Science Herald Press, Budapest, 2000, pp. 85–161.
[57] K. Szpila, T. Pape, The first instar larva of *Apodacra pulchra* (Diptera: Sarcophagidae, Miltogramminae), Insect Syst. Evol. 36 (2005) 293–300, https://doi.org/10.1163/187631205788838447.
[58] P. Skidmore, The biology of the Muscidae of the World, Ser. Entomol. 29 (1985) 1–550.
[59] A. Grzywacz, Third instar larva morphology of *Hydrotaea cyrtoneurina* (Zetterstedt, 1845) (Diptera: Muscidae) – a species of forensic interest, Pol. J. Entomol. 82 (2013) 303–315, https://doi.org/10.2478/v10200-012-0044-5.
[60] P. Ferrar, The immature stages of dung-breeding muscoid flies in Australia, with notes on the species, and keys to larvae and puparia, Aust. J. Zool. Suppl. Ser. (73) (1979) 1–106, https://doi.org/10.1071/AJZS073.
[61] M. Thomsen, A Comparative Study of the Development of the Stomoxydinae (especially *Hæmatobia stimulans* Meigen) with Remarks on other Coprophagous Muscids, J. Zool. 105 (1935) 531–550, https://doi.org/10.1111/j.1096-3642.1935.tb01679.x.

Article 4

Walczak, K., Piwczyński, M., Pape, T., Johnston, N. P., Wallman, J. F., Szpila, K., & Grzywacz, A. (2025). Unravelling phylogenetic relationships within the genus *Lispe* (Diptera: Muscidae) through genome-assisted and de novo analyses of RAD-seq data. Molecular Phylogenetics and Evolution, Volume 204, March 2025, 108291.

https://doi.org/10.1016/j.ympev.2025.108291

Molecular Phylogenetics and Evolution 204 (2025) 108291

Contents lists available at ScienceDirect

Molecular Phylogenetics and Evolution

journal homepage: www.elsevier.com/locate/ympev

Unravelling phylogenetic relationships within the genus *Lispe* (Diptera: Muscidae) through genome-assisted and *de novo* analyses of RAD-seq data

Kinga Walczak [a,*], Marcin Piwczyński [a], Thomas Pape [b], Nikolas P. Johnston [c,d], James F. Wallman [d,e], Krzysztof Szpila [a], Andrzej Grzywacz [a,*]

[a] Department of Ecology and Biogeography Faculty of Biological and Veterinary Sciences Nicolaus Copernicus University in Toruń Toruń Poland
[b] Natural History Museum of Denmark University of Copenhagen Copenhagen Denmark
[c] Molecular Horizons, School of Science, University of Wollongong Wollongong New South Wales Australia
[d] Faculty of Science, University of Technology Sydney Ultimo New South Wales Australia
[e] School of Earth, Atmospheric and Life Sciences, University of Wollongong Wollongong New South Wales Australia

ARTICLE INFO

Keywords:
De novo assembly
Genome
Nanopore sequencing
Phylogeny
Reference-based assembly

ABSTRACT

Lispe represents a species-rich genus within the family Muscidae. The current subdivision of *Lispe* species into species groups is based mainly on adult morphology and ecology, with the only available phylogenetic study based on three molecular markers. Nonetheless, certain species groups remain unclear and the relationships and composition of these groups are still unresolved. This study employs restriction-site associated DNA sequencing (RAD-seq) with both reference-based and *de novo* reads assembly approaches to investigate relationships within *Lispe*. To apply a reference-based approach we utilised Oxford Nanopore Technologies (ONT) long read sequencing to assemble a draft genome of *L. tentaculata*. We evaluated various assemblers for ONT reads of *L. tentaculata* in order to demonstrate the highest effectiveness in terms of completeness and assembly quality. The resulting phylogenetic trees topologies are well supported and present a consistent division into three main clades: 1) the *palposa*-, *rigida*- and *caesia*-groups, 2) the *nicobarensis*-, *nivalis*-, *scalaris*- and *tentaculata*-groups and 3) the *longicollis*-, *desjardinsii*-, *uliginosa*- and *kowarzi*-groups. The primary discrepancy between topologies obtained under our various analytical approaches is the relationship between the *leucospila*-group and all other ingroup taxa, being a sister taxon either to all remaining *Lispe* or to a clade consisting of the *longicollis*-, *desjardinsii*-, *uliginosa*- and *kowarzi*-groups. *Lispe polonaise*, included for the first time in a molecular phylogenetic analysis, is nested within the *caesia*-group. Similarly, *L. capensis* and the hitherto unassigned *L. mirabilis* belong to the *tentaculata*-group. Our study confirms the validity of the 14 species groups currently recognised in the genus *Lispe*.

1. Introduction

Lispe Latreille, 1796 is a genus of Diptera (Fig. 1) widespread in all biogeographical regions, but with a notable absence from New Zealand (Hennig, 1965; Vikhrev, 2015). The genus contains 163 described species (Pont, 2019), but extensive taxonomic changes and descriptions of new species are ongoing (Vikhrev, 2014, 2016, 2020, 2021; Zielke, 2018; Pont, 2019). Species of *Lispe* can be easily distinguished from other muscid genera by the combination of an apically dilated palpus and a setulose anepimeron (Curran, 1937; Snyder, 1954; Pont, 2019). Adults are mainly observed on river banks, along the shores of lakes, seas and oceans or in other wetlands (Snyder, 1954; Vikhrev, 2011a), and they are commonly known as predators of small insects, e.g., Diptera (Pont, 2019) and Coleoptera (Steidle et al., 1995). Their most common prey are other flies of families such as Psychodidae, Milichiidae (Williams, 1938), Muscidae (Hennig, 1960), or Chironomidae and Culicidae (Snyder, 1954; Shinonaga & Kano, 1983; Pont, 2019). Due to their predation of culicid and simuliid populations, species of *Lispe* serve as natural biological control agents and thus can be considered of economic and medical importance (Snyder, 1954; van Emden, 1965; Werner et al., 2014). However, representatives of *Lispe* exhibit various feeding strategies (Vikhrev, 2011a). *Lispe binotata* Becker, 1914 feeds on invertebrate carrion (Vikhrev, 2011a), and active hunting was observed for example in *L. geniseta* Stein, 1909, *L. tentaculata* (De Geer, 1776) and

* Corresponding authors at: Department of Ecology and Biogeography, Nicolaus Copernicus University in Toruń, Lwowska 1, 87-100 Toruń, Poland.
E-mail addresses: walczak.kinga00@gmail.com (K. Walczak), hydrotaea@gmail.com (A. Grzywacz).

https://doi.org/10.1016/j.ympev.2025.108291
Received 5 July 2024; Received in revised form 5 January 2025; Accepted 21 January 2025
Available online 26 January 2025

L. pygmaea (Fallén, 1825) (Vikhrev, 2011a; Werner et al., 2014). *Lispe caesia* Meigen, 1826 successfully attacks much larger flies (Hennig, 1960) and *L. candicans* Kowarz, 1892 can penetrate the cuticle of adult beetles (Steidle et al., 1995). In some species of *Lispe*, males perform spectacular courtship dances around passive females, making them valuable models for studying mating behaviour (Frantsevich & Gorb, 2006; Butterworth & Wallman, 2022). Larvae of *Lispe* are obligatory carnivores (Skidmore, 1985), which develop in wet sand or mud with high organic content (Séguy, 1937; Hennig, 1960; Skidmore, 1985), where they feed on aquatic invertebrates (Pont, 2019).

Lispe is recognised as a monophyletic group, supported by several autapomorphies listed by Hennig (1960, 1965) and more recently confirmed by molecular data (Gao et al., 2022). The systematic position of *Lispe* within Muscidae has changed over the years. Initially, the genus was placed in its own subfamily Lispinae (Malloch, 1923; Séguy, 1937; van Emden, 1941, 1965; Snyder, 1949) or in the tribe Limnophorini of Mydaeinae (Karl, 1928). Hennig (1960) later reclassified *Lispe* in the Limnophorini of Coenosiinae based on morphological characters of the eggs, larvae and adults. He argued that *Lispe* exhibits specific derived features also present in some genera of Limnophorini, particularly *Limnophora* Robineau-Desvoidy, 1830, indicating a probable sister-group relationship. This classification has been widely accepted (Skidmore, 1985; Werner et al., 2014; Pont, 2019; but see Fan, 2008 for an exception) and the sister-group relationship between *Lispe* and *Limnophora* has recently been confirmed by molecular studies (Kutty et al., 2010, 2014; Ge et al., 2016; Grzywacz et al., 2021; Gao et al., 2022). Attempts to organise species of *Lispe* into smaller units have been a matter of debate for many years. Currently, the genus is divided into several species groups defined by leg and body chaetotaxy, characters of the male terminalia, as well as the ecology of adults (Hennig, 1960; Pont, 2019). Even though Snyder (1954) is believed (Hennig, 1960) to be the first to have proposed a subdivision, van Emden (1941) tentatively used the term '*tentaculata*-group' and Paterson (1953) used '*Lispe leucospila*-group'. To date, *Lispe* has been classified into 14 species groups (Supp. Table S1). Snyder (1954) proposed three species groups for Nearctic *Lispe*, i.e., the *tentaculata*-group, the *uliginosa*-group and the *palposa*-group. Hennig (1960) complemented Snyder's classification by adding Palaearctic species of *Lispe*, and he established another three species groups: the *scalaris*-group, the *caesia*-group and the *longicollis*-group, with the latter divided into two subgroups, and he also left several Palaearctic species unassigned. Most recently, Vikhrev has contributed significantly to the ordering of *Lispe* by proposing and defining further species groups and revising the existing ones, such as: *leucospila* (Vikhrev 2011b), *nivalis* and *rigida* (Vikhrev 2012b), *desjardinsii*, *kowarzi* and *nana* (Vikhrev 2014), *nicobarensis* (Vikhrev 2015) and *ambigua*, *dichaeta*, *geniseta*, *pumila* and *pygmaea* (Vikhrev 2016). Some groups are well-defined, like the *nivalis*-group (Vikhrev, 2012a) and the *palposa*-group (Vikhrev, 2015), while others remain unclear, e.g., the *caesia*-group (Vikhrev et al., 2016). Moreover, five species complexes have been proposed based on similarities in ecology rather than morphology (Vikhrev, 2016). Previous authors did not conduct formal morphology-based phylogenetic analyses, yet hypotheses based on morphological evidence suggest that the *nivalis*-group is closely related to the *tentaculata*-group (Vikhrev, 2012a) and that the *nana*-complex has an intermediate position between the *tentaculata*-group and the *scalaris*-group (Vikhrev, 2014). These four groups form the *tentaculata* supergroup, which is additionally supported by a shared similar ecological association with freshwater habitats (Vikhrev, 2014). Furthermore, Vikhrev (2014) stated that species of the *desjardinsii*-group resemble those of the *longicollis*-group, and that the *palposa*-group appears to be closely related to the *rigida*-group. A recent molecular study based on three genes investigated the limits of some species groups and confirmed some of those phylogenetic hypotheses (Gao et al., 2022). However, tree topologies were susceptible to changes depending on the inference methods, and the relationships between species groups emerged with low to moderate nodal support values, especially along the backbone of the phylogenetic tree.

The rapidly decreasing costs of next-generation sequencing (NGS) make it feasible to obtain genomic-scale data in a relatively short time (Metzker, 2010). Advances in high-throughput sequencing approaches

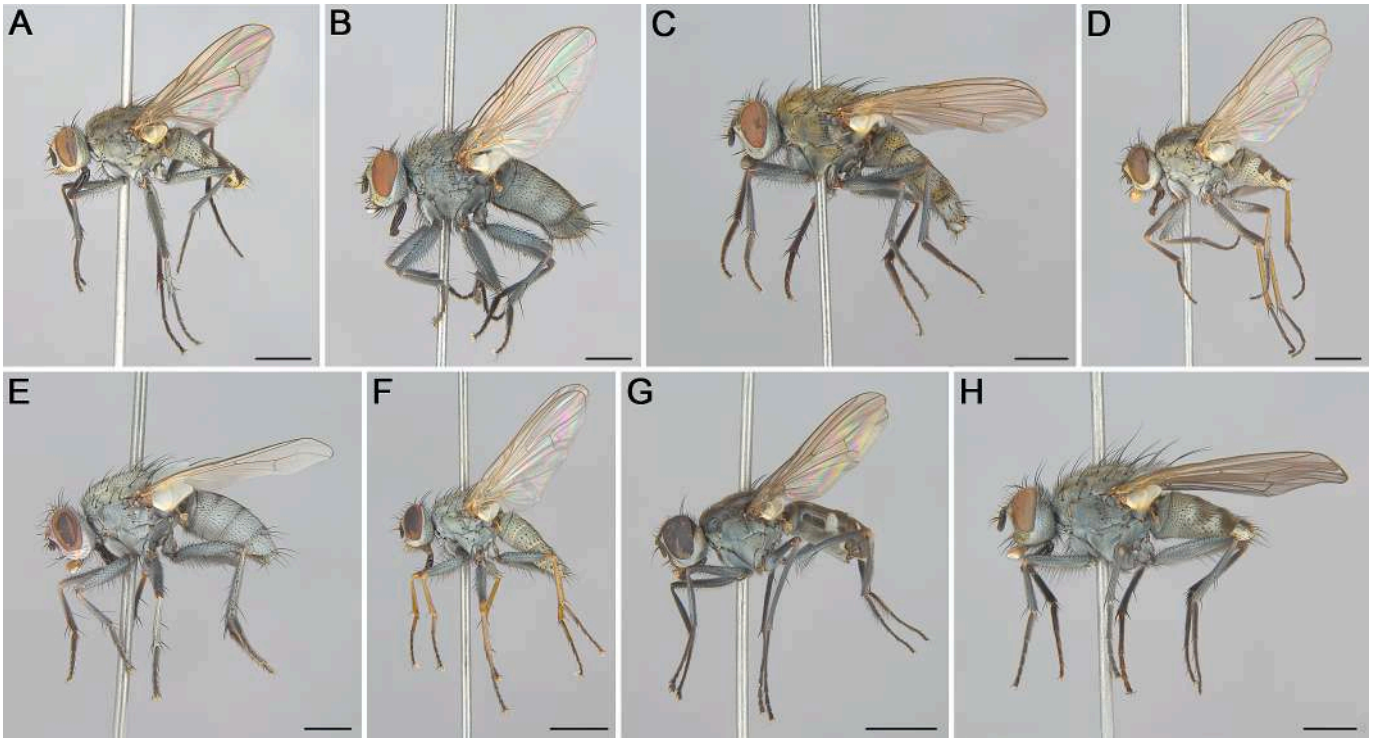

Fig. 1. Representative taxa of Lispe. (A) *Lispe assimilis* Wiedemann, 1824; (B) *Lispe caesia* Meigen, 1826; (C) *Lispe loewi* Ringdahl, 1922; (D) *Lispe nana* Macquart, 1835; (E) *Lispe polonaise* Vikhrev, 2021; (F) *Lispe pygmaea* (Fallén, 1825); (G) *Lispe sydneyensis* Schiner, 1868; (H) *Lispe tentaculata* (De Geer, 1776). Scale bars 3 mm.

over the past decade have proven to be advantageous for phylogenetics and population genetics studies (Hohenlohe et al., 2010; Rubin et al., 2012). Restriction site-associated DNA sequencing (RAD-seq) is one method that has revolutionised ecological, biogeographical and evolutionary studies (Hohenlohe et al., 2010; Etter et al., 2011; Andrews et al., 2016). The ongoing development of whole-genome sequencing remains challenging compared to RAD-seq, which targets a reduced representation of the genomic regions flanking restriction sites (Baird et al., 2008; Davey & Blaxter, 2010). RAD sequencing provides an efficient method for the discovery and genotyping of thousands of single nucleotide polymorphisms (SNPs) at sites scattered throughout the genome, when no, or limited, prior genomic resources are available for the organisms under study (Davey & Blaxter, 2010; Emerson et al., 2010). Therefore, RAD-seq has been utilised for non-laborious and relatively cost-effective phylogenetic inference of model and non-model organisms (Cariou et al., 2013; Suchan et al., 2017; Wagner et al., 2018). Raw RAD-seq reads can be mapped to a reference genome, if available, or processed *de novo* by clustering together reads based on a certain level of sequence similarity (clustering threshold or CT, see *2.3* below). The CT defines the minimum percentage of sequences similarity below which two reads are considered to have come from different loci. Consequently, *de novo* assembly is highly sensitive to changes in this parameter, as both too low and too high CT values can adversely affect the analysis (McCartney-Melstad et al., 2019).

Despite recent advancements in *de novo* assembly pipelines (Willing et al., 2011; Paris et al., 2017; Díaz-Arce & Rodríguez-Ezpeleta, 2019), this approach continues to face significant challenges, including sequencing errors, sequencing bias, repetitive region complexity and high computational requirements (Rubin et al., 2012; Dida & Yi, 2021; Kunvar et al., 2021). However, one of the critical considerations is that the final results of *de novo* assembly may strongly depend on the chosen filtering parameters, which can influence the accuracy and reliability of the assembly. On the other hand, studies have suggested that assembling raw RAD-seq reads to a reference genome can yield improved results compared to a *de novo* method, as it facilitates the determination of the genomic locations of loci and subsequently a higher number of SNPs calls (Manel et al., 2016; Shafer et al., 2017; Kunvar et al., 2021). Reference sequences can be either the genome of the target species or a species closely related to the study group (Manel et al., 2016). In some cases even a draft genome from a distant relative can be used with success (Shafer et al., 2017; Kunvar et al., 2021). However, an increase in evolutionary distance between ingroup taxa and reference genome can result in considerably lower phylogenetic signal and a failure in the reconstruction of relationships between deeper nodes (Tripp et al., 2017; Grzywacz et al., 2021).

Due to the unclear status of some of the proposed species groups within *Lispe*, this work aims to examine relationships within *Lispe* with the main objective to clarify the division of *Lispe* into species groups and analyse their phylogenetic relationships. To achieve this goal, and to investigate whether mapping short RAD-seq reads to a draft genome increases the phylogenetic signal, we applied RAD-seq using both *de novo* assembly and mapping to a reference genome under different analytical schemes. We utilised long read sequencing to obtain a reference genome sequence of *L. tentaculata*, and to achieve a high-quality genome assembly, we compared several assemblers for ONT reads to determine their effectiveness in producing accurate and reliable genomic data.

2. Methods

2.1. Taxon sampling and DNA isolation

For phylogenetic analysis, we sampled 49 species of *Lispe* representing all recently proposed and/or revised species groups (Snyder, 1954; Hennig, 1960; Vikhrev, 2016, 2020, 2021, 2011a, 2011b, 2012a, 2012b, 2012c, 2014, 2015; Vikhrev et al., 2016; Gao et al., 2022) and including taxa from the Afrotropical, Australasian and Palaearctic regions, as well as one from the Nearctic region (Supp. Table S2). All adult specimens were identified by Nikita Vikhrev and AG using keys provided by Hennig (1955), Pont (2019) and Vikhrev (2020, 2021). Outgroups included four representatives of *Limnophora*. Voucher specimens, where available, have been deposited in the collection of the Department of Ecology and Biogeography, Faculty of Biological and Veterinary Sciences, Nicolaus Copernicus University in Toruń.

Prior to DNA extraction, ethanol-soaked samples were rinsed three times for 30 min in distilled water and dried on a thermoblock at 40℃. Pinned specimens were directly used for DNA extraction. Total genomic DNA was isolated from entire specimens using a DNeasy Blood & Tissue Kit (Qiagen, Valencia, CA, USA) according to the manufacturer's protocol with the following modifications: (i) for each individual, 40 μL of proteinase K (>600 mAU/ml; Qiagen) was used; (ii) after initial incubation at 56 °C, 4 μL of RNase A (100 mg/ml; Qiagen) was added to each sample. The extracted DNA was quantified with a Qubit 3.0 fluorometer using a dsDNA High Sensitivity Assay Kit (Life Technologies, Inc., Carlsbad, CA, USA) following the manufacturer's protocol. Samples with DNA concentrations below 0.1 ng/μL based on Qubit measurements were further amplified using the REPLI-g Mini Kit (Qiagen) to increase DNA concentration. Extractions were electrophoresed in a 1 % agarose gel, stained with GelRed (Biotium, Darmstadt, Germany) and photographed with a gel documentation system.

Specimens of *Lispe tentaculata* for nanopore sequencing were collected in Toruń, Poland (53°00′14.4″N 18°36′19.2″E) in June of 2021. Adults were placed in a freezer for a few minutes for immobilisation. The material was subjected to DNA extraction, as described above. The two *L. tentaculata* isolates with the highest concentration and the longest DNA fragments were selected based on results from the Qubit 3.0 assay and electrophoresis. The samples were subsequently purified with AMPure XP beads (Beckman Coulter, Carlsbad, CA, USA; 0.4 × ratio of beads to sample volume) to remove short DNA fragments and then resuspended in TE buffer. The purified products were quantified with a Qubit 3.0 fluorometer using the dsDNA High Sensitivity Assay Kit following the manufacturer's protocol.

2.2. Library preparation for genome sequencing and data processing

Two libraries were prepared simultaneously, one for each *L. tentaculata* individual. We could not limit our approach to a single adult of *L. tentaculata* due to the low concentration of gDNA, insufficient for four sequencing runs on two flow cells. We used the SQK-LSK110 Ligation Sequencing Kit (Oxford Nanopore Technologies, Oxford, United Kingdom) to prepare libraries according to the manufacturer's protocol with the following modifications: to minimise pipetting steps, the input DNA was prepared by transferring 1 μg of gDNA into a 0.2 ml PCR tube and adjusted with nuclease-free water to 47 μl. Times recommended for the initial 65 °C binding incubation, incubation during a bead-based AMPure XP clean-up after DNA repair, end-prep, and adapter ligation steps, as well as incubation with a NEBNext Quick T4 DNA Ligase (New England BioLabs Inc., Ipswich, MA, USA) were doubled. For the beads washing step that follows the adapter ligation, the Long Fragment Buffer (LFB) was used. The incubation in the increased volume of 26 μl of Elution Buffer (EB) was performed at 37 °C. After the completion of the library preparation protocol, half of the library (12 μl) was loaded onto a SpotON Flow Cell Rev D (R.9.4.1; FLO-MIN106D), while the other half and the second library were stored in 4 °C according to the manufacturer's recommendations. After the first run, the flow cell was washed with the Flow Cell Wash Kit (EXP-WSK002) following the manufacturer's protocol and the second half of the library was immediately loaded for sequencing. A total of four sequencing runs were performed on two flow cells using a MinION Mk1C device (MIN-101C) (Oxford Nanopore Technologies, Oxford, United Kingdom).

The FAST5 ONT (Oxford Nanopore Technologies) reads were basecalled using *Guppy* v.5.0.7 with the super-accuracy mode (SUP), and

output fastq files were then concatenated together into a single file before subsequent data processing. Adapter sequences were trimmed using *PoreChop* v.0.2.4 (https://github.com/rrwick/Porechop) (Wick et al., 2017) with an option to discard reads with internal adapters. Next, reads were additionally filtered using *NanoFilt* (https://github.com/wdecoster/nanofilt) and sequences shorter than 500 nucleotides or with Phred quality scores (Q) below 10 were removed. The quality check of overall raw and trimmed ONT reads was performed using *NanoPack* scripts (De Coster et al., 2018).

In this study, five state-of-the-art *de novo* long-read only assemblers were utilised and compared to determine their efficiency and capacity to produce complete assembled genomes. To assemble the *L. tentaculata* genome, we used: *Raven* v.1.5.1 (Vaser & Šikić, 2021), *SMARTdenovo* (Liu et al., 2021), *wtdbg2* (Ruan & Li, 2020), *Canu* v.2.2 (Koren et al., 2017) and *Flye* v.2.9-b1768 (Kolmogorov et al., 2019). Default parameters were used in *Raven* assembler with two polishing rounds of *Racon* (Vaser et al., 2017). In *SMARTdenovo* and *wtdbg2* assemblers, a minimum length of alignment was set to 1000 bp (−J and −L, respectively). For *wtdbg2*, *Canu* and *Flye* an approximate genome size was set to 700 Mb (Scott et al., 2014). The accuracy and completeness of each *de novo* genome assembly was evaluated using *BUSCO* v.5.2.1 (Manni et al., 2021). Analyses were performed with the odb10 Diptera lineage dataset from 56 genomes that were available in NCBI GenBank in July 2022. Summary assembly statistics (number of contigs, total length, the longest contig, N50) and assembly quality (QV) were obtained using *Inspector* (Chen et al., 2021). QV score was calculated based on the identified structural and small-scale errors scaled by the total base pairs of the assemblies. For subsequent analyses we selected the most complete assembly according to *BUSCO* assay and that with the highest QV.

2.3. Rad-seq library preparation and data processing

Genomic DNA for each species was individually barcoded and processed into a reduced complexity library based on the original RAD-seq protocol described by Ali et al. (2016) with the following modifications: (i) for each sample, two separate repetitions of 75 ng DNA each were digested using *Sbf*I-HF restriction enzyme (New England BioLabs) at 37 °C for 2 hr to mitigate the risk of reaction failure; (ii) 5 μL of P1 adapter-ligated fragments of each of the 106 samples (2 repetitions × 53 species) were pooled and then divided into three equal parts before the clean-up step; (iii) sonication was performed for 60 s using a Covaris M220 (Covaris, Inc. Woburn, MA, USA); (iv) Pippin Prep (Sage Science, Beverly, MA, USA) was used to select fragments between 300 and 500 bp with prior library cleaning with AMPure XP beads (1:1 ratio of beads to sample volume); (v) four independent PCRs (15 cycles) were carried out and subsequently pooled; and (vi) PCR products were purified twice with AMPure XP beads (1:1 ratio of beads to sample volume) to completely remove the remaining primers. A final library check was performed using a Qubit 3.0 fluorometer and 2100 Bioanalyzer with the High Sensitivity DNA Analysis Kit (Agilent Technologies, Santa Clara, CA, USA). Commercial paired-end sequencing (Macrogen) of the multiplexed library was conducted using an Illumina HiSeq 2500.

Raw sequence read quality was analysed using *FastQC* v.0.11.9 (https://www.bioinformatics.babraham.ac.uk/projects/fastqc/; accessed 27.03.2021). Illumina-specific adapters and low-quality bases were removed using *Trimmomatic* v.0.36 (Bolger et al., 2014) with the following options: TRAILING:3 SLIDINGWINDOW:4:20 MINLEN:50. For downstream phylogenetic analyses, the raw RAD-seq R1 reads were processed with the *ipyrad* v.0.9.81 pipeline (Eaton, 2014). Reads were demultiplexed and assigned to species based on sequence barcodes (allowing one mismatch).

Further, two assembly pipelines were performed for 1) *de novo* assembly and 2) reference- guided assembly using the newly obtained reference genome sequence. For *de novo* assembly, various combinations of clustering thresholds (CT) were tested. Since this parameter is known to alter assembly results (Rubin et al., 2012; Cariou et al., 2013; Grzywacz et al., 2021; Piwczyński et al., 2021), we implemented a wide range of CT values from 0.70 to 0.90 incremented by 0.01. Other parameters used for *ipyrad* analysis were as follows: *min_samples_locus* = 4, *max_SNPs_locus* = 0.6, *max_Indels_locus* = 8. For each alignment we performed phylogenetic tree reconstruction using maximum likelihood (ML) approach implemented in *RAxML* v.8.2.12 with 100 rapid bootstrap repetitions (Stamatakis, 2014). To select the best CT, we considered the highest average bootstrap support and the highest number of obtained SNPs. For the reference-based approach, we performed an assembly guided by a draft genome of *L. tentaculata* obtained in this study. The remaining parameters were kept unchanged, as previously mentioned.

2.4. Phylogenetic inference

Four alignments were analysed by maximum likelihood (ML) using *RAxML* v.8.2.6 (Stamatakis, 2014) under the concatenation approach: two *de novo* alignments with the highest average bootstrap support from preliminary study (Supp. Fig. S3), one *de novo* alignment with the highest number of SNPs and one alignment obtained from mapping to reference genome. We applied nucleotide substitution model GTR + G. In the ML analysis, a search for the best scoring ML tree was performed with 100 replicates, and branch support for each node was assessed by 1000 nonparametric bootstrap replicates and summarised on the best ML tree. For the analysis of results, bootstrap support (BS) values were classified as follows: poor support (BS ≤ 75 %), moderate support (75 % < BS < 90 %) and high support (BS ≥ 90 %) (e.g., Johnston et al., 2024).

We used the multispecies coalescent model as implemented in *BPP* v.4.0 software (Flouri et al., 2018) to analyse RAD-seq data assembled with the reference-based approach and under 0.74 CT. This approach allows investigation of the potential incomplete lineage sorting and can be used to account for sites in the genome that are evolutionarily linked which may lead to highly supported, yet incorrect species trees when analysed using concatenation-based approach. To infer a species tree using *BPP* we used the A01 analysis (speciesdelimitation = 0 and speciestree = 1). We performed inference on two data sets: the first consisting of all 11 693 loci retrieved from reference-based assembly, and the second with 9 540 loci retrieved from assembly under 0.74 CT. We conducted four independent MCMC runs with burn-in set to 10 000, a sample frequency of 5 and with 50 000 total samples. For each dataset we used the corresponding *RAxML* output as the starting species tree topology for the analysis. We specified inverse gamma priors for both population sizes (θ) and the divergence time of the root (τ0). We assigned the inverse gamma priors for θ with $\alpha = 3$ and $\beta = 0.02$, and for root age we set $\alpha = 3$ and $\beta = 0.234$. The divergence time between *Lispe* and *Limnophora* lineages was derived from Haseyama et al. (2015).

3. Results

3.1. Nanopore sequencing and genome assemblies

Long-read sequences of *L. tentaculata* were obtained in two sequencing runs on MinION Mk1C. A total of 9.06 x 10^5 reads (6.01 Gb) were generated for the first run and 1.34 x 10^6 (5.3 Gb) for the second run. The N50 read lengths were 9.4 kb and 9.2 kb, respectively. We benchmarked five *de novo* tools for genome assembly from long ONT-only reads. The evaluation of genome completeness using *BUSCO* (Table 1; Supp. Fig. S1) revealed that *Flye* yielded the lowest percentage of missing genes (6.3 %), with 90.1 % of complete and 3.6 % of fragmented genes. The lowest percentage of genome completeness values were observed in *Raven* (49.9 %) and *SMARTdenovo* (60.9 %). *SMARTdenovo* generated the lowest assembly length (~282 Mb), followed by *Raven* (~335 Mb). *wtdbg2* resulted in an intermediate total length (~550 Mb), but the most contiguous assembly (N50 = 81.7 kb). *Flye* produced the longest assembly length of 989 Mb, yet the assembly was highly fragmented with the largest number of contigs (46 646) and

Table 1
Evaluation summary of genome completeness (*BUSCO*) and genome assembly quality (*Inspector*) for five assemblers: *Raven*, *SMARTdenovo*, *wtdbg2*, *Canu* and *Flye*. *BUSCO* assessment used the dipteran dataset (3285 genes).

Parameter	*Raven*	*SMARTdenovo*	*wtdbg2*	*Canu*	*Flye*
***BUSCO*, n = 3285**					
Complete [single, duplicated]	49.9 % [49.5 %, 0.4 %]	60.9 % [60.1 %, 0.8 %]	77.3 % [77.1 %, 0.2 %]	82.5 % [60.8 %, 21.7 %]	90.1 % [67.9 %, 22.2 %]
Fragmented	6.1 %	5.7 %	7.5 %	3.8 %	3.6 %
Missing	44.0 %	33.4 %	15.2 %	13.7 %	6.3 %
Inspector					
Number of contigs	6049	7870	14,130	23,668	46,646
Number of contigs > 1000 bp	6049	7870	14,127	23,668	45,777
Number of contigs > 10000 bp	6042	7595	9775	21,765	28,848
Total length	334,979,448 (335 Mb)	281,692,310 (281,7 Mb)	549,512,882 (549,5 Mb)	748,791,779 (748,8 Mb)	988,956,643 (989 Mb)
Longest contig	447,123	795,484	1,985,679	572,497	384,705
N50	68,227	42,005	81,745	38,417	35,162
Mapping rate	85.06 %	82.59 %	94.02 %	91.56 %	93.77 %
Split-read rate	44.76 %	41.45 %	41.43 %	36.49 %	38.95 %
Depth	31.72	37.08	20.17	14.64	12.33
Small-scale assembly error/Mbp	3686.95	2355.19	7463.49	2362.22	719.94
Total small-scale assembly error	1,235,053	663,439	4,101,272	1,768,812	645,359
Quality Value (QV)	23.00	24.89	20.59	25.43	30.97

the lowest N50 value (35.1 kb). Similarly, *Canu* produced a low contiguity assembly (N50 = 38.4 kb) with a total length of 748.8 Mb. The N50 value is commonly used as a parameter to reflect the contiguity of the assembly results. However, a larger N50 value is not always a useful parameter for assessing assembler performance, because longer contigs may be less accurate (Wang et al., 2021). The Quality Value (QV), which estimates overall assembly quality, was the highest for *Flye* (30.97), followed by comparable values for *Canu* (25.43) and *SMARTdenovo* (24.89). *wtdbg2* showed the lowest QV (20.59). In general, *Raven* was the assembler with the lowest memory and computational requirements with the trade-off of poor statistical report in comparison to the other long-read assemblers. *Canu* and *Flye* performed better than the other three assemblers, not only by generating the highest assembly length but also having the highest QV and completeness. We selected the *Flye* assembler for the downstream analysis based on the *BUSCO* assessment (Supp. Fig. S1) and QV (Table 1).

3.2. RAD-seq assembly results

Alignment length, number of retrieved loci, percentage of missing data, number of variable sites, proportion of parsimony informative sites (PIS) and mean bootstrap for nodes generally increased as the clustering threshold decreased (Table 2). The highest number of PIS, a proxy for phylogenetic signal strength (Table 2) and the greatest number of SNPs (Supp. Fig. S2) were obtained under 0.74 CT. In contrast, the highest mean bootstrap support (BS) was observed under 0.85 CT (BS = 93.75 %) and 0.75 CT (BS = 93.42 %) (Supp. Fig. S3). Although all aligments from the three CT (0.74, 0.75, and 0.85) were utilised for subsequent phylogenetic analyses, only the results for 0.74 CT are visually represented in Fig. 2 to emphasise the highest bootstrap support for *de novo* processed alignments, together with reference-based approach with the highest number of loci and variable sites. The summary statistics for alignments obtained under 0.74 and 0.75 clustering thresholds were relatively similar, but the 0.74 CT obtained the highest mean bootstrap support (96 %) (Table 2). The lowest number of retrieved loci (8 877), variable sites (113 339), PIS (28 234) and the lowest mean bootstrap value (84.2 %) were recovered under 0.85 CT. Mapping reads to the *L. tentaculata* reference genome resulted in increased alignment length (1 786 362 bp), number of retrieved loci (11 693) and number of variable sites (197 320), but simultaneously produced the lowest number of PIS (27 250) of all assembly methods (Table 2) and a mean bootstrap support of 87.7 %.

The resulting ML topologies varied between assembly methods, particularly in terms of nodal support. The percentage of nodes with poor support differed across methods with 25 % for the reference-based approach, 4 % for *de novo* 0.74 CT, 15 % for *de novo* 0.75 CT and 31 % for *de novo* 0.85 CT (Fig. 2; Supp. Fig. S4). Most other nodes were resolved with either high nodal support values or moderate support. In contrast, the topologies produced from each assembly method were generally congruent (Fig. 2; Supp. Fig. S4), except for the placement of *L. pumila* Wiedemann, 1824 and *L. pygmaea* and the position of the *leucospila*-group. These taxa resolved in two alternative topologies, one for both the *de novo* 0.74 (Fig. 2) and 0.75 CT (Supp. Fig. S4: topology A) assemblies, and the other for the reference-based (Fig. 2) and *de novo* 0.85 CT (Supp. Fig. S4: topology B) assembly analyses.

Our results are henceforth primarily described for the topologies derived from the reference-based and *de novo* 0.74 CT assemblies, as these are the datasets with the highest number of loci and highest mean bootstrap support, respectively (Fig. 2; Table 2). Subsequent descriptions of the bootstrap values for reference-based, *de novo* 0.74 CT, *de novo* 0.75 CT and *de novo* 0.85 CT assemblies are as follows: BS_{rb}, $BS_{0.74}$, $BS_{0.75}$ and $BS_{0.85}$.

3.3. Concatenated maximum likelihood phylogenies

Our results, similarly to previous studies (Kutty et al., 2010, 2014; Ge et al., 2016; Grzywacz et al., 2021; Gao et al., 2022), confirm the monophyly of *Lispe* (Fig. 2; Supp. Fig. S4). A division into three highly

Table 2
Summary statistics of analysed data and summary of bootstrap support values for phylogenies inferred from restriction site associated DNA sequencing (RAD-seq) alignments with maximum likelihood approach. RAD-seq data were processed with *de novo* approach under 0.74, 0.75 and 0.85 clustering thresholds and with the reference-based approach with the genome sequence of *Lispe tentaculata*. Abbreviations: PIS, parsimony informative sites; CV, coefficient of variation.

Analysed data		Aligment (bp)	Loci	Missing data (%)	Variable sites	PIS	Bootstrap support		
							Mean	Median	CV
Reference-based	*Flye*	1 786 362	11 693	90.44	197 320	27 250	87.7 %	100	0.20
de novo	Threshold								
	0.74	783 882	9 540	89.00	155 298	38 929	96 %	100	0.08
	0.75	788 761	9 640	89.02	154 955	38 830	92.6 %	100	0.14
	0.85	731 488	8 877	88.73	113 339	28 234	84.2 %	100	0.27

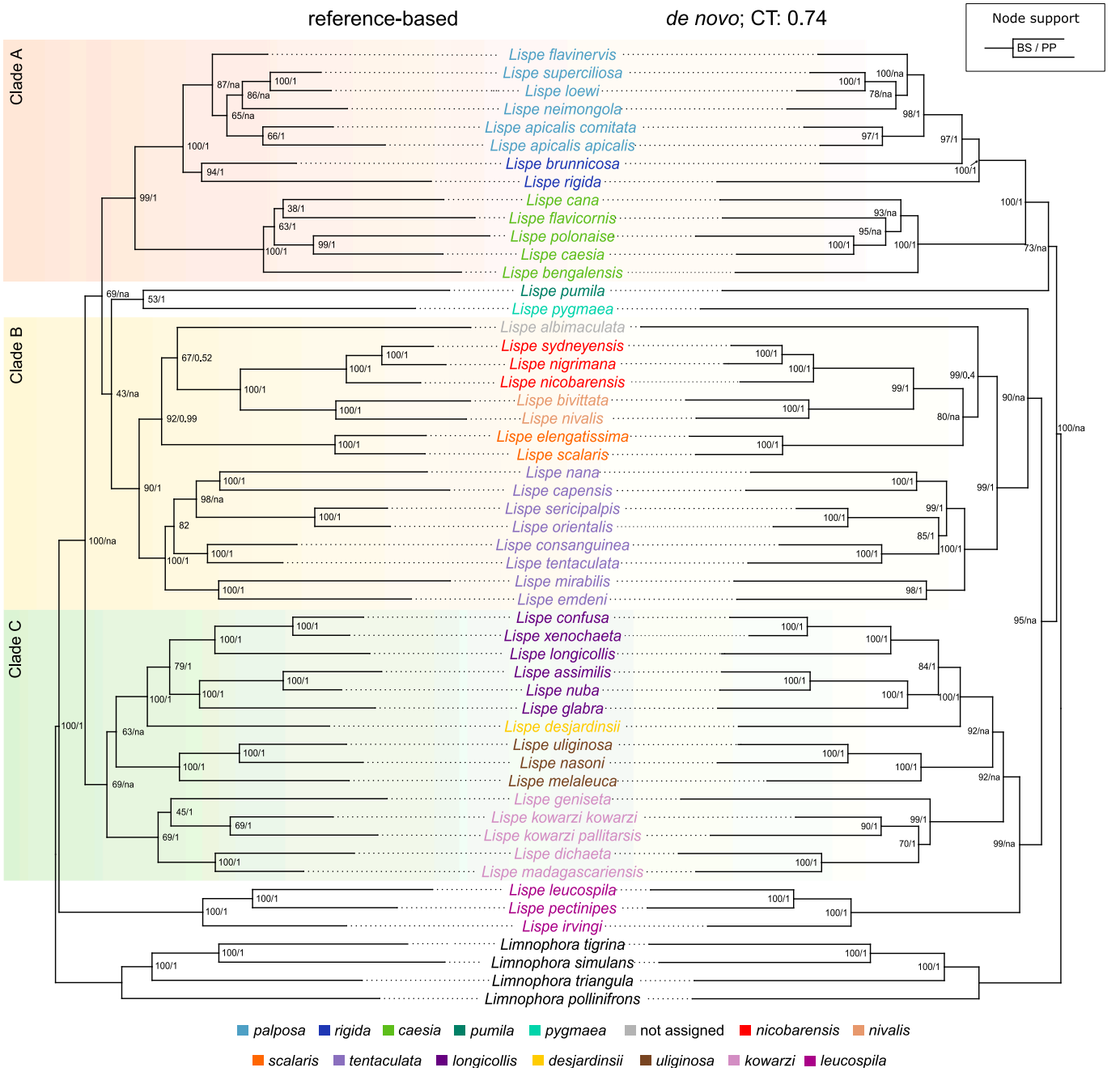

Fig. 2. Comparison of *RAxML* and *BPP* tree topologies inferred from reference-based approach and *de novo* assembly under 0.74 clustering threshold. Node support values are shown for 1 000 nonparametric bootstrap replicates (BS) and posterior probability (PP). Species groups of *Lispe* are marked with different colours as provided and outgroup marked with a black colour includes representatives of *Limnophora*. Clades consistently observed in this study are indicated by specific colours. Clade A consists of the *palposa*-, *rigida*-, and *caesia* groups, Clade B includes the *nicobarensis*-, *nivalis*-, *scalaris*- and *tentaculata* groups and Clade C includes the *longicollis*-, *desjardinsii*-, *uliginosa*- and *kowarzi* groups. In this study, the placement of *L. pumila*, *L. pygmaea*, and *L. leucospila* was influenced by assembly method and therefore they were not assigned to any clade. Abbreviation: CT, clustering threshold.

supported (BS $\geq$ 90 %) clades is observed, both for reference-based and *de novo* assemblies. For the sake of transparency in the presentation of results and discussion, 'Clade A' includes the *palposa*-group, the *rigida*-group and the *caesia*-group; 'Clade B' is composed of *L. albimaculata* Stein, 1910 (not assigned to a group), the *nicobarensis*-group, the *nivalis*-group, the *scalaris*-group and the *tentaculata*-group; while 'Clade C' consists of the *longicollis*-group, the *desjardinsii*-group, the *uliginosa*-group and the *kowarzi*-group.

In the reference-based and *de novo* 0.85 CT assemblies, the *leucospila*-group is revealed to be the sister group to all other *Lispe* ($BS_{rb} = 100$ %; $BS_{0.85} = 100$ %) (Fig. 2; Supp. Fig. S4: topology B), while in the *de novo* 0.74 and 0.75 CT assemblies the *leucospila*-group is a sister taxon of (*kowarzi*-group + (*uliginosa*-group + (*longicollis*-group + *desjardinsii*-group))) ($BS_{0.74} = 99$ %; $BS_{0.75} = 94$ %) (Fig. 2; Supp. Fig. S4: topology A). In *de novo* assembly under 0.74 CT (Fig. 2), a clade consisting of *palposa*-group, *rigida*-group and *caesia*-group ($BS_{0.74} = 100$ %) with *L. pumila* at the base ($BS_{0.74} = 73$ %) emerges as a sister group to the remaining *Lispe* ($BS_{0.74} = 100$ %).

Two species groups, the *pumila*-group and the *pygmaea*-group, each represented by a single representative, significantly differed in their position on the obtained phylogenetic trees. In the analysis of the reference-based assembly *L. pumila* is a sister taxon to *L. pygmaea* and

this clade emerges a sister to the Clade B (Fig. 2). In *de novo* assemblies *L. pumila* and *L. pygmaea* do not form a monophyletic clade, and the former is sister to Clade A, while the latter is sister to Clade B (Fig. 2).

The majority of the relationships within species groups are highly supported for the *leucospila-*, *longicollis-*, *nicobarensis-*, *nivalis-*, *rigida-*, *scalaris-*, *tentaculata-* and *uliginosa*-groups, and moderately or poorly supported for the *kowarzi-*, *caesia-* and *palposa*-groups (Fig. 2; Supp. Fig. S4). In Clade A, the *palposa*-group is monophyletic with *L. flavinervis* (Becker, 1904) being sister (BS_{rb} = 87 %) to (*L. neimongola* Tian et Ma, 2000 + (*L. superciliosa* Loew, 1861 + *L. loewi* Ringdahl, 1922)) and these species form a sister group to *L. apicalis comitata* (Becker, 1904) + *L. apicalis apicalis* Mik, 1869 (BS_{rb} = 66 %). Alternatively, in the *de novo* assemblies *L. apicalis comitata* + *L. apicalis apicalis* is sister to the rest of the *palposa*-group ($BS_{0.74}$ = 97 %). The *rigida*-group either emerges as the sister group to the *palposa*-group (BS_{rb} = 100 %) or is paraphyletic with regard to the *palposa*-group (Fig. 2 *de novo* CT: 0.74; Supp. Fig. S4). *Lispe cana* (Walker, 1849), traditionally representing the *cana*-group, is nested within the *caesia*-group, and emerges as a sister taxon to *L. flavicornis* Stein, 1909 (BS_{rb} = 38 %) or to (*L. flavicornis* + (*L. polonaise* Vikhrev, 2021 + *L. caesia*)) ($BS_{0.74}$ = 93 %). The *caesia*-group with *L. cana* is sister to the *palposa-* + *rigida*-groups (BS_{rb} = 99 %; $BS_{0.74}$ = 100 %).

In Clade B, *L. nana* Macquart, 1835, traditionally representing the *nana*-complex, is nested with *L. capensis* Zielke, 1971 (BS_{rb} = 100 %) within the *tentaculata*-group, and *L. mirabilis* Stein, 1918 emerges as a sister taxon to *L. emdeni* Vikhrev, 2012 (BS_{rb} = 100 %). The *nicobarensis*-group is sister to the *nivalis*-group (BS_{rb} = 100 %; $BS_{0.74}$ = 99 %). The *scalaris*-group is sister to (*L. albimaculata* + (*nigrimana* + *nivalis* groups)) with high branch support (BS_{rb} = 92 %), and this clade is sister to the *tentaculata*-group (BS_{rb} = 90 %) or to the (*nigrimana* + *nivalis*) groups with moderate support ($BS_{0.74}$ = 80 %). *Lispe albimaculata* is sister taxon to the (*nicobarensis* + *nivalis*) groups (BS_{rb} = 67 %) or to the (*scalaris* + (*nicobarensis* + *nivalis*)) groups ($BS_{0.74}$ = 99 %).

In Clade C, a moderately supported dichotomy (BS_{rb} = 79 %; $BS_{0.74}$ = 84 %) splits the *longicollis*-group into subgroup I with (*L. longicollis* Meigen, 1826 + (*L. xenochaeta* Malloch, 1923 + *L. confusa* Vikhrev, 2021)) (BS_{rb} = 100 %), and subgroup II with (*L. glabra* Wiedemann, 1824 + (*L. assimilis* Wiedemann, 1824 + *L. nuba* Wiedemann, 1830)) (BS_{rb} = 100 %; $BS_{0.74}$ = 100 %). *Lispe desjardinsii* is a sister taxon to the *longicollis*-group (BS_{rb} = 100 %; $BS_{0.74}$ = 100 %). The *uliginosa*-group is sister to the (*longicollis* + *desjardinsii*) groups, with moderate or high support (BS_{rb} = 63 %; $BS_{0.74}$ = 92 %). The poorly (BS_{rb} = 69 %) or highly ($BS_{0.74}$ = 90 %) supported *kowarzi*-group is revealed as a sister to the traditionally separated *geniseta*-complex represented by *L. geniseta* (BS_{rb} = 45 %), and the former *dichaeta*-complex (*L. dichaeta* + *L. madagascariensis*) is sister (BS_{rb} = 69 %) to the *kowarzi*-group + *L. geniseta*. In the *de novo* 0.74 CT topology, *L. geniseta* emerged as a sister taxon to the remaining representatives of *kowarzi*-group and the former *dichaeta*-complex ($BS_{0.74}$ = 99 %).

3.4. Multispecies coalescence-based phylogenies

Assembly type did not influence the final *BPP* topologies, with both reference-based and *de novo* + 0.74 CT data sets producing congruent phylogenetic trees (Fig. 2; Supp. Fig. S5). For the reference-based assembly, all species groups were monophyletic with maximum support (PP = 1). For the *de novo* + 0.74 CT assembly, similarly to the ML phylogenetic tree, the *rigida*-group is paraphyletic with regard to the *palposa*-group (PP = 1).

The resultant phylogenetic trees from the *BPP* analysis were also highly congruent with the ML topologies obtained for reference-based and *de novo* + CT 0.74 assemblies, including the *leucospila*-group sister to remaining *Lispe*. *Lispe albimaculata* is sister to (*nivalis* + *nicobarensis*) groups (PP = 0.52 and 0.41 for reference and *de novo* assembly, respectively).

Alternatively, both reference-based and *de novo* + CT 0.74 *BPP* topologies disagree with their corresponding ML topologies in terms of the position of the clade *L. pumila* + *L. pygmaea*, which under *BPP* is sister to the remaining *Lispe* (PP = 1), with the exception of the *leucospila*-group.

4. Discussion

4.1. Systematics of Lispe

The definition and species-groups limits within *Lispe* have primarily relied on morphological data, lacking formal phylogenetic reconstruction. Gao et al. (2022) provided the first molecular phylogeny, revealing four major clades, but with low backbone support. In this study, we consistently observed the following three clades: Clade A (*palposa-*, *rigida-* and *caesia*-groups), Clade B (*nicobarensis-*, *nivalis-*, *scalaris-* and *tentaculata*-groups) and Clade C (*longicollis-*, *desjardinsii-*, *uliginosa-* and *kowarzi*-groups). Clade B and Clade C of this study are congruent in terms of species-group composition with the second and third clades of Gao et al. (2022), but the limits of the remaining clades are incongruent between both studies. All incongruences between our generated topologies are related to relationships between these three clades. None of our phylogenetic hypotheses are considered conclusive and future research is still needed to comprehensively resolve relationships in the backbone of the *Lispe* tree of life. Despite this, we can certainly review of the state of *Lispe* phylogenetics in light of our current results.

4.1.1. Relationships within Clade A

The *palposa*-group, originally proposed by Snyder (1954), is the most clearly defined group based on adult morphology and is closely related to the *rigida*-group, as concluded by Vikhrev (2015) and this study (BS = 100 %). Neither the *leucospila*-group nor the *pygmaea*-group was found to be sister to the *palposa*-group as shown by Gao et al. (2022). The *caesia*-group, characterised by a widened ocellar triangle with convex margins, ventral spines on fore and mid femora and abdomen with a characteristic pattern, was one of the better-supported groups within *Lispe* according to Hennig (1960). Since then, species within the *caesia*-group have undergone re-examination, leading to a redefinition of this group by Gao et al. (2022). The present criterion for classifying species within the *caesia*-group is the presence of at least one of the character states indicated by Hennig. In line with this, *L. polonaise*, included for the first time in a molecular analysis, is nested within the *caesia*-group despite exhibiting only a slightly widened ocellar triangle with slightly convex margins (Vikhrev, 2021). *Lispe cana*, previously classified in the *cana*-group (Pont, 2019), is also nested within the *caesia*-group in our analysis, suggesting the inclusion of *L. cana* and its relatives within this group (Vikhrev, 2020). Our analyses revealed that the *caesia*-group is closely related to the (*uliginosa* + *rigida*) groups and it is not found to be sister to all other *Lispe* species as reported by Gao et al. (2022).

4.1.2. Relationships within Clade B

The systematic position of the *nana*-group and *L. mirabilis* within the *tentaculata*-group is congruent with previous molecular study, thereby supporting the extended *tentaculata*-group sensu Gao et al. (2022). Additionally, we propose to include *L. capensis* in the *tentaculata*-group, as it is placed as sister to *L. nana* with very high support. This is in agreement with Vikhrev (2021), who stated that the intermediate character states of *L. capensis* support a relationship of *L. nana* with the *tentaculata*-group.

Our analyses show a sister-group relationship between the clade composed of *scalaris*-group and (*nivalis* + *nicobarensis*) groups, as well as the *tentaculata*-group, with variable nodal support (Fig. 2; Supp. Fig. S4). These results, in conjuction with Gao et al. (2022), support Vikhrev's (2012a, 2014) conclusion that the *tentaculata* supergroup includes species from the *nivalis-*, *scalaris-* and extended *tentaculata*-groups (Vikhrev, 2014). Furthermore, we also propose to include the *nicobarensis*-group within this supergroup.

4.1.3. Relationships within Clade C

We confirm the split of the *longicollis*-group into subgroup I and II, as proposed by Hennig (1960), and further expanded on by Vikhrev (2014, 2020, 2021), with moderate ($BS_{rb} = 79$ %; $BS_{0.74} = 84$ %; $BS_{0.75} = 60$ %) or high support ($BS_{0.85} = 99$ %). Gao et al. (2022) suggested that *L. pennitarsis*, the only representative of the *desjardinsii*-group in their study, is nested within the *longicollis*-group. However, while *L. pennitarsis* appeared the intermediate position between the two subgroups of the *longicollis*-group (*assimilis*-subgroup and *longicollis*-subgroup), this position lacked significant support. Nevertheless, authors proposed merging the *desjardinsii*-subgroup within the *longicollis*-group. Despite morphological similarities between the *desjardinsii*- and *longicollis*-groups (Vikhrev, 2014), our study does not support the relationships reported by Gao et al. (2022). In all our analyses, *L. desjardinsii* is placed as a sister to the *longicollis*-group with full support (BS = 100 %), not nested within it. We propose retaining the *desjardinsii*-group separately until more extensive taxon sampling is implemented to test the validity of the entire species group. Our study also shows that the *uliginosa*-group is sister to the *longicollis*-group + *desjardinsii*-group, which in turn is sister to the *kowarzi*-group sensu Gao et al. (2022). This is in conflict with Gao et al. (2022) who showed the *longicollis*-group (including the *desjardinsii*-group) as sister to the *uliginosa*-group + *kowarzi*-complex. As for the former *geniseta* and *dichaeta* complexes, our results are congruent with those of Gao et al. (2022), which showed that these complexes clustered as sisters to the *kowarzi*-group. Therefore, we support the proposal of Gao et al. (2022) to extend the *kowarzi*-group to include all species assigned to the *dichaeta*, *geniseta* and *kowarzi* complexes.

4.1.4. Uncertain relationships of L. pumila, L. pygmaea and L. leucospila

The placement of *L. pumila* and *L. pygmaea* was influenced by the assembly method in our results. In the reference-based analysis, *L. pygmaea* emerged as sister to *L. pumila*, with moderate support (Fig. 2: reference-based), while the *de novo* + 0.74 CT analysis separated these species between the main three clades (Fig. 2: *de novo*, 0.74; Supp. Fig. S4). These two species were initially classified together in the *pumila*-group by Vikhrev (2012b), but later considered as monotypic complexes by the same author (Vikhrev, 2016), who proposed five complexes (*ambigua*, *dichaeta*, *geniseta*, *pumila* and *pygmaea*) that were regarded as the *L. pygmaea* ecological group based on a shared ecology. *Lispe pumila* was excluded from the analysis in the previous study (Gao et al., 2022), and we do not have a reference for its position on the *Lispe* tree. Thus, future studies with greater sampling are necessary to confirm the relationships between the *pumila*- and *pygmaea*-groups within *Lispe*.

The present study does not resolve the relationship between the *leucospila*-group and the other groups. The systematic position of the *leucospila*-group differed between our analyses. In the reference-based approach it is sister to all other *Lispe* (Fig. 2: $BS_{rb} = 100$ %), while in the *de novo* approach it is sister to the clade consisting of the *longicollis*-, *desjardinsii*-, *uliginosa*- and *kowarzi*-groups (Fig. 2: $BS_{0.74} = 99$ %; Supp. Fig. S4). Ge et al. (2016) also proposed that *L. leucospila* is at the base of the *Lispe* tree of life with high nodal support (BS = 98 %, PP = 1.0), however this study had incomplete taxon sampling, only including representatives of the *nivalis*-, *palposa*- and *tentaculata*-groups (Fig. 2 in Ge et al. 2016). Our results do not support the previous results of Gao et al. (2022) which suggestes a close relationship between the *leucospila*- and *palposa*-groups.

4.2. Ecology of Lispe

Species of the *leucospila*-group differ ecologically from other *Lispe* species. According to Vikhrev (2014), "their typical habitats are grassy lawns being seasonally or artificially watered, or similar natural habitats, usually secondary sites with short or sparse grass and moderately wet soil", while other *Lispe* inhabit semi-aquatic environments with wet mud or sand and high organic content. While some species of *Lispe* can surely be distinguished by their ecology and are only encountered in selected habitats, the habitat preferences for many species are unknown or inconclusive. *Lispe sericipalpis* Stein, 1904 and *L. manicata* Wiedemann, 1830 were reported from limnic habitats (Vikhrev, 2011a, 2012c), while *L. candicans* and *L. caesia* were reported from habitats influenced by saltwater, and *L. orientalis* from habitats containing dirty and organically polluted water (Vikhrev, 2011a). In contrast, *L. pygmaea* and *L. uliginosa* were found in both limnic and saline habitats (Hennig, 1960). Therefore, using ecology to infer phylogenetic relationships or ancestral state reconstruction should be approached with great caution. In this study we do not assess whether the habitat preferences observed within the *leucospila*-group, i.e., an association with grassy lawns and seasonally watered habitats, provide sufficient evidence to draw conclusions about the ancestral habitat preferences of *Lispe*. It is worth noting that many representatives of the closely related genus *Limnophora* are also associated with water bodies (Ivković & Pont, 2016). Thus, species of the *leucospila*-group may also exhibit a derived strategy, and an association with stagnant or running water could potentially be an ancestral strategy within a larger clade comprising several muscid genera.

4.3. Oxford nanopore reads assemblers performance

Many projects have recently been launched with the aim of providing high-quality genomes, e.g., Darwin Tree of Life, the Bird 10 000 Genomes (B10K) Project, the Vertebrate Genomes Project (VGP) and the BAT1K Genome Project. To date, the number of available dipteran genomes in public repository databases clearly indicates that model species (e.g., of *Drosophila* Fallén, 1823) or economically important species (e.g., of *Anopheles* Meigen, 1818) are of great interest. Among the Muscidae, genomes are available for ten species, that is *Eudasyphora cyanicolor* (Zetterstedt, 1845), *Haematobia irritans* (Linnaeus, 1758), *Hydrotaea cyrtoneurina* (Zetterstedt, 1845), *Hydrotaea diabolus* (Harris, 1780), *Musca domestica* Linnaeus, 1758, *Musca vetustissima* Walker, 1849, *Muscina levida* (Harris, 1780), *Phaonia tiefii* (Schnabl, 1888), *Polietes domitor* (Harris, 1780) and *Stomoxys calcitrans* (Linnaeus, 1758) (Scott et al., 2014; Konganti et al., 2018; Olafson et al., 2021; Romine et al., 2022; Falk et al., 2024a, 2024b, 2024c, 2024d), which represent a small percentage, considering that Muscidae are known from approximately 6 000 species. Nonetheless, this number is increasing especially due to the Darwin Tree of Life initiative.

Genome sequencing significantly advances phylogenetic research by providing extensive genetic data that enhances the resolution phylogenetic trees. This capability enables researchers to reconstruct phylogenetic relationships with greater comprehensiveness and reliability (McCormack et al., 2013; Shakya et al., 2020). In light of the progressive reduction of costs and computational requirements, genome sequencing is now achievable and affordable for individual laboratories, rather than only for international consortia (Brandies et al., 2019). Despite only a few years of commercial use, nanopore sequencing has revolutionised genomic studies owing to facilitating *de novo* genome assembly by increasing read length and significantly reducing sequencing time (Leggett & Clark, 2017; Senol Cali et al., 2018; Nature, 2023). Both long-read sequencing, i.e., ONT and PacBio, do not require PCR, which helps avoid biases during library preparation and facilitates the assembly of repetitive genome regions (Jansen et al., 2017). However, ONT stands out particularly for its lower cost and availability, making it a more widely used method in large-scale sequencing and routine applications. As the availability of genome sequencing technology has increased, attention has also shifted to the pivotal step of genome assembly. This process may produce different results, depending on the use of various assemblers, each of which has its own algorithms and methodologies (Guiglielmoni et al., 2021). To address crucial time and cost considerations, we used ONT reads to obtain the genome of *L. tentaculata*, evaluating five different assemblers, commonly used at the time of the study. Among the selected assemblers, *Flye* appeared to be the most

effective, achieving the highest percentage of completeness (90.1 %) in the *BUSCO* assessment and demonstrating the lowest small-scale assembly error rate per megabase of genome. Additionally, *Flye* exhibited the highest Quality Value (QV), indicating high genome reconstruction accuracy. Following *Flye*, *Canu* also showcased competitive performance, particularly in terms of completeness and assembly accuracy. This is in agreement with recent studies that compared different assemblers and in most of them *Flye* and *Canu* performed best, on both eukaryotic and prokaryotic genomes (Jung et al., 2020; Latorre-Pérez et al., 2020; Sun et al., 2021; Cosma et al., 2023). On the other hand, in this study *Raven* appeared to perform relatively poorly compared to the other assemblers, showing lower completeness percentages and quality values, whereas in other genome comparison studies, it was noted as the best-performing assembler (Chen et al., 2020). As previous studies have shown, there is no single assembler that stands out as the best, as various assemblers exhibit differences in terms of structural accuracy, completeness and contiguity of assembled genomes (Wick & Holt, 2019). This is due to the use of distinct algorithms, optimisations for different data types and qualities and varied approaches to handling genomic complexity and error correction. Additionally, assembler performance can depend on specific settings, computational resources and ongoing software updates (Cosma et al., 2023). Hence, the selection of the most appropriate assembler should depend on study-specific factors, including genome assembly goals such as the characteristics of the sequencing data and the complexity of the genome being studied. Furthermore, given the ongoing introduction of new assemblers and improvements to existing ones, it is advisable for users to keep updated with these advancements to ensure optimal performance that meets their specific needs.

Genomes of Muscidae, similarly to those of many other insects (Hotaling et al., 2021), contain a large proportion of transposable elements. In case of muscid flies even more than 50 % of the genome is present as repeated content (Romine et al., 2022). The first genome of *Musca domestica* obtained with a short reads sequencing approach, resulted in the assembly of a 691 Mb genome (GCA_000371365.1), while the application of long reads overcame the issue of highly repetitive regions and led to genomes assemblies ranging from 907 Mb (GCA_030504385.2) to 1.3 Gb (GCA_032878625.1) in length. Among all of the available genomes, only that of *Musca vetustissima* and the one obtained in this study for *Lispe tentaculata* were sequenced using nanopore sequencing, with the genome of the former species also incorporating short reads from Illumina. The remaining genomes were predominantly sequenced using PacBio technology, with some supplemented by short Illumina reads. With a genome size of 989 Mb assembled using *Flye* (Table 1), *L. tentaculata* falls in the mid-range of genome sizes among all available muscid genomes. It is larger than several genomes, like *H. cyrtoneurina* (575 Mb) and *M. vetustissima* (850 Mb), but smaller than others, such as those of *E. cyanicolor* and *P. tiefii*, which exceed 1.5 Gb.

5. Conclusions

The results of this study are congruent with species-group concepts established using adult morphology, particularly those proposed by Vikhrev (2020, 2021), but they differ both in relationships between and within species groups from the findings of Gao et al. (2022), who provided the only previous phylogenetic hypothesis for the classification of *Lispe*. We propose expanding the *tentaculata* supergroup *sensu* Vikhrev (2014), which presently comprises the *tentaculata*-, *nivalis*- and *scalaris*-groups, to also include the *nicobarensis*-group. Our results corroborate the proposal of Gao et al. (2022) to expand the *kowarzi*-group to include the traditionally recognised *dichaeta*-complex and *geniseta*-complex. Given that our results provide strong support for *L. desjardinsii* as the sister taxon of the *longicollis*-group, we retain the validity of the *desjardinsii*-group, thus confirming the presence of 14 distinct species groups in the genus *Lispe*. Our results yielded two alternate, but highly supported phylogenetic tree topologies, resolving most of the relationships between and within species groups and between species within those groups. Future studies focusing on the genus *Lispe* should prioritise improving taxon sampling, including species from recognised species groups as well as many of those that have not yet been assigned to any group (Supp. Table S1).

CRediT authorship contribution statement

Kinga Walczak: Writing – review & editing, Writing – original draft, Visualization, Methodology, Investigation, Conceptualization. **Marcin Piwczyński:** Writing – review & editing, Resources, Investigation. **Thomas Pape:** Writing – review & editing, Resources. **Nikolas P. Johnston:** Writing – review & editing, Resources. **James F. Wallman:** Writing – review & editing, Resources. **Krzysztof Szpila:** Writing – review & editing, Resources. **Andrzej Grzywacz:** Writing – review & editing, Visualization, Methodology, Investigation, Funding acquisition, Conceptualization.

2.5. Data availability

Data obtained during this study have been submitted to NCBI (National Center for Biotechnology Information, Bethesda, MD, USA) and are available under the BioProject PRJNA1059801 accession number. Specifically, ONT long reads are available under SRR27397080 and RAD-seq reads under SRR27504576-SRR27504628 accession numbers in Sequence Read Archive (SRA). A Whole Genome Shotgun project for *Lispe tentaculata* has been deposited at DDBJ/ENA/GenBank under the accession JBBFKM000000000. The version described in this paper is version JBBFKM010000000.

Declaration of Competing Interest

The authors declare that they have no known competing financial interests or personal relationships that could have appeared to influence the work reported in this paper.

Acknowledgements

We would like to express our appreciation to Nikita E. Vikhrev and Konstantin Tomkovich (Moscow, Russia), Adrian C. Pont (Oxford, UK), Alessandra Rung, Martin Hauser and Stephen D. Gaimari (Sacramento, CA, USA), Mike E. Irwin (Urbana-Champaign, IL, USA), Thai Hong Pham (Hanoi, Vietnam), Oleg Kosterin and Natalya Priydak (Novosibirsk, Russia) and Doreen Werner (Müncheberg, Germany) for their help in obtaining material. This research was supported by the National Science Centre of Poland (grant no. 2019/33/B/NZ8/02316 to AG). We gratefully acknowledge Poland's high-performance computing infrastructure PLGrid (HPC Center: ACK Cyfronet AGH) for providing computer facilities and support within computational grant no. PLG/2022/015448 to AG.

Appendix A. Supplementary data

Supplementary data to this article can be found online at https://doi.org/10.1016/j.ympev.2025.108291.

Data availability

Data will be made available on request.

References

Ali, O.A., O'Rourke, S.M., Amish, S.J., Meek, M.H., Luikart, G., Jeffres, C., Miller, M.R., 2016. RAD capture (Rapture): Flexible and efficient sequence-based genotyping. *Genetics* 202, 389–400.

Andrews, K.R., Good, J.M., Miller, M.R., Luikart, G., Hohenlohe, P.A., 2016. Harnessing the power of RADseq for ecological and evolutionary genomics. *Nat. Rev. Genet.* 17, 81–92.
Baird, N.A., Etter, P.D., Atwood, T.S., Currey, M.C., Shiver, A.L., Lewis, Z.A., Selker, E.U., Cresko, W.A., Johnson, E.A., 2008. Rapid SNP discovery and genetic mapping using sequenced RAD markers. *PLoS One* 3, 1–7.
Bolger, A.M., Lohse, M., Usadel, B., 2014. Trimmomatic: A flexible trimmer for Illumina sequence data. *Bioinformatics* 30, 2114–2120.
Brandies, P., Peel, E., Hogg, C.J., Belov, K., 2019. The value of reference genomes in the conservation of threatened species. *Genes* 10, 846.
Butterworth, N.J., Wallman, J.F., 2022. Flies getting filthy: The precopulatory mating behaviours of three mud-dwelling species of Australian *Lispe* (Diptera: Muscidae). *Ethology* 128, 369–377.
Cariou, M., Duret, L., Charlat, S., 2013. Is RAD-seq suitable for phylogenetic inference? An *in silico* assessment and optimization. Ecol. Evol. 3, 846–852.
Chen, Y., Zhang, Y., Wang, A.Y., Gao, M., Chong, Z., 2021. Accurate long-read *de novo* assembly evaluation with Inspector. Genome Biol. 22, 1–21.
Chen, Z., Erickson, D.L., Meng, J., 2020. Benchmarking long-read assemblers for genomic analyses of bacterial pathogens using Oxford Nanopore Sequencing. Int. J. Mol. Sci. 21, 1–27.
Cosma, B.M., Zade, S.H., R., Jordan, E.N., Van Lent, P., Peng, C., Pillay, S., & Abeel, T, 2023. Evaluating long-read *de novo* assembly tools for eukaryotic genomes: insights and considerations. *GigaScience* 12, 1–12.
De Coster, W., D'Hert, S., Schultz, D.T., Cruts, M., Van Broeckhoven, C., 2018. NanoPack: Visualizing and processing long-read sequencing data. *Bioinformatics* 34, 2666–2669.
Curran, C.H., 1937. African Muscidae - IV (Diptera). *Am. Mus. Novit.* 1–14.
Davey, J.L., Blaxter, M.W., 2010. RADseq: Next-generation population genetics. *Brief. Funct. Genomics* 9, 416–423.
Díaz-Arce, N., Rodríguez-Ezpeleta, N., 2019. Selecting RAD-Seq data analysis parameters for population genetics: The more the better? *Front. Genet.* 10, 1–10.
Dida, F., Yi, G., 2021. Empirical evaluation of methods for *de novo* genome assembly. *PeerJ Comput. Sci.* 7, 1–31.
Eaton, D.A.R., 2014. PyRAD: Assembly of *de novo* RADseq loci for phylogenetic analyses. *Bioinformatics* 30, 1844–1849.
van Emden, F.I., 1941. Key to the Muscidae of the Ethiopian Region: Scatophaginae, Anthomyiinae, Lispinae, Fanniinae. *Bull. Entomol. Res.* 32, 251–275.
van Emden, F.I., 1965. Diptera 7, Muscidae. Part I. The fauna of India and the adjacent countries, Government of India, Delhi, p. 647.
Emerson, K.J., Merz, C.R., Catchen, J.M., Hohenlohe, P.A., Cresko, W.A., Bradshaw, W. E., Holzapfel, C.M., 2010. Resolving postglacial phylogeography using high-throughput sequencing. *PNAS* 107, 16196–16200.
Etter, P.D., Bassham, S., Hohenlohe, P.A., Johnson, E.A., Cresko, W.A., 2011. SNP discovery and genotyping for evolutionary genetics using RAD sequencing. *Methods Mol. Biol.* 772, 157–178.
Falk, S., Grzywacz, A., University of Oxford and Wytham Woods Genome Acquisition Lab, et al., 2024a. The genome sequence of a muscid fly, Hydrotaea cyrtoneurina (Zetterstedt, 1845) [version 1; peer review: 2 approved]. *Wellcome Open Res.* 9 (60), 1–12.
Falk, S., Grzywacz, A., University of Oxford and Wytham Woods Genome Acquisition Lab, et al., 2024b. The genome sequence of a muscid fly, Hydrotaea diabolus (Harris, [1780]) [version 1; peer review: 1 approved]. Wellcome Open Res. 9 (176), 1–10.
Falk, S., Grzywacz, A., University of Oxford and Wytham Woods Genome Acquisition Lab, et al., 2024c. The genome sequence of a muscid fly, Muscina levida (Harris, 1780) [version 1; peer review: awaiting peer review]. *Wellcome Open Res.* 9 (537), 1–11.
Falk, S., Sivell, D., Webb, J., et al., 2024d. The genome sequence of a muscid fly, *Polietes domitor* (Harris, 1780) [version 1; peer review: 2 approved]. Wellcome Open Res. 9 (58), 1–12.
Fan, Z.-D., 2008. Fauna Sinica Insecta. Diptera Muscidae (i) vol. 49, 1–1180.
Flouri, T., Jiao, X., Rannala, B., Yang, Z., 2018. Species tree inference with BPP using genomic sequences and the multispecies coalescent. *Mol. Biol. Evol.* 35, 2585–2593.
Frantsevich, L., Gorb, S., 2006. Courtship dances in the flies of the genus *Lispe* (Diptera: Muscidae): From the fly's viewpoint. *Archives of Insect Biochemistry and Physiology* 62, 26–42.
Gao, Y., Ge, Y., Yan, L., Vikhrev, N.E., Wang, Q., Butterworth, N.J., Zhang, D., 2022. Phylogenetic analyses support the monophyly of the genus *Lispe* Latreille (Diptera: Muscidae) with insights into intrageneric relationships. *Insects* 13, 1015.
Ge, Y., Gao, Y., Yan, L., Liu, X., Zhang, D., 2016. Review of the *Lispe tentaculata*-group (Diptera: Muscidae) in China, with one new synonym. *Zoosystema* 38, 339–352.
Grzywacz, A., Trzeciak, P., Wiegmann, B.M., Cassel, B.K., Pape, T., Walczak, K., Bystrowski, C., Nelson, L., Piwczyński, M., 2021. Towards a new classification of Muscidae (Diptera): a comparison of hypotheses based on multiple molecular phylogenetic approaches. *Syst. Entomol.* 46, 508–525.
Guiglielmoni, N., Houtain, A., Derzelle, A., Van Doninck, K., Flot, J.F., 2021. Overcoming uncollapsed haplotypes in long-read assemblies of non-model organisms. *BMC Bioinf.* 22, 1–23.
Haseyama, K.L.F., Wiegmann, B.M., Almeida, E.A.B., de Carvalho, C.J.B., 2015. Say goodbye to tribes in the new house fly classification: A new molecular phylogenetic analysis and an updated biogeographical narrative for the Muscidae (Diptera). *Mol. Phylogenet. Evol.* 89, 1–12.
Hennig, W., 1955. Family Muscidae. In: Lindner, E. (Ed.), Die Fliegen Der Paläarktischen Region, 63b. Schweizerbart'sche Verlagsbuchhandlung, Stuttgart, pp. 625–672.
Hennig, W., 1960a. 63 b. Muscidae (Lieferung 225). In: Lindner, E. (Ed.), Die Fliegen Der Palaearktischen Region. Schweizerbart'sche Verlagsbuchhandlung, Stuttgart, pp. 399–432.
Hennig, W., 1960b. Muscidae (Lieferung 209). In: Lindner, E. (Ed.), Die Fliegen Der Palaearktischen Region. Schweizerbart'sche Verlagsbuchhandlung, Stuttgart, pp. 399–432.
Hennig, W., 1965. Vorarbeiten zu einem phylogenetischen System der Muscidae (Diptera: Cyclorrhapha). *Stuttgarter Beiträge Zur Naturkunde* 141, 1–100.
Hohenlohe, P.A., Bassham, S., Etter, P.D., Stiffler, N., Johnson, E.A., Cresko, W.A., 2010. Population genomics of parallel adaptation in threespine stickleback using sequenced RAD tags. *PLoS Genet.* 6, e1000862.
Hotaling, S., Sproul, J.S., Heckenhauer, J., Powell, A., Larracuente, A.M., Pauls, S.U., Kelley, J.L., Frandsen, P.B., 2021. Long reads are revolutionizing 20 years of insect genome sequencing. *Genome Biol. Evol.* 13, evab138.
Ivković, M., Pont, A.C., 2016. Long-time emergence patterns of *Limnophora* species (Diptera, Muscidae) in specific karst habitats: tufa barriers. *Limnologica* 61, 29–35.
Jansen, H.J., Liem, M., Jong-Raadsen, S.A., Dufour, S., Weltzien, F.A., Swinkels, W., Koelewijn, A., Palstra, A.P., Pelster, B., Spaink, H.P., Thillart, G.E.V.D., Dirks, R.P., Henkel, C.V., 2017. Rapid *de novo* assembly of the European eel genome from nanopore sequencing reads. *Sci. Rep.* 7, 1–13.
Johnston, N.P., Pape, T., Piwczyński, M., Wallman, J.F., Wiegmann, B.M., Cassel, B.K., Akbarzadeh, K., Szpila, K., 2024. Anchored phylogenomics and revised classification of the Miltogramminae (Diptera: Sarcophagidae). *Syst. Entomol.* 49 (1), 138–155.
Jung, H., Jeon, M.S., Hodgett, M., Waterhouse, P., Eyun, S.I., 2020. Comparative evaluation of genome assemblers from long-read sequencing for plants and crops. *J. Agric. Food Chem.* 68, 7670–7677.
Karl, O. (1928) Zweiflügler oder Diptera. II: Muscidae. Die Tierwelt Deutschlands und der angrenzenden Meeresteile nach ihren Merkmalen und nach ihrer Lebensweise. p. 1–232.
Kolmogorov, M., Yuan, J., Lin, Y., Pevzner, P.A., 2019. Assembly of long, error-prone reads using repeat graphs. *Nat. Biotechnol.* 37, 540–546.
Konganti, K., Guerrero, F.D., Schilkey, F., Ngam, P., Jacobi, J.L., Umale, P.E., Perez de Leon, A.A., Threadgill, D.W., 2018. A whole genome assembly of the horn fly, *Haematobia irritans*, and prediction of genes with roles in metabolism and sex determination. *G3 Genes|genomes|genetics* 8, 1675–1686.
Koren, S., Walenz, B.P., Berlin, K., Miller, J.R., Bergman, N.H., Phillippy, A.M., 2017. Canu: Scalable and accurate long-read assembly via adaptive κ-mer weighting and repeat separation. *Genome Res.* 27, 722–736.
Kunvar, S., Czarnomska, S., Pertoldi, C., Tokarska, M., 2021. In Search of Species-Specific SNPs in a non-model animal (European bison (*Bison bonasus*))—comparison of *de novo* and reference-based integrated pipeline of STACKS using genotyping-by-sequencing (GBS) Data. Animals 11, 1–13.
Kutty, S.N., Pape, T., Wiegmann, B.M., Meier, R., 2010. Molecular phylogeny of the Calyptratae (Diptera: Cyclorrhapha) with an emphasis on the superfamily Oestroidea and the position of Mystacinobiidae and McAlpine's fly. *Syst. Entomol.* 35, 614–635.
Kutty, S.N., Pont, A.C., Meier, R., Pape, T., 2014. Complete tribal sampling reveals basal split in Muscidae (Diptera), confirms saprophagy as ancestral feeding mode, and reveals an evolutionary correlation between instar numbers and carnivory. *Mol. Phylogenet. Evol.* 78, 349–364.
Latorre-Pérez, A., Villalba-Bermell, P., Pascual, J., Vilanova, C., 2020. Assembly methods for nanopore-based metagenomic sequencing: a comparative study. *Sci. Rep.* 10, 1–14.
Leggett, R.M., Clark, M.D., 2017. A world of opportunities with nanopore sequencing. *J. Exp. Bot.* 68, 5419–5429.
Liu, H., Wu, S., Li, A., Ruan, J., 2021. SMARTdenovo: a de novo assembler using long noisy reads. *Gigabyte* 2021, 1–9.
Malloch, J.R., 1923. Notes on Australian Diptera with descriptions. [No. i.]. *Proc. Linnean Soc. NSW* 48, 601–622.
Manel, S., Perrier, C., Pratlong, M., Abi-Rached, L., Paganini, J., Pontarotti, P., Aurelle, D., 2016. Genomic resources and their influence on the detection of the signal of positive selection in genome scans. *Mol. Ecol.* 25, 170–184.
Manni, M., Berkeley, M.R., Seppey, M., Simão, F.A., Zdobnov, E.M., 2021. BUSCO update: novel and streamlined workflows along with broader and deeper phylogenetic coverage for scoring of eukaryotic, prokaryotic, and viral genomes. *Molecular Biology and Evolution* 38, 4647–4654.
McCartney-Melstad, E., Gidiș, M., Shaffer, H.B., 2019. An empirical pipeline for choosing the optimal clustering threshold in RADseq studies. *Mol. Ecol. Resour.* 19, 1195–1204.
McCormack, J.E., Hird, S.M., Zellmer, A.J., Carstens, B.C., Brumfield, R.T., 2013. Applications of next-generation sequencing to phylogeography and phylogenetics. *Mol. Phylogenet. Evol.* 66, 526–538.
Metzker, M.L., 2010. Sequencing technologies - the next generation. *Nat. Rev. Genet.* 11, 31–46.
Nature., 2023. Method of the Year 2022: long-read sequencing. *Nat. Methods* 20.
Olafson, P.U., Aksoy, S., Attardo, G.M., Buckmeier, G., Chen, X., Coates, C.J., Davis, M., Dykema, J., Emrich, S.J., Friedrich, M., Holmes, C.J., Ioannidis, P., Jansen, E.N., Jennings, E.C., Lawson, D., Martinson, E.O., Maslen, G.L., Meisel, R.P., Murphy, T.D., Nayduch, D., Nelson, D.R., Oyen, K.J., Raszick, T.J., Ribeiro, J.M.C., Robertson, H. M., Rosendale, A.J., Sackton, T.B., Saelao, P., Swiger, S.L., Sze, S.-H., Tarone, A.M., Taylor, D.B., Warren, W.C., Waterhouse, R.M., Weirauch, M.T., Werren, J.H., Wilson, R.K., Zdobnov, E.M., Benoit, J.B., 2021. The genome of the stable fly, *Stomoxys calcitrans*, reveals potential mechanisms underlying reproduction, host interactions, and novel targets for pest control. *BMC Biol.* 19, 41.
Paris, J.R., Stevens, J.R., Catchen, J.M., 2017. Lost in parameter space: a road map for stacks. *Methods Ecol. Evol.* 8, 1360–1373.
Paterson, H.E., 1953. New *Lispe* species (Dipt., Muscidae) from Southern Africa. *J. Entomol. Soc. South. Afr.* 16, 168–178.

Piwczyński, M., Trzeciak, P., Popa, M.O., Pabijan, M., Corral, J.M., Spalik, K., Grzywacz, A., 2021. Using RAD seq for reconstructing phylogenies of highly diverged taxa: A test using the tribe Scandiceae (Apiaceae). *J. Syst. Evol.* 59, 58–72.
Pont, A.C., 2019. Studies on the Australian Muscidae (Diptera). VIII. The genus *Lispe* Latreille, 1797. Zootaxa 4557 (1), 1–232.
Romine, M.G., Knutie, S.A., Crow, C.M., Vaziri, G.J., Chaves, J.A., Koop, J.A.H., Lamichhaney, S., 2022. The genome sequence of the avian vampire fly (*Philornis downsi*), an invasive nest parasite of Darwin's finches in Galápagos. *G3 Genes|genomes|genetics* 12, jkab414.
Ruan, J., Li, H., 2020. Fast and accurate long-read assembly with wtdbg2. *Nat. Methods* 17, 155–158.
Rubin, B.E.R., Ree, R.H., Moreau, C.S., 2012. Inferring phylogenies from RAD sequence data. *PLoS One* 7, 1–12.
Scott, J.G., Warren, W.C., Beukeboom, L.W., Bopp, D., Clark, A.G., Giers, S.D., Hediger, M., Jones, A.K., Kasai, S., Leichter, C.A., Li, M., Meisel, R.P., Minx, P., Murphy, T.D., Nelson, D.R., Reid, W.R., Rinkevich, F.D., Robertson, H.M., Sackton, T.B., Sattelle, D.B., Thibaud-Nissen, F., Tomlinson, C., van de Zande, L., Walden, K.K., Wilson, R.K., Liu, N., 2014. Genome of the house fly, *Musca domestica* L., a global vector of diseases with adaptations to a septic environment. *Genome Biol.* 15, 466.
Séguy, E., 1937. Diptera, family Muscidae. In: Wytsmann, P. (Ed.), Genera Insectorum. Bruxelles, Desmet-Verteneuil, pp. 1–604.
Senol Cali, D., Kim, J.S., Ghose, S., Alkan, C., Mutlu, O., 2018. Nanopore sequencing technology and tools for genome assembly: Computational analysis of the current state, bottlenecks and future directions. *Brief. Bioinform.* 20, 1542–1559.
Shafer, A.B.A., Peart, C.R., Tusso, S., Maayan, I., Brelsford, A., Wheat, C.W., Wolf, J.B.W., 2017. Bioinformatic processing of RAD-seq data dramatically impacts downstream population genetic inference. *Methods Ecol. Evol.* 8, 907–917.
Shakya, M., Ahmed, S.A., Davenport, K.W., Flynn, M.C., Lo, C.C., Chain, P.S.G., 2020. Standardized phylogenetic and molecular evolutionary analysis applied to species across the microbial tree of life. *Sci. Rep.* 10, 1–15.
Shinonaga, S., Kano, R., 1983. Two new species and a newly recorded subspecies of the genus *Lispe* Latreille from Japan with a key to Japanese species (Diptera, Muscidae). *Medical Entomology and Zoology* 34, 83–88.
Skidmore, P., 1985. The biology of the Muscidae of the World. *Series Entomologica* 29, 1–550.
Snyder, F.M., 1949. New genera and species of Lispinae (Diptera, Muscidae). *Am. Mus. Novit.* 1403, 1–9.
Snyder, F.M., 1954. A review of Nearctic *Lispe* Latreille (Diptera, Muscidae). *The American Museum of Natural History* 1–40.
Stamatakis, A., 2014. RAxML version 8: A tool for phylogenetic analysis and post-analysis of large phylogenies. *Bioinformatics* 30, 1312–1313.
Steidle, J.L.M., Dettner, K., Hübner, G., Köpf, A., Reinhard, J., 1995. The predaceous fly *Lispe candicans* (Diptera: Muscidae) and its chemically protected prey, the rove beetle *Bledius furcatus* (Coleoptera: Staphylinidae). *Entomol. Gen.* 20, 11–19.
Suchan, T., Espíndola, A., Rutschmann, S., Emerson, B.C., Gori, K., Dessimoz, C., Arrigo, N., Ronikier, M., Alvarez, N., 2017. Assessing the potential of RAD-sequencing to resolve phylogenetic relationships within species radiations: The fly genus *Chiastocheta* (Diptera: Anthomyiidae) as a case study. *Mol. Phylogenet. Evol.* 114, 189–198.
Sun, J., Li, R., Chen, C., Sigwart, J.D., Kocot, K.M., 2021. Benchmarking Oxford Nanopore read assemblers for high-quality molluscan genomes. *Philos. Trans. R. Soc., B* 376, 20200160.
Tripp, E.A., Tsai, Y.H.E., Zhuang, Y., Dexter, K.G., 2017. RADseq dataset with 90% missing data fully resolves recent radiation of *Petalidium* (Acanthaceae) in the ultra-arid deserts of Namibia. *Ecol. Evol.* 7, 7920–7936.
Vaser, R., Šikić, M., 2021. Time- and memory-efficient genome assembly with Raven. *Nature Computational Science* 1, 332–336.
Vaser, R., Sović, I., Nagarajan, N., Šikić, M., 2017. Fast and accurate *de novo* genome assembly from long uncorrected reads. *Genome Res.* 27, 737–746.
Vikhrev, N., 2011a. Review of the Palaearctic members of the *Lispe tentaculata* species-group (Diptera, Muscidae): Revised key, synonymy and notes on ecology. *ZooKeys* 84, 59–70.
Vikhrev, N.E., 2011b. Taxonomic notes on the *Lispe leucospila* species-group (Diptera: Muscidae). *Russian Entomological Journal* 20, 215–218.
Vikhrev, N.E., 2012a. Four new species of *Lispe* Latreille, 1796 (Diptera: Muscidae) with taxonomic notes on related species. *Russian Entomological Journal* 21, 423–433.
Vikhrev, N.E., 2012b. Revision of the *Lispe longicollis*-group (Diptera, Muscidae). *ZooKeys* 235, 23–39.
Vikhrev, N.E., 2012c. Notes on taxonomy of *Lispe* Latreille (Diptera: Muscidae). *Russian Entomological Journal* 21, 107–112.
Vikhrev, N.E., 2014. Taxonomic notes on *Lispe* (Diptera, Muscidae), Parts 1-9. Amurian Zoological Journal, VI, pp. 147–170.
Vikhrev, N.E., 2015. Taxonomic notes on *Lispe* (Diptera, Muscidae), Parts 10-12. *Amurian Zoological Journal* 7, 228–247.
Vikhrev, N.E., 2016. Taxonomic notes on *Lispe* (Diptera, Muscidae), Part 13. Amurian Zoological Journal, VIII, pp. 171–185.
Vikhrev, N.E., 2020. *Lispe* (Diptera, Muscidae) of the Palaearctic region. *Amurian Zoological Journal XII* 2, 158–188.
Vikhrev, N.E., 2021. *Lispe* (Diptera, Muscidae) of Africa. *Amurian Zoological Journal XIII* 3, 369–400.
Vikhrev, N.E., Ge, Y.Q., Zhang, D., 2016. On taxonomy of the *Lispe caesia*-group (Diptera: Muscidae). *Russian Entomological Journal* 25, 407–410.
Wagner, N.D., Gramlich, S., Hörandl, E., 2018. RAD sequencing resolved phylogenetic relationships in European shrub willows (*Salix* K. subg. *Chamaetia* and subg. *Vetrix*) and revealed multiple evolution of dwarf shrubs. *Ecol. Evol.* 8, 8243–8255.
Wang, J., Chen, K., Ren, Q., Zhang, Y., Liu, J., Wang, G., Liu, A., Li, Y., Liu, G., Luo, J., Miao, W., Xiong, J., Yin, H., Guan, G., 2021. Systematic comparison of the performances of *de novo* genome assemblers for Oxford Nanopore Technology reads from piroplasm. *Front. Cell. Infect. Microbiol.* 11, 2235–2988.
Werner, D., Pont, A.C., Kampen, H., 2014. *Lispe tentaculata* (De Geer) and *Lispe pygmaea* Fallén (Muscidae) as natural predators of mosquitoes (Culicidae), with a review of mosquito predation by *Lispe* Latreille. *Studia Dipterologica* 21, 11–22.
Wick, R.R., Holt, K.E., 2019. Benchmarking of long-read assemblers for prokaryote whole genome sequencing. *F1000Research* 8, 1–22.
Wick, R.R., Judd, L.M., Gorrie, C.L., Holt, K.E., 2017. Completing bacterial genome assemblies with multiplex MinION sequencing. *Microb. Genomics* 3, e000132.
Williams, F.X., 1938. Biological studies in Hawaiian water-loving insects. Part III. Diptera or flies. A, Ephydridae and Anthomyiidae. *Proc. Hawaiian Entomol. Soc.* 10, 85–119.
Willing, E.M., Hoffmann, M., Klein, J.D., Weigel, D., Dreyer, C., 2011. Paired-end RAD-seq for de novo assembly and marker design without available reference. *Bioinformatics* 27, 2187–2193.
Zielke, E., 2018. Revalidation of an erroneously synonymized *Helina* species and reminder of a forgotten *Lispe* species from the Afrotropical Region. Contrib. Entomol. 68, 371–372.

Table S1. List of *Lispe* species (Pont, 2024) classified into species groups based on recent taxonomic changes. References for the species groups and individual species within each group are given to the author who proposed and/or revised the respective group or species. The table also includes species that have not yet been assigned to any specific species group.

Species-group/species	Author	References
***caesia*-group**		(Hennig, 1960; Vikhrev *et al.*, 2016; Gao *et al.*, 2022)
absentiseta	Pont, 2019	this study
albicorpus	Shinonaga & Kano, 1989	(Shinonaga & Kano, 1989)
aquamarina	Shinonaga & Kano, 1983	(Zhang *et al.*, 2016)
astakhovi	Vikhrev, 2020	(Vikhrev, 2020)
bengalensis	Robineau-Desvoidy, 1830	(Vikhrev, 2020)
caesia	Meigen, 1826	(Hennig, 1960; Vikhrev *et al.*, 2016)
cana	Walker, 1849	(Vikhrev, 2020)
candicans	Kowarz, 1892	(Hennig, 1960)
cilitibia	Pont, 2019	this study
collessi	Pont, 2019	this study
flavicornis	Stein, 1909	(Zhang *et al.*, 2016)
halophora	Becker, 1903	(Hennig, 1960)
inaequalis	(Malloch, 1922)	this study
lanceoseta	Wang & Fan, 1981	(Zhang *et al.*, 2016)
leucocephala	Loew, 1856	(Hennig, 1960)
marina	Becker, 1913	(Vikhrev, 2020)
odessae	Becker, 1904	(Hennig, 1960; Vikhrev *et al.*, 2016)
palawanensis	Shinonaga & Kano, 1989	(Zhang *et al.*, 2016)
patellitarsis	Becker, 1914	(Zhang *et al.*, 2016)
***desjardinsii*-group**		(Vikhrev, 2014)
desjardinsii	Macquart, 1851	(Vikhrev, 2014)
neo	Malloch, 1922	(Vikhrev, 2021)
pennitarsis	Stein, 1918	(Vikhrev, 2014)
tuberculitarsis	Stein, 1913	(Vikhrev, 2014)
zumpti	Paterson, 1953	(Vikhrev, 2021)
***kowarzi*-group**		(Vikhrev, 2014; Gao *et al.*, 2022)
dichaeta	Stein, 1913	(Vikhrev, 2016)
fulvitarsus asiatica	Vikhrev, 2014	(Vikhrev, 2014)
fulvitarsus fulvitarsus	(Snyder, 1949)	(Vikhrev, 2014)
geniseta macfiei	Emden, 1941	(Vikhrev, 2016, 2021)
geniseta setigena	Vikhrev & Pont, 2016	(Vikhrev, 2016, 2021)
kowarzi kowarzi	Becker, 1903	(Vikhrev, 2014)
kowarzi pallitarsis	Stein, 1909	(Vikhrev, 2014)
madagascariensis	Zielke, 1972	(Vikhrev, 2016)
stuckenbergi	Zielke, 1970	(Vikhrev, 2016)
leucosticta	Stein, 1918	(Vikhrev, 2016)
miochaeta	Speiser, 1910	(Vikhrev, 2016)
***leucospila*-group**		(Paterson, 1953; Vikhrev, 2011b; Gao *et al.*, 2022)
leucospila	(Wiedemann, 1830)	(Vikhrev, 2011b)

irvingi	Curran, 1937	(Vikhrev, 2014)
maculata	Stein, 1913	(Vikhrev, 2014)
pectinipes	Becker, 1903	(Vikhrev, 2011b)
***longicollis*-group**		(Hennig, 1960; Vikhrev, 2012a; Gao *et al.*, 2022)
assimilis	Wiedemann, 1824	(Hennig, 1960; Vikhrev, 2012a)
barbipes	Stein, 1908	(Vikhrev, 2012a)
cilitarsis	Loew, 1856	(Hennig, 1960; Vikhrev, 2012a)
confusa	Vikhrev, 2021	(Vikhrev, 2021)
dmitryi	Vikhrev, 2014	(Vikhrev, 2014)
glabra	Wiedemann, 1824	(Vikhrev, 2012a)
longicollis	Meigen, 1826	(Hennig, 1960; Vikhrev, 2012a)
manicata	Wiedemann, 1830	(Vikhrev, 2012a)
microptera	Séguy, 1937	(Vikhrev, 2012a)
nuba	Wiedemann, 1830	(Hennig, 1960; Vikhrev, 2012a)
pacifica	Shinonaga & Pont, 1992	(Vikhrev, 2012a)
paraneo	Zielke, 1972	(Vikhrev, 2021)
xenochaeta	Malloch, 1923	(Vikhrev, 2014)
weschei	Malloch, 1922	(Vikhrev, 2012a)
wittei	Paterson, 1956	(Vikhrev, 2012a, 2021)
***nicobarensis*-group**		(Vikhrev, 2015; Gao *et al.*, 2022)
aceponti	Vikhrev, 2015	(Vikhrev, 2015)
flaveola	Vikhrev, 2015	(Vikhrev, 2015)
nicobarensis	Schiner, 1868	(Vikhrev, 2015)
nigrimana	Malloch, 1925	(Vikhrev, 2015)
sydneyensis	Schiner, 1868	(Vikhrev, 2015)
***nivalis*-group**		(Vikhrev, 2012b; Gao *et al.*, 2022)
bivittata	Stein, 1909	(Vikhrev, 2012b)
hennigi	Vikhrev, 2012	(Vikhrev, 2012b)
medvedevi	Vikhrev, 2014	(Vikhrev, 2014)
nivalis	Wiedemann, 1830	(Vikhrev, 2012b)
ochracea	Becker, 1910	(Vikhrev, 2021)
tomkovichi	Vikhrev, 2014	(Vikhrev, 2014)
***palposa*-group**		(Snyder, 1954; Hennig, 1960; Vikhrev, 2015; Gao *et al.*, 2022)
apicalis	Mik, 1869	(Hennig, 1960; Vikhrev, 2015)
approximata	Huckett, 1966	(Vikhrev, 2015)
appendibacula	Xue & Zhang, 2005	(Vikhrev, 2015)
bahama	Snyder, 1958	(Vikhrev, 2015)
bohemica	Becker, 1904	(Snyder, 1954)
brevipes	Aldrich, 1913	(Snyder, 1954)
cinifera	Becker, 1904	(Hennig, 1960; Vikhrev, 2015)
desertorum	Huckett, 1966	(Vikhrev, 2015)
elkantarae	Becker, 1907	(Hennig, 1960; Vikhrev, 2015)
ezensis	Shinonaga & Kano, 1983	(Vikhrev, 2015)
flavicincta	Loew, 1847	(Hennig, 1960; Vikhrev, 2015)
flavinervis	Becker, 1904	(Hennig, 1960; Vikhrev, 2015)
frigida	Erichson, 1851	(Snyder, 1954; Hennig, 1960; Vikhrev, 2015)
hebeiensis	Ma & Tian, 1993	(Vikhrev, 2015)
hydromyzina	Fallén, 1825	(Hennig, 1960; Vikhrev, 2015)
jamesi	Snyder, 1954	(Snyder, 1954)
johnsoni	Aldrich, 1913	(Snyder, 1954)

litorea	Fallén, 1825	(Hennig, 1960; Vikhrev, 2015)
loewi	Ringdahl, 1922	(Hennig, 1960; Vikhrev, 2015)
monochaita	Mou et Ma, 1992	(Vikhrev, 2015)
neimongola	Tian & Ma, 2000	(Vikhrev, 2015)
palposa	Walker, 1849	(Snyder, 1954; Vikhrev, 2015)
parcespinosa	Becker, 1900	(Vikhrev, 2015)
parcespinosa appendibacula	Xue & Zhang, 2005	(Vikhrev, 2015)
parcespinosa bohemica	Becker, 1904	(Vikhrev, 2015)
parcespinosa parcespinosa	Becker, 1900	(Vikhrev, 2015)
probohemica	Speiser, 1914	(Snyder, 1954; Vikhrev, 2015)
salina	Aldrich, 1913	(Snyder, 1954; Vikhrev, 2015)
sordida	Aldrich, 1913	(Snyder, 1954; Vikhrev, 2015)
superciliosa	Loew, 1861	(Hennig, 1960; Vikhrev, 2015)
superciliosa monochaita	Mou et Ma, 1992	(Vikhrev, 2015)
superciliosa superciliosa	Loew, 1861	(Vikhrev, 2015)
tarsocilica	Xue & Zhang, 2005	(Vikhrev, 2015)
***pumila*-group**		(Vikhrev, 2012c, 2016)
angustipalpis	Stein, 1920	(Vikhrev, 2012c, 2016)
pumila	Wiedemann, 1824	(Vikhrev, 2012c, 2016)
***pygmaea*-group**		(Vikhrev, 2016; Gao *et al.*, 2022)
ambigua	Stein, 1913	(Vikhrev, 2016)
bipunctata	Séguy, 1938	(Vikhrev, 2016)
biseta	Stein, 1913	(Vikhrev, 2016)
keiseri	Zielke, 1972	(Vikhrev, 2016)
pygmaea	Fallén, 1825	(Vikhrev, 2016)
pygmoza	Vikhrev & Pont, 2016	(Vikhrev, 2016)
setuligera	Stein, 1911	(Vikhrev, 2016)
surda	Curran, 1937	(Vikhrev, 2016)
vilis	Stein, 1911	(Vikhrev, 2016)
***rigida*-group**		(Vikhrev, 2012b)
brunnicosa	Becker, 1904	(Vikhrev, 2012b)
kozlovi	Vikhrev, 2012	(Vikhrev, 2012b)
rigida	Becker, 1903	(Vikhrev, 2012b)
***scalaris*-group**		(Hennig, 1960; Vikhrev, 2012c; Gao *et al.*, 2022)
elengatissima	Stackelberg, 1937	(Hennig, 1960; Vikhrev, 2012c)
nubilipennis	Loew, 1873	(Hennig, 1960; Vikhrev, 2012c)
selena	Vikhrev, 2021	(Vikhrev, 2021)
scalaris	Loew, 1847	(Hennig, 1960; Vikhrev, 2012c)
***tentaculata*-group**		(Snyder, 1954; Hennig, 1960; Vikhrev, 2011a; Gao *et al.*, 2022)
capensis	Zielke, 1971	(Vikhrev, 2021)
consanguinea	Loew, 1858	(Hennig, 1960; Vikhrev, 2011a)
emdeni	Vikhrev, 2012	(Vikhrev, 2014)
martirei	Vikhrev 2014	(Vikhrev, 2014)
nana	Macquart, 1835	(Vikhrev, 2014)
orientalis	Wiedemann, 1824	(Vikhrev, 2011a)
patellata	Aldrich, 1913	(Snyder, 1954; Hennig, 1960; Vikhrev, 2014)
sociabilis	Loew, 1862	(Snyder, 1954; Hennig, 1960; Vikhrev, 2014)
sericipalpis	Stein, 1904	(Vikhrev, 2011a)
mirabilis	(Stein, 1918)	this study

tentaculata	(De Geer, 1776)	(Snyder, 1954; Hennig, 1960; Vikhrev, 2011a)
tentaculata draperi	Séguy, 1933	(Hennig, 1960; Vikhrev, 2011a, 2021)
triangularis	Vikhrev 2014	(Vikhrev, 2014)
***uliginosa*-group**		(Snyder, 1954; Hennig, 1960; Vikhrev, 2015; Gao *et al.*, 2022)
albitarsis	Stein, 1898	(Snyder, 1954; Vikhrev, 2015)
antennata	Aldrich, 1913	(Snyder, 1954; Vikhrev, 2015)
cotidiana	Snyder, 1954	(Snyder, 1954; Hennig, 1960)
latana	Snyder, 1949	(Vikhrev, 2015)
levis	Stein, 1911	(Vikhrev, 2015)
lisarba	Snyder, 1949	(Vikhrev, 2015)
melaleuca	Loew, 1847	(Vikhrev, 2015)
mexicana	Vikhrev, 2015	(Vikhrev, 2015)
nasoni	Stein, 1898	(Snyder, 1954; Vikhrev, 2015)
neouliginosa	Snyder, 1954	(Snyder, 1954)
nudifacies	Snyder, 1954	(Snyder, 1954; Vikhrev, 2015)
polita	Coquillett, 1904	(Snyder, 1954; Vikhrev, 2015)
septentrionalis	Xue & Zhang, 2005	(Vikhrev, 2015)
serotina	Wulp, 1896	(Vikhrev, 2015)
uliginosa	Fallén, 1825	(Snyder, 1954; Hennig, 1960; Vikhrev, 2015)
Unassigned species		
affinis	Pont, 2019	(Pont, 2019)
albifacies	Malloch 1929	
albimaculata	Stein, 1910	
alete	Walker, 1849	
alkalina	Vikhrev, 2021	(Vikhrev, 2021)
andrefana	Vikhrev, 2021	(Vikhrev, 2021)
argentata	Couri, Pont & Penny, 2006	(Vikhrev, 2021)
armata	Malloch, 1925	(Pont, 2019)
attenuata	Pont, 2019	(Pont, 2019)
aurocochlearia	Séguy, 1950	(Vikhrev, 2021)
baluchistanensis	Shinonaga, 2010	(Vikhrev, 2020)
boninensis	Snyder, 1965	
bimaculata	Walker, 1859	
brendana	Pont, 2019	(Pont, 2019)
caespitosa	Pont, 2019	(Pont, 2019)
ceylanica	Shinonaga & Tewari, 2008	
chui	Shinonaga & Kano, 1989	(Shinonaga & Kano, 1989)
congensis	Zielke, 1970	(Zielke, 2018)
crinitarsis	Pont, 2019	(Pont, 2019)
cristata	Pont, 2019	(Pont, 2019)
erratica	(Malloch, 1932)	
esuriens	Pont, 2019	(Pont, 2019)
floccosa	Pont, 2019	(Pont, 2019)
freidbergi	Vikhrev, 2012	(Vikhrev, 2020)
glauca	Pont, 2019	(Pont, 2019)
gracilitarsis	Pont, 2019	(Pont, 2019)
grisea	Pont, 2019	(Pont, 2019)
fuscipes	(Ringdahl, 1930)	
hamulifera	Pont, 2019	(Pont, 2019)
hispida	Walker, 1849	
howeana	Pont, 2019	(Pont, 2019)

incana	Pont, 2019	(Pont, 2019)
isolata	Malloch, 1929	
lamellata	Pont, 2019	(Pont, 2019)
longicornia	Wei in Li & Jin, 2006	
metatarsata	Stein, 1900	(Pont, 2019)
niveimaculata	Stein, 1906	(Vikhrev, 2021)
nigrimanoides	Pont, 2019	(Pont, 2019)
orbitalis	Pont, 2019	(Pont, 2019)
patersoni	Vikhrev, 2021	(Vikhrev, 2021)
penicillata	Pont, 2019	(Pont, 2019)
polonaise	Vikhrev, 2021	(Vikhrev, 2021)
pseudohirsutipes	Kakinuma & Kurahashi, 2015	
rufitibialis	Macquart, 1843	(Fogaça & De Carvalho, 2018)
sexnotata	Vikhrev, 2021	(Vikhrev, 2021)
siamensis	Shinonaga & Kano, 1989	(Shinonaga & Kano, 1989)
uniseta	Malloch, 1922	(Pont, 2019)
vikhrevi	Pont, 2019	(Pont, 2019)
vittipennis	Thomson, 1869	

References

Fogaça, J.M. & De Carvalho, C.J.B. (2018) Neotropical *Lispe* (Diptera: Muscidae): Notes, redescriptions and key to species. *Journal of Natural History*, **52**, 2147–2184.

Gao, Y., Ge, Y., Yan, L., Vikhrev, N.E., Wang, Q., Butterworth, N.J., & Zhang, D. (2022) Phylogenetic Analyses Support the Monophyly of the Genus *Lispe* Latreille (Diptera: Muscidae) with Insights into Intrageneric Relationships. *Insects*, **13**, 1015.

Hennig, W. (1960) 63 b. Muscidae (Lieferung 225). In: Lindner E., editor. Die Fliegen der Palaearktischen Region. Stuttgart: Schweizerbart'sche Verlagsbuchhandlung. p. 399–432.

Paterson, H.E. (1953) New *Lispe* species (Dipt., Muscidae) from Southern Africa. *Journal of the Entomological Society of Southern Africa*, **16**, 168–178.

Pont, A.C. (2019) Studies on the Australian Muscidae (Diptera). VIII. The genus Lispe Latreille, 1797. pp. 1–232. .

Pont, A.C. (2024) Muscidae. Systema Dipterorum, Version 5.2. http://diptera.org/ (accessed on 30-06-2024).

Shinonaga, S. & Kano, R. (1989) Four New Species of *Lispe* (Diptera, Muscidae) from Oriental Region. *The Entomological Society of Japan*, **57**, 815–821.

Snyder, F.M. (1954) A review of Nearctic *Lispe* Latreille (Diptera, Muscidae). *The American Museum of Natural History*, 1–40.

Vikhrev, N. (2011a) Review of the Palaearctic members of the *Lispe tentaculata* species-group (Diptera, Muscidae): Revised key, synonymy and notes on ecology. *ZooKeys*, **84**, 59–70.

Vikhrev, N.E. (2011b) Taxonomic notes on the *Lispe leucospila* species-group (Diptera: Muscidae). *Russian Entomological Journal*, **20**, 215–218.

Vikhrev, N.E. (2012a) Revision of the *Lispe longicollis*-group (Diptera, Muscidae). *ZooKeys*, **235**, 23–39.

Vikhrev, N.E. (2012b) Four new species of *Lispe* Latreille, 1796 (Diptera: Muscidae) with taxonomic notes on related species. *Russian Entomological Journal*, **21**, 423–433.

Vikhrev, N.E. (2012c) Notes on taxonomy of *Lispe* Latreille (Diptera: Muscidae). *Russian Entomological Journal*, **21**, 107–112.

Vikhrev, N.E. (2014) Taxonomic notes on *Lispe* (Diptera, Muscidae), Parts 1-9. *Amurian zoological journal*, **VI**, 147–170.

Vikhrev, N.E. (2015) Taxonomic notes on *Lispe* (Diptera, Muscidae), Parts 10-12. *Amurian zoological journal*, **7**,

228–247.

Vikhrev, N.E. (2016) Taxonomic notes on *Lispe* (Diptera, Muscidae), Part 13. *Amurian zoological journal*, **VIII**, 171–185.

Vikhrev, N.E. (2020) *Lispe* (Diptera, Muscidae) of the Palaearctic region. pp. 1–158–188. .

Vikhrev, N.E. (2021) *Lispe* (Diptera, Muscidae) of Africa. pp. 1–369–400. .

Vikhrev, N.E., Ge, Y.Q., & Zhang, D. (2016) On taxonomy of the *Lispe caesia*-group (Diptera: Muscidae). *Russian Entomological Journal*, **25**, 407–410.

Zhang, D., Ge, Y.-Q., Li, X.-Y., Liu, X.-H., Zhang, M., & Wang, R.R. (2016) Review of the *Lispe caesia*-group (Diptera: Muscidae) from Palaearctic and adjacent regions, with redescriptions and one new synonymy. *Zootaxa*, **4098**, 43.

Zielke, E. (2018) Revalidation of an erroneously synonymized *Helina* species and reminder of a forgotten *Lispe* species from the Afrotropical Region. *Beiträge zur Entomologie = Contributions to Entomology*, **68**, 371–372.

Table S2. List of 53 species used in study, including authorship, collecting data and voucher ID. The table includes 49 species of *Lispe* and 4 species of *Limnophora* representing the outgroup.

No.	Species	Voucher information	Voucher ID
1	*Lispe albimaculata* Stein, 1910	Australia, Seven Mile Beach 34°46'22.2"S 150°48'48.2"E; 27.11.2019 leg. KEiB exp., det. A. Grzywacz	KEIB_DIP_01426
2	*Lispe apicalis apicalis* Mik, 1869	Russia, Kalmyia reg. 47°52'30.0"N 44°36'03.6"E; 08.06.2012 leg. N. Vikhrev, det. N. Vikhrev	KEIB_DIP_01453
3	*Lispe apicalis comitata* Becker, 1904	Uzbekistan, Tudakul Lake 39°47'56.0"N 64°44'26.5"E; 21.06.2019 leg. KEiB exp., det. A. Grzywacz	KEIB_DIP_01439
4	*Lispe assimilis* Wiedemann, 1824	Australia, Northern Teritory, Darwin 06.11.2017 leg. K. Szpila, det. A. Grzywacz	KEIB_DIP_01428
5	*Lispe bengalensis* Robineau-Desvoidy, 1830	Australia, Berrara Creek 35°11'43.8"S 150°31'01.2"E; 01.12.2019 leg. KEiB exp., det. A. Grzywacz	KEIB_DIP_01435
6	*Lispe bivittata* Stein, 1909	India, Assam st, Chapar env Champamati R 26°19'12.0"N 90°27'36.0"E; 01-03.01.2014 leg. K. Tomkovich, det. N. Vikhrev	KEIB_DIP_01441
7	*Lispe brunnicosa* Becker, 1904	Russia, West Siberia, Omsk Reg 10.05.2009 leg. O.E. Kosteri, det. N. Vikhrev	KEIB_DIP_01451
8	*Lispe caesia* Meigen, 1826	Croatia, Stobreč 43°30'01.6"N 16°31'05.5"E; 13.08.2020 leg. K. Szpila, det. A. Grzywacz	KEIB_DIP_01655
9	*Lispe cana* Walker, 1849	Australia, Seven Mile Beach 34°46'22.2"S 150°48'48.2"E; 27.11.2019 leg. KEiB exp., det. A. Grzywacz	KEIB_DIP_01430
10	*Lispe capensis* Zielke, 1971	Namibia, Walvis Bay, Bird Sanct. 22°58'01"S 14°31'56"E; 21.11.2018 leg. KEiB exp., det. A. Grzywacz	KEIB_DIP_01477
11	*Lispe confusa* Vikhrev, 2021	Namibia, Walvis Bay, Bird Sanct. 22°58'01"S 14°31'56"E; 21.11.2018 leg. KEiB exp., det. A. Grzywacz	KEIB_DIP_01476
12	*Lispe consanguinea* Loew, 1858	Poland, Wojnicz, Dunajec 49°57'01.0"N 20°52'20.8"E; 14.06.2012 leg. K. Szpila, det. A. Grzywacz	KEIB_DIP_01485
13	*Lispe desjardinsii* Macquart, 1851	Tanzania, Dodoma env. 7.385S 37.015E; 11-13.02.2017 leg. N. Vikhrev, det. N. Vikhrev	KEIB_DIP_01447
14	*Lispe dichaeta* Stein, 1913	Kenya, Nyandarua Co 0°07'12.0"S 36°25'48.0"E; 20.12.2013 leg. N. Vikhrev, det. N. Vikhrev	KEIB_DIP_01450
15	*Lispe elengatissima* (Stackelberg, 1937)	Uzbekistan, Tudakul Lake 39°47'56.0"N 64°44'26.5"E; 21.06.2018 leg. KEiB exp., det. A. Grzywacz	KEIB_DIP_01434
16	*Lispe emdeni* Vikhrev, 2012	India, Rajasthan, Jodhpur 26°13.42' S 73°01.96' E; 11-15.08.2008 leg. M. Irwin, D.M. Pnyadarsanan, det. A. Grzywacz	KEIB_DIP_01585
17	*Lispe flavicornis* Stein, 1909	India, Andhra Pradesh, Samalkot 16°59'34.8"N 82°16'19.2"E; 29.01-02.02.2014 leg. K. Tomkovich, det. N. Vikhrev	KEIB_DIP_01524
18	*Lispe flavinervis* Becker, 1904	Russia, Omsk reg. 53°57'36.0"N 73°45'36.0"E; 15.05.2010 leg. N. Priydak, det. N. Vikhrev	KEIB_DIP_01452
19	*Lispe geniseta* Stein, 1909	Cambodia, Siem Reap env. 13°18'00.0"N 103°48'00.0"E; 21-28.02.2017 leg. N. Priydak, O. Kosterin, det. N. Vikhrev	KEIB_DIP_01446

20	*Lispe glabra* Wiedemann, 1824	Malaysia, Selangor st, Sungai Pelek 2°36'00.0"N 101°42'00.0"E; 06-07.02.2014 leg. N. Vikhrev, det. N. Vikhrev	KEIB_DIP_01438
21	*Lispe irvingi* Curran, 1937	Namibia, Windhoek env. 22°32'24.0"N 17°12'00.0"E; 02-04.12.2018 leg. N. Vikhrev, det. N. Vikhrev	KEIB_DIP_01444
22	*Lispe kowarzi kowarzi* Becker, 1903	Portugal, Rio Torto, Guarda D. 40°31'19"N 7°38'23.6"W; 03.10.2015 leg. A. Grzywacz, det. A. Grzywacz	KEIB_DIP_01482
23	*Lispe kowarzi pallitarsis* Stein, 1909	Malaysia, Selangor st, Sungai Pelek 2°36'00.0"N 101°42'00.0"E; 06-07.02.2014 leg. N. Vikhrev, det. N. Vikhrev	KEIB_DIP_01469
24	*Lispe leucospila* (Wiedemann, 1830)	India, Rajasthan, Jodhpur 26°13.42' S 73°01.96' E; 11-15.08.2008 leg. M. Irwin, D.M. Pnyadarsanan, det. A. Grzywacz	KEIB_DIP_01586
25	*Lispe loewi* Ringdahl, 1922	Uzbekistan, Olot II 39°18'11.2"N 63°52'26.4"E; 23.06.2019 leg. KEiB exp., det. A. Grzywacz	KEIB_DIP_01460
26	*Lispe longicollis* Meigen, 1826	Uzbekistan, Tudakul Lake 39°79'89"N 64°74'07"E; 21.06.2018 leg. KEiB exp., det. A. Grzywacz	KEIB_DIP_01431
27	*Lispe madagascariensis* Zielke, 1972	Mozambique, Sofala Prov., Gorongosa Park 18°41'14.8"S 34°04'28.0"E; 18-30.04.2015 leg. M.Hauser & A.Rung, leg. A. Grzywacz	KEIB_DIP_01497
28	*Lispe melaleuca* Loew, 1847	Russia, Volgograd reg, Breslavka 48°32'07.8"N 44°07'51.6"E; 30.04.2013 leg. N. Vikhrev, det. N. Vikhrev	KEIB_DIP_01440
29	*Lispe mirabilis* Stein, 1918	Cambodia, Siem Reap env. 13°18'00.0"N 103°48'00.0"E; 21-28.02.2017 leg. N. Priydak, O. Kosterin, det. N. Vikhrev	KEIB_DIP_01640
30	*Lispe nana* Macquart, 1835	Uzbekistan, Machitly 39°51'41.0"N 67°15'55.4"E; 26.06.2019 leg. KEiB exp., det. A. Grzywacz	KEIB_DIP_01473
31	*Lispe nasoni* (De Geer, 1776)	United States, Kern Co., Short Canyon 35°42'62"N 117°55'09"W; 21-29.05.2006 det. M.E. Irwin, leg. A. Grzywacz	KEIB_DIP_01512
32	*Lispe neimongola* Tian et Ma, 2000	Uzbekistan, Olot II 39°18'11.2"N 63°52'26.4"E; 23.06.2019 leg. KEiB exp., det. A. Grzywacz	KEIB_DIP_01475
33	*Lispe nicobarensis* Schiner, 1868	Vietnam, Ninh Binh Province; Cuc Phuong National Park 20°12'36.0"N 105°21'00.0"E; 24-28.03.2012 leg. Gaimari, Hauser & Pham, leg. A. Grzywacz	KEIB_DIP_01525
34	*Lispe nigrimana* (Malloch, 1923)	Australia, Royal National Park 34°08'55"S 151°01'49"E; 02.12.2019 leg. KEiB exp., det. A. Grzywacz	KEIB_DIP_01433
35	*Lispe nivalis* Wiedemann, 1830	Namibia, Windhoek env. 22°36'00.0"N 17°08'24.0"E; 25-28.11.2018 leg. N. Vikhrev, det. A. Grzywacz	KEIB_DIP_01507
36	*Lispe nuba* Wiedemann, 1830	Tanzania, Mikumi NP. env. 7.385S 37.015E; 24-25.02.2017 leg. N. Vikhrev, det. N. Vikhrev	KEIB_DIP_01456
37	*Lispe orientalis* Wiedemann, 1824	India, Meghalaya st, Sohra (Cherrapunjee) 25°18'00.0"N 91°42'00.0"E; 14-26.12.2013 leg. K. Tomkovich, det. N. Vikhrev	KEIB_DIP_01471
38	*Lispe pectinipes* Becker, 1903	Portugal, Vila do Conde, Porto D. 41°21'06.6"N 8°44'53"W; 06.10.2015 leg. A. Grzywacz, det. A. Grzywacz	KEIB_DIP_01493
39	*Lispe polonaise* Vikhrev, 2021	Namibia, Walvis Bay, Bird Sanct. 22°58'01"S 14°31'56"E; 21.11.2018 leg. KEiB exp., det. A. Grzywacz	KEIB_DIP_01494
40	*Lispe pumila* Wiedemann, 1824	Australia, Berrara Creek 35°11'43.8"S 150°31'01.2"E; 01.12.2019 leg. KEiB exp., det. A. Grzywacz	KEIB_DIP_01429
41	*Lispe pygmaea* Fallén, 1825	Russia, Ryazan reg., Kasimov env. 54°56'24.0"N 41°20'24.0"E; 17-19.06.2013 leg. N. Vikhrev, det. N. Vikhrev	KEIB_DIP_01470
42	*Lispe rigida* (Becker, 1903)	Uzbekistan, Olot II 39°18'11.2"N 63°52'26.4"E; 23.06.2019 leg. KEiB exp., det. A. Grzywacz	KEIB_DIP_01474

43	*Lispe scalaris* Loew, 1847	Namibia, Windhoek env. 22°32'24.0"N 17°16'12.0"E; 21-24.11.2018 leg. N. Vikhrev, det. N. Vikhrev	KEIB_DIP_01458
44	*Lispe sericipalpis* Stein, 1904	India, Meghalaya st, Sohra (Cherrapunjee) 25°18'00.0"N 91°42'00.0"E; 14-26.12.2013 leg. K. Tomkovich, det. N. Vikhrev	KEIB_DIP_01436
45	*Lispe superciliosa* Loew, 1861	Belarus, Gomel reg. 51°56'45.6"N 29°20'56.4"E; 30.07.2019 leg. N. Vikhrev, det. N. Vikhrev	KEIB_DIP_01442
46	*Lispe sydneyensis* Schiner, 1868	Australia, Seven Mile Beach 34°46'22.2"S 150°48'48.2"E; 27.11.2019 leg. KEiB exp., det. A. Grzywacz	KEIB_DIP_01427
47	*Lispe tentaculata* (De Geer, 1776)	Poland, Różankowo 53°05'41.3"N 18°32'12.0"E; 15.09.2015 leg. A. Grzywacz, det. A. Grzywacz	KEIB_DIP_01500
48	*Lispe uliginosa* (Fallén, 1825)	Poland, Toruń, Kępa Bazarowa 53°00'27.7"N 18°37'35.7"E; 19.09.2020 det. A. Grzywacz, leg. A. Grzywacz	KEIB_DIP_01670
49	*Lispe xenochaeta* Malloch, 1923	Australia, Wattamolla, RNP 34°08'15"S 151°07'E; 28.11.2019 leg. KEiB exp., det. A. Grzywacz	KEIB_DIP_01432
50	*Limnophora pollinifrons* Stein, 1916	Poland, Toruń, Port Drzewny 53°01'12.0"N 18°29'47.7"E; 30.05.2020 leg. A. Grzywacz, det. A. Grzywacz	KEIB_DIP_01521
51	*Limnophora simulans* Stein, 1913	South Africa, KwaZulu Natal; Drakensberg Mts 29°07'48.0"N 29°19'48.0"E; 14.11.2006 leg. A.C. Pont & D. Werner, det. A.C. Pont	KEIB_DIP_01520
52	*Limnophora tigrina* (Stein, 1860)	Poland, Toruń, Port Drzewny 53°01'11.2"N 18°29'43.5"E; 30.05.2020 leg. A. Grzywacz, det. A. Grzywacz	KEIB_DIP_01523
53	*Limnophora triangula* (Fallén, 1825)	Poland, Toruń, Port Drzewny 53°01'11.2"N 18°29'43.5"E; 30.05.2020 leg. A. Grzywacz, det. A. Grzywacz	KEIB_DIP_01522

Fig. S1 *BUSCO* analysis for the completeness of the *Lispe tentaculata* genome assembly using *Canu*, *Flye*, *Raven*, *SMARTdenovo* and *wtbg2* against Diptera reference dataset. The y-axis indicates five assemblers used in this study, and the x-axis shows the percentage of complete and single-copy, complete and duplicated, fragmented and missing genes in assembled contigs.

Fig. S2 Distribution of SNP numbers for datasets obtained with *de novo* assembly under different clustering thresholds (CT).

Fig. S3 Distribution of bootstrap values for preliminary maximum likelihood (ML) analysis followed with 100 rapid bootstrap repetitions for datasets obtained with *de novo* assembly under different clustering thresholds (CT).

Fig. S4 Alternative topologies of phylogenetic trees obtained by *de novo* assembly under a clustering threshold of 0.75 (topology A), and a clustering threshold of 0.85 (topology B). Node support values are shown for 1000 nonparametric bootstrap replicates (BS). Species groups of *Lispe* are marked with different colours as provided. Outgroups marked with black colour. Nodes with BS = 100 marked with an asterisk (*). Abbreviation: CT, clustering threshold.

Fig. S5 Comparison of *BPP* trees topologies inferred from reference-based approach and *de novo* assembly under 0.74 clustering threshold clustering threshold. Species groups are marked with different colours and collapsed for monophyletic groups which received maximum node support (PP = 1). Outgroup marked with black colour include representatives of *Limnophora*. Abbreviation: CT, clustering threshold.

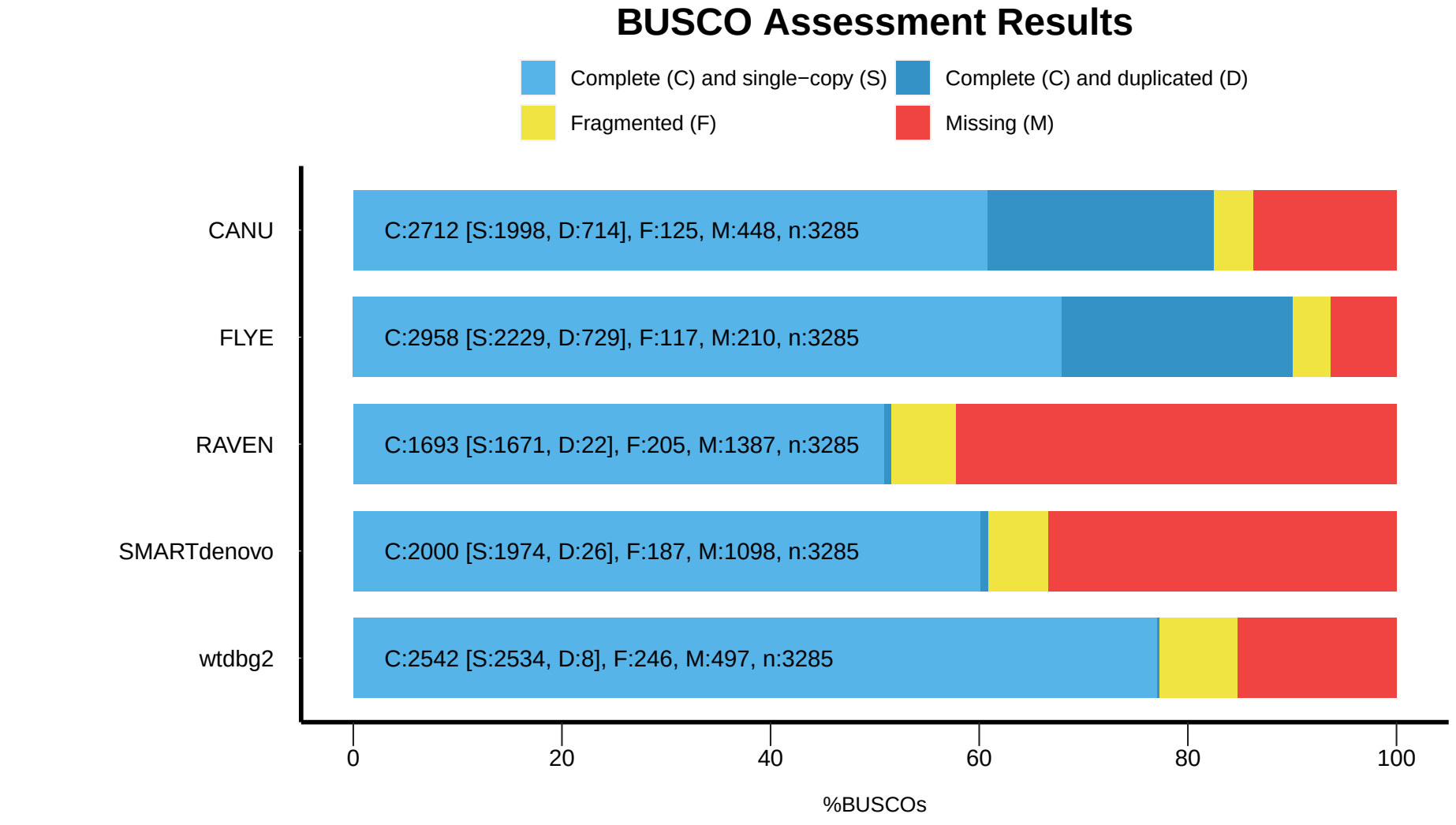
BUSCO Assessment Results
Complete (C) and single−copy (S)
Complete (C) and duplicated (D)
Fragmented (F)
Missing (M)
CANU
C:2712 [S:1998, D:714], F:125, M:448, n:3285
FLYE
C:2958 [S:2229, D:729], F:117, M:210, n:3285
RAVEN
C:1693 [S:1671, D:22], F:205, M:1387, n:3285
SMARTdenovo
C:2000 [S:1974, D:26], F:187, M:1098, n:3285
wtdbg2
C:2542 [S:2534, D:8], F:246, M:497, n:3285
0
20
40
60
80
100
%BUSCOs

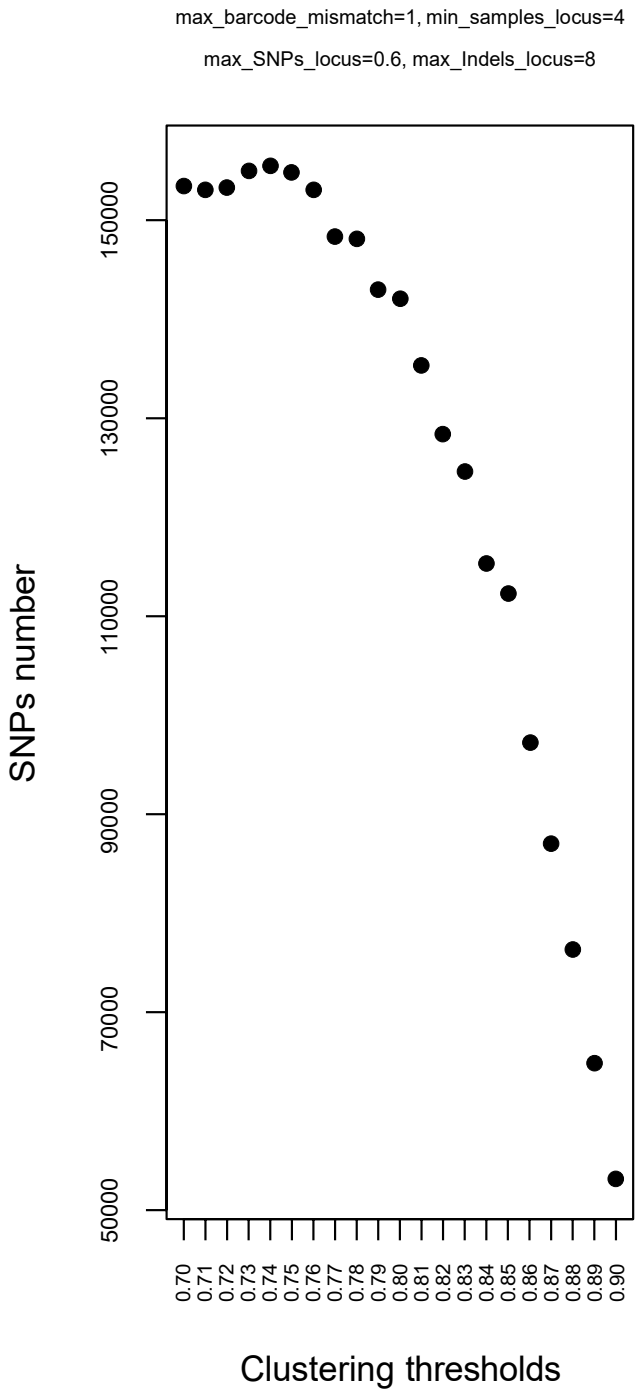

CT	SNP number
0.70	153455
0.71	153025
0.72	153267
0.73	154953
0.74	155298
0.75	154955
0.76	153068
0.77	148363
0.78	148084
0.79	142908
0.80	142062
0.81	135355
0.82	128351
0.83	124538
0.84	114904
0.85	113339
0.86	97177
0.87	86941
0.88	76282
0.89	64823
0.90	53188

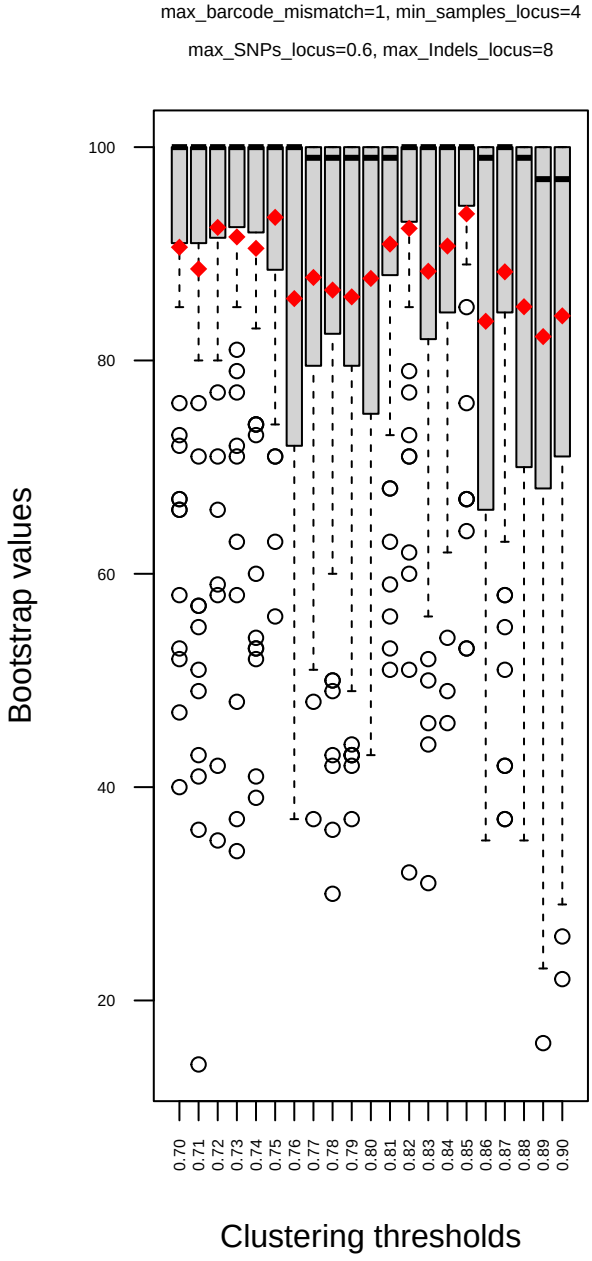

CT	Mean	Median	SD
0.70	90.62	100.00	16.60
0.71	88.58	100.00	21.07
0.72	92.47	100.00	14.73
0.73	91.58	100.00	16.05
0.74	90.51	100.00	17.26
0.75	93.42	100.00	10.74
0.76	85.80	100.00	18.81
0.77	87.78	99.00	17.63
0.78	86.60	99.00	20.60
0.79	85.96	99.00	20.66
0.80	87.69	99.00	17.69
0.81	90.91	99.00	14.00
0.82	92.38	100.00	14.33
0.83	88.36	100.00	18.95
0.84	90.73	100.00	15.09
0.85	93.75	100.00	12.31
0.86	83.67	99.00	20.73
0.87	88.31	100.00	19.57
0.88	85.04	99.00	20.19
0.89	82.24	97.00	26.34
0.90	84.18	97.00	22.41

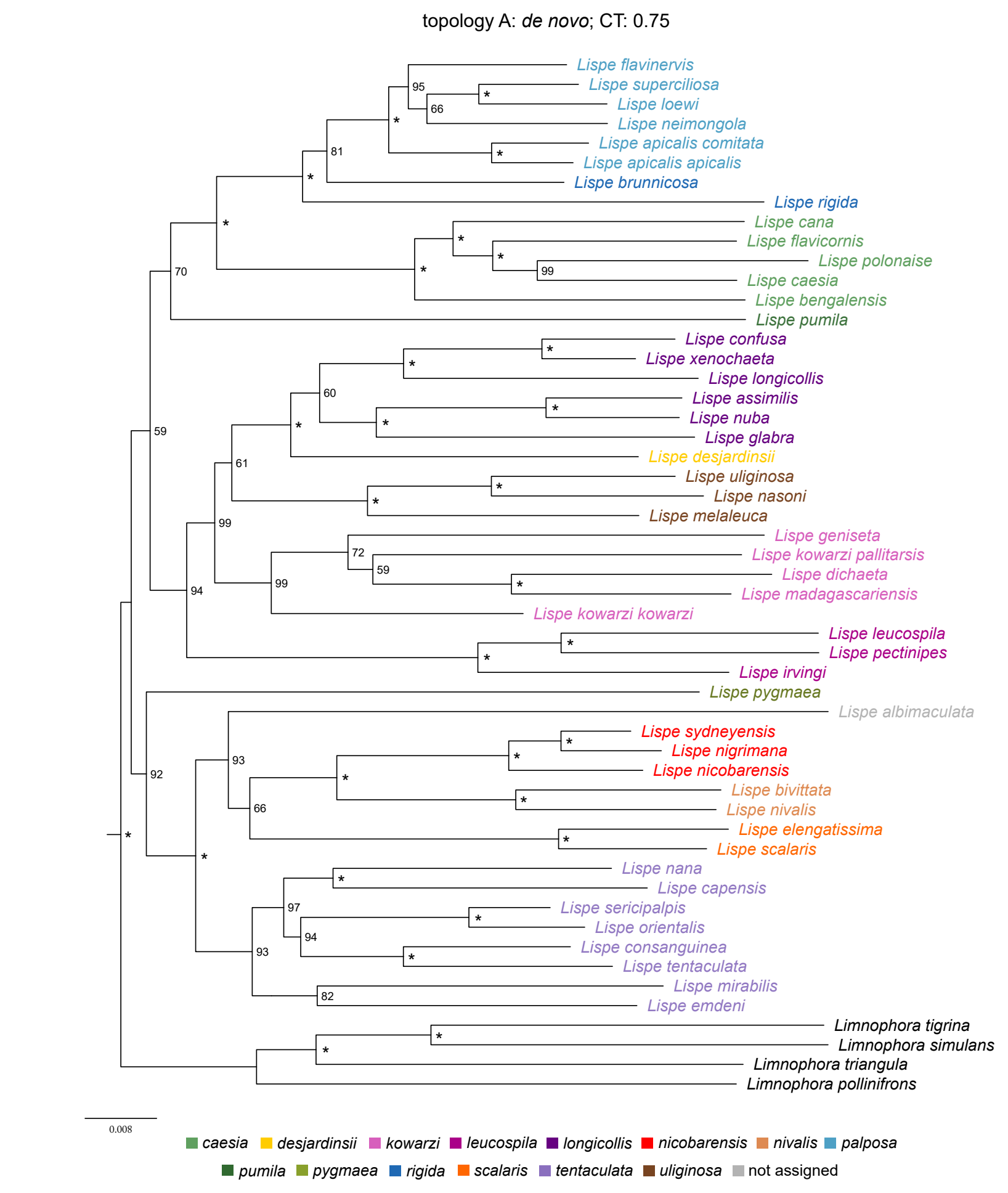
topology A: de novo; CT: 0.75
Lispe flavinervis
Lispe superciliosa
Lispe loewi
Lispe neimongola
Lispe apicalis comitata
Lispe apicalis apicalis
Lispe brunnicosa
Lispe rigida
Lispe cana
Lispe flavicornis
Lispe polonaise
Lispe caesia
Lispe bengalensis
Lispe pumila
Lispe confusa
Lispe xenochaeta
Lispe longicollis
Lispe assimilis
Lispe nuba
Lispe glabra
Lispe desjardinsii
Lispe uliginosa
Lispe nasoni
Lispe melaleuca
Lispe geniseta
Lispe kowarzi pallitarsis
Lispe dichaeta
Lispe madagascariensis
Lispe kowarzi kowarzi
Lispe leucospila
Lispe pectinipes
Lispe irvingi
Lispe pygmaea
Lispe albimaculata
Lispe sydneyensis
Lispe nigrimana
Lispe nicobarensis
Lispe bivittata
Lispe nivalis
Lispe elengatissima
Lispe scalaris
Lispe nana
Lispe capensis
Lispe sericipalpis
Lispe orientalis
Lispe consanguinea
Lispe tentaculata
Lispe mirabilis
Lispe emdeni
Limnophora tigrina
Limnophora simulans
Limnophora triangula
Limnophora pollinifrons
0.008
caesia
desjardinsii
kowarzi
leucospila
longicollis
nicobarensis
nivalis
palposa
pumila
pygmaea
rigida
scalaris
tentaculata
uliginosa
not assigned

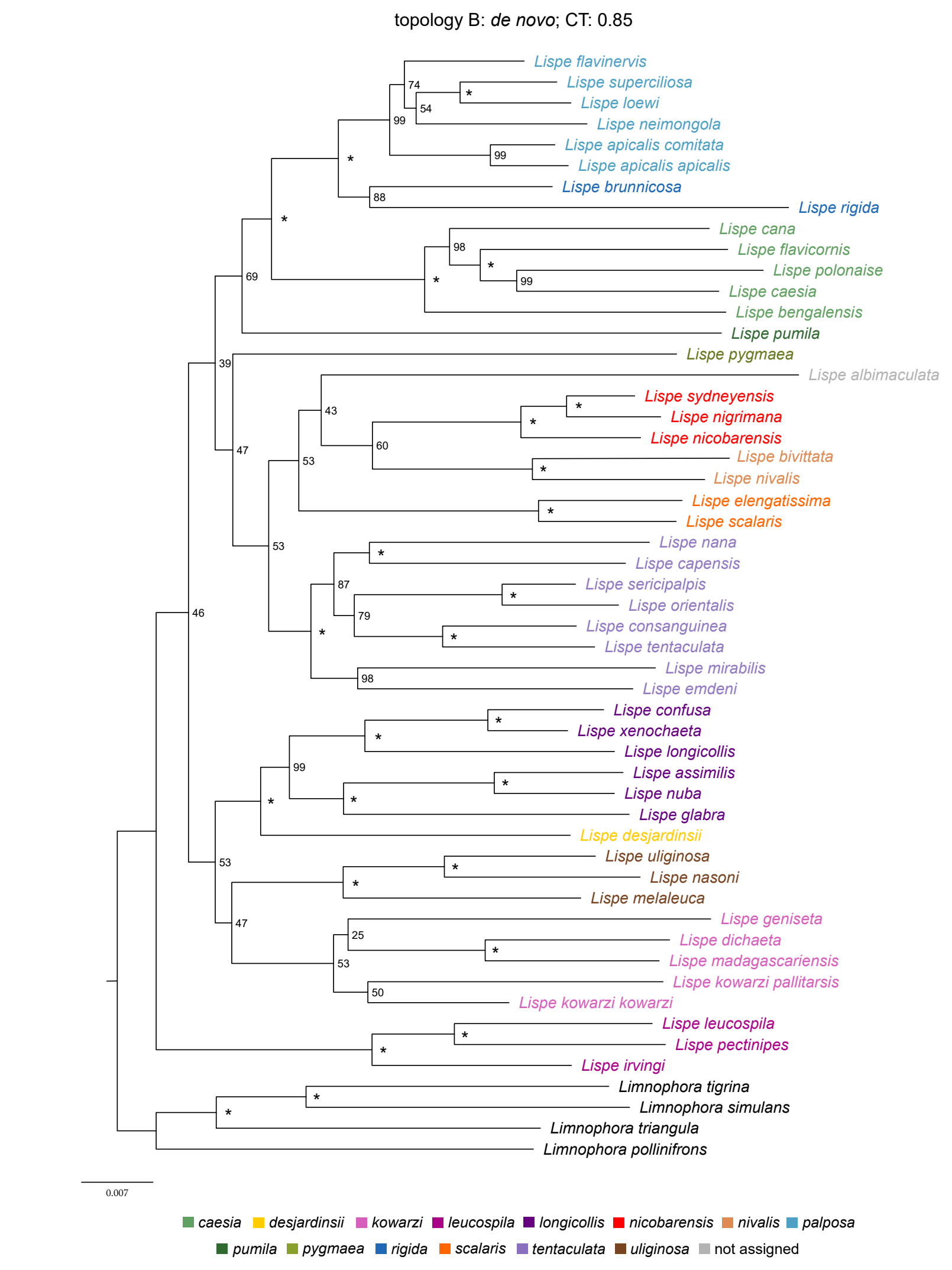
topology B: *de novo*; CT: 0.85
Lispe flavinervis
Lispe superciliosa
Lispe loewi
Lispe neimongola
Lispe apicalis comitata
Lispe apicalis apicalis
Lispe brunnicosa
Lispe rigida
Lispe cana
Lispe flavicornis
Lispe polonaise
Lispe caesia
Lispe bengalensis
Lispe pumila
Lispe pygmaea
Lispe albimaculata
Lispe sydneyensis
Lispe nigrimana
Lispe nicobarensis
Lispe bivittata
Lispe nivalis
Lispe elengatissima
Lispe scalaris
Lispe nana
Lispe capensis
Lispe sericipalpis
Lispe orientalis
Lispe consanguinea
Lispe tentaculata
Lispe mirabilis
Lispe emdeni
Lispe confusa
Lispe xenochaeta
Lispe longicollis
Lispe assimilis
Lispe nuba
Lispe glabra
Lispe desjardinsii
Lispe uliginosa
Lispe nasoni
Lispe melaleuca
Lispe geniseta
Lispe dichaeta
Lispe madagascariensis
Lispe kowarzi pallitarsis
Lispe kowarzi kowarzi
Lispe leucospila
Lispe pectinipes
Lispe irvingi
Limnophora tigrina
Limnophora simulans
Limnophora triangula
Limnophora pollinifrons
0.007
caesia
desjardinsii
kowarzi
leucospila
longicollis
nicobarensis
nivalis
palposa
pumila
pygmaea
rigida
scalaris
tentaculata
uliginosa
not assigned

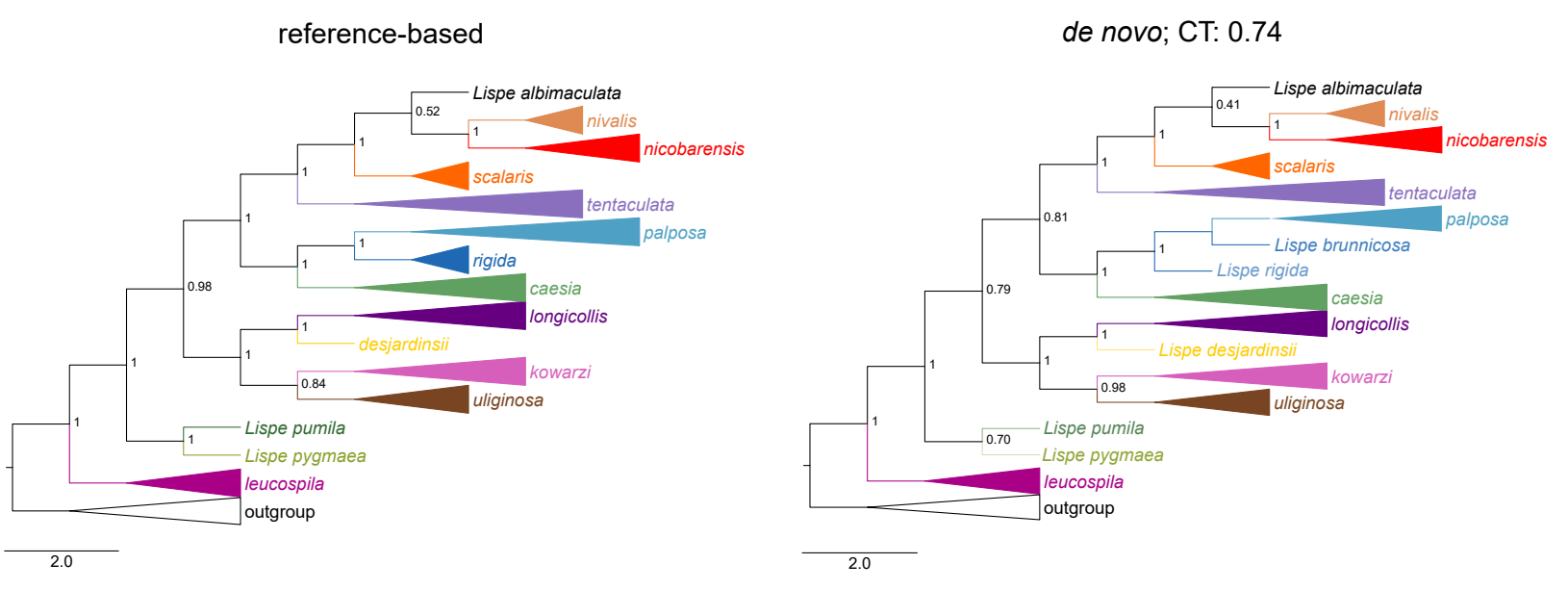
reference-based
Lispe albimaculata
nivalis
nicobarensis
scalaris
tentaculata
palposa
rigida
caesia
longicollis
desjardinsii
kowarzi
uliginosa
Lispe pumila
Lispe pygmaea
leucospila
outgroup
0.52
1
1
1
0.98
1
1
1
1
0.84
1
1
2.0
de novo; CT: 0.74
Lispe albimaculata
nivalis
nicobarensis
scalaris
tentaculata
palposa
Lispe brunnicosa
Lispe rigida
caesia
longicollis
Lispe desjardinsii
kowarzi
uliginosa
Lispe pumila
Lispe pygmaea
leucospila
outgroup
0.41
1
1
1
0.81
1
1
1
0.79
1
1
0.98
0.70
2.0